THE STRENGTH AND DEFORMATIONAL BEHAVIOUR OF A COHESIONLESS SOIL UNDER GENERALISED STRESS CONDITIONS

a thesis presented by

Stuart Dyson

for the degree of

Doctor of Philosophy

Department of Civil Engineering
University of Aston in Birmingham

October 1970

The research work described in this thesis was carried out in the Department of Civil Engineering of the University of Aston in Birmingham during the four-year period from October 1966. For the first two years, the author held a Science Research Council research studentship, and for the remaining period was employed by the University as a lecturer in civil engineering.

VOLUME ONE

SYNOPSIS

Predictions of the stresses and displacements induced within a soil mass by interaction with an engineering structure are made, at present, with only a limited knowledge of the deformational behaviour of soils under generalised stress conditions. The majority of routine testing and laboratory research investigations are performed on cylindrical soil specimens in the conventional triaxial apparatus, which is limited to imposing axially-symmetrical stress conditions. In very few field problems are such conditions strictly relevant. Many problems approximate more closely to plane strain, and recent progress has been made in investigating the behaviour of cuboidal specimens constrained from deformation in one of the principal directions. However, the experimental difficulties are increased, and controversies remain regarding the influence exerted by the apparatus on the soil behaviour.

The general field condition is one in which the stresses and strains are different in each of their three principal directions at a point. Very few satisfactory attempts have been made to overcome the complex problem of testing elements of soil under similar conditions.

The design and development of a new apparatus is described which allows generalised stress or strain conditions to be applied to cuboidal specimens. The methods used to apply the three boundary principal stresses ensure a high degree of stress uniformity, and suitable lubrication encourages uniform strains. Comparisons between the results of tests carried out under simple stress conditions, on specimens of the same sand, in this and in more conventional apparatus, indicate negligible apparatus interference. A further series of tests in plane strain shows that the deformational behaviour of loose specimens is similar to that observed in triaxial compression. For dense specimens, however, considerable strength increases result from the restriction imposed on strains. The results of generalised stress tests suggest that the intermediate principal stress is of most significance when its magnitude is less than that observed at failure in plane strain.

LIST OF CONTENTS

VOLUME ONE

CHAPTER FOUR - ASTON TRIAXIAL APPARATUS - DESIGN DEVELOPMENT AND TESTING TECHNIQUE

CHAPTER SIX - ASTON TRIAXIAL APPARATUS TESTS - RESULTS AND DISCUSSION

NOTATION

ENGLISH

a	constant
	apparatus calibration factor
A	cross-sectional area
ATA	Aston Triaxial Apparatus
b	constant
	Bishop's parameter, $\frac{\sigma_2 - \sigma_3}{\sigma_1 - \sigma_3}$
b_{1-4}	apparatus calibration factors
B.S.	British Standard
c	cohesion intercept
	apparatus calibration factor
C.V.R.	critical voids ratio
CYL	cylindrical
CUB	cuboidal
d_{1-2}	apparatus calibration factors
D	dilatancy factor
D_T	generalised dilatancy factor
D_t	rod diameter
DDG	deflection dial gauge
e	voids ratio
	apparatus calibration factor
exp	exponential
E	Young's modulus
	energy ratio
f	function
	apparatus calibration factor
F	frictional force
G	shear modulus
	specific gravity

H	height
INT	intermediate-stress test
j_o	angle between interparticle contact normal and horizontal
k	constant
κ	gradient of isotropic swelling curve
k	membrane penetration parameter
K	stress-dilatancy factor
	bulk modulus
K_o	coefficient of earth-pressure at rest
K_2	empirical factor
L	length
ΔL	change in length
m	mean projected solid path
M	compression modulus of rubber
n	porosity
N	normal load
p	mean principal stress
P	load
PDG	pedestal dial gauge
PRDG	proving-ring dial gauge
PS	plane strain test
q	axial deviator stress
q_w	corrected deviator stress
R	stress ratio, $\frac{\sigma_1}{\sigma_3}$
R_{oct}	octahedral stress ratio
S	material matrix
T	stress ratio, $\frac{\sigma_2}{\sigma_3}$
TC	triaxial compression test

TE	triaxial extension test
u	pore pressure
U	recoverable energy
v	volumetric strain
V	volume
ΔV	change in volume
ΔV_p	membrane penetration correction
W	energy dissipated during shear distortion
x, y, z	orthogonal axes
Y	yield stress in simple tension
z	shear strain

GREEK

α	constant
	compressibility parameter
tan α	degree of anisotropy
β	angle of interparticle sliding
β_1	maximum possible value of β
β_2	minimum value of β to comply with $\Delta V = 0$
β_c	preferred angle of interparticle sliding
γ	shear strain
	bulk density
γ_d	dry density
Γ	voids ratio at critical state for unit σ
δ	increment
Δ	change
ε	strain
	axial distortion shear strain
$\varepsilon_{1,2,3}$	principal strains
ε_v	volumetric strain

ε_{vc}	volumetric strain during consolidation
ε_{vf}	volumetric strain at failure
ε_{vs}	volumetric strain during shearing
$\dot{\varepsilon}_{vf}$	volumetric strain rate at failure
η'	stress ratio, $\frac{\sigma_1 - \sigma_3}{\sigma_1 + \sigma_3}$
θ	octahedral plane parameter
λ	gradient of virgin-compression curve
	incremental constant
μ	Lode's parameter
	coefficient of friction
M	critical state frictional constant
ν	Poisson's ratio
σ	total stress (effective stress)
σ'	effective stress
$\sigma_{1,2,3}$	principal stresses
$(\sigma_1)_{PR}$	proving-ring measurement
$(\sigma_1)_{SC}$	stress-cell measurement
$(\sigma_1)_{un}$	uncorrected measurement
$(\sigma_1)_t$	stress at top of specimen
$(\sigma_1)_b$	stress at bottom of specimen
$(\sigma_1-\sigma_3)_f$	deviator stress at failure
$(\sigma_1-\sigma_3)_{ms}$	membrane strength correction
τ_θ	octahedral plane parameter
ϕ	angle of internal shearing resistance
ϕ_{cv}	value of ϕ during shearing at constant volume
ϕ_μ	angle of interparticle friction
ϕ_R	value of ϕ_μ at rest
ϕ_s	value of ϕ_μ during sliding
ϕ_f	stress-dilatancy parameter

χ	total length of stress path to critical state
χ_o	remaining length of stress path to critical state

SUFFICES

a	axial
c	consolidation
cv	constant volume
f	failure
i	initial
max	maximum
min	minimum
oct	octahedral
p	plastic
r	radial
	recoverable
v	volumetric
x, y, z	directions
1, 2, 3	principal
$\cdot$	rate of change

CHAPTER ONE

INTRODUCTION

1.1 OBJECT AND SCOPE OF RESEARCH PROGRAM

The solution of many problems in soils engineering involves the prediction of the stresses and displacements induced in a soil mass by its interaction with a contiguous structure. The mechanical properties of the soil will govern its stress-deformational behaviour.

Because of the complex nature of soil material, the variability of its physical properties and the variation in its response with differing environmental conditions, many experimental investigations have been undertaken to assist the formulation of suitable behavioural theories. However, few theories allow accurate prediction of strains, largely because of the unrealistic assumptions necessary to make solutions tractable. Frequently the engineer has been prepared to ignore any pre-failure deformations, and to concentrate instead on whether the soil is capable of withstanding the applied stresses without collapse.

Theories of strength and stress-deformational behaviour will be discussed in Chapter 2, particular attention being given to cohesionless soils.

Laboratory investigations of soil behaviour, for the purposes of scrutinizing theories, necessarily need to be carried out on simple specimens, such as uniform dry sand or saturated remoulded clay which, in certain circumstances, may be assumed homogeneous. In most investigations, unless it is further assumed that the boundary stresses and strains are uniformly distributed throughout the interior of the specimen, a complete analysis of its deformational behaviour is impossible. No single laboratory test suffices for the study of all important aspects of soil behaviour, mainly because of the wide variety of stress and strain paths

relevant to common field conditions.

The role of soils testing in the overall study of mechanical properties will be considered in Chapter 3.

The primary objective of this research program was to begin an investigation into the strength and stress-deformational behaviour of soils under generalised conditions of stress.

The conventional triaxial apparatus, though remaining one of the most prolific in both routine and research studies, is limited to imposing axially-symmetrical stress conditions. Such conditions are appropriate to only a minority of field problems, and therefore important assumptions need to be made in order to extrapolate these findings to other situations.

Many attempts have been made to subject specimens to plane strain deformation, which is of considerable engineering interest. However, the more general problem is one in which the magnitudes of the three principal stresses at a point in the soil mass are different. Many practical difficulties have been encountered in attempting to apply such conditions to laboratory specimens, some of which have not yet been overcome.

Various apparatuses designed to allow generalised stress testing of soils will be reviewed in Chapter 3, together with the more important developments in experimental technique.

Chapter 4 is devoted to the work done in developing a new apparatus capable of imposing a wide variety of stress conditions on a cuboidal specimen without significant interference with the specimen deformation.

The results of drained triaxial compression, plane strain, triaxial extension and "intermediate-stress" tests on saturated specimens of a coarse sand will be discussed in Chapter 6.

In order to assess the effectiveness of this apparatus, which is

necessarily of greater complexity than the more conventional, it is essential to investigate the behaviour of similar specimens, subjected to the same simple stress conditions, in each type of apparatus. Any significant differences may be attributable to an "apparatus effect". Therefore in addition to the extensive tests carried out in the new apparatus, a series of triaxial compression tests was performed on both cylindrical and cuboidal specimens of the same soil. Cylindrical triaxial extension tests were also included in this program.

Several refinements of the conventional triaxial apparatus and testing technique, developed during these test series, will be presented in Chapter 5. The analysis and discussion of the experimental results are covered in Chapter 7.

In the final chapter, the overall conclusions from the complete investigation are summarized.

1.2 DEFINITION OF TERMS AND UNITS

The majority of terms used in this work are common to much current soil mechanics research, and as such are widely accepted and unambiguous. For instance, the "deviator stress" in conventional triaxial tests is understood to be the difference between the major and minor principal stresses, as distinct from the term "deviatoric stress" which, in a more general field, expresses the difference between the major and mean principal stresses.

However, several other terms, such as "elastic" and "plastic", and "failure" and "yield", are often used to convey different meanings by different investigators. These will be given consideration at relevant points in the text and the definitions used will be stated. In Chapters 2 and 3, where the investigations of other workers have been reviewed, the original authors' terms have usually been preserved. Attention will be drawn to any differences between these and the current definitions.

The terms "uniaxial", "biaxial" and "triaxial", used with respect to soil test conditions, are frequently given various meanings depending upon whether stresses or strains are being considered and whether symmetry is regarded as important. In this research program, the phrases "triaxial compression" and "triaxial extension" are used in the conventional sense. However, this in no way simplies that the "Aston Triaxial Apparatus" described in Chapter 4 is limited to imposing these stress and strain conditions. The various types of test that are made possible with the use of this apparatus will be defined in the relevent sections.

Natural strains are used throughout, and compression is taken to be positive. The volumetric strain rate at failure, $\dot{\varepsilon}_{vf}$, was always negative for the cohesionless soil tested in this research program, and therefore relative magnitudes refer to the modulus of this quantity.

All tests were carried out under fully drained conditions, the rate

of strain being sufficiently small to ensure negligible excess pore-pressure. Effective and total stresses were therefore assumed equal. Each has been denoted as σ, except where ambiguity is possible, in such cases the conventional symbol σ' has been used for effective stress.

During the period in which the research program was undertaken, much of the laboratory apparatus was being replaced with equipment consistent with the S.I. system of units. In some instances this has resulted in the use of "mixed" units, but the majority of the experimental work was carried out with apparatus calibrated in British units. No attempt has been made to convert all measured quantities to the S.I. system. The most useful conversion, that between the units of stress, is given below.

$$10 \text{ lbf/in}^2 = 68.9 \text{ kN/m}^2.$$

1.3 GENERAL LAYOUT

The main text of each chapter, minor diagrams, and tabulated data are included in Volume I.

The corresponding graphs, diagrams, photographs and engineering drawings are grouped consecutively in Volume II, which also includes the appendices. The latter are each complete with their respective graphs and diagrams.

In general, units have not been shown on individual graphs, since these are quoted frequently in the text. For instance, it may be assumed that σ is in lbf/in^2, ΔV in ml and ε in %, unless otherwise stated.

CHAPTER TWO

STRESS-DEFORMATIONAL BEHAVIOUR AND STRENGTH OF COHESIONLESS SOILS

2.1 INTRODUCTION

The laws of gravity dictate that the majority of civil engineering problems at some stage involve interaction between the structure and the surrounding soil. The solution of such problems usually requires the resulting stresses and displacements in the soil mass, both during and after construction, to be predicted. In other problems, for instance earth-dam construction or land reclamation, the soil itself forms the whole or part of the structure, and selection of the appropriate material, with respect to its mechanical properties, and control over its placement are of major importance. The mechanical properties of the soil govern its deformational behaviour under applied stress systems or under stresses induced by given displacements.

Many studies of soil behaviour have been concerned with the conditions necessary for failure, and have led to the development of new failure theories for soils or the verification of those currently employed.

At any point within a soil mass, providing the principal effective stresses are known, together with the relevant soil properties, the chosen failure criterion predicts whether or not failure will occur at that point. The soil properties which need to be known in order to make this prediction vary depending upon the chosen criterion.

Estimation of the stability of engineering structures in soils involves comparison between the magnitudes of the applied stresses and the ability of the soil to withstand them. Therefore the factors of safety of retaining-walls and slopes, and the bearing capacity of

foundations, are usually determined by idealizing the soil as a rigid-plastic material, thus ignoring any pre-failure deformation. The soil, and hence the structure, is assumed not to move until the resistance to applied shear stress along some surface through the mass is no longer sufficient to prevent relative movement on each side of that surface. The resulting displacements are catastrophic.

However, the strength of soils and their deformational behaviour under applied stress are not totally independent properties.

In many soils engineering problems, prediction of settlements is vital in order to meet the design requirements of the superstructure. Therefore, having established that the factor of safety against failure is adequate, the soil is commonly idealized as a linearly elastic, isotropic material for the purpose of determining displacements. In some cases, the soil profile may be complex, and hence far removed from the semi-infinite medium to which it is often approximated. Therefore a solution for the stresses and displacements in layered media, either isotropic or axially-symmetrical anisotropic, may be more appropriate. However, despite the complexity of some solutions, accurate predictions of deformation are usually much more difficult to obtain than those concerned with failure, mainly because of the effect of time-dependent inelastic behaviour on displacements.

Soils are neither ideally rigid-plastic nor linearly elastic; they are polyphase particulate materials having widely differing physical properties. The individual particles vary in shape, size and mineral composition, factors which influence their geometrical arrangement, or "packing", within the soil mass and their interaction with the fluid phases. The stress-deformational behaviour of soils will therefore depend upon the interparticle stresses and deformations, and the relative movement of the particles. Particle crushing and fracture may also

occur, even at low stresses.

Because of the nature of their deposition, soils are rarely either homogeneous or isotropic, and the degree of anisotropy is likely to depend heavily upon subsequent deformation. However, in order to assist in the solution of boundary value problems, it is necessary to formulate realistic relationships between stress and strain as the soil deforms along various stress paths.

For the majority of problems, economic and time factors dictate that the soil properties are determined from limited sampling and experimentation. Therefore the engineer needs to be able to call upon a general knowledge of soil behaviour, and engineering judgement, in extrapolating information obtained from testing to the given field conditions. Frequently, very approximate methods of predicting stresses and strains are suitable for particular types of problem, more exact solutions being unjustified having regard to the available information on the soil properties. However, rigorous investigations of soil behaviour will lead to the development of more realistic solutions to field problems and provide a common basis for engineering judgement.

Clearly it would not be possible, in developing analytical solutions to stress-deformation problems, to take into account the true nature of the interparticle contacts. Therefore the properties of soil material must be idealized in a manner which will hold good for a wide variety of soils over a wide range of stress or strain paths. No single theory has yet been found satisfactory in describing accurately the behaviour of soils under such conditions.

The only means by which a theory may be assessed is the accuracy with which it fits observed behaviour. Therefore careful experimentation is required using soils with known physical properties.

In order to eliminate as many variables as possible, most

investigators have confined their attention to laboratory-prepared specimens with a single pore fluid, such as saturated remoulded clay or clean dry sand, and have attempted to obtain a high degree of initial homogeneity. Others have simplified their experiments even further by testing artificial particulate materials, for instance uniform steel spheres or glass ballotini, and hence have eliminated particle shape and size distribution as factors affecting the results. Also, by arranging the spheres in regular geometrical packings, the effect of the degree of initial anisotropy could be investigated.

Having developed theories for stress-deformational behaviour which are in general agreement with results from tests on small elements subjected to "uniform" stresses and strains, some workers have then attempted to predict behaviour in model tests on mixed boundary problems. However, the experimental techniques are often complex in model tests which allow realistic comparisons to be made between theoretical and observed behaviour.

Basically, theories of mechanical behaviour have been derived using either the methods of continuum mechanics, in which the discrete nature of soil material is disregarded, or those of particulate mechanics, in which the relationships between individual particles are of primary importance. A further category, which may be termed "macroscopic" research, has been concerned largely with describing observed stress-deformational behaviour using a variety of empirical factors.

2.2 PARTICULATE MECHANICS

Much early work in solving stability problems in soils engineering used the rigid-plastic idealization for the soil material, the most popular theory being that now frequently described as the Mohr-Coulomb failure criterion. This postulates that, for a cohesionless soil, deformation will occur if, and only if, the major and minor principal stresses are such that $\sigma_1 = \sigma_3 \tan^2(45+\phi/2)$, where ϕ is described as the "angle of internal shearing resistance". A planar surface is formed at an angle $(45+\phi/2)$ to the direction of the major principal plane, along which the two sections of the soil mass slide at constant volume.

This type of model takes no account of the large distortional strain required to reach failure and the large accompanying volumetric deformation, which are characteristics of real soils. Terzaghi was the first to realize the deficiencies of this type of approach, and suggested that a more fundamental treatment of soil properties should be based on acceptance of their particulate nature.

Many investigators have studied the properties of regular geometrical arrangements of equal spheres in order to isolate the various factors determining their behaviour under stress. Attempts have then been made to extend these findings to random assemblies of irregular particles, that are natural soils. Clearly such assemblies are statically indeterminate to a high degree. However, one of the major factors governing their behaviour will be the relative positioning of the particles, i.e. their packing.

The six basic regular packings of uniform spheres (Graton and Fraser 1935) are shown in Fig. 2.1. The porosities range from 0.2595 for the densest packings, pyramidal and tetrahedral to 0.4764 for the loosest, simple cubic, and the coordination numbers, representing the

number of contacts per sphere, range from 12 to 6 for the respective packings. The greater the number of contacts, the more stable will be the arrangement, and therefore initially loose packings will tend to increase their coordination numbers when conditions are favourable. Smith, Foote and Busang (1929) determined the number of contacts of random packings of lead shot experimentally, using acetic acid, and derived an expression relating the average coordination number with the proportion of spheres in their densest possible arrangement. In order to calculate the latter, it was assumed that the packing was composed entirely of small cubic and face-centered cubic arrays, present in proportions consistent with the measured average porosity.

If the packing of uniform spheres is random, it is possible that spaces large enough to accommodate spheres become arched over, thus increasing the maximum porosity. Similarly, graded spheres are likely to have lower minimum porosities. Consequently, an assembly of natural soil particles, which differ in shape and size, must inevitably be random, and the limiting porosities cannot be determined theoretically.

The stresses and deformations at the particle contacts will govern the macroscopic behaviour of particulate materials.

In regular packings of equal spheres, the contact loads resulting from an applied ambient stress should be equal. Dantu (1961) investigated the distribution of contact load between glass spheres under hydrostatic stress, using the photoelasticity technique, and found that the statistical bell-shaped distribution did not apply. Instead, a large number of contacts carried loads much less than the average, and a smaller number carried loads much greater than the average. It was suggested that the latter group governed the overall deformation of the assembly.

Observed deformations were compared with those predicted using

Hertz's contact theory for two elastic spheres (Timoshenko and Goodier 1951), which gives a non-linear relationship between stress and deformation resulting from the generated shape of the contact surfaces. Despite the wide deviation from the assumed distribution of contact forces, the basic form of the stress-strain curve was similar to the predicted relationship given by $\varepsilon = (\sigma/E)^{2/3}$, although the observed strains were much greater.

In a further study (1968), the same worker analysed the contact forces between two thousand plastic spheres of two diameters contained in a rubber membrane and stressed hydrostatically. By heating and then cooling the spheres, the contact areas were preserved and measured, and the interparticle forces were calculated using Hertz's theory. Both the coordination numbers and contact forces were approximately uniformly distributed about their mean values.

Deformations of elastic spheres resulting from oblique loading are not only non-linear but also inelastic, relative displacements having both normal and tangential components. Therefore the stress-deformation relationship is dependent upon loading history. Thurston and Deresiewicz (1959), developed a stress-strain theory for face-centered cubic packings of equal spheres by integrating an incremental form of this relationship along the triaxial compression stress path. The failure process was envisaged as one in which sliding occurred in one direction only, the minimum required stress ratio being

$$\frac{\sigma_1}{\sigma_3} = 2\left(\frac{\sqrt{6} + 2\tan\phi_\mu}{\sqrt{6} - 4\tan\phi_\mu}\right).$$

Ko and Scott (1967) assumed non-linear elastic contact behaviour under ambient stress in their granular model. The packing was assumed to consist of regular loose and dense arrays of particles. In each array, larger spheres were considered to arch over slightly smaller

ones until the pressure was great enough for deformation to result in new contacts. Consequently the predicted deformations were less than those which would be obtained for exactly equal spheres in continuous contact.

In general, non-linear elasticity relationships of the form $\varepsilon \propto \sigma^{-m}$, have been used in the analysis of arrays of spheres, even when the contact forces deviate from the normal as a result of either applied shear stresses or initial anisotropy. Moreover, the assumption that contact forces are equal is inevitably less reliable for natural soils, even if the particles do deform as Hertzian spheres.

Therefore although overall deformations of particulate materials depend on the deformations of the particles themselves, as well as their geometrical arrangement, many investigators have chosen to assume the latter to be rigid.

Because soils are deposited under gravity their initial geometry is rarely simple, the number of contact planes with major components in the vertical direction exceeding those with major components in the horizontal direction. The degree of initial anisotropy is determined by the distribution of particle contacts. Despite earlier workers' claims to the contrary, it is an established phenomenon that vertically-deposited cohesionless soils show greater compression in horizontal directions when subjected to ambient stress (El-Sohby 1964). Therefore, because of anisotropy, the forces between particles, even under ambient stressing, deviate from the normal to the contact surfaces. The normal component causes elastic deformation of the particles, assuming they are sufficiently hard to resist local failure, or crushing, at the contacts, and the tangential component is resisted by friction between the particles. When the frictional resistance is exceeded, relative movement occurs, and is arrested only when new contacts are formed such

that the tangential force is suitably reduced.

Frequently it is assumed that the number of rolling contacts between particles is negligible compared with those that slide. Rowe (1962) studied the behaviour of parallel stacks of uniform rods, under plane stress, and that of three-dimensional packings of spheres under triaxial stress conditions. From these studies the "stress-dilatancy" theory was developed.

Ignoring elastic and plastic deformation and rotation of the particles, deformation of the soil mass was considered to depend entirely upon the relative movements of groups of particles as contact friction was overcome, the groups constantly changing as contacts were broken and new ones formed. For a random assembly of rotund, rigid, cohesionless particles, the principle of "maximum energy transmission" was postulated.

Fig. 2.2 shows two such particles under axially-symmetrical stress conditions, $\sigma_1 > \sigma_2 = \sigma_3$. L_1 and L_3 are the components of the inter-particle resultant force, R, resolved in the principal directions, and β is the angle between the major principal direction and the plane of contact, i.e. the instantaneous direction of sliding. The angle of friction between the particles is ϕ_μ, and is governed by their mineral content, decreasing slightly with the load per particle. At the instant of sliding, $\frac{L_1}{L_3} = \tan(\phi_\mu + \beta)$, and the energy ratio, E, is defined as the ratio of the energy supplied in the direction of the major principal stress to the work done in the direction of the minor principal stress. Since $\tan\beta = -\frac{\delta x}{\delta z}$, the incremental energy ratio becomes

$$E = \frac{L_1 \delta z}{-L_3 \delta x} = \frac{\tan(\phi_\mu + \beta)}{\tan\beta},$$

and therefore the energy dissipated in internal friction is

$$L_1 \delta z + L_3 \delta x = L_1 \delta z (1 - 1/E).$$

This is a minimum when E is a minimum, i.e. when $\beta = (45-\phi_\mu/2)$, and therefore the minimum energy ratio is

$$E_{min} = \tan^2(45+\frac{\phi_\mu}{2}) = K_\mu,$$

giving

$$\frac{L_1 \delta z}{-L_3 \delta x} = K_\mu.$$

Generalising for a random assembly of particles with many groups having differing instantaneous slip directions, using the principle of

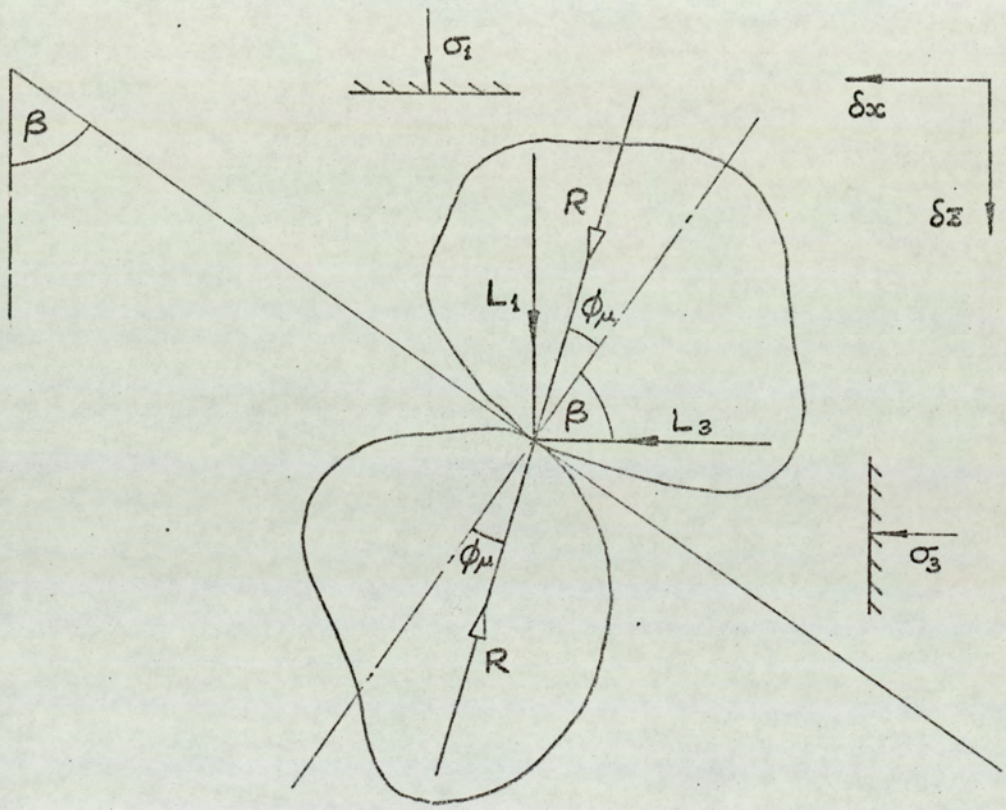

FIG. 2.2

virtual work :-

$$\frac{\sigma_1 d\varepsilon_1}{-2\sigma_3 d\varepsilon_3} = K_\mu, \text{ and since } d\varepsilon_v = d\varepsilon_1 + 2d\varepsilon_3,$$

$$\frac{\sigma_1}{\sigma_3} = (1 - \frac{d\varepsilon_v}{d\varepsilon_1})\tan^2(45+\frac{\phi_\mu}{2}), \text{ or}$$

$$R = D\, K_\mu.$$

The mechanism of deformation visualizes a random assembly to be composed of weak and strong groups of particles, and hence β varies. The weak groups slide first, and transfer stress to adjacent groups, β changing continuously. As the stress increases, the obliquity of inter-particle forces increases, and therefore more contacts instantaneously slide. Rearrangement will occur most economically if β is such that the energy dissipated in internal friction is a minimum, this value being denoted as β_c. All other contacts are static, and hence all deformation is due to the movement of instantaneously rigid groups, at the prefered angle β_c, the groups continuously dividing and forming.

Criticisms of this theory and the deformation mechanism have been concerned with Rowe's assumption that elastic deformation and rolling of the particles were insignificant, and with the logic of minimizing E for a random assembly. Horne (1965) indicated that medium to dense packings are far more likely to deform in large groups by translation rather than by rotation, especially since the former allows at least one more contact, resulting in a more stable mode of deformation with a lower dilatancy rate. The principle of maximum energy transmission leads directly to that of preferred directions, and hence to the conclusion that the number of sliding contacts is small compared with the total number of contacts, and that deformation occurs in large groups.

Using a different approach, Horne derived upper and lower bounds for the number of sliding contacts and for the total number of contacts, leading to the derivation of the strain rates in the principal directions and confirmation of Rowe's stress dilatancy equation, $R = D K_\mu$.

The structure of a deforming assembly of particles constantly changes, the resulting anisotropy depending on the rate at which new contacts are formed and old ones disappear. For axially-symmetrical stress conditions, Horne used the ratio of the "mean projected solid

paths" in the major and minor principal directions as a measure of the degree of anisotropy. The m.p.s.p. was defined as the ratio of the number of particles required to trace a solid path parallel to a principal stress direction to the length of the path itself, and was denoted by m. Therefore for $\sigma_1 > \sigma_2 = \sigma_3$, $\frac{m_1}{m_3} \geq 1$.

Assuming that after an initial period, the initial contacts, and hence the initial anisotropy, had been destroyed, the following relationships between the principal stresses, the strain rates and the degree of induced anisotropy were obtained:-

$$\frac{\sigma_1}{\sigma_3} = \frac{4m_1}{\pi m_3} \tan(45 + \frac{\phi_\mu}{2}),$$

$$\frac{d\varepsilon_3}{d\varepsilon_1} = \frac{-2m_1}{\pi m_3} \tan(45 - \frac{\phi_\mu}{2}).$$

The ratio $\frac{m_1}{m_3}$ is equivalent to tan α, the ratio of the number of contacts per unit area on the major and minor principal planes respectively, used by Rowe to describe the arrangement of uniform spheres in regular packings, the interpretation of which was unclear for random assemblies.

At the maximum dilatancy rate, by assuming that the only contacts were those occurring at maximum frequency, and that anisotropy was governed by these alone, the "maximum degree of anisotropy" was derived as

$$\left(\frac{m_1}{m_3}\right)_{max} = \frac{\pi}{2}\tan(45 + \frac{\phi_\mu}{2}),$$

therefore

$$\left(\frac{\sigma_1}{\sigma_3}\right)_{max} = 2\tan^2(45 + \frac{\phi_\mu}{2}),$$

and

$$D_{max} = \left(1 - \frac{d\varepsilon_v}{d\varepsilon_1}\right)_{max} = 2, \text{ i.e. } \left(\frac{d\varepsilon_3}{d\varepsilon_1}\right)_{max} = -1$$

Hence the upper limit on the dilatancy rate, expressed in terms of the dilatancy factor D, is 2.

As the assembly dilates further, more contacts are at incipient sliding and the average size of the particle groups decreases, so that instantaneous sliding in directions deviating from β_c is more likely.

Horne suggested that at any instant in a fully dilated assembly, sliding occurs with uniform frequency within a range of β values from β_1 to β_2, where β_1 is the maximum possible angle of sliding, $(90 - \phi_\mu)$, and β_2 is the minimum angle necessary to comply with the constant volume condition, $\delta\varepsilon_1 = -2\delta\varepsilon_3$. β_2 was also expressed in terms of ϕ_μ, and therefore since $\frac{\sigma_1}{\sigma_3} = \tan^2(45 + \frac{\phi_{cv}}{2})$, a relationship between ϕ_μ and ϕ_{cv} was obtained (Horne 1969).

The Mohr-Coulomb peak value of ϕ and the shape of the stress-strain curve depends largely upon the initial porosity, and the difficulties of relating this to the degree of anisotropy, particularly when sliding occurs in small groups, were pointed out.

Several previous attempts at deriving a relationship between ϕ and ϕ_μ had been based on an "energy correction" for the work done during volumetric deformation. However, Rowe et al (1964) pointed out that although the corrections applied by Taylor (1948) to direct shear tests, and by Bishop (1954) to triaxial compression and plane strain tests, were correct, they did not isolate a fundamental soil property. Energy was dissipated internally due to dilatancy, in addition to that expended in expansion against confining pressure. Bishop had obtained the following approximate expressions using energy corrections:-

$$\sin\phi = \frac{15\tan\phi_\mu}{(10 + 3\tan\phi_\mu)} \quad \text{for triaxial compression,}$$

and assuming $\sigma_2 = (\sigma_1 + \sigma_3)/2$,

$$\sin\phi = \frac{3}{2}\tan\phi_\mu \quad \text{for plane strain.}$$

The latter was compared with a theoretical relationship proposed by Caquot (1934) for plane strain:-

$$\tan\phi = \frac{\pi}{2}\tan\phi_\mu.$$

The relationship between ϕ_μ and ϕ_{cv} was confirmed experimentally by Parikh (1967) using a variety of particulate materials, and varying

the value of ϕ_μ by changing the pore-fluid. However, Skinner (1969) obtained a coefficient of friction for submerged glass ballotini which was more than ten times greater than that for the same material when dry. Since ϕ, ϕ_{cv} and dilatancy rates were similar in shear box tests on dry and saturated specimens, it was concluded that rolling must predominate for the latter, in order to maintain the energy balance. Clearly, reliable measurement of ϕ_μ is essential to the verification and use of the stress-dilatancy theory.

Rowe had observed the formation of slip zones after peak stress ratio in tests on regular packings of spheres, and Horne confirmed theoretically that they could not occur before peak, since the value of ϕ_{cv} within the slip zones would need to be greater than ϕ_{cv} for the fully-dilated assembly. Therefore slip zones are the result of failure, not the cause.

In practice it was found that particulate materials deform according to the stress-dilatancy equation:-

$$\frac{\sigma_1}{\sigma_3} = \left(1 - \frac{d\varepsilon_v}{d\varepsilon_1}\right) \tan^2 \left(45 + \frac{\phi_f}{2}\right), \text{ or } R = D\,K_f,$$

where ϕ_f varies depending upon the porosity, stress level and stress path, between a lower limit ϕ_μ and an upper limit ϕ_{cv}. Experimental data from tests on a wide variety of particulate materials indicated that for dense packings in both triaxial compression and extension $\phi_f \rightarrow \phi_\mu$ up to peak stress ratio, and for loose packings $\phi_f \rightarrow \phi_{cv}$ throughout deformation.

The deviation of ϕ_f from its lower limit occurs when particle groups are small, i.e. in loose or highly-dilated assemblies, when sliding takes place in other than the preferred direction β_c, and rolling may become significant.

Similarly in the case of plane strain, the number of potential

sliding planes is restricted, and therefore variations from β_c again occur, ϕ_f approaching the upper limit ϕ_{cv}. Therefore, R varies from K_{cv} to $2K_{cv}$ as the packing varies from the loosest to the densest arrangement. Barden et al (1969) demonstrated experimentally, using a variety of materials, that this concept was valid for plane strain deformation, providing that ϕ_{cv} measured at large strain in triaxial compression was applicable to plane strain. El-Sohby (1964) showed that deformation during unloading under constant stress ratio could be considered totally elastic.

By subtracting the elastic components from total deformation during loading under constant stress ratio, the stress-dilatancy equation was confirmed for the "slip" components.

Leussink and Wittke (1963) investigated the stress-deformational behaviour of glass and steel spheres arranged in regular packings, both theoretically and experimentally. The theoretical assumptions regarding particle rearrangement were similar to those of the stress-dilatancy theory.

In each layer, the spheres were positioned at the corners of squares or equilateral triangles, those of one layer resting on four or three spheres, respectively, of the layer beneath. These packings were described as "quadratic" and "hexagonal".

The porosities were expressed in terms of the angle between the contact normal and the horizontal, j_o. It was assumed that, under triaxial compression stress conditions, the basic geometry was preserved and only the distance between layers, and hence the angle of contact, changed. Rotation was excluded, failure resulting from translation as the frictional resistance at the points of contact was overcome.

From considerations of equilibrium between the principal stresses and the contact forces in the major and minor principal directions, the

critical stress ratio at failure, for both packings, was derived as:-

$$\frac{\sigma_1}{\sigma_2} = 2 \tan j_o \tan(j_o + \phi_R),$$

where ϕ_R was the angle of friction between the spheres at rest. Therefore for any given value of ϕ_R , the failure stress condition, and hence the Mohr-Coulomb value of ϕ, could be related to the porosity.

The post-failure critical stress ratios were determined for different axial strains, using current j-values and ϕ_S, the sliding angle of friction, in the above equation. Therefore the stress-deformation curves show a peak at zero axial strain, which is inevitable in this type of rigid particle model, which drops instantaneously to a value consistent with ϕ_S, and then decreases continuously with strain.

In the case of plane strain, clearly the basic packing geometry must change after failure, the frictional forces and the deformation being limited to parallel planes. The failure stress ratios were again determined from equilibrium of the components of the contact forces and the major and minor principal stresses, leading to more complex expressions for ϕ in terms of ϕ_R and j_o, the hexagonal packing yielding higher values. Post-failure stress-strain curves, being dependent upon the mode of deformation, were again different for the two packings investigated.

Experiments confirmed the relatively higher shear strength in plane strain, for the same packings. However, the test results were always lower than the theoretical ones, especially at low strains. The out-of-roundness of the spheres and restraint from the apparatus were suggested as the main causes of this discrepancy.

These investigations emphasized that stress-deformational behaviour depends largely on the geometrical arrangement of the particles; the relationship between ϕ and n is not unique.

Rennie (1959) used the rigid sphere model in an investigation into the strength of sand, firstly assuming that the spheres were smooth, and then introducing frictional forces.

By considering the densest array of equal smooth spheres, i.e. each sphere in contact with twelve neighbours, it was shown that in order to remain stable, the maximum principal stress ratio should not exceed 2. By assuming a similar mode of collapse, this solution was extended for small coefficients of friction, and if coincidence of the intermediate principal stress and strain axes was also assumed, an upper bound to the value of σ_2 was obtained:-

$$\sigma_2 = \frac{\sigma_1 + \sigma_3}{3}.$$

Rennie's solution was valid for a restricted range of σ_2, although it was independent of the magnitude of σ_2, and, in an attempt to relate this study to the more common stress conditions in soil mechanics, Parkin (1965) considered the remaining range:-

$$\frac{\sigma_1 + \sigma_3}{3} > \sigma_2 \geq \sigma_3.$$

In the former investigation, it was necessary to consider only one pair of broken contacts at opposite points on a diameter of each sphere. For the above stress condition, two pairs were considered on perpendicular diagonals, the solution depending significantly upon the magnitude of the intermediate principal stress. Therefore, combining the two solutions, the strength of the densest regular packing of uniform spheres under generalised principal stress conditions could be represented in two zones. For magnitudes of $\sigma_2 \geq \frac{\sigma_1 + \sigma_3}{3}$, the principal stress ratio $\frac{\sigma_1}{\sigma_3}$, at failure, was independent of σ_2; for the remaining range between the triaxial compression condition and $\sigma_2 = \frac{\sigma_1 + \sigma_3}{3}$, strength increased steadily, almost linearly, as σ_2 increased. Obviously the absolute magnitude of the peak stress ratio depended upon the assumed interparticle

friction angle ϕ_μ.

Based on this model, a dense assembly of irregular natural sand particles would exhibit a single failure plane as soon as the critical stress ratio was reached and overall collapse would occur. This is in contrast to the stress-dilatancy model, in which the stress ratio increases steadily, as large deformations occur, and many groups of particles may be sliding at any instant. Moreover, the critical stress ratio may occur in more than one sliding direction simultaneously, and single failure planes are only the result of post-failure conditions.

However, the Rennie-Parkin model may represent an upper limit to the strength of dense cohesionless soils for all magnitudes of σ_2. Conveniently, for most sands the maximum principal stress ratio at failure is such that the intermediate principal stress given by $\sigma_2 = \frac{\sigma_1 + \sigma_3}{3}$ is very similar to that commonly measured in plane strain tests, though this is not assumed in the model. Therefore, the failure criterion effectively predicts an increase in strength between triaxial compression and plane strain, after which no further change occurs up to and including the triaxial extension condition.

This will be considered together with other failure criteria in section 2.4.

2.3 CONTINUUM MECHANICS

In the previous section, theories for the stress-deformational behaviour of soils developed from consideration of the relationships between individual particles were discussed. Each, at some stage, idealized the true behaviour of the material, for instance by assuming that the particles were perfectly spherical, perfectly elastic or perfectly rigid, or that they moved by sliding only when a constant frictional force was overcome. An alternative approach is to idealize the whole assembly as a continuum, and attempt to describe its observed mechanical behaviour, under particular conditions, using a mathematical approximation. The value of such an approximation may be measured by the degree of success with which it predicts behaviour under differing conditions. Generally, the wider the range of its proven application, the greater is its suitability for solving real problems.

The homogeneous, isotropic, linearly-elastic idealization has frequently been used to predict stresses and strains within a soil mass, e.g. using the Boussinesq equations to determine stresses, and the coefficient of compressibility to calculate vertical settlement. Because of the principle of superposition associated with linearity, and the isotropy of the material, two constants only are required to completely describe its mechanical properties, the bulk modulus, K, and the shear modulus, G, given by:-

$$\varepsilon_{oct} = \frac{\sigma_{oct}}{3K} \text{ , and } \gamma_{oct} = \frac{\tau_{oct}}{G} \text{ .} \quad *$$

The alternative elastic constants, E, Young's modulus, and, ν, Poisson's ratio, are often used.

Finn and Mittal (1963) used this idealization in proposing a theory which predicted the effect of the intermediate principal stress on the strength of cohesionless soil. By assuming that $\nu = 0.5$ and that failure

* The octahedral stresses and strains are defined at the end of section 2.3.

occurred at the same axial strain in both plane strain and triaxial compression, it was shown that

$$\left(\frac{\sigma_1}{\sigma_3}\right)_{ps} = \frac{4}{3}\left(\frac{\sigma_1}{\sigma_3}\right)_{tc} - \frac{1}{3}.$$

However, since it was commonly observed that failure in plane strain tests was reached at smaller axial strains, the equation could be regarded as giving an "upper bound" only. For triaxial extension tests, no change in strength was predicted.

Clearly, this simple idealization would have greater appeal if it approximated more closely to realistic soil behaviour. However, soils deforming under increments of shear stress usually exhibit significant volumetric deformation, unrelated to the octahedral normal stress, σ_{oct}.

Because of the manner of their deposition, soils have also been idealized as linearly elastic anisotropic materials, frequently assuming horizontal isotropy. In general, assuming that the material has three orthogonal planes of elastic symmetry, and that these coincide with the coordinate axes, the stresses and strains are related by

$$[\varepsilon_{ij}] = [S_{ij}][\sigma_{ij}],$$

where the material matrix is symmetric, and therefore six independent constants are required. All components of strain depend upon all components of stress, so that volumetric and shear behaviour may not be separately represented.

Natural soils, in addition to being dilatant, are non-linear. To overcome the difficulty of describing non-linear behaviour in suitable mathematical form, incremental strains have been related linearly to incremental stresses using tangent or secant moduli, described as "pseudo-elastic constants".

Girijavallabhan and Reese (1968) used the finite element technique to predict the deformations of sand behind a retaining-wall. In developing a non-linear stress-strain relationship from triaxial compression

tests, it was assumed that ε_{oct} was predominantly due to τ_{oct}, and that $\frac{\tau_{oct}}{(\sigma_{oct})_i}$, where the suffix i indicates the initial condition, was principally a function of γ_{oct}. The value of ν, $(= -\frac{\varepsilon_3}{\varepsilon_1})$, was determined as a secant modulus from the experimental curve for various axial strains, and its mean value over the range $0 < \varepsilon_1 < 0.01$ was taken as a material constant.

Assuming a value of E, the shear strain, γ_{oct}, could be calculated for any given applied shear stress, τ_{oct}, using the pseudo shear modulus, G, $(= \frac{E}{2(1 + \nu)})$. For this value of γ_{oct}, the corresponding shear stress was obtained from the $\frac{\tau_{oct}}{(\sigma_{oct})_i}$ v. γ_{oct} experimental curve. A new Young's modulus was determined from $G = \frac{\tau_{oct}}{\gamma_{oct}}$ until satisfactory agreement between successive values was obtained.

The predicted plane strain behaviour of the sand mass agreed well with the experimental results at low porosity, but less well at high porosity.

The stress-strain relationships used were obtained from tests on triaxial compression specimens, for which $\sigma_1 > \sigma_2 = \sigma_3$ and the principal axes were fixed. Hence these relationships should only strictly be applied to deformations occurring under the same conditions.

In typical boundary value problems, such as the plane strain model tests described, the relative magnitude of the principal stresses and their orientation each vary throughout the mass, and the stress-deformational behaviour of soils is not independent of stress history. Therefore, although the use of empirical stress-strain relationships obtained from simple tests does allow complete solutions of these problems, the degree of extrapolation required is considerable.

In order to develop a generalised stress-strain relationship for soils, it is necessary to observe their behaviour over a wide range of applied stress paths. The conventional triaxial test is incapable of

imposing other than axially-symmetrical stress conditions and therefore its value is limited.

Behaviour of soils under pure hydrostatic stress has frequently been of secondary interest only, in tests where deformation was continued up to or beyond failure. Consequently, because the apparatus and the measuring systems were not specially designed for the small strains which usually occur under these conditions, errors were made both in observation and interpretation.

Investigation of the effect of the intermediate principal stress on stress-deformational behaviour involves many practical difficulties, and reliable results from tests under generalised principal stress conditions are few. (This subject will be discussed more fully in Chapters 3 and 4). Nevertheless, an acceptable constitutive relationship should incorporate the effect of all three principal stresses.

Studies of soil deformations under pure shear stresses, and the effect of the magnitude of σ_{oct} have been facilitated by the use of mechanical or pneumatic analogues of the octahedral plane in principal stress space. However, the mechanical properties of soils are, in general, dependent upon stress history and strain history, and therefore applied stress and strain paths should each be multifarious.

Plastic idealizations of soil behaviour are of many types, ranging from rigid-plastic, used widely in the solution of stability problems in soils engineering, to elastic-strain-hardening plastic.

The determination of the point at which "yielding" of a material, i.e. the onset of permanent plastic deformation or "flow", will occur under any applied stress system is of major importance. In the case of rigid-plastic idealizations it represents the "failure" condition, the material yielding indefinitely without change in the stress conditions.

Many studies of the failure condition have involved the testing of

many specimens, under a variety of stress states, and attempting to find an empirical failure criterion to fit the results. These will be discussed in a subsequent section.

The locus of all points at which the stresses satisfy the yield criterion forms a yield surface in principal stress space. Of many yield criteria which have been proposed, those due to Tresca and von Mises are commonly used to predict the yielding of metals. The former suggests that yield occurs when the maximum shear stress reaches a critical value k, i.e. when

$$(\sigma_1 - \sigma_3) = \pm 2k,$$

and therefore the yield surface takes the form of a regular hexagonal cylinder, coaxial with the space diagonal in stress space.

Von Mises' criterion defines the yield condition in terms of the octahedral shear stress, τ_{oct}, yield occurring when

$$[(\sigma_1 - \sigma_2)^2 + (\sigma_2 - \sigma_3)^2 + (\sigma_3 - \sigma_1)^2] = 2Y^2,$$

where Y is the yield stress determined from a simple tension test. The yield surface is a circular cylinder in principal stress space circumscribing Tresca's surface, for $2k = Y$.

Neither of the above criteria takes into account the effect on yielding of the octahedral normal stress, σ_{oct}, which for soils is highly significant. Consequently, modifications have been proposed which lead to the Extended Tresca and Extended von Mises yield criteria respectively:-

$$\frac{(\sigma_1 - \sigma_3)}{\sigma_{oct}} = a,$$

$$[(\sigma_1 - \sigma_2)^2 + (\sigma_2 - \sigma_3)^2 + (\sigma_3 - \sigma_1)^2]/[\sigma_{oct}]^2 = a,$$

where a is a constant. The corresponding yield surfaces are hexagonal and cylindrical cones, coaxial with the space diagonal, with their apexes at the origin. Right sections of these surfaces are, respectively, regular hexagons and circles, their size being directly proportional to their distances from the origin. The projections of the surfaces onto the $\sigma_1 - \sqrt{2}\sigma_3$ "triaxial stress plane" are shown in Fig. 2.3.

Under all stress states represented by a point within the space bounded by the chosen yield surface, the material either behaves elastically or is rigid. A point outside the yield surface is meaningless.

Both sands and clays strain considerably before failure. Therefore it is more realistic to idealize natural soils as strain-hardening plastic materials, the yield surface expanding, from that corresponding to the initial stress state at yield, as the stresses are increased. This concept of progressive yielding prior to failure is more likely to represent their real stress-deformational behaviour. Because the stress conditions necessary for yielding of soils depend on the octahedral normal stress and the porosity, the assumption that strain-hardening is isotropic would not be invalidated by the observation that yield strength varies if the stresses are re-ordered during a test.

If the three axes of principal strain space are aligned with the corresponding axes of principal stress space, then for an ideal plastic material, the plastic strain-increment vectors must be normal to the yield surface. The yield function f, in addition to defining the stress conditions required for yielding, also serves as the plastic potential function for flow, and the plastic strain-increments, $\delta^{p}{}_{ij}$, may be obtained by partial differentiation of f.

Therefore, $$\delta^{p}{}_{ij} = \lambda \frac{\partial f}{\partial \sigma_{ij}},$$

where λ depends on the work done in the strain increments, and hence determines their absolute magnitudes. However, for any point on the yield surface, their relative magnitudes are given by the associated-flow rule which obeys the normality condition.

The stability of a yielding plastic material under uniaxial stress conditions is denoted by a rising curve of stress against plastic strain, i.e. the net work done by a stress increment is positive. Under generalised stress conditions, where some stress components could increase

while others decrease, Drucker (1959) defined a stable work-hardening plastic material as one for which an external agency, applying and then removing a small stress, does a non-negative net quantity of work. It follows that stress-increment vectors must be directed outwards from the yield surface in order to produce stable hardening, and that the surface is convex. Since the yield function is also the plastic-potential function, any yield surfaces which have, or develop, corners give rise to ambiguities regarding plastic strain-increments.

It has been stated that the octahedral normal stress is likely to be significant in determining a yield function for soils. Mohr's theory of failure assumes that the shear and normal stresses on a failure plane are related by some function $\tau = f(\sigma)$, which may be represented as a curve, symmetrical about the σ-axis, in a τ v. σ plot. Only planes containing the major and minor principal stresses need be considered.

A special case of the Mohr theory occurs when the τ v. σ relationship is linear, giving the well-known Mohr-Coulomb failure criterion:-

$$\tau = c + \sigma \tan \phi.$$

In principal stress space, the failure surface has the form of an irregular hexagonal cone with its apex at the origin, (Fig. 2.3).

Early attempts to apply plasticity theory to soils used this failure surface as a yield function and therefore the associated flow rule gave excessive volumetric plastic strain-increments. Drucker et al (1957) used a series of hemispheres to represent successive yield surfaces in conventional triaxial compression tests. The strain-increments were determined assuming normality with yield loci projected onto the σ_1 v. $\sqrt{2}\,\sigma_3$ plane, the soil strain-hardening until failure was reached at the Mohr-Coulomb envelope.

Rendulic (1937) investigated the relationship between voids ratio and effective stress during drained and undrained triaxial compression

tests on saturated specimens of clay, consolidated under ambient stress. It was concluded that a unique function existed, and therefore that the change in voids ratio was independent of stress path. All tests were carried out under increasing stresses, and it was suggested that the findings would apply equally to anisotropically-consolidated specimens.

In developing Hvorslev's concept of a unique function connecting the shear and normal effective stresses and the voids ratio in a saturated remoulded cohesive soil at failure, Roscoe et al (1958) considered the progressive yielding of soils along drained and undrained triaxial compression loading paths in (p, e, q) space, where $p = (\sigma_1 + 2\sigma_3)/3$, and $q = (\sigma_1 - \sigma_3)$. To investigate whether loading paths ended at any specific point on the yield surface, should such a surface exist in this space, the concept of "critical voids ratio" which for drained tests implied continuous shear distortion at constant volume without change in the stress condition, was extended to include undrained tests.

The "C.V.R. line" in (p, e, q) space was defined as the unique line to which all loading paths converge, thus incorporating the effect of the octahedral normal stress on the ultimate state of the soil in undrained tests. To obtain the drained yield surface, an energy correction was applied to allow for the work done in changing the boundaries of the specimen.

The analysis of experimental results demonstrated that saturated remoulded clay did have a characteristic yield surface containing a C.V.R. line, and therefore the ultimate state of specimens tested from a known initial state, and under known drainage conditions, could be predicted.

Although reservations regarding the nature of the boundary energy correction were expressed, the coincidence of drained and undrained yield surfaces suggested that the resulting errors were small. It was pointed

out that any number of drained yield surfaces could be obtained depending upon the drainage conditions and the corrections, if any, that were applied, the only common feature being possibly the C.V.R. line, at which the boundary energy correction was zero.

The difficulties associated with interpreting the results from tests on heavily-overconsolidated specimens, which dilate during shear, were pointed out. Because localized shear deformations result in zones of weakness, in which subsequent deformations become concentrated, overall measurements grossly underestimate the strains in these zones, and hence also the boundary energy corrections.

These difficulties are even more relevant to shear tests on most cohesionless particulate materials. In addition, the rapidly decreasing pore-pressures associated with undrained testing may lead to the liberation of vapour from the pore-fluid of "saturated" specimens even before cavitation (Newland and Allely 1959). This effect, together with membrane penetration in tests on triaxial specimens, makes testing along truly undrained loading paths, and interpretation of measured quantities, very difficult. Similar arguments apply to tests carried out on such materials under drained conditions.

The analysis of triaxial compression tests, performed on various cohesionless materials by several workers, indicated the possibility of a yield surface, common to both drained and undrained loading paths.

Clearly, it was impossible to demonstrate the existence of a common C.V.R. line, since all drained specimens approached the undrained line from the "dry" side and consequently developed zones of localized shear deformation. However, specimens of 1 mm. dia. steel spheres were prepared, in random packing, for drained tests in the "simple shear apparatus" (3.3.2), which allowed the C.V.R. to be approached from the "wet" side. When plotted in (σ, e, τ) space the voids ratio of these specimens in their ultimate state agreed very closely with those of "dry"

specimens prepared over a range of initial density and sheared under the same normal stress. Similar tests at different values of σ confirmed the existence of a well-defined drained yield surface containing the C.V.R. line.

Natural sands and glass ballotini showed a greater scatter when tested in this apparatus, particle crushing and fracture affecting the results obtained using the former material.

. Many subsequent publications have described the development, at Cambridge, of these investigations into the suitability of the elastic-plastic isotropic continuum idealization for soils, and into the nature of their yielding. Several changes in terminology have been made, including the introduction of the "critical state" to avoid any ambiguity associated with the C.V.R. line.

Poorooshasb and Roscoe (1961) considered the problem of energy correction in more detail, and indicated that boundary energy correction alone was insufficient. It was suggested that the energy absorbed in shear distortion should be the basis of comparison of tests carried out under different drainage conditions . Since this could not be separated from that absorbed in consolidation, a further parameter was introduced which depended largely on the nature of specimen volume change.

For specimens which decreased in volume during shear, it was concluded that drained and undrained results could be directly correlated, whereas for dense cohesionless media, assumed to have little internal energy to assist dilatancy, the boundary energy correction only was necessary. Triaxial compression tests on normally-consolidated clay indicated common drained and undrained yield surfaces, and after applying the energy correction to the results of simple shear tests on steel spheres, a similar phenomenon was observed for various controlled conditions of partial drainage.

In developing a stress-strain relationship for normally consolidated saturated clays in triaxial compression tests, Roscoe and Poorooshasb (1963) attempted to determine the conditions under which water-content was a unique function of stress.

The family of yield curves for a soil generated a closed surface in (p, w, q) space which contained all permissible states of specimens, and was termed the "stable-state boundary surface". Using a two-dimensional method of representing yield surfaces in three-dimensional space, it was shown that, for this surface, water-content was a unique function of stress. State paths obtained from triaxial compression tests in which the axial stress was kept constant while the radial stress was reduced, were different from those obtained from the more conventional test. It was suggested that only the unique yield surface obtained from the latter was coincident with the state boundary surface, and therefore attention was confined to this type of test.

For an incremental change of state on this surface, it was assumed that the axial strain-increment was the sum of two components, a constant volume increment resulting from shear distortion and an anisotropic consolidation increment during which the stress ratio remained constant. Therefore the axial strain-increment for any change of stress could be determined, providing the deformational behaviour in these two types of test was known.

Using the volumetric strain, v, and the "axial distortion" shear strain, $\varepsilon = \varepsilon_1 - v/3$, as the strain parameters, the slope of the plastic strain-increment vector was shown to be given by:-

$$\frac{\delta\varepsilon^p}{\delta v^p} = \frac{1}{(1 - \frac{\delta v^+}{\delta v})}\left(\frac{\delta\varepsilon_1}{\delta v} - \frac{1}{3}\right),$$

assuming that the recoverable axial-distortion increment ε^+ was negligible. If the elastic component of volumetric strain was also ignored,

the vectors obtained from the results of a series of anisotropic consolidation tests could be used to construct a yield curve for the soil, assuming this was also the plastic potential function.

Roscoe et al (1963) derived a new-energy equation, by relating increments of recoverable elastic energy δU, per unit volume, to the slope, κ, of the isotropic swelling curve, e v. $\log_e p$. Energy dissipated during shear distortion, δW, was considered independent of the magnitude of volumetric strain and therefore given by $q\delta\varepsilon$, or $Mp\delta\varepsilon$, which was clearly so for the critical state when internal energy was constant. Since plastic volumetric strains involved structural change of the soil, the resulting dissipated energy was included in the term $Mp\delta\varepsilon$, so that the energy equation became:-

$$q\delta\varepsilon + p\delta v = \frac{\kappa\delta p}{1+e} + Mp\delta\varepsilon,$$

giving the corrected deviator stress in terms of a boundary energy and an elastic energy correction:-

$$q_w = Mp = q + p\frac{\delta v}{\delta\varepsilon} - \frac{\kappa}{1+e}\cdot\frac{\delta p}{\delta\varepsilon}.$$

However, for isotropic virgin-consolidation, the energy equations predicted plastic shear distortion in addition to plastic volume change:-

$$\frac{\delta\varepsilon}{\delta v} = \frac{(1 - \kappa/\lambda)}{M},$$

where λ is the slope of the virgin-consolidation curve, e v. $\log_e p$. This condition was associated with the point of the bullet-shape yield surface, and it was postulated that predicted plastic distortions were localized so that the overall distortion was zero.

Calladine (1963) suggested that a yield locus could be constructed for any point on a yield surface in (p, e, q) space, such that a normal vector would predict the ratio of plastic strain-increments. A vertical "elastic wall" was constructed using the isotropic (e v. p) swelling curve through the given point as a base. The projection of the top of

the elastic wall onto the q v. p plane was taken to be the appropriate current yield locus.

In an attempt to distinguish between stress changes which caused yielding and those resulting in elastic behaviour, Roscoe and Schofield (1963) considered unloading stress paths. It was concluded that yielding occurred for stress-increment vectors which, when projected onto the e v. $\log_e p$ plane, were directed below the isotropic swelling line through the point concerned. Other stress increments caused elastic volumetric strains only, these being determined by the slope of the swelling line.

Lewin and Burland (1970) carried out "stress-probe" experiments on a powdered slate dust in order to investigate the effect of both loading and unloading stress-increments on the specimen strains. The choice of this material was dictated by the need to minimize the effects of creep in tests on clays lasting several days.

The triaxial apparatus allowed close control of the applied stresses so that stress probes having any $\frac{\Delta\sigma_3}{\Delta\sigma_1}$ ratio could be directed from the basic stress state point in the σ_1 v. σ_3 plane. Four basic stress states were established between the isotropic consolidation line and the peak stress failure envelope, for specimens anisotropically-consolidated to the same octahedral normal stress, p. Eight different stress probes were applied to each set of specimens, their magnitude in each case being approximately 5% of the distance between the origin and the basic stress point.

The observed volume changes for increased loading probes were found to be in reasonable agreement with those predicted using Rendulic's concept of a unique yield surface, but the test results showed that increased anisotropy of the basic stress state caused a marked increase in volumetric strain.

Stress probes resulting in a stress decrease gave volume changes in general agreement with those predicted by Roscoe and Schofield (1963) based on the isotropic swelling curve.

An abrupt changeover from elastic to plastic behaviour was observed, which was dependent upon the direction of the stress-probe. Yield loci were constructed from the yield surfaces using the method suggested by Calladine, and hence, assuming normality of the plastic strain-increment vector, the ratio between the axial distortion shear strain-increment and the plastic volumetric strain-increment, $\Delta\varepsilon/\Delta v^p$, could be determined.

Knowing Δv^p, the values of $\Delta\varepsilon$ were calculated for the various stress-probes, and were found to compare well with those observed. However, there was a slight rotation of the plastic strain increment vector towards the direction of the stress-probe.

Burland (1969) presented a flow rule for the yielding of "wet" clays under constant stress ratio q/p in triaxial compression:-

$$\frac{\delta\varepsilon}{\delta v^p} = \frac{2q/p}{M^2 - (q/p)^2} ,$$

where M is the value of q/p at failure, and hence

$$M = \frac{6 \sin \phi}{3 - \sin \phi} .$$

In contrast to Roscoe et al (1963) this equation predicted $\delta\varepsilon = 0$ for virgin-consolidation, and at failure the volume change was zero.

Assuming that a unique relationship existed between voids ratio and effective stress, the volumetric strain increment resulting from small stress-increments was expressed in terms of the slopes of the isotropic consolidation and swelling curves, λ and κ. The corresponding total increment of shear strain during yielding was considered to consist of a component from compression under constant stress ratio, and a component resulting from change in this ratio, following Roscoe and Poorooshasb (1963). Since the recoverable volumetric strain was given

by $\delta v^+ = \frac{\kappa}{1+e}.\frac{\delta p}{p}$, the former component of $\delta\varepsilon$ could be obtained directly from the above flow rule. The latter component, being independent of δv^p, was assumed to be that obtained directly from an undrained triaxial test. Similar expressions were derived for plane strain by assuming that $\kappa = 0$, and replacing M with $M/\sqrt{3}$.

Plane strain tests on "wet" clay in the Cambridge biaxial apparatus (3.3.1) were reported by Hambly (1969). Both increasing and decreasing stress paths were investigated, following either one- or two-dimensional consolidation, and comparison between them was facilitated by dividing each principal stress by $(\sigma_1)_o$, the value of the major stress at the end of consolidation.

The ratio $\frac{\sigma_2}{\sigma_1 + \sigma_3}$ was found to vary by less than 10% from its magnitude at the end of consolidation, approximately 0.4, during subsequent stressing along various paths. The generalised stress-strain relationship of Roscoe and Burland (1968), which predicted

$$\frac{\sigma_2}{\sigma_1 + \sigma_3} = \frac{18 - M^2 + 9(\eta')^2}{4(M^2 + 9)} ,$$

where M is the value of q/p at failure in triaxial compression and $\eta' = \frac{\sigma_1 - \sigma_3}{\sigma_1 + \sigma_3}$, was shown to overestimate this ratio. In all other respects the theoretical and experimental stress paths were in close agreement.

The relationship between the major and minor principal stresses at failure in all types of plane strain test, and in conventional triaxial compression tests, was found to be unique, therefore favouring the Mohr-Coulomb failure criterion. However, the shear strength $(\sigma_1 - \sigma_3)_f$, at any given voids ratio, was dependent upon the stress path. Tests involving reduction of stress, and hence reorientation of the principal stresses, resulted in significantly lower strengths when change in voids ratio to failure was small.

The observed principal strains were compared with those predicted

by the theories of Roscoe and Schofield (1963), and Roscoe and Burland (1968). Better agreement was obtained, however, for both increasing and decreasing stress, using a revision of the latter authors' theory in which the predicted strain-increments were increased by adding the magnitudes of strain-increments observed in undrained tests for the same change in η'.

In summarising the basic principles underlying the critical state concept and the treatment of soils as isotropic continuous media, Schofield and Wroth (1968) introduced the rigid-plastic Granta-gravel model as a fore-runner of the more sophisticated elastic-plastic Cam-clay model.

It was pointed out, however, that comparison between Granta-gravel and real cohesionless soils, tested under normal laboratory conditions, was unlikely to be satisfactory. These specimens were always initially denser than critical, and therefore measured strains were rarely reliable because of the development of weak zones during shear distortion. In addition, peak stress was reached in the Granta-gravel model while it remained rigid.

Clearly the practical difficulties associated with verification of a plastic idealization for cohesionless soils are great.

Roscoe (1967) reported tests on coarse sand by Cole in the Mk.6 simple shear apparatus, in which γ-rays were used to measure the local voids ratio in the dilating zone. The local change was found to exceed the average value, based on overall measurements, by as much as 60% at large strains. Up to peak stress ratio, the difference was not so great.

Tests on specimens prepared at widely differing densities showed that they all reached the same local voids ratio at the critical state, if subjected to equal normal stress. However, assuming uniform shear

distortion, the changes in overall average voids ratio were found to be in agreement with Rowe's stress-dilatancy equation (2.2).

Poorooshasb et al (1966) performed triaxial tests on sands with different stress paths passing through a common point. The direction of the plastic strain-increment vector was found to be independent of the direction of the stress-increment vector, and therefore it was possible to obtain expressions for a family of plastic potentials. However, these were shown to be different from the family of yield loci, and therefore indicated that normality did not apply for sands.

The stress-dilatancy theory for the behaviour of particulate material (2.2), which applies strictly to plastic strains, was used by Barden and Khayatt (1966) to determine a family of plastic potentials in the triaxial stress plane.

For stress paths involving increasing values of R, $(= \frac{\sigma_1}{\sigma_3})$, the basic stress-dilatancy equation, R = DK, had been verified experimentally and therefore, when plotted in the conventional triaxial stress plane, gave the simple plastic strain rate function:-

$$\frac{-\sqrt{2}\,\delta\varepsilon_3}{\delta\varepsilon_1} = \frac{\sigma_1}{\sqrt{2}\,\sigma_3} \cdot \frac{1}{K} ,$$

where K varied between the limits $K_\mu < K < K_{cv}$. Therefore the plastic potential function became:-

$$f = \frac{\sigma_1^K}{\sqrt{2}\sigma_3} ,$$

and by assuming K to be constant, a family of plastic potentials could be drawn which were compatible with the observed strain rates in triaxial compression. However, since the above equation was unlikely to be that appertaining to the family of yield loci, the conclusions regarding normality were in agreement with those of Poorooshasb et al.

The corresponding stress-dilatancy equation and plastic potential function for plane strain (Barden et al 1969) were:-

$$\frac{-\delta\varepsilon_3}{\delta\varepsilon_1} = \frac{\sigma_1}{\sigma_3} \cdot \frac{1}{K} \text{ , and } f = \frac{\sigma_1 K}{\sigma_3} .$$

Since it had been shown that $K \rightarrow K_{cv}$ throughout deformation in plane strain for all initial porosities, the same family of plastic potential curves was applicable to all specimens.

Dense specimens of sand were consolidated at zero lateral strain and then subjected to increasing and decreasing stress paths in plane strain, in which previous maximum values of R were exceeded. Marked changes occurred in both volumetric and shear strains, the former changing sign, when the previous maximum value was reached during reloading. However, difficulties of defining the exact point of yield and complications associated with particle crushing for large increases in octahedral normal stress, meant that the previous maximum R could only be regarded as a first approximation to the yield criterion. Nevertheless, the plastic potential function would be identical with this criterion only for K = 1, which would give $\phi_f = 0$, indicating that normality did not apply.

It was pointed out that sudden rotation of the principal stresses would also be likely to affect yielding.

Whether soils in general, and cohesionless soils in particular, could be justifiably idealized as isotropic strain-hardening plastic materials was investigated by Roscoe et al (1967). A coarse uniform sand was tested in the Mk.6 simple shear apparatus (3.3.2), which allowed the principal axes of stress and strain, and also of their increments, to be determined. Each rotates during a test in simple shear.

It was assumed that in the central one-third of the specimen the stresses and strains were uniform. The average stresses on the horizontal boundaries of this element were determined directly from load-cell measurements, and those on the initially vertical boundaries were calculated by considering the equilibrium of the two outer-thirds of

the specimen. Strains were obtained directly from the observed displacements during any increment of shear strain.

The inclinations to the horizontal of the major principal planes of stress, stress-increment and strain-increment were plotted against shear strain, and close agreement between those of stress- and strain-increment was apparent for both loose and dense specimens, especially for strains between minimum voids ratio and peak stress ratio. Only for very small initial strains did the axes of principal stress-increment and strain-increment coincide, showing elasticity theories to be generally inapplicable. At the critical state, the intermediate principal stress was found to approximate to the mean of the major and minor principal stresses, again suggesting that the plastic idealization was reasonable.

The common assumption that the horizontal plane is the plane of $(\tau/\sigma)_{max}$ was shown to be totally invalid, and τ_{max} was horizontal only for tests on loose specimens.

Wroth and Bassett (1965) used an empirical mathematical function, based on the critical state concept, to represent the observed shearing behaviour of cohesionless soils tested under various controlled drainage conditions in simple shear.

Using an energy equation similar to that of Roscoe et al (1963) and the parameter $\alpha = \Delta e/\Delta \log \sigma$ to denote the degree of volume change, the progress along any α-path towards the critical state was expressed as an exponential function of the shear strain z. At any stage of deformation, the ratio of the remaining length of the test path, in the e v. log σ plane, to its total length from initial condition to critical state, was given by the ratio χ/χ_o, where

$$\chi/\chi_o = (1 + bz) \exp(-az).$$

The constants a and b for any test were functions of the initial con-

ditions, e_o and σ_o, and α. Since χ/χ_o could be expressed in terms of the conditions at the critical state and the geometry of the critical state line in the e v. log σ plane, τ, σ and e could be uniquely related with z for all stages of a test, providing the soil constants λ, k and M were known, together with the specific test conditions. The constant a was assumed to be the same for all tests, and therefore b could be determined from the initial conditions of any given test. For drained tests, the unique relationship was shown to be given by:-

$$\frac{\tau}{\sigma} = M + \frac{a}{2}(\Gamma - \lambda \log \sigma + e) \quad ,$$

where Γ is voids ratio at the critical state under unit normal stress σ.

Tests were carried out in the simple shear apparatus on 1 mm. steel spheres and coarse sand, in order to investigate the proposed relationships for a variety of α-paths. The measured ratio of τ/σ, $(=\tan\phi)$, was found to vary from its assumed constant value of M, i.e. at the critical state, particularly during the early stages of a test.

Although there was a noticeable difference between the predicted τ/σ v. z curves and those obtained, the agreement being less for the tests on sand, the general shape of the curves was similar and it concluded therefore that exponential functions were applicable to the stress-deformational behaviour of cohesionless soils.

In dealing with the behaviour of soils in generalised stress or strain states, it is frequently convenient to use the following invariants:-

octahedral normal stress,

$$\sigma_{oct} = (\sigma_1 + \sigma_2 + \sigma_3)/3;$$

octahedral shear stress,

$$\tau_{oct} = \sqrt{[(\sigma_1 - \sigma_2)^2 + (\sigma_2 - \sigma_3)^2 + (\sigma_3 - \sigma_1)^2]}/3 \; ;$$

octahedral normal strain,

$$\varepsilon_{oct} = (\varepsilon_1 + \varepsilon_2 + \varepsilon_3)/3 = \varepsilon_v/3 \ ;$$

octahedral shear strain,

$$\gamma_{oct} = 2\sqrt{[(\varepsilon_1 - \varepsilon_2)^2 + (\varepsilon_2 - \varepsilon_3)^2 + (\varepsilon_3 - \varepsilon_1)^2]}/3 \ .$$

2.4 MACROSCOPIC STUDIES

Numerous investigations have been carried out on soils, particularly cohesionless soils, in order to determine the conditions under which they "fail", and to attempt to fit the observed behaviour to established failure criteria or suitable amendments thereof.

The generally accepted meaning of "failure" as applied to soils is the condition corresponding to peak strength, either in terms of maximum effective stress ratio or maximum deviator stress; the former will be used throughout this discussion.

Three of the more common criteria for cohesionless soils, the Mohr-Coulomb, Extended Tresca and Extended von Mises, were presented in the previous section. It is usually convenient to represent these failure surfaces in three dimensional principal stress space, in which the space diagonal, or "hydrostatic axis" is equally inclined at $\cos^{-1}(1/\sqrt{3})$ to each principal axis, (Fig. 2.3). A further useful representation for the purposes of comparison, is the "right section", taken perpendicular to the hydrostatic axes. The equation of any such plane is $(\sigma_1 + \sigma_2 + \sigma_3) = k$, and stress paths lying wholly within the plane represent changes in deviatoric stresses only.

Normally, investigations in soil mechanics are restricted to compressive stress space, and therefore only one set of "octahedral planes" is necessary to represent the failure condition. Various failure criteria are shown in the octahedral plane of Fig. 2.4. Any point in the plane is defined by the cylindrical coordinates:-

$$\tan\theta = \frac{\sqrt{3}(\sigma_2 - \sigma_3)}{2\sigma_1 - \sigma_2 - \sigma_3}\ , \text{ and}$$

$$\tau_\theta = \frac{1}{\sqrt{3}}\left[(\sigma_1 - \sigma_2)^2 + (\sigma_2 - \sigma_3)^2 + (\sigma_3 - \sigma_1)^2\right]^{1/2}.$$

One of the more controversial aspects of soil strength studies is the influence of the intermediate principal stress, σ_2, on the failure

condition, as it varies between σ_1, the triaxial extension stress state, and σ_3, the triaxial compression stress state. Several methods have been used to express its magnitude relative to the other principal stresses, including Lode's parameter

$$\mu = \frac{2\sigma_2 - \sigma_1 - \sigma_3}{\sigma_1 - \sigma_3} ,$$

and that proposed by Bishop (1966):-

$$b = \frac{\sigma_2 - \sigma_3}{\sigma_1 - \sigma_3} .$$

The value of μ varies from -1 to +1 over the full compression to extension range, whereas b varies from 0 to +1. The latter parameter will be used throughout the remainder of this discussion.

The Mohr-Coulomb and Extended Tresca and von Mises criteria each depict a failure surface in principal stress space which expands linearly with the hydrostatic stress. Bishop (1966) has shown that for the range of stresses normally of engineering interest, this is probably a close approximation. The conclusion was based on the results of triaxial compression tests, performed using a wide range of confining pressures.

At pressures above about 100 lbf/in^2, the failure envelope in triaxial compression was shown to curve concavely towards the hydrostatic axis. The major factor causing this variation is the crushing and fracture of particles, which is particularly severe at high pressures. Although it has been reported (e.g. Rowe 1962) that the interparticle friction angle, ϕ_μ, decreases with load per particle, it would appear that this effect is largely compensated by the increasing number of contacts.

It is not implied, however, that crushing is absent at much lower pressures, and several workers have demonstrated that the grading curves of cohesionless soils, determined before and after tests carried out

within the pressure range of conventional laboratory apparatus, were significantly different. However, for cell pressures less than 50 lbf/in^2 it has consistently been shown (Barden and Khayatt 1967) that the effect of particle crushing on stress-deformational behaviour, represented as curves of stress ratio against both axial and volumetric strains, is negligible.

The predominant effect of higher stress levels on the behaviour of sands is to suppress dilatancy, especially that of dense specimens, so that at pressures in excess of about 1000 lbf/in^2 the dilatancy rates at failure, and hence the failure envelopes, of loose and dense specimens converge.

Although the majority of studies concerning the effect of stress level have been confined to triaxial compression, Barden et al (1969) and Lee (1970) have observed the same effect in plane strain tests. However, it has been frequently demonstrated, e.g. Cornforth (1961), Wightman (1967), Finn et al (1967), that the volumetric and axial strains at failure in plane strain are usually much smaller than those in the axially-symmetrical test, the difference increasing with decrease in initial porosity. Consequently, the "critical voids ratio", at which no overall change in volume is observed between the end of consolidation and the attainment of peak stress ratio, is less for specimens tested in plane strain.

In reviewing the use of the more common failure criteria, Bishop (1966) demonstrated that, for the majority of cohesionless soils, the Extended von Mises and Extended Tresca criteria are unacceptable from both practical and theoretical standpoints.

For values of ϕ in triaxial compression of 36.9°, each criterion predicts a strength in triaxial extension equivalent to $\phi = 90°$. For greater triaxial compression strengths, which are very common for

cohesionless soils, surfaces representing the Tresca and von Mises failure condition encroach into negative stress space, which for cohesionless soils is meaningless.

Therefore, accepting the Mohr-Coulomb criterion as sensibly representing the strength of sand in both triaxial compression and extension, Bishop used an empirical factor K_2, determined from a plane strain test, to allow for the increase in strength frequently observed for values of b:-

$$\frac{\sigma_1 - \sigma_3}{\sigma_1 + \sigma_3} = \frac{\sin \phi}{1 - K_2\sqrt{(b(1 - b))}} ,$$

where sin ϕ is determined from either triaxial compression or triaxial extension tests.

Sutherland and Mesdary (1969) have since found that this expression, of several empirical formulae tried, gave the best agreement with their results from tests on sand under generalised stress conditions. The parameter K_2 was found to be a linear function of the initial porosity, given by $K_2 = 0.425 - 0.605n_i$. However, this form of failure criterion is only one of the many proposed to represent the stress conditions at failure for soils. It will be worthwhile at this stage to discuss some of the experimental data upon which these criteria are based.

Many investigators have attempted to determine the strength of both cohesive and cohesionless soils over a wide range of applied stress conditions, by carrying out laboratory stress-deformation tests in other than the conventional triaxial compression apparatus. The majority have been concerned either with the plane strain or triaxial extension stress conditions, but several have tried to impose more generalised stresses, allowing the magnitude of the intermediate principal stress to be varied independently. The apparatuses used will be discussed fully in Chapter 3; for the present, the results of these investigations will be of

primary interest.

Table 2.1 summarizes some of the more important findings, using the peak strength ϕ, as defined by the Mohr-Coulomb criterion, in cylindrical triaxial compression as the basis for comparison. Unless otherwise stated in the accompanying notes, the maximum principal effective stress ratio has been used to define both the point of failure and the magnitude of ϕ. The increase or decrease in ϕ is shown as positive or negative with respect to triaxial compression, and the parameter b, $(= \frac{\sigma_2 - \sigma_3}{\sigma_1 - \sigma_3})$, describes the relative magnitude of the intermediate principal stress.

The type of apparatus used in the various investigations is listed in the table, together with a reference to the appropriate section in Chapter 3, in which a fuller description is given. The following abbreviations have been used:-

Cyl TE - cylindrical triaxial extension;

Cub PS - cuboidal plane strain;

Cub 3-d - cuboidal "three-dimensional" apparatus (i.e. three independent principal stresses);

H'w Cyl - hollow cylinder;

Tri-SBox - "triaxial shear box".

All strengths have been quoted to the nearest $\frac{1}{2}^\circ$ in ϕ, even though, in a few investigations, a greater accuracy may have been claimed.

TABLE 2.1

	NAME OF INVESTIGATORS	SOIL TESTED	TRIAXIAL EXT'SION	PLANE STRAIN	INTER-b TESTS	APPA'TUS USED
(1)	Barden & Khayatt (1966)	sand	= TC			Cyl TE (3.3.1)
(2)	Barden et al (1969)	sand		+3°→ +4°		Cub PS (3.3.1)
(3)	Bell (1965)	sand	+12°		+12°	Cub 3-d (3.3.1)
(4)	Bishop & Eldin (1953)	sand	= TC			Cyl TE
(5)	Bjerrum Kummeneje (1961)	sand		+3°→ +4°		Cub PS (3.3.1)
(6)	Broms & Casbarian (1965)	rem'l'd clay	+7°		+7°	H'w CyL (3.3.3)
(7)	Cornforth (1961)	sand	= TC	$+\frac{1}{2}°$→ +4°		Cub PS (3.3.1)
(8)	Daniel (1957)	sand			>> TC	Cub 3-d (3.3.1)
(9)	Duncan & Seed (1966)	undis'd clay		$+3\frac{1}{2}°$		Cub PS (3.3.1)
(10)	Esrig & Bemben (1965)	sand	0°→ +2°,+5°		+5°	Solid & H'w Cyls
(11)	Finn & Mittal (1963)	compact clay		+2°→ +4°		Cub PS
(12)	Green (1969)	sand	+2°, +5°		+5°	Cub TE Cub 3-d (3.3.1)
(13)	Habib (1953)	sand	-7°		+4°→ -7°	Torsion (3.3.2)
(14)	Hambly (1969)	"wet" clay		= TC		Cub PS (3.3.1)
(15)	Haythornthwaite (1960)	crushed quartz	< TC			Cyl TE
(16)	Henkel & Wade (1966)	satur'd clay		+1°		Cub PS (3.3.1)

Table 2.1 (cont'd)

	Investigators	Soil	Triaxial Ext'sion	Plane Strain	Inter-b	Appa'tus
(17)	Jakobson (1957)	sand	> TC			Cub 3-d (3.3.1)
(18)	Kirkpatrick (1957)	sand	= TC		+2°	Solid & H'w Cyls (3.3.3)
(19)	Kjellman (1936)	sand			+8°	Cub 3-d (3.3.1)
(20)	Ko & Scott (1967)	sand	+4°→ +6°		+5°→ +6°	Cub 3-d (3.3.1)
(21)	Lee (1970)	sand		+6°→ +8°		Cub PS (3.3.1)
(22)	Lence (1966)	sand			+8°	Cub 3-d (3.3.3)
(23)	Leussink & Wittke (1963)	glass spheres		+2°→ +13°		Cub PS (3.3.1)
(24)	Lomize & Kryzanovsky (1967)	sand	+9°,+21°		+12°, +22°	Cub 3-d (3.3.1)
(25)	Lomize et al (1969)	various soils	> TC		> TC	Cub 3-d (3.3.1)
(26)	Lorenz et al (1965)			no con-clusion		Cub PS (3.3.1)
(27)	Marsal (1965)	rock-fill		+13°		Cub PS (3.3.1)
(28)	Peltier (1957)	sand	$-6\frac{1}{2}°$→ -9°		-11°	Cyl TE Tri-SBox (3.3.2)
(29)	Procter (1967)	sand	0°→ +2°	+7°→ $+9\frac{1}{2}°$	+13 °	H'w Cyl (3.3.3)
(30)	Roscoe et al (1963)	sand	no con-clusion			Cyl TE (3.3.1)
(31)	Shibata Karube (1965)	rem'l'd clay	= TC		+2° → 4°	Cub 3-d (3.3.1)
(32)	Shibata Karube (1967)	satur'd clay		+4°→ +9°		Cub 3-d (3.3.1)

Table 2.1 (cont'd)

Investigators		Soil	Triaxial Ext'sion	Plane Strain	Inter-b	Appa'tus
(33)	Sultan & Seed (1967)	sand		$+\frac{1}{2}^{o} \rightarrow +3\frac{1}{2}^{o}$		Cub PS (3.3.1)
(34)	Sutherland & Mesdary (1969)	sand	= TC		$+3^{o} \rightarrow +5\frac{1}{2}^{o}$	Cub 3-d (3.3.1)
(35)	Whitman & Luscher (1962)	sand		$+6^{o}$		H.Cyl PS (3.3.3)
(36)	Wightman (1967)	sand & glass spheres		$+4^{o} \rightarrow +5^{o}$		Cub PS (3.3.1)
(37)	Wood (1958)	grav'ly silty sand		$+2^{o}$		Cub PS (3.3.1)
(38)	Wu et al (1963)	sand & rem'l'd clay	= TC		$+5^{o}$	Solid & H'w Cyls (3.3.3)

(1) By using specimens with length to diameter ratios of 1 : 1 and adequate end lubrication, deformations in both triaxial compression and extension tests were shown to be more uniform than is usually the case. Providing it was arranged for the mean principal stress at failure to be the same in both tests, the "short" specimens showed equal strengths. The strengths of "long" (2 : 1) triaxial extension specimens were equal with this value only if the cross-sectional area of the "necked" zone was measured and used in stress computations.

(2) Drained plane strain tests were carried out on specimens of different sands and bronze spheres at several initial porosities in order to investigate the validity of the stress-dilatancy theory under these conditions. Assuming that the R. Welland sand was very similar to that used by Wightman (1967), it would appear that the peak strengths obtained from plane strain tests under conventional cell pressures exceeded those from triaxial tests by between 3° and 4°, the lower value corresponding to lower initial densities. At a cell pressure of 850 lbf/in^2, a decrease of 10° in ϕ below the previous value in plane strain was observed. No comparison with triaxial tests at this stress level was reported.

(3) Despite the unusual proportions of the specimen dimensions, reasonable agreement was obtained with the conventional triaxial test for the b = 0 condition. An increase in ϕ of up to 12° occurred as b was raised to about its plane strain value, and this strength was maintained for all other intermediate principal stress magnitudes, including that corresponding to triaxial extension.

(4) Triaxial extension tests were performed either by increasing the cell pressure with the axial stress constant, or by decreasing the axial stress at constant cell pressure. Corrections were applied to allow for the effects of necking at large strains. The results were widely scattered but the measured strengths were in general agreement with triaxial compression values.

(5) For both loose and dense specimens, an increase in ϕ of between 3° and 4° was obtained in plane strain using a fixed top platten. When this was replaced by a ball-bearing seating, which allowed the platten to tilt, the observed difference was reduced by about 1°.

(6) In a series of undrained hollow cylinder tests, without applied torque, in which the average radial stress was taken to be the intermediate principal stress, an increase of 5° in ϕ was observed as b increased for 0 to 0.25. Maximum strength occurred under triaxial extension stress conditions.

(7) Peak and ultimate strengths of cylindrical triaxial compression and extension tests were similar for all initial porosities for specimens having the same value of σ_{oct} at failure, after being consolidated under ambient stress. The plane strain specimens exhibited a strength increase approximately in proportion to their initial relative density. It was assumed that the manner of consolidation had no effect on strength, and in the ultimate condition, at large strains, the values of ϕ in triaxial compression and plane strain were found to be equal. However, significant non-uniformities of deformation had taken place before this condition was reached. Although the overall volume changes in plane

strain tests were smaller, the maximum dilatancy rates, occurring approximately at peak stress ratio, were similar.

(8) Under triaxial compression conditions, strengths were obtained which were in agreement with conventional cylindrical tests on the same dry sand. At greater values of b, excessive strengths were recorded, almost certainly due to apparatus interference.

(9) The undrained failure of a clay slope was simulated by carrying out "vertical" and "horizontal" plane strain tests on undisturbed specimens consolidated, under K_o conditions, to pressures in excess of those appertaining to the field condition. In the former tests, a strength increase of $3\frac{1}{2}°$ was observed, whereas in the "horizontal" tests, which involved a 90° rotation of the principal stresses following consolidation, the increase was only $\frac{1}{2}°$. The comparisons were made with respect to the strength of undrained triaxial specimens in terms of effective stress, the cohesion intercept being negligible.

(10) Tests on solid cylinders showed increased values of ϕ in triaxial extension, ranging from +5° for dense specimens to zero for loose. Although the hollow cylinder tests showed a similar trend, the maximum extension increase being +2°, the strengths observed in both compression and extension were different from those for the solid specimens. Tests over a range of b values showed that the maximum ϕ occurred at plane strain, and for a relative porosity of about 0.7 the increase above triaxial compression strength was 5°.

(11) Cuboidal and cylindrical triaxial compression tests, in addition to plane strain tests, were carried out at constant σ_3 values of

30, 60 and 75 lbf/in². All were undrained with pore-pressure measurement. Since the lowest cell pressure gave rise to a cohesion intercept these results were not reported. The maximum difference in ϕ was observed for the highest cell pressure. However, the design of the apparatus did not allow plane strain conditions to be imposed until axial strains of about 2% had occurred, failure being reached at about 10%. In each case the strength of the cuboidal specimen apparently slightly exceeded that of the cylindrical specimen in triaxial compression.

(12) All triaxial compression tests gave the same strengths, irrespective of specimen shape. Cylindrical and cuboidal triaxial extensions tests showed increases in ϕ of 2° and 5° respectively. Tests on cuboidal specimens of thesame density in the "independent stress control apparatus" verified the compression and extension strengths, and showed that ϕ increased steadily until the value of b appertaining to plane strain was reached, from which point no further change was observed.

(13) By applying torsion to "dumb-bell" shaped sand cylinders the value of σ_2 was varied, a maximum strength, up to about 4° in excess of triaxial compression strength, occurring for values of b generally between 0 and 0.5. Considerable necking was apparent in the triaxial extension tests.

(14) Using peak deviator stress $(\sigma_1 - \sigma_3)_{max}$ as the point of failure, a comparison was made between the peak stress ratios in plane strain tests involving stress increase after either one- or two-dimensional consolidation, and stress decrease following one-dimensional consolidation. The points were found to lie on a unique curve, common to that obtained for specimens in conventional triaxial

compression.

(15) Triaxial extension tests on "long" specimens of crushed quartz indicated strengths considerably less than that in triaxial compression. However, specimen necking was considerable, and the definition of failure was different from that used by other investigators.

(16) K_o-consolidation was used in both plane strain and cylindrical triaxial compression tests, and the pore-pressure was measured during the subsequent undrained shearing stage. In terms of effective stress, at the maximum deviator stress an increase in ϕ of approximately 1° was observed for plane strain. A similar difference was obtained using peak effective stress ratio as the definition of failure. The undrained strength in plane strain was also shown to be greater, by about 8%, for specimens consolidated to the same major principal stress.

(17) The limitations of strain did not allow peak stress ratios to be reached under either triaxial compression or extension conditions. However, it was clear that the influence of the intermediate principal stress was significant.

(18) Similar triaxial extension and compression strengths resulted from solid cylinder tests. The axial stress was always the intermediate principal stress during the hollow cylinder tests, and its magnitude was approximately equal to the mean of the other two. Based on a linear distribution of radial stress through the specimen wall a strength slightly in excess of that for triaxial compression was obtained for a b value of about 0.5. Using this as confirmation of the Mohr-Coulomb criterion, ϕ at the inner and outer surfaces

was determined, corresponding to 0.35 and 0.65 values of b. At each point, the increase was about 2°.

(19) Equal strengths, $\phi = 43°$, were obtained in the cubical apparatus for b values of 0.38 and 0.50, compared with $\phi = 35°$ under triaxial compression stress conditions.

(20) Peak stress ratios were not obtained during tests in this apparatus, and therefore failure was defined in terms of the rate of increase of volumetric deformation with respect to octahedral normal stress. The equivalent values of ϕ at these "failure" points increased as σ_2 was varied between the triaxial compression and plane strain conditions, the differences being +5° and +6° respectively for loose and dense specimens. The strength of loose specimens then increased by a further 1° as b was increased to its maximum value at triaxial extension, whereas for the dense specimens ϕ decreased by 2° over the corresponding range.

(21) Imposed plane strain deformation caused the maximum strength increase for dense specimens at low stress levels, whereas the lower limit of +6° was associated with loose specimens and also with denser specimens at higher stress levels. In some tests, the mean principal stress at failure was in excess of 250 lbf/in^2.

(22) Because of the limitations of the method used to apply the intermediate principal stress, the maximum attainable value of b was 0.1, corresponding to a maximum lateral deviator stress, $(\sigma_2 - \sigma_3)$, of 3 lbf/in^2. The major principal stress at failure was calculated using the initial dimensions of the specimen.

(23) Plane strain and triaxial compression tests were performed on regular

hexagonal and quadratic packings of glass spheres (2.2). In plane strain a minimum increase in strength of about 2° was observed for low density quadratic arrangements, while dense hexagonal packings showed the maximum increase, giving strengths up to 13° in excess of the corresponding triaxial compression value.

(24) Each of the two sands tested were found to have a triaxial compression strength of $\phi = 36°$, in the three-dimensional apparatus. As b was increased, maximum strengths of 48° and 58° respectively were reached at corresponding b values of 0.7 and 0.9. Each then reduced slightly as the triaxial extension stress condition was approached. Almost certainly, interference from the apparatus was largely responsible for these peculiar results. Even the von Mises criterion underestimated these strengths.

(25) In a similar, but apparently modified apparatus, tests on a variety of soils showed comparable trends, a typical undisturbed clay reaching its maximum strength at approximately b = 0.6, which then reduced slightly to the triaxial extension value.

(26) No failure was observed in plane strain, even at major principal strains in excess of 7%, and apparently no comparison was made with stress-strain curves from conventional triaxial compression tests.

(27) Two gradings of rockfill were tested at a relative density of about 0.9, and grain crushing was considerable.

(28) On average, strengths in triaxial extension tests on solid cylindrical specimens were found to be about 7° lower than those in compression. Tests in the "triaxial shear box", in which the

intermediate principal stress could be varied, showed a complete reversal of this trend, the equivalent "extension" ϕ being up to 11° greater than the equivalent "compression" ϕ. In addition to the usual non-uniformity of strain associated with direct single shear tests, the stress distribution was unknown, and likely to have been extremely variable, rendering the results practically useless. However, the results from the former tests were shown to be in good agreement with those of Habib (1953).

(29) The strengths of thin-walled hollow cylinders of dense sand were found to be similar for stress conditions corresponding to triaxial compression and extension, whereas in plane strain ϕ had increased by $9\frac{1}{2}$°. A further increase of 1° was observed for an intermediate value of b. The thick-walled hollow cylinders, having the same triaxial compression strength, showed increases in ϕ of 2° and 7° respectively for triaxial extension and plane strain. Plane strain strengths exceeded those obtained by Wightman (1967) on specimens of the same soil.

(30) Conventional $1\frac{1}{2}$ in. dia. "long" triaxial specimens were tested in both extension and compression. Calculation of the stresses at failure on the assumption that deformations were uniform, showed that strengths in these two stress conditions were approximately equal. If, however, the local minimum cross-sectional area was measured in triaxial extension tests, a substantial increase in the calculated magnitude of ϕ was obtained. Depending upon the local voids ratio, the increase could have been greater than 10° above the corresponding compression strength. Because of the uncertainties regarding measured quantities, overall judgement was reserved.

(31) Consolidated-undrained tests with pore-pressure measurement on cuboidal specimens showed that the peak deviator stress was similar in triaxial compression and extension tests, but increased above this value for intermediate values of b. The maximum increase in ϕ appeared to be between 2° and 4°, depending upon the cell pressure, and occurred when b was approximately 0.6.

(32) Because of the unknown effect of specimen size and shape, plane strain and triaxial compression tests were performed on the same type of cuboidal specimen. Both ambient and K_o-consolidation were used and all tests were completed in the undrained manner with pore-pressure measurement. At failure, defined as the maximum principal stress difference, tne strengths of the plane strain specimens were greater by between 4° and 9° in the value of ϕ, depending upon the mean principal effective stress at failure.

(33) Two sands were tested in vacuum plane strain and triaxial compression apparatuses. Increases in ϕ of from $\frac{1}{2}$° to $3\frac{1}{2}$° and from 1° to 3° respectively were observed in plane strain, the densest specimens showing the greatest difference.

(34) Identical strengths were obtained in preliminary cylindrical and cubical triaxial compression. In the three-dimensional apparatus, in both triaxial extension and compression, very similar ϕ values were obtained for comparable initial porosities. As b increased from 0 to 1, strength increased rapidly at first, reaching a maximum at about b = 0.4, and then decreased to its original value. The maximum strength increase was greatest for the densest specimens.

(35) With the tangential stress as the major principal stress, the

increased strength in plane strain was found to be constant for all initial porosities.

(36) Over the whole range of initial porosities tested, the strength of R. Welland sand, the behaviour of which was typical of the other materials tested, was between 4° and 5° greater in plane strain than in triaxial compression. It was anticipated that specimens prepared close to their maximum porosity would have the same strength in these two types of test.

(37) Following K_o-consolidation, specimens of well-graded gravelly-silty-sand were tested under undrained plane strain conditions, and the pore-pressure was measured. Using $(\sigma_1 - \sigma_3)_{max}$ to define the point of failure, both shear strength parameters, in terms of effective stresses, showed an increase above their corresponding magnitudes in undrained triaxial compression, ϕ having increased from 35.1° to 36.9° and the cohesion intercept from 0.2 to 1.9 lbf/in^2.

(38) Tests on both remoulded clay and sand were performed under undrained conditions with pore-pressure measurement. Solid cylinders gave equal strengths in triaxial compression and extension for each soil, and hollow cylinders tested under the triaxial compression stress state showed good agreement. An increase in ϕ of up to 5° was observed for hollow sand cylinders, when b was varied, the majority of test points falling in the range of b from 0 to 0.5.

The majority of results from the investigations covered in Table 2.1 and the accompanying notes must, for various reasons which will have to be discussed more fully in subsequent chapters, be ignored when attempting to "fit" a suitable failure criterion to observed soil behaviour.

Interpretation of the results of hollow cylinder tests, for instance, depends largely on the chosen assumption regarding the manner in which stresses are distributed through the wall thickness (3.3.3). However, the effect of stress non-uniformity on the deformational behaviour of the soil is likely to be considerable, and this must be one of the major reasons for the wide variety of strengths reported. Procter's tests on hollow cylinders of two different thicknesses emphasize the uncertainties; although similar trends were apparent for each (nearly all investigators report strength increases as b varies), discrepancies of several degrees in ϕ occurred.

Clearly, categorical statements regarding strength differences observed in different apparatuses can be made only if the soil specimens tested have very similar properties. However, because of the large quantity of data available from tests on loose and dense sands in both triaxial extension and plane strain, it is possible to dismiss certain procedures as unsuitable.

The calculated strengths from triaxial extension tests depend to a large extent on the assumed mode of deformation. This is particularly so for "long" specimens which usually neck at strains much less than those at the peak stress ratio. The results of tests reported by Roscoe et al showed that considerably higher strengths could be computed from measurements of local cross-sectional areas, when compared with those based on the overall average strains. However, even for long specimens, the illustration of non-uniform deformation presented by the above

workers was slightly misleading, since the state of the specimen was appropriate to an axial strain of 17½%, greatly in excess of that at peak.

The use of "short", 1 : 1, specimens with adequate end lubrication, has improved the uniformity of deformations in triaxial extension and hence the reliability of stress calculations. Therefore, the results from tests by Green, and Barden and Khayatt, are likely to be of more significance than those from several other workers. However, many earlier studies, e.g. Bishop and Eldin, show general agreement with the conclusion that the strength of cohesionless soils in cylindrical triaxial extension is either equal to, or a maximum of about 2° in excess of, the triaxial compression strength. The more limited amount of information from tests on clays, suggests that this may apply to soils in general.

Cuboidal specimens tested in plane strain have almost universally exhibited a strength increase relative to triaxial compression. In the majority of apparatuses, lateral constraint is provided by a pair of rigid plates usually connected together. Despite the fact that lubrication is often used on all rigid surfaces, the stress distribution is unlikely to be uniform. However, since the magnitude of the intermediate principal stress is ignored in the Mohr-Coulomb failure criterion, the complex arrangements necessary for its measurement are frequently not undertaken, or the results considered only of secondary importance.

When making comparisons of soil strengths in plane strain, it should be remembered that this is not a unique stress condition, and in consequence the properties of the soil under test will determine the stress path in principal stress space.

For the majority of cohesionless soils the value of the parameter b at failure in a plane strain test varies between 0.2 and 0.3,

depending largely upon the initial porosity. Initial porosity also appears to be a major factor influencing the strength increase, several investigators demonstrating that for very loose specimens, the magnitudes of ϕ in plane strain and triaxial compression are similar.

Wightman, Barden et al, and Lee report plane strain strengths which for a major proportion of the density range exceed the compression value by a constant amount, varying between 3° and 8°. Sultan and Seed, and Cornforth, among others, show a linearly increasing strength difference with increasing density.

Most workers have observed similar behaviour of cohesive soils in plane strain, though the results appear to be more variable, possibly because of the differing nature of the soils tested. Shibata and Karube report a 9° increase in ϕ for a saturated clay, whereas Hambly, using the sophisticated Cambridge biaxial apparatus, observed negligible increase above the strength in conventional triaxial compression, hence supporting the Mohr-Coulomb criterion for failure.

The strengths of soils under generalised stress conditions have been studied using a variety of apparatuses, many quite unsuited to the task.

The major problems to be overcome in the design of a suitable apparatus are interference of the stress systems when more than one pair of boundaries is stress controlled, and the prevention of significant gaps forming between two or more pairs of rigid strain-controlled boundaries. Such problems will be dealt with in more detail in the two following chapters. For the present, it will suffice to say that the very wide range of strengths reported from tests in which generalised principal stresses were applied are due largely to the deficiencies in many of the apparatuses. Extreme examples are the results from tests by Ko and Scott, and Lomize and Kryzanovsky.

The former investigators redefined the failure condition, probably because of the high stresses obtained at very small strains, and the fact that a peak stress ratio was not reached, whereas the latter reported stress ratios at failure, for sands, which exceeded those predicted by the von Mises criterion.

The more reliable data of Sutherland and Mesdary, Green,and Shibata and Karube, indicate that little further increase in strength occurs, in sands and clays, above the value at plane strain, as b is increased to unity at triaxial extension. The first and last-mentioned workers report maximum strengths for b values of about 0.5, and equal minimum compression and extension strengths. Green, however, observed no change in ϕ between plane strain and extension, and a surprising difference of 3° between the strengths of cuboidal and cylindrical specimens tested in triaxial extension.

Although in the direct shear box test the soil specimen is subjected to a form of plane strain deformation, results obtained using this type of apparatus are not worthy of serious consideration in research investigations of stress-deformational behaviour.

Quite unlike the majority of tests which attempt to fulfil a similar purpose, the specimen is deliberately subjected to severely non-uniform strain conditions (Roscoe 1953), which in turn must increase the non-uniformity of stress distribution. In addition, Roscoe et al (1967) demonstrated that, even in the sophisticated Mk.6 simple shear apparatus, horizontal planes were far from being planes of maximum obliquity, i.e. $(\tau/\sigma)_{max}$, and the alternative assumption that they are planes carrying maximum shear stress was warranted, in drained tests, for loose specimens only. This being the case in simple shear, it would appear that agreement between the results from conventional direct shear tests and those from tests in triaxial and other apparatuses is

purely fortuitous.

To adequately represent the stress conditions at failure in various specific test programs, many workers have attempted to "fit" failure surfaces, usually by amending either the Mohr-Coulomb or von Mises criteria, to the test results. It is the usual convention, especially with cohesionless soils, to make strength comparisons, under different stress conditions, of specimens prepared at the same initial porosity. However, it must be remembered that the latter scalar quantity is inadequate in defining the structural properties of the soil, as is clearly demonstrated by the results from tests on different regular packings of equal spheres at equal porosities (Leussink and Wittke 1963).

Therefore, the aim of most investigators is to produce homogeneous specimens of known initial porosity, using standard methods of preparation (4.5). In this way, it is hoped that the initial degree of anisotropy of the specimens will be the same in each case.

For sand specimens consolidated under the same ambient stress, the porosity at the end of consolidation would probably be a suitable alternative description, enabling strength comparisons to be made. However, many studies of soil behaviour under other than axially-symmetrical stress conditions have involved consolidation at zero lateral strain. Since this is not a unique stress condition, care must be exercised in interpreting the resulting strains. El-Sohby (1964) has shown that the ratio of volumetric to axial strain, indicative of the degree of anisotropy, varies considerably with the stress ratio during anisotropic consolidation.

Possibly a more significant means of comparison would be in terms of the specimen porosity at failure. However, apart from the errors in overall strain measurements which are likely to occur between the initial

and failure states (4.4), it is possible that such a quantity would not truly represent the soil properties in local failure zones.

Roscoe (1967) reported tests in the simple shear apparatus which show significant differences between overall and local porosity measurements, although this was most marked after peak stress ratio. Such difficulties are likely to be less for normally-consolidated clays which compress during shear, and therefore tend to deform in a more uniform manner.

Coleman (1960) attempted to extend the Mohr-Coulomb failure criterion to a three-dimensional stress state. Accepting evidence that the strength of soil was the same in triaxial compression and extension, a simple invariant expression was derived to represent a convex failure surface passing through the six known points on the octahedral plane. Hence the influence of the intermediate principal stress was incorporated in the criterion, without disturbing the observed equality of strengths from the two axially-symmetrical tests.

The results of tests on dense sand by Green (1969) favoured a failure criterion of the type presented by Parkin (2.2) for a densely-packed idealized particulate medium.

It was found that cuboidal specimens exhibited the same strength for all values of b between plane strain and triaxial extension conditions. No satisfactory explanation for the apparent difference, 3°, between this strength and that from triaxial extension tests on cylindrical specimens could be found. It was suggested, however, that for some reason the plane strain deformation mechanism was appropriate to cuboidal extension specimens.

Haythornthwaite (1960) carried out triaxial tests on crushed quartz, and obtained inferior strengths in extension, (though a peculiar definition of failure was used). All extension test results,

when plotted on an octahedral plane, were shown to lie well inside the predicted Mohr-Coulomb failure surface. A new failure criterion was proposed, which took the form of an equilateral triangle passing through the three triaxial compression points and just inside the points representing the lowest triaxial extension strengths. Since no correction was apparently applied to the extension test results to allow for necking of the specimen, the calculated strengths, and the failure criterion of which they form the basis, are each likely to be gross underestimates of the true behaviour.

The most reliable experimental data concerning soil strength would seem to indicate that for loose sands, the Mohr-Coulomb failure criterion is a reasonable approximation. The maximum strength of dense sands is probably only a little in excess of that observed in plane strain. Whether a subsequent decrease occurs between this condition and triaxial extension is still controversial. If it does, it may be convenient to preserve the basic form of the Mohr-Coulomb criterion, and allow for any increase, for intermediate values of b, by using an empirical factor, e.g. Bishop (1966), which may be related to initial porosity. If, however, no change in strength occurs over the majority of the intermediate principal stress range, a criterion similar to that of Parkin (1965) would be more suitable. However, since the latter was derived for ideal dense packings of equal spheres, predicted strengths will almost certainly represent an upper limit to the failure condition. Therefore, without amendments for the random, irregular nature of real soils, such a theory would appear to be of limited use.

Some of the failure surfaces described are shown in Fig. 2.4, bounding widely-differing areas in an octahedral plane.

The curves representing the Mohr-Coulomb, Bishop, and Parkin criteria have been drawn for a value of ϕ in triaxial compression of 37°.

In addition, in plotting the Bishop curve, it was assumed that plane strain occurred at b = 0.25, and that the corresponding increase in ϕ was 4°. The shape of the Parkin surface is appropriate to an inter-particle friction angle of about 22°.

It should be remembered that in the majority of soil stress-deformation investigations it is assumed that both the stresses and the strains are the same at every point in the specimen, and therefore that overall measurements accurately depict local conditions. In conventional triaxial tests, it is further assumed that two of the principal stresses are equal. The validity of these assumptions, and their consequences, will be discussed more fully in the following chapter.

2.5 SUMMARY

The mechanical properties of a soil govern its deformational behaviour when subjected to applied stresses or, conversely they dictate the nature of the stresses induced by applying or preventing displacements. In this chapter, various methods have been described by which these properties have been, and are being, investigated.

Since the stress-deformational behaviour of soils must depend upon the interparticle stresses and deformations, and the relative movements between particles, many studies have been undertaken in the loosely-defined field of particulate mechanics.

Some of the more prominent theories for the behaviour under stress of, firstly, regular packings of equal spheres, and then random arrangements of irregular particles, were discussed in section 2.2. Of these, the stress-dilatancy theory, developed under Rowe at the University of Manchester, has been thoroughly investigated using laboratory stress-deformation tests on cohesionless soils carried out over a wide range of conventional triaxial stress paths, and in plane strain.

Other theoretical and experimental studies were described concerning the behaviour, under stress, of regular packings of spheres, which emphasized the important influence of soil structure. Finally, a mathematical treatment of the strength of densely-packed spheres was mentioned, leading to the definition of a failure surface in principal stress space.

In section 2.3, several fields of study involving the idealization of soils as continua were described, ranging from those assuming isotropic linearly-elastic behaviour to the more complex elastic-plastic-strain-hardening theories. The extensive work at Cambridge University, under Roscoe, on the development of the latter type of model was considered, and the difficulties associated with experimental investigation of "dry" soils were pointed out.

Normality of the plastic strain-increment vector to the yield surface would considerably simplify the prediction of soil deformations under applied stresses, but although this would appear to be a reasonable assumption for "wet" clays, the same cannot be said for cohesionless soils.

Section 2.4 covered some of the work concerning the "failure" of soils. The more common criteria for failure were described, and some of the more significant experimental evidence, from soil tests carried out over a wide range of stress conditions, was discussed.

Many of the apparatuses used in these investigations will be reviewed in the following chapter and, in particular, attention will be paid to the degree of success which has been achieved in subjecting laboratory specimens to generalised stress conditions.

CHAPTER THREE

LABORATORY STRESS-DEFORMATION INVESTIGATIONS

3.1 INTRODUCTION

Laboratory experimentation and testing are probably more prolific in soil mechanics than in any other branch of civil engineering. This chapter is concerned with laboratory methods of investigating the relationship between stress and deformation in soil specimens.

Section 3.2 discusses the needs of laboratory testing in relation to field problems, either in formulating theories of behaviour or in extrapolation to predict behaviour under specific conditions. The difficulties involved in attempting to standardize testing and the requirements of an "ideal" stress-deformation test are outlined.

Section 3.3 goes on to review developments in apparatus, in categories based on the assumed test conditions. Tests subjecting specimens to principal stresses at their boundaries are considered in 3.3.1., firstly axially-symmetrical stress conditions, 3.3.1.1, and secondly asymmetrical stress conditions, 3.3.1.2. Early methods of triaxial testing are reviewed together with more recent variations and improvements in testing technique, including the evaluation of stress-strain homogeneity and its improvement. A frequent implicit assumption concerning the magnitudes of principal stresses in the triaxial test is discussed.

Many of the topics in 3.3.1.1 are relevant in category 3.3.1.2, which covers the majority of experimental work carried out by the author as part of his research program. Past and present methods of applying three independent principal stresses to laboratory specimens, including the special case of plane strain deformation, are described and an attempt is made to assess their relative merits.

Section 3.3.2 covers tests in which the specimen is subjected to boundary shear stresses or torsion, and finally, in 3.3.3., other stress-deformation tests are discussed including the hollow cylinder method of varying the magnitude of the intermediate principal stress.

3.2 BASIC REQUIREMENTS OF APPARATUS

Knowledge of the strength and deformational behaviour of a soil under stress is necessary in the analysis of most field problems in soil mechanics. Usually this implies laboratory investigation of the relationship between stress and strain carried out on representative samples of the soil.

Information from laboratory tests may be used in formulating or scrutinizing theories of soil behaviour or, for more immediate practical purposes, extrapolated to predict behaviour under specific field-loading conditions. The former objective is essentially research and is intended principally to assist in gaining a fundamental understanding of the mechanical behaviour of soils. Methods of fulfilling the latter objective, including indirect measurement of strength-related properties, are not always compatible with research and have occasionally hindered understanding.

Because of the complex nature of polyphase soil material and the wide variation in its behaviour, not only with composition but also with environmental conditions, no one test suffices for the study of all important aspects of stress-strain behaviour. Furthermore for these reasons it seems highly unlikely that any one standard test will be developed which would be capable of supplying comprehensive information relevant to all field problems.

Often attempts are made to subject laboratory samples to the environmental conditions that are assumed to apply in field problems, in terms of either loading or deformation or a combination of both. The triaxial test, which allows a wide variety of such stress conditions to be imposed, has therefore proved to be one of the most commonly used methods for studying stress-strain properties of soils.

Among the many limitations of the conventional triaxial test, the

confinement to axially-symmetrical stress conditions is one of the most significant when extrapolating information on behaviour to the field-loading condition. Therefore, despite the attention which has been given to many of its remaining limitations, the triaxial test is unable to simulate many common field conditions, such as those in earth-dams, embankments and natural slopes, around excavations and earth-retaining structures, and beneath strip footings. Consequently the condition of axial symmetry implicit in the triaxial test is relevant to only a minority of field problems, e.g. square or circular footings and vertical piles.

Many common field problems will approximate more closely to the plane strain condition. The general case, however, will be one in which both the stresses and strains are different in each of their three principal directions at a point. Also the principal directions themselves may reorientate with deformation at any point and vary from point to point within the mass. An "ideal" laboratory test for use in the study of strength and deformational behaviour of soils would therefore need to be fully versatile with respect to the general field condition. The suitability of apparatus permitting such tests would further depend upon the validity of assumptions concerning the distribution of stress and strain within the test specimen.

A complete analysis of the deformational behaviour of the specimen is possible only if all components of stress and strain at any point are determinable. Usually this necessitates controlling or measuring the boundary stresses and strains and assuming homogeneous distribution of stress and strain within the specimen. Alternatively the specimen may be sub-divided into elements, within which the homogeneous condition is assumed, and the stress-strain behaviour of each element separately monitored. Such measurements also provide a basis for assessing the

degree of homogeneity within specimens tested in apparatus permitting only boundary measurement of stress and strain.

It is unfortunate, though not surprising, that attempts at tests allowing general three-dimensional stress-strain states often decrease the credibility of the homogeneous stress-strain assumption, due largely to the increased complexity of the apparatus. In tests where rotation of the principal directions has been possible, apart from the special case of orthogonal reorientation, the homogeneous condition has not generally been assumed, resulting in even greater apparatus complexity.

3.3 HISTORICAL REVIEW

Apparatus for stress-deformation and strength investigations will be reviewed under the following headings according to the assumed test conditions rather than the efficiency with which these conditions are met:-

3.3.1 Principal stresses applied at specimen boundaries.

3.3.1.1 Axially-symmetrical stress conditions.

3.3.1.2 Asymmetrical stress conditions.

3.3.2 Shear stresses or torsion applied to specimen boundaries.

3.3.3 Other stress-deformation tests.

3.3.1 PRINCIPAL STRESSES APPLIED AT SPECIMEN BOUNDARIES

3.3.1.1 Axially-Symmetrical Stress Conditions

Cylindrical compression tests have long been used to determine the mechanical properties of many materials including rocks and concrete. The specimen is loaded axially without lateral confinement and hence the stress conditions represent a special case of the triaxial compression test which would, in general, involve the application of lateral stress. Although used extensively for testing unfissured clays at constant water-content, the unconfined compression test is clearly limited as a research tool and is wholly unsuitable for testing cylinders of cohesionless soils which normally will not stand without confinement.

Early triaxial compression tests were performed, around 1900, on cylinders of rock laterally confined within thin-walled hollow metal cylinders. Hence the magnitude and distribution of the lateral stresses induced by axial loading were unknown, irrespective of whether the metal cylinder allowed small lateral strains or was effectively rigid.

In 1911 the Journal of the German Society of Engineers reported an experimental study of the stability of rocks, in which an all-round

fluid pressure was used (Karman 1911). However, it was not until the early 1930's that the fore-runner of the modern triaxial compression apparatus was first used to study the behaviour of soils.

In Holland the "limit of internal equilibrium" of a soil was investigated experimentally (Buissman 1934), using apparatus similar to that developed concurrently in Germany from a device for measuring the consolidation of clays under "negligible side friction" (Seiffert 1933). In the United States, Berry (1935) first reported the development of Housel's "stabilometer" (Housel 1936) for assessing the stability of road-surfacing materials.

The stabilometer (Fig. 3.1a) incorporated the main features of the triaxial compression apparatus and represented an improvement on Hveem's stabilometer (Stanton and Hveem 1934) which allowed measurement, but not control, of lateral stress. Dense, cylindrical, dry sand specimens prepared by vibration and enclosed in sealed, rubber membranes, were tested over a range of cell pressure. The axial stress was increased, through a plunger of diameter equal to that of the specimen, and the maximum stress ratio was found to be similar in each case.

Housel was one of the first to recognise that lateral restraint at the ends of the specimen could be reduced by increasing the length to diameter ratio. He recommended that this should be not less than "the cotangent of the angle of pressure transmission", which effectively set the lower limit for the length to diameter ratio at $\cot(45 - \phi/2)$, in terms of Coulomb's angle of friction. It was concluded that "such a test would be a direct measure of the shearing resistance ... and at the same time eliminate some boundary effects which complicate the analysis".

At the same time Rendulic (1936) carried out a series of classic experiments on specimens of remoulded silty-clay using an oil-filled

triaxial cell which allowed close control of lateral stress. Following ambient consolidation, the axial stress could be increased independently under either drained or undrained conditions.

Several variations of the triaxial compression apparatus were developed under the supervision of Casagrande during the 1930's and 1940's, including the vacuum triaxial (Chen 1948) and the transient triaxial compression apparatus (Casagrande and Shannon 1948). Using the latter apparatus, soil behaviour under rapid cycles of loading and unloading could be studied, simulating the effect of stress waves caused by earthquakes and explosions. Reports of investigations into the effects of transient loading on strength and deformational behaviour have since been numerous (Lee et al 1969).

Geuze (1948) also used a vacuum triaxial apparatus in a careful study of the dilatancy of sand in shear (Fig. 3.2a). Volume change of the specimen was determined from the volume of water entering or leaving the cell, since cell pressure was maintained atmospheric and the lateral stress induced by applying a partial vacuum to the pore space. Obviously this method of applying lateral pressure limits its magnitude to one atmosphere and is suitable only for cohesionless soils. Geuze also noted that "friction on the plunger considerably reduced the top load" and therefore used a hydraulic pressure cell to measure vertical load on the bottom platten.

During the 1940's Taylor supervised investigations into the stress-deformation and strength of soils carried out at Massachusetts Institute of Technology, and developed both apparatus and testing technique, particularly in the field of pore-pressure measurement (Taylor 1948).

The triaxial compression test currently used for routine testing (Bishop and Henkel, 1957) developed from this early work and, in modified and improved form, has been the basis of much recent research into

stress-deformation of soils.

The specimen, set up within the pressure vessel, or cell, is surrounded by a flexible rubber membrane sealed to rigid, cylindrical end plattens to prevent the confining fluid, usually de-aired water, from penetrating into the pore space. In some short-term tests a combination of air and water has been used in the cell, enabling instruments for measuring load and deformation to be accommodated in air immediately above the specimen which itself remains submerged in water (Barden and Khayatt, 1966). However, to retard the diffusion of air, under pressure, through the water and specimen sleeve, it is necessary to use a thin layer of olive oil between the two fluids.

The results of long-term tests on partially-saturated soils are particularly subject to errors caused by the diffusion of air through the rubber membrane. Bishop and Donald (1961) employed a mercury-filled jacket within the cell to apply lateral stress. The rise or fall of mercury with the jacket also provided an independent method of measuring lateral strain.

In the conventional test axial force is applied through a loading piston, or plunger, protruding into the cell and is transferred to the specimen through the end plattens. This force is commonly measured outside the cell using a proving ring. Hence friction between the piston and bushing causes a discrepancy between measured and applied loads. Many investigators have attempted to evaluate this error or have devised methods to reduce it, e.g. by rotating the bushing (Wood, 1958), or eliminate it, e.g. by using a proving ring within the cell (Barden and Khayatt, 1966).

Axial deformation of the specimen is normally measured by the movement of the loading piston, but direct measurement of lateral deformation is hindered by the presence of the cell. Therefore it is

usual practice to calculate this quantity from the volumetric deformation, determined by the volume of pore fluid entering or leaving the specimen, and the axial deformation.

In normal testing, after applying a uniform ambient stress to the specimen, it is usual to hold the cell pressure constant and either increase the axial stress at a steady rate, "stress-controlled conditions", or increase the axial strain at a steady rate, "strain-controlled conditions". The latter allows post-failure deformations to be studied.

Most so-called stress-controlled tests are truly load-controlled, the axial load being applied in increments. The resulting stress will remain constant only if the specimen cross-sectional area does not change under a given load increment. Ingenious methods of stress-compensation have been devised by Prater (1965), based on the cam principle, and by Saada (1967), using a pneumatic analogue. Saada's analogue further permits soil testing under constant octahedral normal stress. Lundgren and Mitchell (1968) describe a machine capable of imposing either load- or strain-control or any combination of the two.

An alternative loading condition in triaxial compression is to maintain a constant axial stress and decrease the cell pressure under either stress- or strain-control. In the"cell test" (de Beer 1950) this type of loading was used to determine "the lateral supporting pressure just satisfying the equilibrium of a sample under a given axial principal stress", (Fig. 3.1b). An axial load was applied to the specimen and the volume of cell water kept constant so that a lateral stress was induced under zero lateral strain. By bleeding off a little of the cell water the lateral stress was slowly reduced, without change in axial stress, until failure occurred.

De Josselin de Jong and Geuze (1957) developed a form of cell test in which the specimen surface was used as one electrode of a

capacitor, the rigid metal cell being the other. Consequently any change in capacity of the system during a test could then be related to lateral strain of the specimen. Conversely the zero lateral strain condition could be achieved by maintaining constant capacity.

The majority of attempts to measure lateral strain directly without disturbing the uniformity of lateral stress have, however, used optical methods. Systems which establish the soil profile over its entire length, e.g. Escario and Uriel (1961), are particularly advantageous when testing triaxial compression specimens with large length to diameter ratios or high end friction; in either case the tendency to bulge is increased.

Development of the triaxial extension test widened the range of axially-symmetrical loading conditions by rotating the principal stresses through 90° with respect to triaxial compression.

By pulling upwards on the top platten the axial stress is reduced, making it the minor-principal stress, while all-round fluid pressure maintains equality between the major- and intermediate- principal stresses. Alternatively the top platten can be connected to a loading piston having a diameter equal to that of the specimen. Consequently the axial and radial stress systems are independent and it is possible to carry out triaxial tests over a full range of compression or extension stress paths, including sudden orthogonal reorientation of principal stresses, using a single apparatus.

Early workers in this field soon recognised the difficulties of interpretation associated with "necking" in specimens approaching failure (Schraerer et al 1948). This was exaggerated by the use of specimens with initially large length to diameter ratios which became even greater with strain.

Knowledge of the variation in cross-sectional area of triaxial

extension specimens is especially important when computing the peak stress ratio from axial load at large strains. Roscoe et al (1963) used an optical method to measure local lateral and axial strains at various stages of deformation.

Uni-axial tension tests on soil specimens are uncommon, being relevant only to the study of cohesion in clays (Tschebotarioff 1953, Bishop and Garga 1969).

Many investigations have been concerned with the overall size of test specimens. The greater the overall size, the greater will be the statistical probability that an undisturbed sample is representative, particularly for gravelly soils. More importantly from the point of view of stress-deformation research, an increase in specimen size often reduces specimen boundary effects in a disproportionate manner so that the accuracy of measured quantities is increased. However, although apparatuses for testing gravelly soils and rockfill have been heavily documented, comparative studies of the effect of specimen size, e.g. Fukuoka(1957), have been few. Therefore with an assumed preference for overall sizes greater than the 1½ in. diameter triaxial specimen used in much early research, investigators have concentrated on establishing an optimum shape, with respect to boundary effects, by varying the relative dimensions.

A great deal of research work has been concerned with the degree of stress-strain homogeneity within stress-deformation test specimens, and the extent to which the boundaries are free from shear stress.

Early workers were aware that platten friction restrained lateral expansion at the ends of the specimen, introducing inhomogeneous strain conditions and violating the assumption that normal stresses only were applied. By increasing the length to diameter ratio it was hoped that the overall influence of end restraint was reduced sufficiently for it

to be reasonably ignored.

Nowadays it is common practice to reduce end friction by interposing one or more suitably lubricated rubber membranes between the specimen and the end plattens. Lee and Seed (1964) investigated several lubricants and found silicone grease the most successful. It is now widely used in strength testing.

Rowe and Barden (1964), Bishop and Green (1965) and others have shown that efficient end lubrication is essential when testing specimens with a 1 : 1 length to diameter ratio, since the absence of such lubrication results in a significantly different overall stress-strain response and a greater apparent strength. The effect of end restraint on strength decreases with increase in length to diameter ratio, Bishop and Green concluding that for 2 : 1 specimens it becomes negligible. However, experiments by Lee and Seed have indicated that there may be a difference in apparent strength of sands tested at low stress levels. It is agreed that the provision of lubricated ends improves the accuracy of volume change measurements at large strains.

Roscoe et al (1963) measured local variations in the axial and lateral strains of conventional "long" triaxial compression and extension specimens using an optical method to observe local boundary displacements. In both types of test, strains in the region of the end plattens were found to be considerably less than the overall average strains.

By inserting stress- and strain-gauges within triaxial compression specimens, Januskevicius and Vey (1965) demonstrated the improvement in homogeneity obtained with end lubrication. Unfortunately measurements were reliable only for small strains.

Methods of reducing end friction are relatively simple and clearly increase the likelihood of obtaining uniform strains. The problem of

non-uniform stress is, however, not as easily resolved.

There is clear evidence that the application of stress through rigid surfaces is liable to produce non-uniform stress distribution both at the boundaries and in the interior of the specimen (Roscoe, Bassett and Cole, 1967). It is probably that this effect increases with the proportion of specimen surface area subjected to rigid boundary constraint, and therefore is of particular significance when considering apparatuses capable of imposing other than axially-symmetrical stress conditions. These will be considered in the following section. Because triaxial specimens are rigidly constrained at their end surfaces only, the effects are likely to be less important.

When considering the homogeneity of stress in the triaxial test it should be remembered that although the cell pressure gives rise to a uniform radial stress, normal to the surface of the specimen, the assumed equality between intermediate- and minor-principal stresses has no theoretical justification.

In any rigorous treatment the radial stress, which by nature of its application is the only boundary stress known to be uniformly distributed, may represent one principal stress only. If it can be shown that shear stresses at the end plattens are negligible, the direction of the major principal stress will be known. Rigidity of the end plattens will mean, however, that its distribution will almost certainly be non-uniform.

The remaining principal stress is not radial but tangential to any element of the cylindrical specimen, and therefore indeterminate unless elastic theory is assumed. Fortunately experimental indications (Kirkpatrick and Belshaw 1968) are that, providing precautions are taken to minimise end platten friction, the radial and tangential stresses are approximately equal.

Triaxial tests applying axially-symmetrical stress conditions to specimens with other than circular cross-sections have been used primarily as control tests prior to stressing the specimen under different conditions in a more elaborate apparatus.

Green (1969) carried out cuboidal triaxial compression and extension tests on dense sand, varying the dimensions of the specimen in an attempt to determine its optimum geometry for tests in the "independent stress control" apparatus.

3.3.1.2 Asymmetrical Stress Conditions

The stress conditions in many geotechnical field problems do not approximate to those of axial symmetry implicit in the conventional triaxial test. However, if it can be shown that the influence of the intermediate principal stress on the stress-deformational behaviour of a soil is slight, the continuing use of cylindrical triaxial compression tests to determine the mechanical properties of the soil, and hence permit solution of these problems, may be justified. Even if this is the case, experimental investigation into soil deformation under generalised stress conditions is still necessary, if a fundamental understanding of the factors controlling their mechanical behaviour is to be gained.

The plane strain condition is appropriate to many common field problems. Although not strictly a unique stress condition, the three principal stresses are different. Several investigators have attempted to measure the intermediate principal stress induced in the direction of constraint. Others have ignored this value, or have been unsuccessful in measuring it, and have concentrated on relating strains to the major and minor stresses.

The majority of apparatuses in which generalised stress conditions

can be applied to cubic or cuboidal specimens, are also capable of imposing the condition of plane strain. These will be considered later, in their general context.

The usual form of plane strain apparatus is typified by that developed at Imperial College, London, firstly by Wood (1958), (Fig. 3.3a).

The specimen, 4 in. × 2 in. × 16 in. long and enclosed in a rubber membrane, was constrained in the direction of its major dimension by two rigid aluminium end plates, connected together with four tie-bars, and covered by lubricated membranes. In order to measure the intermediate principal stress, a rigid circular disc was attached to one of the end plates. The remote face of the disc was itself connected to the rubber diaphragm of a pressure-cell, so that stress from the specimen was transmitted to de-aired water confined within the pressure-cell and hence measured. A mercury thread null-indicator was balanced to maintain constant volume of the de-aired water, and therefore zero strain of the specimen in this direction.

Two loading rams, acting at the quarter-points of a rigid top platten, were used to apply the axial deviator stress, the complete assembly being contained within a water-filled cell. The cell pressure was applied and measured in the usual way. Because axial load was measured externally with proving-rings, the loading rams were equipped with rotating bushing to reduce friction. Axial deformation was determined from the displacement of each ram.

Four porous discs set in the bottom platten allowed specimen drainage or pore-pressure control. In this type of apparatus, where the end plates are at a fixed separation, K_o-consolidation of the specimen is essential, since otherwise the specimen will lose contact with the plates or the end stress will be indeterminable.

Following Wood's undrained tests on a well-graded sandy-gravel,

Cornforth (1961) used the apparatus to test medium-fine sand under fully-drained conditions. Henkel and Wade (1966) automated the K_o-consolidation process, during tests on remoulded clay, by using the movement of the mercury thread to stop or start an electric motor driving the moveable pot of a self-compensating mercury pressure control system.

Bjerrum and Kummeneje (1961) carried out plane strain tests on similar cuboidal specimens of sand 12 cm. high × 4 cm. wide, the length being variable between 30 and 60 cm. Axial deviator stress was applied to the specimen via rigid, unlubricated top and bottom plattens, a vacuum applied to the pore space providing the ambient stress.

No clamps or plates were used at the ends of the specimen, which was tested in the triaxial compression fashion. Measurements of the specimen dimensions taken throughout testing indicated that friction at the loading plattens was sufficient to restrain the specimen from longitudinal deformation. Little advantage was gained from increasing the length to width ratio beyond about 8. Clearly, under these conditions the specimen could not have been homogeneously stressed, since the intermediate stress must have varied considerably.

In the light of this work, Lee (1970) investigated the necessity of end plates in plane strain testing. Using a simplified version of Duncan and Seed's (1966) apparatus, Lee tested specimens 2.4 in. × 1.1 in. × 2.8 in. long, with and without end plates, and concluded, predictably, that they were essential. These were used in the subsequent plane strain tests. The minor principal stress was applied using cell pressure in the normal way, and no measurements of intermediate stress were taken.

Duncan and Seed's apparatus had used a pair of water-filled boxes with flexible diaphragms to apply lateral stress to the two wider faces of a specimen 2.78 in. × 1.10 in. × 2.78 in. long.

In an attempt to simulate the consolidation and subsequent undrained failure of the soil at the top and bottom of a slip surface in a clay slope, the apparatus was designed to permit K_o-consolidation in one of two directions, followed by plane strain deformation. During consolidation of a "vertical plane strain" specimen, four rigid plates prevented lateral deformation. One pair, the side plates, could be withdrawn by decreasing the pressure in the diaphragm-boxes from outside the cell, the second pair, the end plates, constraining the specimen in the other lateral direction, while axial stress was increased to failure. "Horizontal plane strain" was preceded by K_o-consolidation in the direction of the water-filled boxes, this time using the flexible diaphragms to apply the major principal stress. This stress was then rotated through 90°, and failure brought about, again by increasing the axial stress.

In the plane strain apparatus of Leussink and Wittke (1963), the minor principal stress was produced by evacuating the interior of the 60 cm. × 20 cm. × 100 cm. long specimen. Tests were carried out on regular packings of uniform glass balls, 1.5 cm. in diameter, the axial stress being applied by hydraulic presses through a rigid steel loading beam, mounted on roller bearings. The specimen was constrained from longitudinal deformation by water-filled steel boxes, aluminium plates transferring the intermediate stress to the water, and thence to a pressure gauge. Soft soap was used to reduce friction between the aluminium plates and the specimen membrane.

Sultan and Seed (1967), also using a vacuum plane strain apparatus, investigated the mechanical properties of sand used in the model testing of sloping-core earth dams.

Marsal (1965) used a similar system to apply ambient stress in an apparatus designed to subject specimens of rockfill to plane strain

deformation. The specimens, 75 cm. square in cross-section and 180 cm. high, were tested between two rigid walls, formed from box-girders and connected together with twenty hollow bars. Ten of the bars were instrumented with linear variable differential transformers which measured the specimen reaction to within 1%. Greased polyethylene sheets were used to reduce friction, and corrugated cardboard placed inside the membrane prevented its puncture.

Wightman (1967) carried out plane strain tests on specimens of sand and glass ballotini, 4 in. × 4 in. × 8 in. long. Stainless-steel end plates formed an integral part of the bottom platten, and were held at a fixed separation at the top with two tie-bars. Lubricated end-membranes were used on each plate. Axial deformation was measured inside the cell using dial gauges mounted on rods screwed into the cell base, and an internal proving-ring was used to measure the deviator stress. The intermediate principal stress was not measured.

This apparatus was amended by Barden et al (1969), the end plates becoming separate components, so that the number of tie-bars had to be increased to four. The specimen was reduced in length from 8 in. to 6 in., and all four rigid surfaces were lubricated. Tests were performed on specimens with heights of 4 in., 6 in. and 9 in., the observed stress-strain behaviour being similar in each case. The shortest was therefore adopted for general plane strain testing, which covered a range of cell pressure from 5 to 1000 lbf/in^2. High pressure tests, above 100 lbf/in^2, were carried out in a cylindrical steel cell, axial load and deformation being measured externally in the more conventional manner. All specimens were consolidated at zero lateral strain.

Finn et al (1967) used a lateral strain indicator (Bishop and Henkel 1957) in order to consolidate their 4 in. × 2 in. × 16 in. long

plane strain specimen under K_o conditions, the apparatus being similar to that of Wood (1958). The cell pressure was held constant, and the intermediate stress adjusted to prohibit change in length while the deviator stress was increased to failure. Their investigation was concerned mainly with the comparative volume changes in plane strain and triaxial compression specimens tested at the same cell pressure.

Lorenz et al (1965) designed a plane strain apparatus based on that developed by Kjellman (1936) for testing under generalised stress conditions.

A 10 cm. cubic specimen, enclosed in a rubber membrane, was loaded in the two horizontal directions through four sets of 8 metal strips, or "hammers", each 10 cm. long. It was arranged that the loads on each set of 8 hammers were equal, regardless of their individual displacements. These provided the major and minor principal stresses while, in the vertical direction, two sets of 64 rods constrained the specimen from significant deformation and transmitted the intermediate stress to strain gauge blocks, where its magnitude was measured. Horizontal strains were determined from the relative movements of the hammers, as the major principal stress was increased in increments to failure. The specimen was found to deform uniformly in each of the horizontal directions.

In the Cambridge plane strain apparatus (Hambly 1969), the cuboidal specimen was constrained by two horizontal glass plates connected rigidly together with four load cells. Therefore the average value of the intermediate principal stress could be determined from measurements of the induced vertical load. Each of the four vertical plattens overlapped each of its neighbours, to which it was attached by freely-running guides, (Fig. 3.3b). This allowed the lateral dimensions of the specimen to be varied between 6.8 and 13 cm., its cross-section remaining

rectangular and symmetrical about the two horizontal axes.

The cuboidal specimen membrane was made to deform in accordance with the specimen, a remoulded "wet" clay, by fixing its corners into slots in the plattens. Drainage was through filter paper drains, laid inside the lower face, and a central orifice in the membrane; pore pressure was measured at top and bottom, using pressure transducers. A small clearance was always maintained between the upper glass plate and the loading plattens, which rested on P.T.F.E. discs supported by the lower plate.

Deformation could be applied in either the stress-controlled or strain-controlled manner, each pair of horizontal loading rams being mechanically linked by chain gear. Roller-races allowed the plattens to move freely perpendicular to their loading rams as the specimen deformed.

Each platten consisted of eight load cells, arranged so that all eight measured the normal force, three measured the shear force in the intermediate stress direction, and five measured the shear force perpendicular to the latter. The local strains within the specimen were determined by transmitting X-rays vertically through the upper glass plate to a film below the lower plate. Movements of lead shot, probed into the specimen before test, were recorded on successive radiographs and hence the strains calculated. The specimens were consolidated horizontally in either one or two dimensions, and sheared at constant volume in plane strain.

Several investigators have carried out model tests in the laboratory, in which the soil is deformed under plane strain conditions. Many of these have been concerned with the stresses on a retaining wall, and the distribution of strain within the soil mass as the wall moves in either the active or passive manner (Arthur et al 1964, Rowe and

Peaker 1965).

One of the major difficulties encountered in modelling field problems in the laboratory is the limited magnitudes of the stresses that can be applied. This is being overcome with the development of the centrifuge for soil model tests (Roscoe 1970).

However, it is not the purpose of model testing to subject elements of a soil mass to either homogeneous stress or strain conditions, and therefore such investigations do not fall within the general scope of this review.

One of the earliest apparatuses allowing independent control of the three principal stresses was developed at the Swedish Geotechnical Institute (Kjellman 1936). Loads were applied to the specimen, a 62 mm. cube, by filling three suspended water tanks, each connected independently through a system of levers to loading plungers. They were then transferred from each plunger to the specimen surface by 100 brass rods, 6 mm. square and of equal length, so that their ends effectively remained in one plane. An initial separation of 0.2 mm. between rods was designed to allow for subsequent lateral movement, either increased or decreased separation, determined by the deformation of the specimen, (Fig. 3.2b).

In this way it was hoped to eliminate the friction which would otherwise exist between the loading plungers and the specimen surfaces. However, with cohesionless soils in particular, grains tended to wedge in the gaps between bars, thus preventing the independence of movement that the bars were designed to encourage, and possibly accentuating their separation. Also, in order to allow unrestrained lateral movement of the bars, their ends in contact with the loading plungers were spherical, clearly making them unstable in compression.

Jakobson (1957) reported some small improvements to increase

stiffness, but otherwise the apparatus was used unchanged.

In general, deformations are limited in this type of apparatus due to mutual interference of the loading systems along the twelve edges of the specimen. Therefore, for the majority of soils, investigations are restricted to magnitudes of strain much smaller than those required to reach failure.

Daniel (1954) used two pairs of rigid plattens, connected at the sides with rubber sheet, to apply different lateral stresses to a specimen $1\frac{3}{4}$ in. square × $3\frac{1}{2}$ in. long. Systems of hangers and weights allowed the lateral loads to be held constant while the axial stress was increased to failure. The results of tests on dry sand were almost certainly affected by platten friction and non-uniformities of stress and strain along the edges of the specimen.

In Bell's (1965) apparatus, the vertical faces of a specimen 16 in. square and 2 in. thick were stressed through four flexible, water-filled compartments, separated by adjustable hinged plates at the corners. A fifth compartment, covering about 60% of the specimen surface area, was recessed into the lower of two steel-reinforced perspex plates, to provide the remaining principal stress. Windows allowed the corners of the specimen to be observed, and all surfaces were lubricated to reduce friction. The stresses were increased in increments, and the hinged plates adjusted each time to prevent mutual interference of the flexible surfaces. Consequently, the test procedure was rather laborious.

Ko and Scott's "soil test box" (1967) was developed from Bell's apparatus and allowed independent control of the three principal stresses acting on a 4 in. cubic specimen, (Fig. 3.4a). The three pairs of rubber panels, through which the stresses were applied, were separated using a stainless steel spacing frame so that they would not mutually interfere. The panels, 0.010 - 0.012 in. thick, were attached to six aluminium box

sections using rubber O-rings which formed an effective seal when the sections were screwed together. The specimen, sand was used in early experiments, was prepared by deposition into the test box. With the box closed, the specimen was completely surrounded by the six panels, and therefore the experimenters found no reason to use a specimen membrane.

Despite the precautions taken to prevent panel interference, strains were limited to 1 to 1.5% and were determined from the volume of water entering or leaving the compartments in each of the principal directions. It was confirmed by microscope sightings through windows in the box walls that deformations were almost uniform and therefore the measured average strains could sensibly be used. A further check on volumetric deformation, using a hypodermic needle inserted into the specimen (Taylor 1942) through a sealed hole in one corner of the box, was in agreement with the individual strain measurements.

The designers accepted that small volumes of soil at the corners and along the edges of the spacing frame would not be in a homogeneous stress state, but decided that the error would be unimportant because strains were small. Subsequent discussions (Green 1967, Bell 1968, Arthur and Menzies 1968) showed that this was not the case, and that severe stress non-uniformity in these regions probably accounted for the discrepancy between conventional triaxial compression strengths and those obtained under similar stress conditions in the soil test box. Ko and Scott did not in fact obtain peak values of stress ratio at these small strains and attempted to redefine failure in terms of the rate of increase of volumetric deformation with respect to octahedral normal stress.

Bell presented an elastic analysis to compare the axial strain of a cylinder restrained along four edges at its circumference, similar to

the restraint imposed by Ko and Scott's spacing frame, with the axial strain of an unrestrained cylinder. An experimental comparison of the strengths of 4 in. cubic specimens of sand, either unrestrained or restrained along eight edges, showed qualitative agreement with the elastic analysis, thus demonstrating the significant effect of edge restraint.

A modified version of the soil test box was constructed by Arthur and Menzies, the specimen being surrounded by its own rubber membrane, and the spacing frame relieved so that at small strains it did not come into contact with this membrane. X-rays of lead shot placed in specimens of sand confirmed that when contact with the spacing frame did occur, severe distortion resulted.

Using this apparatus, peak strengths in triaxial compression were found comparable with those obtained in conventional tests. However, deformations were found to be non-uniform, contrary to Ko and Scott's observations, so that stress-strain curves based on overall measurements were not in similar agreement.

Using a very similar apparatus, Lomize and Kryzhanovsky (1967) tested 71 mm. cubic specimens of sand under three-dimensional states of stress. Six hollow compartments, approximately triangular in cross-section and covered with flexible membranes, were again used to apply the stresses. Each pair of compartments was water-filled and connected to "volumenometer" tubes, in which the rise or fall of the water-air meniscus was measured, and hence the average specimen strain determined. Controlled air pressure was transmitted to the water in each volumenometer and thence to the specimen surfaces.

The effect of air diffusion on deformation measurements was not discussed, and no indication was given of the influence of edge and corner interference from the apparatus.

In testing undisturbed and remoulded clays, Lomize et al (1969) increased the size of the specimen to 10 × 10 × 10 cm., and inserted a hypodermic pore-pressure probe, through one corner of the box, into its centre. The strains were again calculated from movement of water into or out of each pair of compartments, but the shape of the compartments was changed and a more complex system for applying the pressures was used. Although the reasons were unspecified, it is quite possible that the amendments were aimed at reducing specimen restraint.

Shibata and Karube (1965) carried out tests on a remoulded alluvial clay, reconsolidated in a cylindrical oedometer and then trimmed to the shape of a cuboid 3.5 cm. × 2 cm. × 6 cm. long, for tests under three-dimensional stress conditions.

The specimen was confined within the conventional triaxial cell, and loaded axially in the usual manner. Two water-filled membrane cushions, used to apply the intermediate principal stress, were held against the two smaller vertical faces with aluminium plates, and double lubricated membranes were inserted between the cushions and the specimen to eliminate friction. The complete intermediate stress assemblies were suspended from pulleys within the cell and counterbalanced for the same reason.

Apparently there was no measurement of either lateral strain. This would certainly have been very difficult in the intermediate direction, since volume change of the membrane cushions must have depended largely on the lateral deviator stress, in addition to specimen deformation. The effect of cushion expansion on the stress conditions at the vertical edges of the specimen was not mentioned. Shibata and Karube (1967) reported plane strain tests carried out with this apparatus.

Lenoe (1966) used two half-cylinder boxes, faced with rubber membranes to apply a lateral deviator stress to cuboidal specimens of sand,

the minor principal stress being applied by evacuating the pore-space, (Fig. 3.4b). The specimens were loaded axially through rigid end plattens in the usual way. Since the surface area of each rubber membrane was apparently considerably greater than that of the corresponding face of the specimen, edge restraint must have been significant, despite the fact that tests were carried out at very low stress levels.

Sutherland and Mesdary (1969) also used a pair of flexible side panels to form the faces of two lateral rigid boxes, in their apparatus for testing 4 in. cubical specimens under three-dimensional states of stress. In order to overcome the difficulties of edge restraint, the side panels were reinforced with a brass mesh.

Specimen deformation in the direction of the panels was determined from their change in volume, and in the other horizontal direction, two deflection dial gauges were used on opposite diagonals. All instruments, including an internal proving-ring and two vertical deflection dial gauges, were accommodated in air above the top platten (Barden and Khayatt 1966). A check on the three direct strain measurements was made possible by measuring the volumetric deformation. Lubricated end membranes were used to cover the rigid end plattens and the side panels were smeared with grease before the intermediate stress boxes were connected together with six tie-bars. The edges of the specimen were found to be slightly rounded; the curvature was measured and allowed for in subsequent calculations.

The stress-deformation charactersitics of a medium-fine sand were investigated for a series of intermediate stress conditions ranging from triaxial compression to triaxial extension.

Green (1969) experimented with several different sizes of cuboidal specimen, before choosing one 3.3 in. × 3.2 in. × 2.1 in. for use in the "independent stress control" apparatus. When tested in conventional

triaxial compression with double lubricated membranes at each end, this specimen had a strength which was lower than that of the various other specimens tested, and equal to that obtained from 4 in. × 4 in. dia. cylindrical triaxial compression specimens similarly lubricated.

In the independent stress control apparatus, two rigid, lubricated plattens were used to apply the lateral deviator stress, the complete assembly being enclosed within a conventional water-filled cell which supplied the minor principal stress. The specimen itself was surrounded with a conventional cylindrical membrane, drawn into cuboidal shape prior to specimen preparation. The cell pressure represented the only stress-controlled boundary, since the axial deviator stress was also applied through rigid plattens, in the usual way.

The difficulties of platten interference at the two strain-controlled boundaries were partly overcome by varying the size of the intermediate stress plattens to suit the anticipated specimen deformations, the specimen arching across the rigid boundary gaps. The two pairs of plattens were driven at constant rates of deformation, the rates being adjusted for different tests to obtain various resultant stress conditions. Therefore the apparatus was strictly capable of applying only independent strains, not independent stresses, in these two directions.

Internal proving-rings, incorporating electrical measurement of load, were used to determine the axial and lateral deviator stresses. The two intermediate stress plattens were connected together with four tie-bars and suspended over pulleys to help reduce the frictional force on the specimen, the system being similar to that used by Shibata and Karube. Lateral deformation of the specimen between the plattens was measured using encapsulated dial gauges within the cell, and the axial deformation was determined from the movement of the loading plunger

relative to the cell base.

Drained tests on a medium-fine dense sand were carried out at different relative strain rates, to provide various values of the intermediate principal stress at failure. In a few tests, the principal stresses were interchanged to investigate the influence of platten rigidity on stress-deformation data. The conclusions from such a comparison must, however, be tentative, since the effect of initial specimen anisotropy may also be significant.

The development of the Cambridge biaxial plane strain apparatus to allow the application of three independent strains was reported by Hambly (1969).

The corner and edge effects inherent in apparatuses having two or more sets of rigid surfaces, e.g. Green (1969), were overcome by butting two edges of each platten against the overlapping faces of the two neighbouring plattens. Continuous contact was maintained throughout deformation by three pairs of orthogonal guides in which the plattens were made to move. Therefore the specimen was completely surrounded by a corner area of each of six rigid surfaces. The size of the areas depended upon the original size and shape of the specimen and the current state of deformation. The only restriction on the specimen dimensions was the maximum size of the plattens. The relative magnitude of the three principal stresses could be controlled throughout testing.

Clearly a large majority of apparatuses capable of applying three independent principal stresses to a soil specimen have been based on the conventional triaxial apparatus. Many have used the conventional system for applying axial deviator stress and have enclosed the specimen, altered in shape to a rectangular prism, within a water-filled cell. Cell pressure has then been used to apply the minor principal stress on one pair of exposed vertical faces of the specimen, while

in the perpendicular horizontal direction, the intermediate principal stress has been applied through two independent surfaces, either rigid plattens or flexible diaphragms. The necessary equipment has usually been accommodated within the cell and controlled from outside.

In most recent apparatuses, all surfaces not subjected to direct fluid pressure have been suitably lubricated, usually with silicone grease, to reduce boundary friction and improve the degree of homogeneity of stresses and strains.

An ingenious method of applying the intermediate stress without the necessity for contact with the specimen was that described by Escario (1961). Iron shot was embedded in one pair of parallel faces of the membrane surrounding a cuboidal specimen, (Fig. 3.5b). A magnetic field, applied using an electromagnet, reduced the stress in one of the horizontal directions, so that the cell pressure became the intermediate principal stress. However, difficulties concerning the uniformity of the magnetic field, and undesirable tangential forces on the specimen, complicated the stress-distribution, and little progress seems to have been made with this apparatus.

The majority of investigators have therefore concentrated on applying at least one of the lateral stresses through some form of mechanical component, either flexible or rigid. Although the overall boundary conditions range from three stress-controlled boundaries, e.g. Ko and Scott, to three strain-controlled boundaries, e.g. Hambly, the problems of stress system interference with the former, and the greatly increased sophistication of measurement required with the latter, would appear to favour the use of a combination of boundary conditions in the majority of experimental investigations.

This topic will be discussed more fully in Chapter 4 when considering the Aston Triaxial Apparatus.

3.3.2 SHEAR STRESSES OR TORSION APPLIED TO SPECIMEN BOUNDARIES

The direct shear box test has long been used to subject specimens of cohesive and cohesionless soil to controlled shear displacements.

In the conventional test, a cuboidal specimen is confined within the top and bottom halves of a rigid box, which are subsequently mutually displaced causing the specimen to shear along a horizontal plane. The forces normal to and parallel to the shear plane are measured, but the intermediate principal stress, which acts on the vertical sides of the specimen perpendicular to the direction of shear, is of unknown magnitude and distribution. The other two principal stresses rotate as strain progresses.

Because of the rigidity of the normal loading plattens and the sides of the box, the distributions of all the stresses are unlikely to be uniform. This, together with the extreme non-uniformity of shear strains (Roscoe 1953), render the results of such tests very difficult to interpret with any certainty (Bent Hansen 1961), the apparatus being particularly unsuitable for the study of deformations prior to failure. The use of double direct shear apparatuses does nothing to reduce the uncertainties.

Peltier (1957) performed "triaxial shear box" tests on cohesionless soils, in which it was possible to vary the intermediate principal stress. The shear and normal stresses were applied in the usual way, while moveable rigid plattens, separated at the height of the shear plane, allowed lateral force to be applied perpendicular to the direction of shear. However, the distribution of stress over the plattens was again unknown and therefore its average value only could be determined.

In the "ring shear apparatus", designed by Hvorslev (1936) to overcome the limitation of strain magnitude inherent in the direct shear box, an annular specimen confined within inner and outer metal rings was

subjected to normal and torsional loading. Using this type of apparatus it was possible to apply unlimited shear displacements over a surface parallel to the plane surface of the specimen, facilitating investigation of post-failure conditions. However, in addition to the limitations associated with conventional direct shear box tests, the average shear strains in torsion varied with the distance from the centre of rotation.

The extreme non-uniformity of strains in the conventional test has been partially overcome by subjecting specimens to simple shear.

In the Swedish Geotechnical Institute simple shear box, reported by Kjellman (1951), the specimen, 60 mm. dia. × 20 mm. high, was enclosed within a cylindrical thick rubber tube surrounded with aluminium rings. Normal load was applied through rigid plattens, the specimen consolidating with minimum side friction, and the top platten was displaced horizontally relative to the bottom to apply uniform shear strain, the rubber tube deflecting sideways. However, despite the presence of the closely-spaced rings, it seems likely that there was some lateral deformation of the soil, the tube squeezing out locally between adjacent rings, and therefore the distribution of lateral stress would have been non-uniform.

Bjerrum and Landva (1966) carried out simple shear tests on undisturbed specimens of Norwegian "quick" clay in an improved version of the above apparatus. The cylindrical rubber membrane was reinforced with a spiral winding of 0.15 mm. dia. wire at 25 turns per cm.

Although the strains are more uniform in this type of test, and the drainage conditions more easily controlled, the distribution of stress is still unknown.

In the Cambridge "simple shear apparatus", (Roscoe 1953), a cuboidal specimen, 6 cm. square × approximately 2 cm. high, was used. Two rigid end flaps were connected to upper end plates with hinges, above the top

surface of the specimen, and held against the lower end plates with roller bearings, so that during shearing the end flaps remained mutually parallel. The two vertical sides of the apparatus were each made up of two sections joined at the mid-height of the specimen also with roller bearings. The sides were covered with thin rubber sheet stretched over the surfaces and fixed in position, the interface between the rubber and the box sides being smeared with silicone grease to reduce friction. Similar lubrication was applied to the end flaps. Thin sheets of sand paper were glued to the base of the box and the bottom of the normal loading piston to help improve the uniformity of deformation. The loading piston was made to remain both vertical and clear of the upper surface of the specimen throughout shearing.

In order to investigate the uniformity of deformations, a series of striped plasticine specimens were tested, and the results compared with similar specimens tested in the conventional direct shear box.

The latest model of this apparatus, the Mk.6, was described by Roscoe et al (1967). Major improvements in the design had eliminated the "dead zone" at the top of the specimen, in which shear strains were non-uniform, and had allowed the accurate determination of the magnitudes and directions of the principal stresses independently from the principal strains.

The specimen, 10 cm. square × approximately 2 cm. high, was surrounded with ten load cells, each capable of measuring the shear force and the magnitude and eccentricity of the normal force on its active face. Three load cells beneath the specimen, and another three above, were postioned with their longitudinal axes at right angles to the direction of shear, taking the place of the top and bottom plattens of the conventional direct shear box. The end flaps and the two vertical sides each consisted of a further load cell.

The normal load could be applied by attaching weights to a hanger,

or, alternatively the normal strain, and hence the degree of drainage, could be controlled. A load cell connected to the central column of the apparatus was used to measure the total normal and shear loads acting on the specimen, and displacement transducers were used to measure its horizontal and vertical deformations. Strains within the specimen could be determined by using rigid sides in place of the vertical loads cells, perpendicular to the direction of shear, allowing X-rays to be transmitted through the specimen to determine the movement of lead shot.

In addition to direct and simple shear, torsion has often been used, frequently in combination with conventional triaxial loading, in soil stress-deformation tests.

To investigate the effect of the intermediate principal stress on the mechanical behaviour of sand and clay, Habib (1953) subjected triaxial specimens to torsion, by rotating the top platten, while keeping the bottom platten fixed. Axial and radial stresses were applied in the usual manner. Failure of the specimen adjacent to the plattens was prevented by enlarging its ends, and therefore only over its middle two-thirds was the specimen uniformly cylindrical.

Various intermediate stress conditions were imposed by applying torsion to specimens under differing axial stresses, the lateral stress being the same in each case.

Haythornthwaite (1960) carried out combined torsion and axial loading tests on hollow cylindrical specimens of silt and clay, hoping to improve the uniformity of stress distribution.

3.3.3 OTHER STRESS-DEFORMATION TESTS

A popular method of investigating the influence of the intermediate principal stress on the mechanical behaviour of soils has been the

"hollow cylinder" test.

Kirkpatrick (1957) tested cylindrical annular specimens of sand 4 in. O.D. × 2.5 in. I.D. × 6 in. long, surrounded with an outer membrane in the usual way, (Fig. 3.5a). On the inner surface, a second cylindrical membrane was used to isolate the pore-fluid from the internal pressurized fluid. The latter was itself isolated from the main-cell fluid so that inner and outer pressures could be varied independently, subjecting the element to radial, tangential and axial compressive stresses, the major, minor and intermediate principal stresses respectively. The latter could be varied by applying additional external loads. However, in the tests reported, this was not done, and therefore the axial stress depended only upon the magnitudes of the inner and outer pressures, and the radii of the specimen.

During a series of drained tests on sand, the outside pressure was kept constant while the inner pressure was increased to failure. Allowances were made for the stresses induced in the rubber membranes as the specimen bulged. The tests were stopped as soon as the maximum lateral pressure differential was reached, and the specimen measured. These measurements were then used in calculating the principal stresses at failure.

The distribution of radial stress from inner to outer surfaces was unknown, and a linear variation had to be assumed to calculate the average value at failure. Similarly, the average tangential stress was determined. Using these two stresses, the soil strength was found to approximate closely to that obtained in both triaxial compression and extension. Assuming that the Mohr Coulomb failure criterion was valid for the hollow cylinder tests, the distribution of tangential stress was obtained. Therefore the magnitudes of all three principal stresses were known at any point on both the inner and outer surfaces. Failure

was assumed to have occurred simultaneously throughout the thickness of the specimen.

Whitman and Luscher (1962) investigated the interaction of thin-walled aluminium tubes and surrounding annular cylinders of sand, using the hollow cylinder technique. Firstly tests were performed on the separate components, and then the combined effect was studied.

The sand specimens were 5 in. or 3 in. high and 1 in. I.D., the wall thickness being $\frac{1}{4}$ in., $\frac{1}{2}$ in., or 1 in. The pore space was evacuated while either the inner pressure was decreased or the outer pressure increased to failure. Therefore in each case the tangential stress was the major principal stress and the radial stress was the minor principal stress, failure propagating from the inner surface. Axial strain was prevented by connecting together the top and bottom plattens with a steel rod passing through the bore of the specimen. The mean radial deformation of either the inner or the outer surface could be determined by measuring the volume of water displaced from the bore or main-cell respectively, depending upon which pressure was held constant.

Esrig and Bemben (1965) carried out tests on both solid and hollow cylinders of sand in triaxial compression and extension. The stresses were adjusted at all stages to keep the specimen at constant volume, the pore-pressure remaining atmospheric throughout. Measurement of the axial deformation, and of the volume change in the bore, allowed the average radial and tangential strains to be calculated. The volume of water entering or leaving the bore could be controlled to produce variations in the strain ratios at failure corresponding to undrained triaxial compression or extension, or any intermediate condition, including plane strain.

Wu et al (1963) described hollow cylinder tests on specimens of remoulded clay and sand having dimensions 4 in. O.D. × 3 in. I.D. × 6 in.

high. After hydrostatic consolidation, the specimens were loaded to failure in the undrained manner with pore-pressure measurement. The inside and outside pressure were controlled by applying dead weights to the pistons of constant-pressure cells, and radial deformation of the specimen was determined from volume change in the bore. Stresses were applied incrementally, and failure induced by increasing or decreasing the axial stress, or by increasing the outside pressure, or by combining these two operations.

Broms and Casbarian (1965) tested hollow cylinders of clay in the consolidated undrained manner with measurement of pore-pressure. The specimens, 5 in. O.D. × 3 in. I.D. × 11 in. long, were enlarged to 6 in. O.D. adjacent to each end platten, and to facilitate pore-pressure equalization, filter paper drains were placed along the inner and outer perimeters.

The effect of the intermediate principal stress, in this case the average radial stress, was investigated by adjusting the relative magnitudes of the major and minor principal stresses to obtain stress conditions at failure ranging between triaxial compression and triaxial extension. In a further series of tests, torque was also applied to the specimen, causing the principal stresses to rotate about the intermediate stress axis, which was again radial.

During the same period that Wightman carried out plane strain tests on cuboidal specimens of granular media (3.3.1.2), Procter (1967) made a comparative study using the hollow cylinder method on thin-walled, $2\frac{1}{2}$ in. I.D., and thick-walled, $1\frac{1}{2}$ in. I.D., specimens. In each case the specimens were 6 in. high × 4 in. O.D. For the plane strain condition, the strengths of the two cylinders were unequal, and each exceeded that of the comparable cuboidal specimen.

Procter, in common with many investigators, assumed that the radial

stress, which is necessarily non-uniform in this type of test, was distributed linearly across the wall of the hollow cylinder. The true distribution probably depends upon the wall thickness and end restraint.

Therefore the possibility of buckling, the uncertainties associated with progressive failure and with interpretation of strain data, and the dependence of analysis upon the assumed stress distribution, render the results from hollow cylinder tests inconclusive.

A large number of laboratory tests have been devised to measure soil properties related to strength, such as penetration resistance. However, in most cases these are of little value in improving the understanding of soil behaviour, and will not be considered here.

3.4 SUMMARY

This chapter has outlined the requirements of laboratory soil testing associated with investigation of the fundamental factors controlling stress-deformational behaviour.

Many techniques, which are now common to the majority of testing apparatuses and procedures, were developed initially to improve the uniformity of stresses and strains, and the accuracy of measured quantities, in the triaxial compression test.

After reviewing the development of methods for axially-symmetrical testing, various attempts to subject soil specimens to generalised three-dimensional stress or strain conditions were described.

The design and development of the Aston Triaxial Apparatus, and the procedure used for testing soil under generalised stress conditions, which have constituted a major part of the author's research program, will be discussed in Chapter 4.

The review of previous testing apparatuses was continued by outlining the principles involved, and the practical difficulties encountered, in applying shear stresses or torque directly to specimen boundaries. Finally, attempts to vary the intermediate principal stress by subjecting hollow cylinders of soil to differing inside and outside pressures were discussed, and the disadvantages, particularly the inevitable stress non-uniformity, were stated.

CHAPTER FOUR

THE ASTON TRIAXIAL APPARATUS

DESIGN, DEVELOPMENT AND TESTING TECHNIQUE

4.1 INTRODUCTION

In the preceeding chapter the objectives of laboratory stress-deformation and strength testing of soils were discussed together with their past and present methods of execution. This chapter describes the design and development of the Aston Triaxial Apparatus, its merits and limitations, and current testing techniques. For convenience, the apparatus will be referred to as the "ATA". Where appropriate, distinction will be made between the Mk.I and Mk.II apparatuses. In the absence of such a distinction, it should be assumed that comments relate to the ATA Mk.II.

The basic principles considered in the design of the apparatus, including the choice of one strain-controlled and two stress-controlled boundaries, are discussed in section 4.2. The side stress-cells, used to apply stress to the specimen on one pair of parallel vertical surfaces, are described in detail, since they represent one of the main features of the ATA. Methods of sealing the specimen to its membrane and of providing adequate drainage are considered, and evidence that pore-pressures remain negligible, for the chosen rate of testing, is presented.

In section 4.3 the importance of measuring axial stress at both ends of the specimen and of reducing rigid boundary constraint is emphasized, and the development of the end stress-cells, which help to fulfill these objectives, is described. Various experiments carried out to confirm their suitability are mentioned.

The methods used to measure specimen deformations are covered in

section 4.4, reference being made to the corrections which must be applied to axial and volumetric deformations, and which are described more fully in Appendices B and C. Measurement of the lateral deformations of ATA specimens is discussed, and it is pointed out that there is no redundancy of measured quantities.

In section 4.5, specimen homogeneity is considered in relation to specimen formation. The difficulties of assessing the degree of homogeneity are stated.

The techniques used to test soil specimens under various stress conditions in the ATA are discussed in section 4.6. Many of these techniques are common to the tests carried out under more conventional conditions. They are described in this chapter for the sake of completeness, and will be referred to in subsequent chapters when dealing with triaxial testing of cylindrical and cuboidal specimens.

The advantages and disadvantages of consolidating ATA specimens under ambient and K_o conditions are stated, with respect to the type of test being carried out.

The bulk of the author's research program involved testing under triaxial compression and plane strain conditions, together with tests in which the intermediate principal stress was varied, the orientation of the three principal stresses being the same in each case. These are described in detail.

Further types of ATA tests, with alternative orientations of principal stresses, are discussed, and attention is drawn to certain practical limitations concerning the side stress-cells.

4.2 BASIC PRINCIPLES

The generalised case of stress-deformation of soils under field conditions is one in which the stresses and strains are different in each of their three principal directions at a point.

One method of testing in the laboratory under these conditions is to apply three independent principal stresses to the boundaries of a cuboidal specimen (3.3.1.2). If it is assumed that the distribution of stress and strain within the specimen is initially homogeneous, and remains so throughout a specified period of the test, then measurements of boundary strains together with knowledge of applied stresses will make possible a complete analysis of the deformational behaviour. It is on this principle that the ATA is based. Reorientation of principle stresses with respect to the specimen axes is limited to instantaneous 90° rotations.

4.2.1 STRESS- AND STRAIN-CONTROLLED BOUNDARIES

It was pointed out in 3.3.1.1 that some systems purporting to control the stress on test specimens, do instead control applied load, since the cross-sectional area of the specimen usually is not constant. Similarly, many so-called strain-controlled tests do not apply deformation to the specimen at a constant rate.

Particularly during the early stages of a test, elastic compression of the proving-ring, and other components, reduces the rate of deformation. However, although strain-rate has been shown to affect the behaviour of even cohesionless soils (Lee et al 1969), the variation here is probably negligible. Therefore for most practical purposes the loosely-defined terms "stress-control" and "strain-control" are adequate.

The difficulties that can be encountered in attempting to apply three independent principal stresses to a cubic or cuboidal specimen in a fully stress-controlled manner have been emphasized in discussions on

Ko and Scott's apparatus, (3.3.1.2). Problems of mutual interference of the stress systems along the edges and at the corners of the test specimen are considerable, particularly if it is intended to study stress-deformational behaviour at strains up to and beyond failure.

The difficulties at two strain-controlled boundaries are not so great, since the gap between loading-plattens need be large enough merely to allow relative movement between them without contact. Most soils are capable of arching across such small gaps. However, if all three boundaries are strain-controlled, either the strains are very limited, as in the Kjellman-type apparatus, or a complex mechanical system is necessary to prevent interference of the plattens and, at the same time, keep the gaps between them small.

From a practical point of view, therefore, it would seem that a combination of two strain-controlled boundaries with one stress-controlled boundary is the optimum arrangement. This has been used in the majority of plane strain apparatuses, where clearly the mechanical problems are reduced by the fact that one pair of plattens remains static, and in some "three-dimensional" apparatuses.

A serious drawback to this system, however, is the inevitable non-uniformity of stress resulting from the use of rigid plattens on four surfaces. This is of less significance if analysis is based on knowledge of localized stresses rather than on an assumption of stress homogeneity, but such cases are few and are usually limited to considering stress variation at the boundaries only.

In the Aston Triaxial Apparatus two of the boundaries are stress-controlled, each using fluid pressure. The remaining boundary, though strain-controlled, is not subject to the usual degree of uncertainty regarding stress-distribution, since rigid end plattens are not used (4.3.2).

4.2.2 THE A.T.A. SPECIMEN - SIZE AND SHAPE

Previous methods of varying three independent principal stresses were reviewed (3.3.1.2) in two basic categories - those imposing boundary principal stresses to a cubic or cuboidal specimen, and those using the hollow cylinder technique. Of the two, it was suggested that the former method is preferable provided that boundary stresses and strains are sufficiently uniform for their overall measurements to be used in analysis.

The ATA specimen is cuboidal in shape, being approximately 4 in. in height and $2\frac{1}{4}$ in. square in cross-section. These dimensions have been varied a little from time to time with improvements in testing technique and may also be adjusted to suit chosen test conditions.

Initially, during the development of the Mk.I apparatus, a cylindrical rubber membrane, or sleeve, intended primarily for 2.8 in. diameter triaxial specimens was used to surround the ATA specimen. In addition to the considerable difficulty experienced in sealing the membrane to the top and bottom plattens, the "corners" of the cuboid had noticeable curvature.

It was decided, therefore, to manufacture specimen membranes of exact dimensions in the laboratory using a liquid latex (Appendix A). At the same time flanges and upstands necessary to ensure adequate sealing at top and bottom were incorporated in the design (Fig. 4.1a). The average membrane thickness was approximately 0.013 in., except for surfaces not in direct contact with the specimen, where this was increased to 0.021 in. to reduce susceptibility to leakage. Sand specimens formed within these membranes are cuboidal in shape with well-defined edges.

The specimen membrane is sealed at the top in the conventional way using two or more rubber O-rings. The top platten, and the top

stress-cell (4.3.2), each have a circular upstand, around which the seal is made (Figs. 4.4, 4.5, 4.7).

At the bottom, a flange, approximately $\frac{1}{2}$in. wide, projects inwards from the base of the specimen membrane, and is compressed between the upper and lower sections of the bottom platten, or bottom stress-cell (4.3.2), as they are screwed into the main-cell base. Two soft rubber gaskets, positioned above and below the membrane sealing-flange, ensure that a watertight seal is made (Figs. 4.4, 4.6, 4.8).

4.2.3 APPLICATION OF BOUNDARY STRESSES

The two pairs of vertical surfaces of the ATA cuboid are stress-controlled; the top and bottom horizontal surfaces are strain-controlled.

Fluid pressure has long been used in triaxial and other apparatuses to apply uniformly-distributed stress to the surface of test specimens without impairing freedom of deformation. The ATA specimen is itself fully enclosed within a cylindrical perspex cell, and de-aired water, which fills the cell, is used to apply stress in the x-direction (Fig. 4.4b) to one pair of parallel surfaces. This stress also acts on the top and bottom of the specimen as it does in the conventional triaxial compression test.

Stress in the y-direction is independent of pressure in the "main-cell", being applied through two identical "side stress-cells" (Figs. 4.2a, 4.3) to the remaining pair of vertical surfaces.

Each side stress-cell consists of a stainless-steel side-frame and backplate fixed securely together to form a hollow, rigid compartment 4.66 in. × 2.19 in. × 0.51 in. The front of each compartment is covered with a flexible latex rubber membrane, 0.013 in. thick, which during a test remains in contact with the specimen. The compartments are water-filled and pressurized and hence a uniform stress

is transmitted to the specimen surface in the y-direction. Like the cuboidal specimen membranes, the side stress-cell membranes are manufactured in the laboratory, their size and shape (Fig. 4.1b) being such as to fit neatly into the compartment and be adequately sealed.

Several methods of sealing were attempted before the current one proved consistently successful. The backplate is secured to the side-frame with twenty-eight brass screws spaced evenly around the perimeter. A flange on the side stress-cell membrane, sandwiched between two soft-rubber gaskets, fits between the backplate and side-frame, and is provided with holes to clear the brass screws. Therefore, when these two components are screwed together, the membrane is squeezed tightly between them forming a watertight compartment. This method facilitates easy renewal of the membranes which fatigue with use and possible over-stressing.

The side stress-cells are filled with de-aired water through polythene capillary tubing connected securely into the bottom of each compartment. Air is removed through a de-airing screw at the top of each backplate, the top section of the side-frames being chamferred to assist de-airing. To ensure that an equal pressure is applied through each side-cell, their supply tubes are connected into the same duct in the main-cell base.

Once placed in position on opposite surfaces of the specimen, the two side-cells are connected together with four stainless-steel tie-bars, screwed to the top and bottom of the side-frames (Fig. 4.4b). The length of the tie-bars is such that when each compartment is water-filled flush with the front surface of the side-frames, the side-cell membranes and specimen membrane are in contact. Some variation of specimen width in the y-direction is allowed for in the slightly over-sized holes through which the tie-bars are screwed to the side-cells.

Soft rubber washers enable a secure connection to be made when the screws are tightened.

Because the side-cells remain fixed in position during a test, relative movement between the specimen membrane and side-cell membranes occurs with axial and lateral strains. It is essential to keep friction between these surfaces to a minimum, and therefore each is smeared with silicone grease before every test.

If stresses in the x- and y- directions are to remain independent, there must be no mutual interference of the stress systems. Therefore the specimen should cover the whole surface of each side-cell to prevent differential pressure across the flexible membrane surface. This inevitably means that at some stage during a test, the specimen encroaches a little onto the stainless-steel surround and hence uniformity of stress over this very small area is no longer certain.

In practice it was found that the side-cell membranes could in fact sustain a small pressure differential providing the "exposure", i.e. the visible area of membrane exposed to side-cell pressure, was small, and that the main-cell pressure was the smaller of the two. In early experiments it was noticed that up to 5 lbf/in^2 pressure difference could be tolerated with a 0.1 in. strip of membrane exposed. Conversely with less exposure, the system could withstand greater pressure differences.

Should exposure become excessive, the side-cell membrane may "balloon" into the main-cell in an attempt to equalize pressures or may burst. In either case renewal, rather than repair, of the membrane is essential.

Slight, tolerable membrane exposure is helpful, in certain cases, during the setting up process. However, it is preferable for this to be kept to a minimum because the volume of water entering or leaving the side-cells is used to determine specimen strain in the y-direction,

(4.4.3.1). Large exposures may impair the accuracy of these measurements.

Both x- and y-direction stresses may be controlled manually or connected to a self-compensating mercury pressure control system (Bishop and Henkel 1953).

It is desirable to make regular checks on the side stress-cell membranes, tubing connectors and ancillary components in order to confirm that they are watertight. Two perspex covers (Fig. 4.4a) are secured firmly in position covering the side-cell membranes, making use of the tapped holes provided primarily for the fixing of tie-bars. The pressure is then increased to an appropriate level using the screw-jack. If a significant drop in pressure occurs within a period of at least 10 minutes, the cause may then be further investigated.

4.2.4 DRAINAGE CONDITIONS AND RATE OF TESTING

Investigations into the stress-deformational behaviour using the ATA have, to date, been confined to cohesionless soils. Because their permeability is relatively high, the rate of testing was decided by other factors, such as the ease of measurement of stresses and strains, or adjustment of these quantities to maintain a required stress- or strain-path.

Where stresses or strains were changing continuously, their rates of change were low enough to ensure negligible pore-pressures. In other cases, where stress increments were applied, sufficient time was allowed for full dissipation of pore-pressure. Therefore throughout the experimental program it was assumed that total and effective stresses were equal.

In the Mk.I ATA, where rigid top and bottom plattens were used (Figs. 4.5, 4.6), specimen drainage was through a $\frac{1}{2}$ in. dia. porous disc, $\frac{1}{4}$ in. thick, set into the centre of each platten. Suitable

ducts through each platten connected into the drainage system and thence to a burette. In general, because of the high soil permeability, it was unnecessary to use both top and bottom drainage. However, provision for both allowed de-aired water to be passed slowly through the prepared specimen and drainage connections, in order to purge them of any possible remaining air bubbles.

The end stress-cells of the Mk.II ATA prevent a similar drainage system being used. Since the surface of both top and bottom stress-cells is fully covered with a flexible rubber diaphragm (Figs. 4.2b,d, 4.7, 4.8) the provision of drainage holes is impossible. Therefore water is forced to leave the specimen through filter paper drains laid between the specimen membrane and the sides of the top stress-cell. Rectangular bauxilite porous stones set into a peripheral channel in the stress-cell, below the membrane sealing rings, and in communication with a top drainage tube, complete the drainage path. There is no provision for drainage at the bottom of the specimen.

During one particular test carried out on a cuboidal specimen under conventional triaxial conditions, without side stress-cells, the Mk.I ATA bottom platten was used in conjunction with the Mk.II ATA top stress-cell. Drainage was allowed to take place through the top stress-cell only, as described above. The porous disc in the bottom platten was connected, through the drainage duct, to a pressure transducer.

Using this arrangement, the specimen was tested at the maximum rate of axial strain, approximately 0.1% per min., applied to any ATA specimen during the current research program. Any pore-pressures set up during the test did not exceed 0.05 lbf/in^2, the limit of sensitivity of measurement, hence confirming the assumption regarding effective stresses.

4.3 MEASUREMENT OF AXIAL STRESS

In the conventional triaxial compression test, and in some of its many variations, axial stress, applied to the specimen via rigid end plattens, is known with far less certainty than the lateral stress, resulting from fluid pressure.

The axial load is measured using a proving-ring external to the cell and therefore friction between the loading plunger and cell bushing reduces the load actually applied to the specimen. The frictional loss is usually of unknown magnitude, though Bishop and Henkel (1957), and Olsen and Campbell (1967) suggest methods of correction.

Methods of reducing or eliminating this effect have been used in triaxial and other apparatuses.

Clearly the frictional force will increase with lateral load on the plunger, which normally is either rigidly connected to the top platten or centrally located using a ball-bearing or a half-ball. With large strains, particularly those beyond failure, non-uniformity of lateral deformation and possible tilting of the top platten increases the lateral force on the plunger. Penman (1953) interposed a ball-race between the plunger and top platten in an attempt to minimize this force. The increased use of end lubrication of test specimens has, in addition to its other advantages, had a similar effect.

By rotating the bushing at a high rate relative to the rate of penetration of the plunger, the vertical component of the frictional force is considerably reduced. Wood (1958) incorporated two sets of rotating bushing in his plane strain apparatus. However, although Parikh (1967) has shown that the error can, in this way, be reduced to less than 1% of the axial load, Green (1969) and Thomas (1970) have noticed that the applied load may fluctuate, especially at low strain-rates, after slight wear of the mechanism. Thomas also observed fluctuations of pore-pressure, measured with a pressure transducer, during

undrained loading of Lias clay specimens.

Duncan and Seed (1967) used a ball-bushing to reduce the frictional loss.

The effect of plunger friction on the measured axial stress can be eliminated by measurement inside the cell. Nash and Dixon (1960) incorporated a load cell in the bottom platten of their apparatus for undrained triaxial testing of sands at very high rates of strain. Electrical resistance strain gauges were used.

Geuze (1948) had previously used a hydraulic pressure cell to measure vertical load on the bottom platten in his vacuum triaxial apparatus (Fig. 3.2b).

Internal proving-rings are still subject to errors caused by lateral force transferred from the specimen. A ball-and-socket connection between an internal ring and the top platten was used by Barden and Khayatt (1966). While permitting the application of both tensile and compressive loads, this arrangement allowed the top platten to tilt freely, thus helping to minimise this force.

Bishop and Green (1965) used a flat steel proving-ring within the cell in conjunction with a differential inductance displacement transducer. Careful calibration is necessary to establish both the mechanical and electrical stability of this type of system.

4.3.1 THE Mk.I A.T.A.

In the Mk.I apparatus, axial load was measured with a proving-ring external to the main-cell.

Each end of the specimen was lubricated using a 0.010 in. thick membrane cut to the size and shape of the end plattens and smeared with a thin layer of silicone grease. A $\frac{1}{2}$ in. diameter circular hole cut centrally in each lubricated membrane to expose the porous discs,

allowed unhindered drainage.

The top platten was loaded through a ball-bearing so that the specimen was free to tilt. This arrangement has been shown to reduce lateral force on the plunger, and hence friction, during conventional triaxial testing. However, in the ATA the side stress-cells are fixed rigidly in position around the specimen and therefore any slight eccentricity of initial setting up in the y-direction increases plunger friction despite these precautions. In addition, although the side-cell membranes are lubricated with silicone grease, there will inevitably be a small vertical component of frictional force acting over these surfaces. When axial strain in positive, this will result in the axial stress at the bottom of the specimen being slightly smaller than that at the top.

A situation could develop in certain ATA tests, especially at large strains, where encroachment of the specimen onto the stainless-steel surrounds of the side-cell faces drastically increases this frictional force and hence also increases the difference between top and bottom stresses. This is clearly highly undesirable, for apart from the even greater error incurred in proving-ring measurement of the axial load, the deformational behaviour of the specimen is seriously affected. The situation is similar to that apparent in Ko and Scott's "soil test box".

The results of early plane strain tests carried out in the Mk.I ATA (Appendix G), giving peak strengths highly in excess of most previously reported values, were indicative, at least, of the effect of plunger friction on external proving-ring measurements. The need to measure values of axial stress at the top and bottom of the ATA specimen, both accurately and independently, was evident.

4.3.2 THE Mk.II A.T.A.

Results of experiments using the Mk.II apparatus form the basis of discussion on the behaviour of soils under generalised stress conditions reported herein. The apparatus is also being used, without radical alteration, in a continuation of this research program being carried out at present in the Department.

The end plattens of the Mk.I ATA were amended for use not only in transmitting axial stress to the specimen, but also in measuring its magnitude. In consideration of this rôle they were termed "stress-measuring cells", which became abbreviated to "stress-cells". Hence the descriptions "top stress-cell" and "bottom stress-cell" were consistent with that of the side stress-cells. These terms are not meant to imply that their functions are always identical with the latter, though in the majority of tests carried out in this program, this was the case.

The methods used to seal the rubber membrane at the ends of the specimen, which were found adequate during tests using the Mk.I apparatus, were retained in the Mk.II design. Therefore the shape of each end stress-cell is similar to that of the original end-platten. However, the dimensions were altered to allow a recess to be machined in each working-surface. When covered with a flexible diaphragm, a hollow compartment is formed, similar to those in each side stress-cell (Figs. 4.7, 4.8). Approximately 75% of the total "working-surface" of the perspex top stress-cell is recessed, leaving a 0.15 in. wide peripheral flange to which a soft rubber diaphragm is glued.

The hollow compartment is filled with de-aired water through polythene capillary-tubing sealed into the top of the stress-cell using a brass connector. Because the compartment is non-uniform in section, water entering at the lowest corner displaces air towards the highest

corner, the sloping surface ensuring that no air pockets are formed. A de-airing screw is positioned at the top of the stress-cell, immediately above the highest corner of the compartment.

During the filling process, the stress-cell is placed face-down on a flat surface, in the position it occupies during a test, so that the rubber diaphragm cannot bulge. The remote end of the polythene tubing is connected to the supply via a duct in the main-cell base, and a brass transducer block (Fig. 4.10, 4.11).

The transducer block consists of a rigid, rectangular, brass block into which a pressure transducer (Consolidated Electrodynamics 4-326, 0 - 100 lbf/in^2) is permanently fixed. Two water supply taps and a de-airing screw are interconnected with the transducer through small diameter holes in the block, and the whole assembly is attached to a Klinger tap at the main-cell base.

Therefore, when the de-airing process is complete, with the de-airing screw and the water supply taps closed, a small continuous volume of de-aired water is wholly confined within the following components:- the hollow compartment of the top stress-cell, the polythene capillary-tubing, a duct in the main-cell base, and the transducer block. With the exception of the flexible rubber diaphragm this system can be shown to be effectively rigid, so that a pressure applied directly to the diaphragm will be transmitted, with negligible volume change, to the confined de-aired water and hence measured with the pressure transducer.

The stress-cell is designed to operate using a constant volume of de-aired water and therefore although the diaphragm is flexible its average deflection, with respect to the end plane of the stress-cell, will be zero. During a test, local flexing of the diaphragm no doubt occurs in order to maintain stress uniformity, but this is likely to be

of small magnitude.

Several types of diaphragm and adhesive were used before the optimum combination was decided for the top stress-cell - natural rubber, average thickness 0.052 in., and Araldite AZ/HZ 107.

The bottom stress-cell, like the bottom platten of the Mk.I apparatus, is brass and in two sections, between which the specimen membrane is sealed (Figs. 4.2c,d, 4.8, 4.9d). The upper section is recessed in a manner similar to the top stress-cell, leaving a 0.15 in. flange as before. Rubber used to form the diaphragm is identical with that used for the top stress-cell diaphragm. In this case, Araldite AY/HY 111 was found to be the most suitable adhesive. However, in some early tests, during dismantling of the specimen, sand grains sometimes forced themselves into the joint between the rubber and brass, causing a peeling effect and eventually leading to a complete failure of the stress-cell. This was prevented by dipping the upper section in liquid latex which, when dried, formed a suitable barrier.

The duct in the main-cell base previously used to drain the specimen is now, in the Mk.II apparatus, connected to a transducer block similar and adjacent to the top stress-cell transducer block.

The recess in the upper section of the bottom stress-cell is machined so that when the diaphragm is turned face-down all interior surfaces of the hollow compartment slope upwards towards a central hole. Because the bottom stress-cell must be screwed into the main-cell base, with the specimen membrane sealing-flange in position between the two sections, this hole must be used to both fill and de-air the compartment. Separate provision for each was at first envisaged but early trials showed that the following de-airing system was efficient:-

The upper section of the stress-cell is inverted and submerged in

a container of de-aired water. By continually pressing and then releasing the diaphragm, air is pumped out of the hollow compartment to be replaced by water. During this process the stress-cell is gently tapped and shaken to ensure that no air-bubbles remain adhered to the inside surfaces. When air-bubbles no longer emit from the hole in its base, it is assumed that the stress-cell is de-aired.

This system was checked by de-airing the top stress-cell in the same way. After sealing off the normal supply hole, the de-airing screw was removed and the stress-cell filled by "pumping" the diaphragm. The effect, which could be observed through the transparent perspex, was entirely satisfactory.

After positioning the specimen membrane and lower section, there then remains the delicate operation of righting the complete bottom stress-cell and sealing it into the main-cell base (4.5.1).

When top and bottom stress-cells are used in the Mk.II apparatus approximately 75% of their working-surface area must be uniformly stressed, since this is the area over which fluid pressure is acting. However, the stress-cells are enlarged in the x-direction, in the same way as the previous end plattens, to assist the uniformity of lateral strain. Therefore part of the rubber diaphragm glued to the solid flange is not in contact with the specimen during the initial stages. This means that certainty of uniform stress applies to 80% of the total initial end area of the specimen.

The stress conditions existing over the remaining 20% of the end area are unknown, but it can be assumed that the end lubrication will help to keep variations small (Shockley and Ahlvin 1960). At both top and bottom of the specimen, one 0.010 in. thick rectangular rubber membrane, slightly undersized, is smeared with silicone grease and placed in position covering the diaphragm. Because the width of the

peripheral flange is only 0.15 in., it is also unlikely that the zone of influence of any local stress concentration would be great, relative to the specimen length.

It can be stated with some certainty that stress concentration due to the effects of "arching" (Terzaghi 1936) will be negligible. Terzaghi investigated the variation in load on a trap door, as it was vertically displaced away from a retained sand mass, in an attempt to extend knowledge of stress distribution in sand around tunnels.

The phenomenon is clearly important in the design of any device for measuring stress or strain in granular media. In their investigations into the effectiveness of embedded earth-pressure cells, Trollope and Currie (1957) confirmed the recommendation of the U.S. Waterways Experiment Station (1944) that the diameter to deflection ratio of a circular diaphragm should be not less than 2000 : 1. If this condition is not met, particularly in poorly-graded granular materials, stress concentration and arching could occur.

In order to investigate the deflection of top stress-cell diaphragm, due to compressibility of the confined fluid or expansion of any components under pressure, a small air bubble was introduced into the top of the polythene capillary-tubing which connects the stress-cell eventually to the transducer block. The movement of the air-bubble in the tubing was observed during a test in which the axial stress reached approximately 60 lbf/in^2, and hence the apparent volume of water displaced from the stress-cell could be estimated. An allowance was made for the compression of the bubble itself. However, there is a possibility of compensating errors due to expansion of the stress-cell compartment balancing expansion of the system on the other side of the air-bubble. A second test was therefore devised in which the stress-cell alone was placed in the main-cell. This eliminates

stress-cell expansion when the cell pressure is increased, since internal and external pressures are equal. Unfortunately the same argument applies to the tubing so that it was possible, using this arrangement, to estimate only the combined effect of compression of the confined fluid and expansion of the main-cell duct and transducer block. Based on these two experiments alone, there is still some possibility that compensating expansions of the stress-cell compartment and the tubing could result in a significant underestimation of the diaphragm deflection. However, the total capillary volume of the tubing is small and, in addition, this type of tubing when put to similar use in other apparatuses, shows minimal expansion under pressure.

Combining the results of the two experiments, the volumetric expansion of the system under an internal pressure of 60 lbf/in^2 was estimated at 1.5×10^{-3} in^3, and by assuming an approximately linear mode of deflection from flange to centre, and taking the worst case of the minimum span, an estimate of the maximum span-deflection was made. Although very approximate, the value obtained, 3300 : 1, is well within the limit suggested by the U.S. Waterways Experiment Station to prevent arching across circular diaphragms.

4.4 MEASUREMENT OF STRAINS

If it is possible to apply and measure directly the boundary stresses on a soil specimen then, providing stress homogeneity can be assumed, measurements of strain are unnecessary in the determination of strength. Idealized failure criteria for soils, including the traditional Mohr-Coulomb, take no consideration of strain. However, there are few apparatuses which purport to measure all boundary stresses directly, Ko and Scott's "soil test box" being an example.

In the majority of strength tests, including conventional triaxial compression, at least one of the principal stresses is calculated from measurements of axial load. Therefore it is imperative that the mode of deformation of the specimen, and hence an appropriate cross-sectional area, is known in order to determine the stress.

Unlike some routine commercial testing, research into the behaviour of soils under stress is not normally limited to the failure condition. Usually knowledge of overall or incremental values of principal strains, or direct and shear strains, is sought for all stages of stressing. These quantities must, therefore, be determined with an accuracy compatible with that of stress measurement.

Most apparatuses used in stress-deformation studies rely on boundary measurement of stress and strain, together with the assumption of homogeneous distribution throughout the specimen. Attempts to measure the true distribution of strain fall into two categories, those using strain-gauges embedded in the specimen (Shockley and Ahlvin 1960, Januskevicius and Vey 1965), and those using X-rays.

With the latter technique, the image of lead shot, placed usually in a regular pattern within the specimen, is obtained on a radiograph at various instants during a test. By superposition of successive radiographs, total and incremental strains can be determined. Roscoe,

Arthur and James (1963) described the method with reference to model tests in plane strain and (1964) tests in the Cambridge simple-shear apparatus. Arthur and Shamash (1967) discussed accuracy and methods of reducing errors in detail.

By passing X-rays in two directions, through lead shot embedded in a triaxial compression specimen, Kirkpatrick and Belshaw (1968) were able to investigate the effect of end restraint on strain homogeneity.

The problems to be overcome in extending the technique for use in generalised three-dimensional investigations are, however, considerable. It therefore seems likely that in the near future the majority of this work will continue to rely on the assumption that boundary strains are representative of overall behaviour. This has been assumed, with some reservations, in tests carried out in the ATA.

4.4.1 AXIAL STRAIN

In conventional triaxial testing, axial strain of the specimen is calculated from the displacement of the loading piston relative to a point on the cell top. This basically is the method used to determine strain in the axial- (or z-) direction in the ATA. However, the use of top and bottom stress-cells to measure axial stress allows the proving-ring to be dispensed with, and therefore the deflection dial gauge is instead mounted immediately below the loading crosshead (Fig. 4.11).

Because the gauge is remote from the specimen, there is a clear likelihood of a discrepancy between the measured deflection and the true deflection of the specimen, the major sources of error being expansion of the cell, elastic compression of the various intermediate components, and bedding of the soil at the stress-cell surfaces. Since these errors are common to the majority of apparatuses, many

attempts have been made to reduce or eliminate them.

Bishop and Henkel (1957) suggested the use of an optical micrometer focused onto a convenient reference point, usually a ball-bearing, at the top of the specimen.

El-Sohby (1964), concerned particularly about cell expansion, attempted to provide an alternative reference point not on the cell top. In choosing the pedestal of the loading machine, however, he introduced a further bedding error between this pedestal and the cell base.

Barden and Khayatt (1966) used two dial gauges within the cell to measure the vertical deflection of two diametrically-opposed points at the edge of the top platten. The use of 4 in. × 4 in. dia. specimens allowed these gauges, and an internal proving-ring, to be accommodated in air above the specimen, the gauges being mounted at the top of rigid steel bars fixed to the cell base. Calibration was still necessary in order to allow for bedding of the specimen at the ends, the compression of lubricated membranes, and for the squeezing out of the lubricant under pressure. A comparison was made between this system, that used by El-Sohby, and the conventional method.

Clearly internal measurement is more reliable, but Barden and Khayatt apparently did not attempt to correct for the errors inherent in the other two methods, and expressed doubts regarding the reliability of calibration for cell distortion under varying cell pressure.

A series of careful calibration experiments was carried out (Appendix C) in order to correct the measured deflections of the ATA specimen. Similar calibrations were necessary for all other tests executed on cylindrical and cuboidal specimens in this research program.

The same main-cell was used in all tests and no particular

difficulty was experienced in the calibration for cell distortion under pressure. However, the system for clamping the cell to its base was different from that used by Barden and Khayatt, and the stress level in tests was generally lower.

The axial strain is calculated from the corrected axial deflection and the specimen length (4.5.2), natural strains being used in all cases.

4.4.2 VOLUMETRIC STRAIN

Because of the difficulties associated with measuring lateral strain in the conventional triaxial test, it has been customary to determine an average value for this quantity from axial and volumetric strains.

Attempts to measure lateral strain of the specimen from the volume of water entering or leaving the cell are often unreliable, even at constant lateral stress when distortion of the cell should be negligible, because of leakages, especially around the plunger. Davis and Poulos (1963) eliminated this loss by pressurizing a cavity between the plunger and the bushing, using castor oil. The cavity pressure was always equal to the cell pressure.

In most cases, however, even when lateral strains are measured directly, the measurement of volumetric deformation is a reliable check. More usually, its determination alleviates the need to measure all of the remaining strains where this is impracticable.

Research into the stress-deformational behaviour of cohesionless soils usually involves testing specimens which are either fully-saturated with de-aired water or completely dry. Therefore in either case the pore-fluid may be assumed to be homogeneous. However, the effect of pore-fluid on the frictional characteristics of the mineral surfaces

is not known with certainty.

Horn and Deere (1962) have shown that although water has an anti-lubricating effect between massive-structured minerals, such as quartz, this effect decreases rapidly with surface roughness. Therefore for real sand particles, as opposed to polished blocks of quartz, the frictional properties are very similar in the air-dry and submerged conditions. Use of the latter condition in the testing of cohesionless soils is slightly advantageous from a practical standpoint and eliminates the possibility of surface water films causing capillary forces between particles.

The volumetric strain is determined from the volume of pore-fluid crossing the specimen boundary at one or more specific drainage points. It is assumed that all other points on the surface of the specimen are impermeable. If air is in the pore-fluid, this assumption may be unreasonable, especially in long duration tests, due to diffusion of air through the membrane. This applies equally to cases where specimens are "saturated" with water which has not been de-aired, and where air is used as, or is present in, the confining-fluid.

The use of either air or de-aired water as the sole pore-fluid simplifies measurement of volume change since a single interface can be formed in the measuring device.

All tests carried out in the ATA used de-aired water as the confining-fluid, in both the main-cell and side-cells, and as the pore-fluid. Volume change of the specimen was calculated from readings of meniscus movement in a 50 ml burette, and the strain determined using the initial measured volume (4.5.3).

Considerable errors may be incurred in the measurement of the volumetric deformation of a cohesionless soil if the effect of membrane penetration into the voids between particles is ignored (Newland and

Allely 1959). The apparent volume change exceeds the true volume change of the specimen by an amount dependent upon the size and shape of the particles, the magnitude of the differential pressure across the membrane, the thickness of the membrane, and the shape and size of the specimen.

Attempts have been made to correct volumetric strains in triaxial specimens to allow for this effect. Unfortunately, because of its dependence on the shape and size both of the individual particles and of the specimen, it is impossible for corrections to be generalised and calibration is normally required for each variation of these factors.

Newland and Allely carried out experiments on triaxial specimens of coarse lead shot enclosed within a very thin membrane, to exaggerate the penetration effect, and measured the axial and apparent volumetric deformations during ambient consolidation. They assumed that the specimen behaved isotropically and therefore the true volumetric strain should have been three times the axial strain. The difference between this and the apparent volumetric strain was taken to be the necessary correction.

Roscoe et al (1963b) compared this method with another in which annular cylindrical specimens were used. Cylindrical brass rods, varying in diameter between $\frac{1}{4}$ in. and $1\frac{3}{8}$ in. were placed coaxially within $1\frac{1}{2}$ in. dia. sand specimens, which were then consolidated under ambient pressure and the apparent volume change measured. By assuming that membrane penetration is a surface property unaffected by the presence of the brass rods, they were able to extrapolate the results to the hypothetical condition of a $1\frac{1}{2}$ in. dia. brass rod having surface properties identical with those of the sand. The apparent volume change must then be due entirely to membrane penetration.

It was concluded that this method was less reliable than that based on axial deformation, since the assumption that the rods have no

effect on the surface properties of the specimen may not be justified even if the porosity is the same in each case. However, the possible error from this source is likely to be small and certainly far less than that incurred by assuming isotropic behaviour in the other method. The experiments of McMurdie and Day (1958) quoted to justify the latter assumption, are much less reliable than those carried out by El-Schby (1964), using a refined method of measuring axial deformation. These results showed clearly that, for virgin ambient loading of vertically-deposited specimens, lateral strain exceeds axial strain.

The assumption of isotropy would lead to an overestimation of membrane penetration and therefore explains why Roscoe et al determined a larger correction, using the "axial deformation" method of correction, and questioned the reliability of the "rod method".

A method similar to the latter was used in determining the membrane penetration corrections to be applied to ATA test results (Appendix B).

4.4.3 LATERAL STRAINS

Attempts to measure directly the lateral strain of triaxial specimens have generally been based on changes in cell-water volume.

In the vacuum triaxial apparatus (3.3.1.1), confining fluid is unnecessary so that access to the specimen is possible at all stages of a test. However, lateral pressure is limited to one atmosphere. The ingenious method used by de Josselin de Jong and Geuze in their "capacitive cell apparatus" (3.3.1.1) is impracticable in most cases. Optical methods of determining the profile of cylindrical specimens, especially in triaxial extension (Roscoe et al 1963), enable realistic cross-sectional areas to be used in computing axial stress from load measurements.

None of these methods is particularly suitable for use in generalised three-dimensional testing of cuboidal specimens. The use of optical methods is often precluded by the presence of the apparatus itself.

4.4.3.1 Strain in y-direction

In ATA experiments, stress is applied in one lateral direction, the y-direction, using the side stress-cells described in section 4.2.3. Each side-cell is effectively rigid except for the rubber membrane surface through which the specimen is stressed. Polythene capillary-tubing is used to connect the side-cells into a duct in the main cell base which leads to the pressure control system. Volume change of the tubing, which is of the same type used for the end stress-cells, is negligible. Providing the side-cells and ancillary connections are properly de-aired, and the working-surfaces are brought into full contact with the specimen, movement of water into or out of the side-cells will be a measure of specimen deformation in the y-direction.

This method has been used in other apparatuses in which stress is applied through a flexible surface. Ko and Scott (1967) determined the three direct strains in this way, and Sutherland and Mesdary (1969) measured one of the lateral strains, each type of experiment being carried out using cubical specimens.

Clearly it is difficult to establish the degree of uniformity of deformation using this method since the specimen surface is not visible during a test. Therefore only the average strain can be calculated. However, at the end of ATA tests, by careful removal of the side-cells, it was normally possible to examine the relevant surfaces and hence estimate the likely mode of earlier deformation.

Ko and Scott were unable to examine specimens after tests in their

apparatus , since none were enclosed in a rubber membrane. In order to establish the mode of deformation microscope sightings were made through windows in box walls. Their claim that uniform deformations occur in this type of apparatus was disputed by Arthur and Menzies (1968).

4.4.3.2 Strain in x-direction

The magnitudes of strains in the x-direction are, in the ATA, derived from corrected measurements of strains in the y- and z-directions and volumetric strain. Because the x-direction strain is not determined independently there is no additional check on measured values, such as is possible in Ko and Scott's apparatus.

Sutherland and Mesdary also allow for such a check by measuring one of the lateral strains with two pairs of deflection dial gauges mounted, using Barden and Khayatt's (1966) system, above the specimen in air. They report good overall agreement of strain measurement and good uniformity of lateral strain in the direction of the gauges. Green (1969) used encapsulated dial gauges to determine specimen strain in the direction of the lateral loading plattens in his "independent stress control" apparatus.

In the design of the ATA it was intended that strain in the x-direction be determined from the change in volume of cell water, after correction for cell distortion under pressure. However, in early experiments the loss of cell water due to leakage, predominantly around the plunger, was significant. The size of the main-cell, which is used for triaxial compression and extension tests in addition to ATA tests, further precluded the use of internal dial gauges. Therefore it was decided that, for the present, strain in the x-direction should be derived from corrected measurements of the remaining strains.

4.5 SPECIMEN PREPARATION AND MEASUREMENT

It has been assumed, for the purposes of analysis, that stresses and strains applied to the boundaries of the ATA specimen are distributed homogeneously throughout its interior. This assumption is common to the majority of laboratory stress-deformation tests and, likewise, efforts have been made to reduce boundary effects to a minimum.

In some of the more sophisticated apparatuses, X-ray techniques have provided information on internal strain distribution (4.4) and in others stress-gauges have been embedded in the specimen (4.4).

Homogeneity of the specimen itself is a different, but associated, problem which is relevant, with very few exceptions, to stress-deformation investigations in general. The greater the degree of initial inhomogeneity, the less will be the probability of overall average strains measured at the boundaries being representative, unless the specimen becomes more homogeneous under the applied stresses. Therefore the aim should be to prepare a specimen which is initially homogeneous, and which has not been subjected to any previous significant stressing.

The distribution of porosity, or voids ratio, in the prepared specimen is indicative of its degree of homogeneity. It should be emphasized, however, that initially uniform porosity in no way implies isotropy. The mechanical properties of the soil in various directions cannot be described using a single scalar quantity, i.e. the concentration of particle mass within a given volume as measured by porosity or voids ratio. Initial anisotropy is dependent also upon the geometrical arrangement of the particles. Subsequent behaviour of a specimen will further depend upon additional anisotropy induced by the applied stresses (Horne 1965).

Apart from the desirability of any one prepared specimen being

homogeneous, it is expedient to be able to reproduce initial porosities within close tolerances, so that deformational behaviour over a variety of stress-paths may be reasonably compared. In addition, much research concerned with the strength of cohesionless soils under various boundary conditions attempts to distinguish quite small differences in behaviour, e.g. the difference between peak strengths of specimens under conditions of axial-symmetry and plane strain. Therefore it is important that porosities are known with sufficient accuracy to rule out apparent differences which might otherwise be due entirely to inadequacy in preparation and initial measurement. Consequently many workers have investigated methods of specimen preparation and measurement and have devised means by which to assess their effectiveness.

In general, it is clear that no one system of preparation is suitable for all cohesionless soils, from the viewpoint of both particle size and initial porosity. Very loose and very dense specimens in particular require markedly differing techniques. Methods for measuring the initial physical properties of the specimen are also abundant, and depend more on their suitability to the apparatus and testing procedure.

4.5.1 SPECIMEN FORMATION

All specimens tested in the ATA during this research program were fully saturated. Stress-deformational behaviour was investigated over a range of initial porosity between the maximum and minimum values (Kolbuszewski 1948).

ATA specimens were prepared primarily by vertical deposition, in most cases followed by vibration. These are the two basic components of the formation process used in the majority of apparatuses. Kolbuszewski (1948) showed that the height of fall and rate of deposition, or "density of rain", had an important effect on the resulting

porosity of dry sands. Slightly higher minimum porosities were obtained by pouring through water, but these were due largely to entrapped air. It was not possible to produce higher densities by pouring through water alone, since the rate of deposition was greatly decreased.

Cole (1967), reported by Roscoe (1967), experimented with several different types of hopper for depositing dry sand specimens in the Cambridge Mk.6 simple-shear apparatus, and eventually used three different hoppers to obtain each of three different initial porosities. When preparing medium dense or dense specimens, it was found advantageous to place two $\frac{1}{4}$ in. wire meshes in the flow. Using a collimated γ-ray beam (Coumoulos 1967) it was shown that uniform specimens were produced, uninfluenced by the pattern of holes in the hopper. Without the wire meshes this was not the case, even when pouring from a height of 12 inches. Loose specimens were prepared using a hopper without meshes, which allowed the sand to fall in one mass, the discharge area of the hopper and the area of the specimen container being equal.

However, if it is required to test saturated specimens, these methods may not be practicable. Having deposited dry sand, it is very difficult to achieve subsequent full saturation, even using a slow upward flow of de-aired water, since air bubbles become trapped between the particles. In an attempt to overcome this problem, Shockley and Ahlvin (1960) used ammonia gas in place of air during deposition. Because ammonia is very soluble in water they were able to achieve a degree of saturation of 0.99 when the specimen was flooded.

When preparing saturated sand specimens, it has become common practice to submerge the sand in water and boil thoroughly in order to remove any air (Bishop and Henkel 1957). From this point onwards the particles are kept submerged, any transference from one container to

another being done under water. This principle was adhered to in the formation of all specimens tested in this research program.

The procedure used in the preparation of ATA specimens was as follows:-

Having decided the required porosity and knowing the approximate initial volume, a mass of oven-dried sand, slightly in excess of that required to form the specimen, was weighed together with its container. The sand was then submerged, boiled thoroughly and left to cool.

Meanwhile the bottom stress-cell was de-aired (4.3.2) and a sound, normally freshly-manufactured specimen membrane (Appendix A) together with its two rubber gaskets placed in position between the upper and lower sections of the stress-cell. De-aired water was flooded into the gap between the membrane and the stress-cell, and around the gaskets, so that when the stress-cell was screwed down, simultaneously sealing the specimen membrane to itself and itself into the main-cell base, this water was forced out helping to ensure air-free joints. Excess water was then bled from the bottom stress-cell system until the diaphragm was horizontal in its working-position (Fig. 4.2d), and the specimen membrane was filled with de-aired water to a height about $\frac{1}{2}$ in. above the stress-cell diaphragm. This caused the membrane to bulge out around the sides of the stress-cell allowing inspection for trapped air-bubbles, which could easily be removed.

The four sides of the perspex specimen-former (Fig. 4.12) were then brought into position around the bottom stress-cell and screwed together, taking care not to trap the specimen membrane in the joints as they were closed (Fig. 4.9a).

Both top and bottom stress-cells are enlarged in the x-direction and hence overlap the specimen at the ends. Consequently the two sections of the former which are normal to this direction have been

suitably recessed to clear the stress-cells when in position.

The remainder of the membrane was filled with de-aired water through supply tubing lowered to the level of the stress-cell diaphragm.

Because the membrane is manufactured to the exact size and shape of the required specimen, it fits closely within the former. Therefore it was not necessary to apply a suction to the space between the membrane and former, as is normally done in the preparation of cylindrical specimens. In the ATA system, the gradual increase in the head of water, as the membrane was filled, pressed it firmly against the sides of the former, resulting in four flat, vertical surfaces with well-defined, right-angle intersections.

When the water level reached the top of the former, the filling process was stopped while a lightly-greased end membrane was placed in position fully covering the bottom stress-cell diaphragm. The upper section of the specimen membrane, which encloses the top stress-cell, was, because of its shape, particularly susceptible to trapping air. Therefore, having filled the membrane to its brim, trapped air-bubbles were removed by stretching this section as required.

The membrane was then connected to the deposition vessel, a glass funnel of approximately one litre capacity, and sealed with a rubber O-ring (Fig. 4.9b). Finally the funnel was filled with de-aired water to about half capacity and a temporary plug inserted.

The sand was carefully spooned, under water, from its container into the funnel and the surface levelled. When the funnel plug was removed, particles discharged from its lower orifice, approximately $\frac{1}{2}$ in. in diameter, and settled at an apparently constant rate. When all the particles had been deposited, the excess water was siphoned off and the funnel removed.

Inevitably the use of a central orifice for discharging particles

into a rectangular section resulted in an uneven final surface, sand being slightly "heaped", to about $\frac{1}{4}$ in., towards the centre of the section. Since the majority of specimens were subjected to varying degrees of vibration, which levelled the surface, this was of little consequence in forming a correctly-shaped specimen. However, good shape does not imply homogeneity and it is conceivable that axially-symmetrical non-uniformities of porosity could have resulted from this form of deposition.

Excess water in the top section of the specimen membrane was removed with a pipette, and the membrane turned back over the sides of the former.

At this stage the specimen was densified to the required degree by mechanically vibrating the main-cell base and also, for higher densities, the specimen former. Even with loose specimens, which are not vibrated, the action of turning back the membrane caused slight disturbance and tended to level the surface. Levelling was completed manually if required.

Knowing the approximate dimensions of the specimen and the approximate mass of sand used, assuming the excess left in the container was small, a rough check on porosity could be made by observing the level of sand through the perspex former during vibration. If necessary a small mass of sand could be removed from, or added to, the specimen to ensure the required level surface was obtained. However, even with the use of such a check, producing any one porosity to a close tolerance was still largely a "hit-or-miss" process, the probability increasing sharply towards the dense end of the porosity range.

With the sand levelled and the specimen membrane still turned back, the de-aired top stress-cell complete with its lubricated end membrane was placed in position and the surrounds were flooded with

de-aired water. The four rectangular porous stones, submerged in water and boiled to remove air trapped in the pores, were then replaced in the top stress-cell drainage channel. A rectangular strip of filter paper was inserted between the stress-cell and specimen membrane along each face, so that it projected slightly below the stress-cell diaphragm and slightly above the porous stone, providing a continuous drainage path around the periphery of the specimen at this level (Figs. 4.9c,d).

The specimen membrane could then be carefully rolled back to enclose the stress-cell, slight downward pressure on the latter during this procedure preventing disturbance to the specimen. Again water was flooded around the top stress-cell, this time through the drainage system, and any air-bubbles trapped in the corners of the membrane were removed before the specimen was finally sealed with O-rings.

The burette was lowered to apply a small negative pore-pressure, usually 0.4 lb./in^2, to the specimen, and, having obtained a steady burette reading, the former was removed. This was most efficiently done by removing opposite sections simultaneously, thereby reducing the possibility of lateral force causing disturbance. Burette readings taken before and after removal of the former in all tests were usually very close, indicative of negligible disturbance.

Finally the excess sand was dried and weighed in order to determine the initial mass of the specimen.

It was expected that the initial porosity of ATA specimens formed using the above procedure was reasonably uniform, probably to within a tolerance of a few percent.

In the preparation of specimens for testing in the Mk.I apparatus, it was possible to fill the membrane with de-aired water through the porous disc in the bottom platten. For most purposes, upward filling

is advantageous in de-airing the system. However, in the ATA Mk.I the specimen membrane was sealed between the upper and lower sections of the bottom platten, this basic method being used also in the Mk.II. Therefore it was still necessary to carefully remove any air-bubbles trapped between the membrane and the sides of the stress-cell, below the level of the porous disc.

The difficulties involved in attempting to determine accurately the distribution of porosity throughout a prepared specimen are considerable. One of the few methods enabling this to be done without destroying the preparation is the γ-ray technique, which for this purpose was found to give an accuracy superior to that from X-rays (Coumoulos 1967). Local variations in porosity both before and during testing can be measured with great accuracy.

Cornforth (1961) determined the water-content of medium-fine sand, carefully sampled from prepared specimens. It seems unlikely that such a technique would be accurate enough to reliably distinguish the small variations in porosity that are of interest.

Green (1969) used a more sophisticated method of sampling vertical layers of dry sand specimens prepared using several different techniques. Suction was applied to a narrow-bore glass tube inserted accurately into the specimen to the required depth. By moving this "suction probe" over the surface of the sand at this one level, a known volume of the specimen was sampled, the particles being collected in a "sand trap". Combinations of spooning and static or dynamic compaction in various layers were investigated, in addition to random vibration. However, because these experiments were carried out only on dry specimens it had to be assumed that saturated specimens prepared using similar techniques would show similar variations in porosity. It was not possible to study directly the effects of

deposition through water, followed by vibration.

Shockley and Ahlvin (1960) investigated distribution of porosity by freezing the specimen in order to preserve the original arrangement of particles.

Clearly it would not be a simple matter to determine the degree of homogeneity of a prepared ATA specimen, being cuboidal in shape and fully saturated. In the absence of γ-ray equipment, one of the destructive methods described above would probably be the most suitable. No such attempt was made in this research program. However, all ATA specimens were formed in a systematic manner by deposition followed by careful vibration. Therefore, having no direct evidence to the contrary, it was assumed that the degree of homogeneity achieved was comparable with that obtained by other workers using similar techniques. If reproducibility of overall porosity can be taken as indirect evidence of homogeneity, then dense ATA specimens produced by heavy vibration are likely to be more uniform.

4.5.2 INITIAL MEASUREMENT

The methods used to measure the deformation of ATA specimens under stress were described and discussed in section 4.4. In order to calculate strains in the x-, y- and z-directions and the volumetric strain, it is necessary to determine accurately the initial dimensions of the specimen.

The use of a transparent specimen former in the preparation process is advantageous when placing the top stress-cell in position. By reference to the vertical faces and horizontal recesses in the former, firstly the sand and then the stress-cell can be finally levelled before the specimen is sealed. Thereafter, in the majority of tests, no further check was made to ensure that the ends of the specimen were

parallel, and a single mean height was measured using the following procedure:-

With a small suction applied to the pore space and the former removed, the $\frac{3}{4}$ in. ball-bearing was placed centrally in position in the top stress-cell recess. A height vernier, accurate to 0.001 in., was lowered onto the top of the ball-bearing and the height of this point relative to a fixed point on the main-cell base was measured. The measurement was twice repeated and the average value determined.

The mean height of the specimen was obtained by subtracting the mean height of remaining components, i.e. top and bottom stress-cell, lubricated end membranes, silicone grease and ball-bearing. The latter was determined prior to specimen preparation with respect to the same fixed point on the main-cell base, using the same technique.

In some early ATA tests a check was made on the variation in height at the four corners of the specimen. However, although the average of the measured heights agreed closely with the mean height obtained using the ball-bearing as reference, the results were inconclusive concerning height uniformity. Because it was difficult to clearly define reference points on the sides of the membrane or on the top stress-cell, variations in measurements could have been due entirely to experimental error.

The average widths of ATA specimens in the x- and y-directions were each determined from measurements at fifteen points, distributed uniformly over the surface, using a micrometer gauge accurate to 0.001 in. In all cases allowance was made for the thickness of the specimen membrane by subtracting 0.025 in. from the measured widths, 0.0127 being the average thickness of one surface (Appendix A). By manufacturing membranes to exact size and shape, the difficulties experienced by other workers in obtaining sharp edges to cuboidal specimens were

eliminated, and no corrections to allow for curvature were necessary.

Criticisims have been made, usually in connection with measurement of cylindrical triaxial specimens, of the use of micrometer gauges, vernier calipers and similar mechanical devices which must be brought into direct contact with the specimen in order to function. Apart from the possible specimen disturbance which may result, there is a tendency to vary the pressure on the membrane and hence repeated measurements of the same dimension may show discrepancies. Also, because measurements are made at discreet points, they may not be indicative of the average dimension in a given direction, especially if the specimen surface is irregular.

In order to overcome these difficulties, various other methods have been devised to measure the average diameter of cylindrical specimens. However, they are not generally applicable to cubical or cuboidal specimens, where it is required to measure two lateral dimensions. Therefore systematic measurement at the nodes of an imaginary grid, using the micrometer gauge, was considered the most convenient and accurate way of determining ATA specimen widths. In addition to increasing the likelihood of obtaining a genuine average dimension, this method allows any significant variations to be observed, which is not possible with methods giving only the average widths.

By ensuring that the specimen surface was dry, if necessary by dusting lightly with talc, it was found that a definite contact could be made between the instrument and the specimen which, at any one point, was repeatable to within 0.002 in. This procedure also prevented the membrane adhering to the instrument and hence prevented specimen disturbance when the instrument was removed.

A further study was made of the reliability of micrometer gauge

measurements in the program of testing cylindrical triaxial specimens, (5.5.2). Favourable comparisons were made between average specimen diameters determined in this way and those determined using a method particularly suited to cylindrical specimens.

The initial mass of the ATA specimen was determined from the mass of the originally boiled sand and the mass of the oven-dried residue. Because of the difficulties involved in dismantling the specimen without loss of sand, no attempt was made to dry and weigh the specimen after completion of the test.

Having measured the mass and dimensions of the specimen, the initial porosity calculated from these quantities applies only to the initial stress condition, i.e. an ambient stress of 0.4 lbf/in^2, resulting from the lowered burette. In an ideal method of preparation, the formed specimen should not have been subjected to any pre-stress. However, since saturated cohesionless specimens are incapable of maintaining their shape without lateral support, it is difficult to achieve this ideal. Nakase (1960) used a triaxial specimen former with a remotely-controlled latch, which opened the former only when the lateral stress was applied, in an attempt to overcome this problem, but it is difficult to see how the specimen dimensions can be determined accurately using this system.

In ATA tests, having filled the main-cell, the level of the meniscus in the burette was adjusted to the mid-height of the specimen, and was maintained at this level throughout the test, so that the average pore-pressure was always atmospheric. Therefore the initial sequence of burette movements prior to the test imposed a small cycle of stress on the specimen. An alternative procedure would be to retain the small pore-suction throughout the test and allow for this in calculating the effective stresses. However, the effect of the small stress cycle is

unlikely to be significant except possibly in tests at very low stress levels.

All of the tests in the author's research program were carried out on specimens of "Birmingham Area" sand, passing No.14 and retained on No. 25 B.S. sieves. The following section describes the techniques and procedures used in testing ATA specimens.

4.6 TESTING TECHNIQUE AND PROCEDURE

The primary objective in the design and development of the ATA was to make possible the testing of soils over a wide range of stress paths in three-dimensional stress space. In order to simplify the analysis of stress and strain within the test specimen, it was further intended that the effect of boundary restraints on the soil behaviour should be minimized. Therefore stresses were applied to all six surfaces of the cuboid through flexible boundaries, with the exception of small areas around the edges of the end stress-cells, and a lubricant was used to reduce friction on the y- and z-surfaces, where the application of fluid pressure was indirect.

The effectiveness of the several new techniques incorporated in the ATA design and of the overall suitability of the apparatus, could be rigorously assessed only under test conditions. Consequently, many of the early tests were planned not only to study the stress-deformational behaviour of the soil concerned, but also to investigate the performance of the apparatus. Unless the latter is shown to be satisfactory, experimental data must always be questionable. It was from the point of view of this philosophy that the method of axial stress measurement used in the Mk.I apparatus was superseded.

As a first step in the assessment of the apparatus, it was considered essential to compare the behaviour of a soil under relatively simple stress conditions in the ATA with the behaviour of the same soil under the same conditions in an apparatus more suited to this particular task. The most obvious standard of comparison was the conventional triaxial compression test. Therefore many of the early tests in the ATA were carried out under axially-symmetrical triaxial compression stress conditions. The results from these tests were then compared with those from triaxial tests on cylindrical and cuboidal specimens.

The latter were carried out in the conventional manner, except for the provision of end-lubrication and the use of end stress-cells, each helping to reduce boundary restraint and improve the accuracy of stress and strain measurements.

Because of the uncertainties associated with the interpretation of triaxial extension test data, a simple comparison made under these stress conditions was considered to be an unreliable measure of apparatus performance, and was therefore postponed.

Many of the present testing techniques were developed during tests carried out under plane strain conditions. By maintaining zero strain in the y-direction, exposure of the side stress-cell membranes was minimized. A comprehensive program of testing under triaxial compression and plane strain conditions was undertaken, covering a full range of initial porosities. In addition, failure was induced by either increasing the major principal stress or decreasing the minor principal stress. The latter method usually involves maintaining a constant axial stress, which in most apparatuses is inconvenient and complicated. In the ATA, monitoring this stress is facilitated by the end stress-cell systems. In consequence the results from tests carried out with either increasing or decreasing octahedral normal stress are equally reliable.

During a later series of tests the behaviour of dense specimens only, under a wider variety of stress conditions, was investigated. These included tests at values of intermediate principal stress other than those appertaining to plane strain, termed "intermediate-stress tests", and tests with the principal stresses reorientated, including the triaxial extension condition.

4.6.1 CONSOLIDATION

The majority of stress-deformation studies of cohesionless soils

are carried out on specimens saturated with de-aired water. This was the case in the author's research program.

The variation in slope of the Mohr-Coulomb failure envelope with stress level has been demonstrated by many workers, the curvature being particularly pronounced at low stresses. In order to eliminate this factor when considering soil behaviour along various applied stress paths, it is desirable to be able to control the stress level at which failure, or any other chosen stress condition, occurs. Therefore an essential preliminary stage in most tests is consolidation, the term usually implying that all increments of volumetric strain are positive.

It was not intended that the study of consolidation of soils should be one of the primary functions of the ATA; many other apparatuses have been designed especially for this purpose, often the sophistication of strain measurement having been increased to allow for the relatively small deformations which occur. The two most common forms of consolidation associated with stress-deformation testing are ambient, or all-round, consolidation and zero lateral strain, or K_o-consolidation. Both were used during tests on ATA specimens.

4.6.1.1 Ambient Consolidation

If three equal principal stresses are applied to an isotropic body, the resulting strains in the three directions will also be equal. However, soils are rarely isotropic, and laboratory specimens of cohesionless soils, prepared initially by deposition, usually have different properties in the vertical and horizontal directions. Therefore unequal strains result from the application of equal principal stresses.

In order to distinguish clearly between the applied stress system and the resulting soil behaviour, the terms "isotropic" and "anisotropic", often used loosely to describe a stress condition, will be

reserved for the description of soil properties. The term "ambient" will be used to describe the stress condition in which three equal principal stresses are applied.

In the conventional triaxial test, the cell pressure alone is used to apply ambient stress to the specimen. Because the side stress-cells isolate stress in the y-direction from the main-cell pressure, it is necessary in ATA tests to maintain equality between these two stresses throughout the consolidation process.

The compression of ATA specimens in the two lateral directions during ambient consolidation causes an increase in side stress-cell exposure. Therefore in the early tests, carried out under triaxial compression and plane strain conditions, specimens were consolidated at zero lateral strain.

Ambient consolidation was used as the preliminary stage in all the intermediate-stress tests performed on a series of dense specimens, and was found to be equally satisfactory. The usual procedure was as follows:-

After de-airing the top and bottom stress-cells, the specimen was prepared, as described in section 4.5.1, and a pore-suction of 0.4 lbf/in^2 applied, enabling the perspex former to be removed. Any extraneous material adhering to the surfaces of the specimen, which could cause puncture of the membrane if brought into contact with the side-cell stainless-steel surrounds, was carefully removed, and the initial dimensions of the specimen were measured.

The side stress-cell compartments, having been de-aired, were pressurized and checked for signs of leakage, the two perspex covers (Fig. 4.4a) being used to prevent the membrane surfaces from ballooning during this process. The covers were then removed and a thin layer of silicone grease was applied to each side stress-cell, not only over the

membrane surfaces but also over the stainless-steel surrounds. As the ATA specimen compresses axially, the top stress-cell must move downwards relative to the side-cells. Therefore particular attention was paid to greasing the two $\frac{1}{4}$ in. wide stainless-steel strips at the top of the side-cells, between which the top stress-cell must move. Although friction at this point has no effect on the magnitude of the measured axial stresses, it is desirable to reduce the possibility of frictional build-up and its subsequent dissipation causing erratic response of the loading system.

Each side stress-cell was placed centrally in position resting against the lower section of the bottom stress-cell, and supported away from the specimen at a small angle to the vertical. After checking for lateral alignment, the two side-cells were then brought slowly and simultaneously into contact with the specimen, and connected together with the tie-bars. The side stress-cell pressure was raised to about 0.5 lbf/in^2 to ensure full contact with the specimen and, after a short period, a little water was bled from each de-airing screw to reduce the pressure to zero and complete the de-airing process. Burette readings taken before and after positioning the side-cells were regarded as indicative of the degree of specimen disturbance. Often the difference in readings was not discernible; in the majority of tests it was small enough to be ignored.

The main-cell was clamped to its base and filled with de-aired water, the plunger being supported above the specimen. The burette was then raised to the specimen mid-height and the main-cell and side-cell stress systems interconnected, thus guaranteeing equality of σ_y with σ_x and σ_3 over the full range of consolidation stresses.

Ambient stress increments of 2 or 3 lbf/in^2, depending upon the required maximum stress, were applied to the specimen, and the volume

changes measured. In all cases, the observed volumetric deformations were subsequently corrected for membrane penetration (Appendix B), before calculating the volumetric strains. Therefore, in this section, further references to the volume change of test specimens, whether resulting from ambient or deviatoric stresses, will be taken to imply "apparent volume change".

Each increment of stress was maintained for a minimum of 10 to 15 minutes to ensure that excess pore-pressures were fully dissipated.

During the cuboidal triaxial test described in 4.2.4, in which pore-pressure was measured using a pressure transducer, an ambient stress of 10 lbf/in^2 was applied in a single increment, and full consolidation was observed after about 5 minutes. Therefore it would seem that the periods allowed for consolidation under the smaller stress increments were ample. They also allowed for bedding of the filter paper drains, O-rings and specimen membrane against the end stress-cells.

All stress increments were applied through a self-compensating mercury pressure control system (Bishop and Henkel, 1953), the final increment being maintained for a slightly longer period in order to check finally for signs of leakage.

No attempts were made to measure the axial deformation of the specimen.

Several investigators have attempted to determine the axial strain during ambient consolidation by maintaining contact between the loading plunger and the top platten, or ball-bearing, and observing the resulting displacement of the plunger relative to a point on the top of the cell. Apart from the difficulty of maintaining definite contact between the components without inadvertently applying axial load, bedding errors and errors due to cell distortion have greater significance at low stress levels and when the cell pressure is markedly changing.

Therefore results obtained in this way are unlikely to be reliable when, as is usual during consolidation, the strains being measured are small. Moreover, erroneous measurements may suggest feasible, yet mistaken, conclusions concerning soil behaviour. Fraser (1957), using a strain indicator fitted to the loading ram, concluded that the specimen behaved isotropically under ambient stress, which is improbable for a cohesionless soil.

4.6.1.2 K_o-Consolidation

The K_o, or zero lateral strain, consolidation condition is that under which most sedimentary soil deposits were formed. Most early interest in this condition was, however, concerned with the magnitude of lateral stresses on the sides of bins and silos containing granular material of a comestible nature. More recent experimental studies of the K_o-consolidation of cohesionless soils have concentrated largely on increasing the accuracy with which the stress ratio is measured.

In many types of apparatus, especially those used to investigate plane strain behaviour, K_o-consolidation is a convenient, and often essential, preliminary stage of the test (Wood 1958). Where the plane strain condition is effected by bringing a pair of rigid plattens into contact with two parallel surfaces of a cuboidal specimen, and thereafter maintaining them at constant separation, ambient consolidation would cause the specimen to lose contact with the plattens. Even when the plane strain plattens are positioned after ambient consolidation, a pre-stress is normally required to bed them adequately onto the specimen surfaces.

In ATA tests, it is not essential for the lateral dimensions of the specimen to remain unchanged during consolidation, since the side stress-cell membranes deflect in accordance with deformation in the y-direction. However, consolidation under K_o conditions does limit side-

cell membrane exposure, and was therefore considered preferable to ambient consolidation for the majority of early testing. Furthermore, unless sensible results could be obtained for the magnitude of K_o, the efficiency of the side stress-cells in maintaining plane strain during the subsequent stage would be questionable.

Several techniques for achieving zero lateral strain were tried, with varying degrees of success. The following method was found to be the most useful.

With the side stress-cells positioned and zero ambient stress applied through interconnected σ_x and σ_y stress systems, the loading plunger was slowly lowered into contact with the top stress-cell ball-bearing. In the absence of a proving-ring, a short $\frac{1}{2}$ in. dia. brass bar was used to transfer load from the machine crosshead to the plunger (Fig. 4.11), so that elastic compression of the loading system was negligible. The datum galvanometer trace for each end stress-cell had been recorded at zero stress.

One advantage of this system of axial stress measurement is that it allows very small changes in stress, such as those resulting from plunger contact, to be immediately observed. In conventional triaxial testing it is usually difficult to determine the exact point of contact without applying a stress to the specimen, since inevitable bushing friction affects proving-ring measurements, and visual confirmation is almost impossible when the end of the plunger is countersunk. As soon as the galvanometer traces showed a slight "kick" in the positive direction, contact between the plunger and ball-bearing had occurred.

Rarely was the specimen absolutely central with respect to the loading system. By careful use of the plunger it proved possible to correct small eccentricities without applying significant load to the specimen, trace movement being kept below the equivalent of about

0.2 lbf/in^2. Manual rotation of the plunger was found to be useful during this process. The elimination of errors due to plunger seating was very necessary because of the dependence of applied lateral stress upon measured axial deformation.

Of the many methods devised to achieve zero lateral strain during consolidation, that proposed by Bishop (1950) for triaxial specimens, based on correlation between axial and volumetric strains, has proved one of the more successful.

As the specimen is strained axially, the lateral stress is adjusted to maintain equality between the volume change of the specimen and the volume swept out by the top platten, i.e. the product of axial deflection and initial cross-sectional area. The resulting lateral strain must be zero.

This method was used for ATA specimens, the absence of proving-ring compression permitting the application of a slow and constant rate of axial deformation, which facilitates the necessary manual adjustments. A rate of strain of approximately 0.06% per min. was found to be suitable. A mercury "null-indicator", subsequently used during plane strain tests, was also incorporated in the K_o-consolidation system as a secondary check against volume change of the side-cells. Readings of volume change and lateral stress were taken at regular intervals of axial deformation, and the recording-oscillograph was "run" simultaneously to record the galvanometer deflections subsequently used to calculate the axial stress at each end of the specimen.

In some of the early tests, the null-indicator alone was used to monitor strain in the y-direction. With the two lateral stress systems interconnected, the device proved insensitive to small changes of volume and "spongy" in operation, so that it was possible to increase lateral stress above the K_o value without apparent lateral strain.

Sensitivity was greatly improved by isolating the σ_x and σ_y systems. Movement of the mercury thread was nullified by adjustment to σ_y, the value of σ_x being adjusted by the same amount to maintain equality of the lateral stresses. An increment of σ_y causing movement of the thread in one direction would be counteracted by the corresponding increment of σ_x, and consequently the process was one of continual over-compensation and readjustment. Although the stress increments were always small, the inevitable inequality of σ_x with σ_y had a significant effect on the null datum. As σ_y was increased, the exposed areas of the side-cell membranes expanded. Because of the small time-lag between the adjustment of σ_y and σ_x, the increments of σ_x were rendered ineffective in preventing this happening. With each expansion, the increase in σ_y required to maintain the apparent null datum caused a further expansion. The resulting error in the assessment of side-cell volume change was such that considerable lateral strain of the specimen could occur without detection, causing decreased volumetric compression and underestimation of the magnitude of K_o. Therefore the method used in the majority of ATA tests to achieve K_o-consolidation was that based on volume change control.

One of the disadvantages of this method for use with cohesionless soils is the effect of membrane penetration on volume change measurements. The difference between apparent and genuine volume changes is dependent upon the specimen porosity and the stress on the affected surfaces. Corrections for membrane penetration are usually carried out after the test, since the variation of porosity with applied stresses cannot be predicted accurately beforehand, especially at large strains.

Fortunately the volume changes during consolidation are small and occur steadily, so that it is possible to estimate each increment from its predecessors. Therefore using tables or graphs of membrane

penetration against lateral stress, for various porosities, the necessary corrections can be made to the apparent volumetric deformations and the true specimen volume changes compared with those required for zero lateral strain. Adjustments to the lateral stress can then be made accordingly.

Clearly the use of this method in the study of K_o-consolidation of cohesionless soils is open to criticism. Apart from the difficulties involved in its operation, and the uncertainty of its success until analysis is complete, correction for membrane penetration is less reliable at low stresses. Incorrect allowance for membrane penetration, lack of dexterity with the apparatus, and wayward estimations of porosity and stress changes, led to several of the early tests departing a little from zero lateral strain. However, the method described was found to be substantially better than the alternatives tried, and was therefore considered suitable for use in the preliminary consolidation stage of ATA tests.

4.6.2 TRIAXIAL COMPRESSION TESTS (ATA TC)

Stress-deformation tests under conventional triaxial compression stress conditions were performed on specimens prepared over a wide range of initial voids ratio. All specimens were first consolidated under zero lateral strain conditions as described in the previous section.

4.6.2.1 Increasing σ_{oct}

Following consolidation, the σ_x and σ_y stress systems were switched from manual control to self-compensating mercury pressure control. The lateral stresses thereafter remained at their maximum K_o value. This value varied from test to test depending upon the last stress increment applied at the end of consolidation.

The rate of change of lateral stress increases with axial deformation during K_o-consolidation and therefore a convenient value of total axial deformation was chosen for the end of the stage. After calculating the required corrected volumetric deformation, the lateral stress, σ_3, was adjusted to obtain the appropriate reading on the burette. On occasions, compensation could have been achieved only by a violent change in the rate of increase of σ_3, which was considered inadvisable. In these circumstances, the consolidation stage was often prolonged to allow the correction to be spread over several increments of deformation. Consequently, the final magnitude of lateral stress was not a specific chosen figure, and there was little reason to make it so, since the corresponding value of axial stress, σ_1, also varied depending on the initial density of the specimen. Therefore σ_{oct}, the octahedral normal stress (the mean value of the principal stresses), was slightly different for each test, at the end of consolidation, its value ranging from about 15 to 20 lbf/in^2.

The tests were concluded by applying axial deformation at a constant rate of 0.0024 in. per min., equivalent to a strain rate of approximately 0.06% per min., that used during K_o-consolidation. This was also the rate at which plane strain specimens were tested, the choice being dictated by convenience of taking measurements, and making any necessary adjustments, rather than drainage requirements. A faster rate of strain was later shown to be satisfactory in permitting pore-pressure dissipation (4.2.4).

At regular intervals of axial deformation burette readings were taken and the axial stresses recorded. Usually the recording-oscillograph was run for about 5 seconds, the traces showing the variation in σ_1 over this period, the corresponding axial deformation increment being about 0.0002 in. At regular intervals, and when particular

changes or fluctuations of stress occurred, the run time was extended, sometimes to several minutes' duration. Continuous running throughout the test was not, for most purposes, either necessary or advisable, since even at its lowest paper speed, the recorder would issue several yards of ultra-violet-sensitive recording paper. This increases the possibility of error in correlating the measurements of stress and strain. Each time the recorder is stopped, there is a definite break in the galvanometer traces which can more easily be associated with the appropriate axial deformation. However, the manner in which the axial stresses change shows as a corresponding movement of the traces on the oscillograph, even when the recorder is not being run. Although, during one test in a later series, the recorder was run continuously for long periods prior to the failure condition, little additional information was gained.

It was hoped to investigate the magnitude of lateral strains in the x- and y-directions during ATA triaxial compression testing by measuring the volume change of the side-cell and main-cell systems. It was apparent at an early stage that leakage of water between the plunger and bushing would render measurements of main-cell volume change useless. Moreover, the paraffin gauges (Bishop and Donald 1961) used for measurement were not sufficiently sensitive in determining the side stress-cell volume changes and, being remote from the testing machine, required extensive calibration for expansion of the tubing and connectors under pressure. Judgement was deferred until a more suitable device for lateral strain measruement (4.6.4) could be developed. However, examination of the specimens after test, with the side-cells removed, supported the belief that the magnitudes of the two lateral strains were similar.

Because σ_3 remains constant throughout the second stage of the

test, the value of the octahedral normal stress depends only upon σ_1. Therefore neglecting small fluctuations in the magnitude of the axial stress, increments of σ_{oct} were always positive prior to failure.

The next section describes tests carried out with σ_{oct} decreasing prior to failure. Both series of tests were performed on specimens prepared over a range of initial porosities.

4.6.2.2 Decreasing σ_{oct}

By maintaining a constant value of axial stress and decreasing the lateral stress, after consolidating the specimen at zero lateral strain, failure was brought about with decreasing σ_{oct} and identical ordering of the principal stresses.

In conventional types of apparatus, where axial load rather than axial stress is measured, methods of applying principal stresses in constant proportion or, in general, controlling the value of σ_1 in a strain-controlled test, are complicated and often inaccurate. Usually the load must be calculated, as the test proceeds, from proving-ring readings. The current average cross-sectional area, determined from axial and volumetric deformation measurements, must then be used to calculate the axial stress. If corrections for membrane penetration have to be applied to volume changes, or if adequate provisions have not been taken to limit bushing friction, gross errors may result.

The process is one of continual prediction and correction, similar to that described for K_o-consolidation of ATA specimens, but subject to greater errors as the strains are generally much larger. Some tests on ATA Mk.I specimens were carried out in this way (Appendix G). However, apart from the errors described, no account could be taken of frictional loss over the σ_y surfaces.

In the ATA, axial stress at each end of the specimen, measured

using the stress-cells, is shown as a galvanometer trace on the recording-oscillograph. Therefore, in order to keep σ_1 at a constant value, it is necessary merely to monitor movement of the two traces, no graphs or tables being required.

If specific values of σ_1 are to be applied in correlation with another quantity it is, of course, necessary to know the relevent calibration factors. However, an immediate calculation of the exact magnitude of the top and bottom axial stresses can be made.

During this series of ATA tests, the above method was used to keep σ_1 constant, any adjustment being made by varying the lateral stress. Negative increments of σ_3 were normally necessary prior to failure. The top and bottom axial stresses were normally very similar at the end of K_o-consolidation. A mean value was chosen at which to maintain σ_1 and adjustments were made so that the mean deviation of the two galvanometer traces was zero. In some early tests only one of the traces was monitored, and hence any variation in the other caused a slight change in mean axial stress.

Readings of volume change were taken at regular intervals of axial deformation as before, and the axial stresses simultaneously recorded. A short period was always allowed between adjustment of the stresses and measurement of these quantities.

All ATA triaxial compression tests were continued beyond the peak stress ratio condition in order to investigate post-failure deformations. At the end of each test, the stresses were reduced to zero and a small negative pore-pressure applied, by lowering the burette, before the side stress-cells were removed. The specimen was examined closely before dismantling.

4.6.3 PLANE STRAIN TESTS (ATA PS)

Many engineering problems in soils approximate closely to the

plane strain condition. The deformations of embankments and of the soil behind retaining-walls, for instance, are generally limited almost entirely to directions perpendicular to the longitudinal axis of the structure.

Various apparatuses for subjecting laboratory specimens to plane strain deformations were reviewed in section 3.3.1.2.

ATA plane strain tests were performed by keeping the mean separation of the two side stress-cell membranes constant, thus limiting strains to x-z planes.

4.6.3.1 σ_x- constant

The mercury thread null-indicator, present during K_o-consolidation but not used actively to maintain zero lateral strain, was used in all ATA plane strain tests.

Following consolidation, the lateral stress systems were isolated, σ_x being held constant at its current value by switching from manual to self-compensating mercury pressure control. The null-indicator datum was re-established and thereafter maintained by manual adjustment of σ_y, the intermediate principal stress. A rate of axial deformation of 0.0024 in./min. was applied, and burette and σ_y readings taken at regular intervals, the axial stresses being recorded as before.

Clearly, some of the comments regarding the suitability of the null-indicator in correctly registering lateral strain during consolidation, apply equally to the plane strain stage. However, the nature of specimen deformation is such that the errors probably decrease with strain.

In the preparation of ATA specimens, width in the y-direction may be increased slightly by using rubber gaskets between the sections of the perspex former, hence minimizing side-cell membrane exposure.

This procedure was used in later plane strain tests and is acceptable in all tests where overall strains in the y-direction are positive, since, in these circumstances, the stainless-steel side-cell surrounds should not come into contact with the specimen. Ideally, in the plane strain case, the specimen should be able to slide freely between the surrounds without interference.

Test results and specimen examination after removal of the side-cells suggest that significant departure from this ideal did not occur. Exposure of the side-cell membranes, apparent either at the beginning of the test or at the end of consolidation, decreased with increase in strain, and therefore any deviation from the plane strain condition would have been more likely during the early stages of a test.

4.6.3.2 σ_3-constant

ATA plane strain tests in which failure was brought about by decreasing the minor principal stress, were carried out in a manner very similar to that described in section 4.6.2.2 for ATA triaxial compression tests.

In order to maintain constant axial stress, σ_x was adjusted so that the mean deviation of the two galvanometer traces, from their positions at the end of consolidation, was zero. Prior to failure the applied increments of σ_x were negative. Each adjustment naturally affected the specimen strains, and counteractive adjustment of the intermediate principal stress was necessary in order to balance the null-indicator. This in turn affected the major principal stress, σ_3, thus completing the cycle. Consequently the process was one of continual, and often continuous, adjustment of the three principal stresses, to achieve both constant σ_1 and plane strain.

The rate of deformation and procedure for taking readings were

those described in the previous section. As with the ATA triaxial compression tests, specimens were prepared over a range of initial porosities, and deformation was continued beyond peak stress ratio in order to investigate post-failure behaviour. After test, a small pore-suction was applied and the specimen examined, in particular for planarity of the y-surfaces and the presence of discontinuities.

4.6.4 INTERMEDIATE-STRESS TESTS (ATA INT)

The ATA was designed to allow stress-deformation tests on soil specimens to be carried out over as wide a range of principal stress conditions as possible, without the nature of the apparatus itself becoming a parameter of the soil behaviour. A fundamental limitation of the ATA is the restriction of principal stress reorientations, to sudden 90° rotations. However, with certain ordering of the principal stresses it was hoped to cover the full range of intermediate principal stress values from σ_1 to σ_3. With alternative ordering, relative to the axes of the specimen, it was anticipated that part of this range could again be covered, and hence the effect of initial anisotropy investigated.

Because of certain practical limitations, it is not possible to carry out ATA tests over a full range of σ_2 for all possible ordering of the principal stresses. In particular, tests cannot be performed with the main-cell pressure, σ_x, greater than the side-cell pressure, σ_y, since the water in the main-cell will force its way between the specimen and the side-cell membranes. Even if great efforts were made to ensure that there was no initial membrane exposure, it would be highly optimistic to hope that contact between the specimen and the side-cell surrounds would isolate the two stress systems.

The reverse pressure differential, $\sigma_y > \sigma_x$, can be applied successfully because the strength of the side-cell membranes allows them

to bridge the small gaps, or "exposures", between the specimen and the stainless-steel surrounds. Moreover, if σ_y is never less than σ_x, there is no tendency for the side-cell and specimen membranes to lose contact.

Theoretically it should be possible to apply the three principal stresses ordered in any of the remaining permutations, which are shown in Table 4.1.

TABLE 4.1

CATEGORY	PRINCIPAL STRESSES			TYPE OF TEST	SYMMETRY
	σ_x	σ_y	σ_3		
(i)	σ_3	σ_3	σ_1	ATA TC	z-axis
(ii)	σ_3	σ_2	σ_1	ATA INT	none
(iii)	σ_3	σ_1	σ_1	ATA TE	x-axis
(iv)	σ_3	σ_1	σ_2	ATA INT	none
(v)	σ_3	σ_1	σ_3	ATA TC	y-axis
(vi)	σ_2	σ_1	σ_3	ATA INT	none
(vii)	σ_1	σ_1	σ_3	ATA TE	z-axis

All intermediate-stress tests listed in the table include the special case of plane strain.

During the author's research program, interest was centered on the first two categories. Triaxial compression along the z-axis and plane strain have already been described. This section discusses the remaining intermediate-stress tests in category (ii). Tests in categories (vi) and (vii) were also executed with success, and the methods necessary to perform the triaxial extension tests in category (iii) were attempted. However, no complete tests in categories (iii), (iv) and (v) have, as yet, been carried out using the ATA Mk.II.

Following the plane strain tests, described in section 4.6.3, on

specimens prepared over a range of initial porosities, intermediate-stress tests with the same orientation of principal axes were executed on a series of dense specimens only. The value of σ_2 at failure, relative to the magnitudes of the major and minor principal stresses, was different in each case. A useful way of expressing this relationship is that proposed by Bishop (1966), using the parameter b, given by $\frac{\sigma_2 - \sigma_3}{\sigma_1 - \sigma_3}$. Hence b varies between 0 and 1 as σ_2 varies between σ_3 and σ_1.

In the case of plane strain, the value of b at failure depends upon the density of the soil, and therefore these tests do not represent unique conditions of stress such as are imposed in intermediate-stress tests. The situation is similar to consolidation under zero lateral strain, where a strain condition is specified and the stresses are dependent upon the response of the specimen. Generally the value of b, at failure, in plane strain varied between 0.2 and 0.3. The intermediate-stress tests were intended to investigate the stress-deformational behaviour of dense specimens over the remaining range of b.

All specimens were consolidated under ambient stress to the required value of σ_3. The σ_x stress system was then isolated from the σ_y system and switched to mercury pressure control, so that it remained at this constant magnitude for the remainder of the test. After lowering the plunger into contact with the top ball-bearing and establishing datum readings of galvanometer trace deflections and axial deformation, σ_y and σ_3 were increased together to the required value of σ_2. This was done by increasing axial deformation slowly at a constant rate, and calculating the top and bottom axial stresses from oscillograph readings. The value of σ_y was continually adjusted to the mean of these two stresses. In some intermediate-stress tests, a proving-ring

was used to measure axial load external to the cell for the purpose of comparison with stress-cell measurements.

In general, adjustments were kept small and often made in anticipation of increase in σ_3, since change of one stress slightly affected the other.

Upon reaching the pre-determined value of σ_2, σ_y was switched to mercury pressure control, set in advance to this magnitude of stress so that the change-over could be effected without shock to the specimen. This policy was adopted for all similar switches. Therefore with σ_2 and σ_3 constant, the axial stress was increased to failure.

All of the tests in this series were stopped at peak stress ratio, or just beyond. This allowed the specimen to be examined, after removal of the side-cells, for slip surfaces on the σ_y faces. Discontinuities had been apparent on these surfaces when plane strain specimens were examined, but since deformations were, in all tests, continued well beyond the failure condition, conclusions concerning intermediate states could be based only upon appearance of the σ_x faces. As with all other tests carried out in the research program, sketches were made, or photographs taken, of relevant features either during or after the test.

The usual measurements of specimen volume change and axial stresses were taken at intervals of axial deformation. In addition the change in volume of the side stress-cell compartments was determined by measuring the volume of fluid expelled or taken in. This could not be done during the earlier ATA triaxial compression tests, owing to the lack of a suitably sensitive measuring device.

During the interim period, Thomas (1970) had designed and developed an apparatus with which very small changes in volume, occurring in a pressurized system, could be determined. By observing the movement of mercury threads in rigid capillary tubing, volume changes of less than

0.1 ml could be measured accurately and conveniently. This device was connected into the side stress-cell system, and readings were taken during the two latter stages of all intermediate-stress tests.

The stress levels at which σ_x and σ_y were made constant were chosen so that, at failure, σ_{oct} would be similar in each test, but b would vary suitably from test to test. Strain in the y-direction, and hence exposure of the side-cell membranes, naturally increases with increase of the parameter b. Therefore although measurements of side-cell volume change were precise, the confidence with which they may be used to determine true specimen strains must decrease as b approaches unity.

A test was performed at a value of b close to 1 by re-ordering the principal stresses so that σ_y became the major and σ_x the intermediate principal stress. In this way, as the value of b increases, $(\sigma_y - \sigma_x)$ decreases. Although, in this situation, the side-cell membrane exposure may become as great as before, the pressure differential across the flexible surface becomes less and consequently the magnitude of volume change errors is reduced.

Obviously σ_3 can become the minor principal stress only if a pull is exerted on the top stress-cell, since σ_x, the main-cell pressure acts also in the axial direction. The situation is similar to that appertaining to the conventional triaxial extension test, and is discussed in section 4.6.5.

Tests of the type covered in category (vi) can be carried out most conveniently, in the strain-controlled manner, by increasing σ_x and σ_y to constant values, as described for the intermediate-stress tests of category (ii), and then decreasing σ_3 to failure. An alternative procedure would be to hold σ_x and σ_3 constant and increase σ_y to failure, the possible advantage being that all increments of σ_{oct}

are of the same sign. However, added complexities are introduced by the fact that a pull must still be exerted on the specimen and, throughout the final stage of the test, σ_3 must remain constant.

Although the stress is measured directly on the z-faces of the specimen, this boundary is basically strain-controlled. Unlike the side-cells, the end stress-cells remain at constant volume and are therefore unsuitable for operation in the stress-controlled manner.

Tests in category (iii), triaxial extension along the x-axis, require merely a continuation of the second stage process used in the intermediate-stress tests of category (ii), which have been described in this section. Instead of holding σ_y constant at a predetermined value of σ_2, and increasing σ_3 to failure, the concurrent increase of σ_y and σ_3 would be continued until the peak stress ratio was reached.

The operation of category (iv) tests is again complicated by the strain-controlled nature of the σ_3 boundaries. However, stress-controlled plane strain tests may be performed conveniently, using the loading plunger to keep constant separation between the end stress-cells, which therefore register the value of σ_2. The major principal stress, σ_y, would then be increased slowly to failure. A similar procedure would be necessary for triaxial compression along the y-axis, category (v), the top stress-cell in this case being unrestrained.

Unfortunately, strain in the y-direction is known with less certainty than the axial and volumetric strains. This is likely to be a disadvantage when σ_1 acts in the y-direction, and incremental strain rate ratios are being investigated.

4.6.5 TRIAXIAL EXTENSION TESTS (ATA TE)

The results from triaxial compression tests carried out on ATA specimens, prepared over a range of initial porosities, were compared

with results from triaxial compression tests on similar cuboidal specimens performed in a more conventional manner, without the use of side stress-cells. Significant differences in the behaviour of the soil would have indicated probable interference from the apparatus. A similar comparison based on triaxial extension stress conditions would not have been as reliable, because of the decreased degree of uniformity of lateral deformation and the consequent uncertainty of analysis.

A series of triaxial extension tests were carried out on cylindrical specimens of several different initial densities, and the techniques used are described fully in section 5.6.2. Many of the points discussed are relevant also to the one ATA triaxial extension test performed on a dense specimen.

Before specimen preparation, the top stress-cell was adapted for extension testing by the attachment of a threaded brass bar to its upper surface. After consolidation under ambient stress, this bar was connected to the loading plunger, which itself was attached firmly to the crosshead of the loading machine. Therefore with all of the components connected and the cell clamped to the pedestal of the machine, axial extension deformation could be applied to the specimen, in a strain-controlled manner, and σ_3, the minor principal stress, measured with the end stress-cells.

The interconnected σ_x and σ_y stress systems were switched to mercury pressure control at the end of consolidation, and therefore the value of σ_1 remained constant as σ_3 was decreased to failure. The method used to clamp the main-cell to the loading pedestal was identical with that described in 5.6.2 for cylindrical extension tests.

Burette readings were taken and the axial stresses recorded, as before, at regular intervals of axial deformation. The test was stopped at failure, at which point side-cell membrane exposure had

become considerable, and the specimen was examined closely both before and after removal of the side-cells.

4.7 SUMMARY

In order to develop a full understanding of the relationship between stress and strain in a deforming mass of soil, it is helpful to be able to investigate experimentally the behaviour of homogeneous elements under generalised stress conditions.

It has been the purpose of this chapter to describe the design and development of the Aston Triaxial Apparatus, in which a wide variety of stress conditions may be applied to cuboidal specimens of soil. Arguments have been presented to suggest that the boundary stresses are uniformly applied and correctly measured, and that with suitable calibration, the overall strains may be calculated with only a little less certainty.

The unique components of the apparatus, and the testing techniques used during the author's research program, have been described in detail. Much of this description is relevant to the investigations of soil behaviour under axially-symmetrical stress conditions, carried out using more conventional apparatus, and discussed in the next chapter.

Despite some of its limitations, particularly those concerning the orientation of principal stresses, which have been discussed from both practical and theoretical standpoints, the author believes that the ATA is a suitable apparatus in which to investigate the stress-deformational behaviour of soils.

CHAPTER FIVE

CYLINDRICAL AND CUBOIDAL TRIAXIAL TESTS

APPARATUS AND TESTING TECHNIQUE

5.1 INTRODUCTION

The majority of early soil strength tests in which principal stresses were applied to the boundaries of undisturbed or remoulded specimens were restricted to axially-symmetrical stress conditions. Because of the comparative ease with which cylindrical "undisturbed" samples can be obtained and the stresses applied, triaxial compression testing has remained the most important routine procedure for investigating their mechanical properties. The conventional triaxial test has also been used widely in studies of the fundamental relationships between stress and strain in simpler remoulded laboratory specimens.

In Chapter 3, the objectives of laboratory stress-deformation investigations, and the various apparatuses which have been used, were discussed. Many of the refinements used at present in research tests, particularly those concerning reduction of boundary restraints and improvement in the accuracy of measurements, were developed initially for triaxial tests. These too were presented in Chapter 3, and then considered more fully, where appropriate to laboratory testing under generalised stress conditions, in the following chapter.

Although concerned primarily with the description of the Aston Triaxial Apparatus, and of the techniques employed in performing the various types of ATA test, Chapter 4 covered many topics common to the majority of the author's experimental work. These will not be repeated here, and the reader will constantly be referred to the relevant sections of the preceeding chapter.

The present chapter covers cylindrical triaxial tests, carried

out in both compression and extension, and triaxial compression tests on cuboidal specimens. The basic principles are discussed in section 5.2, and then, in 5.3 and 5.4, the means by which the stresses were measured and the specimen strains determined, are described for each type of test.

Unless the degree of homogeneity of the prepared specimen is satisfactory, and the measurement of its initial dimensions accurate, it is unlikely that test data will be reliable enough to distinguish the cause of small variations in behaviour. The methods of specimen formation and initial measurement are covered in section 5.5, and an investigation into the accuracy of vernier micrometer measurements of the diameter of cylindrical specimens is described.

Finally, in 5.6, the procedures used during all three types of test are stated, attention being given especially to the triaxial extension test, in which faulty technique may often be more critical.

5.2 BASIC PRINCIPLES

All of the tests discussed in this chapter were executed in the same triaxial cell, which was also that in which the ATA tests were performed. The dimensions of the ATA specimen were chosen originally so that the side stress-cells and other attachments could be accommodated within the cell, and a commercially-available cylindrical membrane used to surround the cuboidal specimen. Of the several basic sizes of specimen that may be tested in the Clockhouse Universal Triaxial Cell, that of 2.8 in. diameter was most convenient in this respect. Although it was eventually decided to manufacture cuboidal membranes, the optimum size of the ATA specimen had been determined by these considerations.

Providing specimens are homogeneous, relative size should not affect their behaviour. However, measurement errors in particular, and possibly boundary effects also, become less significant with increasing specimen size. Therefore, other factors being equal, it should be advantageous to test larger specimens.

All cylindrical specimens tested were 2.8 in. in diameter, and the cuboidal specimens were approximately $2\frac{1}{4}$ in. square in cross-section, similar to those used in the ATA.

5.2.1 CYLINDRICAL TRIAXIAL COMPRESSION TESTS (CYL TC)

In the solution of many types of engineering problems in cohesionless soils, the value of ϕ, as determined from a cylindrical triaxial compression test, is the sole parameter used to describe the soil's mechanical properties. In more sophisticated treatments, the nature of the relationship between stress and strain determined from such tests may be extrapolated to predict soil behaviour under field conditions.

Providing it may be assumed that the minor and intermediate

principal stresses are equal (3.3.1.1), and that boundary friction is negligible, two principal stresses are known with certainty, and the average stress in the third principal direction is also known. However, since rigid end plattens are used to apply axial load, it is almost certain that the latter stress is not uniformly distributed, even though lubricated end-membranes may be used, (Shockley and Ahlvin 1960).

In this program, fully drained tests using both conventional rigid end plattens and flexible top and bottom cylindrical stress-cells were executed. Combinations of one rigid platten and one stress-cell were used in a few tests. All of the specimens tested were nominally 5 in. long, saturated with de-aired water, and lubricated at each end using 0.010 in. thick membranes smeared with silicone grease, which fully covered the end surfaces.

The drainage system was similar to that employed for ATA Mk.II specimens. Because the end stress-cells precluded the use of end surface drainage, pore fluid was forced to drain through filter paper, positioned between the sides of the top stress-cell and the specimen membrane, into the peripheral drainage channel, and thence to a burette. The same arrangement was used for cylindrical specimens, whether tested using rigid plattens or stress-cells (Figs. 5.1, 5.2).

Because the top platten, and top stress-cell, were circular in cross-section, it was not possible to use a bauxilite porous stone in the 0.10 in. deep drainage channel. Therefore strips of fine gauze were pressed into the recess, and overlaid with filter paper. Hence the longer strip of filter paper, which was placed in position around the circumference during specimen preparation, formed a second layer. As in ATA tests, drainage was from the top only.

Most of the early tests in this series were carried out, in the

strain-controlled manner, at a rate of deformation of 0.0024 in. per min., equivalent to an axial strain rate of about 0.05% per min. This was later increased to 0.004 in. (0.08%) per min., which was found to be equally suitable for specimen drainage and recording test data.

5.2.2 CYLINDRICAL TRIAXIAL EXTENSION TESTS (CYL TE)

Opinion regarding the influence of the intermediate principal stress on the strength and stress-deformational behaviour of soils has been scanty and controversial. One way in which this influence may be investigated, to a very limited extent, in the conventional triaxial apparatus, is to rotate the principal stresses through 90°, so that the cell pressure becomes the major principal stress and also the intermediate principal stress, the system remaining axially-symmetrical. Again the assumption of equality of the two horizontal principal stresses is necessary. The stress conditions then represent the special case of b = 1, (4.6.4), the triaxial extension condition.

In order to make the axial stress the minor principal stress, a pull is usually exerted at the top of the specimen, partially counteracting the cell pressure. An alternative system employs a loading piston with a diameter equal to that of the specimen, so that axial load may be applied independently of the cell pressure. This has the added advantage of allowing tests to be carried out with increasing octahedral normal stress, which is difficult when using the former method.

In the triaxial compression test, the major principal stress is applied in the strain-controlled manner, and almost certainly stress non-uniformities occur at these boundaries. The opposite conditions exist in triaxial extension tests, where the lateral boundaries are stress-controlled. As a result, lateral strain non-uniformities result, a

"neck" commonly occurring in the specimen in which both axial and lateral strains become concentrated.

When end friction is high, a neck usually forms at about the mid-height of the specimen. The use of shorter specimens with efficient end-lubrication increases the uniformity of deformation, and the point of maximum lateral contraction tends to be displaced towards one end of the specimen (Barden and Khayatt 1966). However, there is still uncertainty associated with the computation of stresses from axial load measurements.

The cylindrical triaxial extension tests reported herein were all performed on 2.8 in. diameter specimens, 3 in. long, with 0.010 in. thick lubricated membranes at top and bottom. The rigid top platten used in some of the triaxial compression tests was adapted for extension testing by attaching a cylindrical brass bar to its upper surface.

The bar (Fig. 5.4), $1\frac{1}{4}$ in. dia. and 3 in. long, and hollowed out in order to reduce its mass, was screwed securely into the top platten, replacing the ball bearing used in compression testing. A female thread at the remote end of the bar allows the plunger to be connected. Axial stress was measured at the bottom of the specimen only, using the same bottom stress-cell that was employed in the majority of triaxial compression tests.

The cell-base must be clamped to the loading machine pedestal, during extension tests, to prevent the cell becoming suspended from the crosshead as soon as the tensile force in the plunger exceeds the weight of the cell and its contents. This was done using two specially-designed clamps formed from $\frac{3}{4}$ in. square mild steel bar. The clamps pass fully beneath the loading pedestal and have vertical upstands at each end, at the top of which four short horizontal steel sections are bolted. When positioned and tightened, these four

sections grip the base of the cell (Fig. 5.3b), hard rubber strips being used to ensure even distribution of the load. Once tightened, the clamps were not readjusted until the test series was complete.

5.2.3 CUBOIDAL TRIAXIAL COMPRESSION TESTS (CUB TC)

In general, triaxial tests on specimens other than cylindrical in shape have been performed either as control tests, used to assess the merits of certain types of apparatus, or as preliminary tests to determine the optimum shape of specimens to be used in such apparatus. Triaxial compression tests on cuboidal specimens were, in this research program, carried out primarily to compare the stress-deformational behaviour of the soil with that observed during ATA triaxial compression tests. Discrepancies could then be investigated from the point of view of apparatus interference.

The results could also be compared with those from tests on cylindrical specimens. Providing the specimens are initially homogeneous, and the stresses and strains uniform, shape should have no influence on the soil behaviour. However, it is probable that shape has some effect on the boundary restraints.

The prepared cuboidal specimens were identical with those prepared for ATA tests, the end stress-cells of the Mk.II ATA being used for axial stress measurement. In one test, the bottom stress-cell was replaced with the Mk.I bottom platten in order to confirm that porepressures were negligible, the porous drainage disc being connected to a pressure transducer (4.2.4).

5.3 MEASUREMENT OF STRESSES

In all of the tests described in this chapter, lateral stresses, resulting from the applied cell pressure, are equal in all directions. The normal nomenclature, σ_a and σ_r respectively, will be used for the axial and radial stresses in cylindrical tests.

For cuboidal tests, despite the absence of side stress-cells, the x-y-z system will be preserved, the x-direction being that in which the end stress-cells overlap the lateral extremities of the specimen (Fig. 4.4b).

5.3.1 CYL TC TESTS

When tests were carried out using rigid plattens at both ends of the specimen, the axial load was measured using a proving-ring external to the cell. Therefore the measurements were affected by friction between the plunger and the bushing. Although lubricated end membranes were used, and hence lateral force on the plunger reduced, it is likely that the magnitude of the frictional force was similar to that observed in a series of tests where, in addition to the proving-ring, end stress-cells were used to measure axial stress. The latter series accounted for the majority of triaxial compression tests on cylindrical specimens.

To form the top stress-cell, an aluminium rigid cylindrical platten, 2.8 in. in diameter, was recessed to a uniform depth of 0.25 in., leaving a 0.15 in. wide circumferential flange, onto which was glued a flexible diaphragm (Fig. 5.2). The rubber had an average thickness of 0.052 in., and was identical to that used to form the ATA end stress-cell diaphragms. However, the same adhesive was not as successful in gluing this material to aluminium, and the diaphragms of both end stress-cells had to be replaced at frequent intervals, usually

after showing signs of peeling from the flanges. A more suitable alternative adhesive was not discovered.

Polythene capillary-tubing connects the top stress-cell, through a duct in the main-cell base, to one of the transducer blocks, a $\frac{1}{4}$ in. dia. hole, diametrically opposite the narrow-bore filler hole, housing the de-airing screw and rubber sealing washer.

Unlike the ATA top stress-cell, the interior surfaces do not slope towards the de-airing point. The situation is similar with the bottom stress-cell which also has a $\frac{1}{4}$ in. deep uniform recess, and a similar flange. However, unlike the ATA bottom stress-cell, once de-aired and screwed firmly into the main-cell base, it need not be again disturbed throughout a series of tests, since the specimen membrane is sealed externally, in the conventional manner, with rubber O-rings.

In order to prevent sand grains from forcing themselves into the glued joint between the rubber diaphragm and the brass stress-cell body, during dismantling of the specimen, the stress-cell was inverted and immersed to a depth of about 1 inch in liquid latex. When dried, the thin rubber skin formed a suitable barrier.

The techniques used to de-air the respective cylindrical end stress-cells were similar to those found most suitable for their ATA counterparts.

The top stress-cell was placed on a flat surface and inclined so that the de-airing screw was at the uppermost point. A de-aired water supply was connected to the appropriate transducer block and the stress-cell filled. Continual shaking and tapping ensured that no air-bubbles adhered to the inside surfaces, and when no further air was emitted from the de-airing screw, the stress-cell was finally sealed. Having once completed the de-airing satisfactorily, it was unnecessary to repeat the process for each test, unless the performance or appearance

of the stress-cell was suspect.

Air was purged from the bottom stress-cell by submerging it in de-aired water and pumping the diaphragm, as described in section 4.3.2. However, because the compartment is uniform in section, it was additionally important, in this case, to incline the stress-cell at all attitudes, so that air would be forced into the central orifice.

Water was flooded into the bottom stress-cell duct in the main-cell base, through the transducer block, and the stress-cell was inverted and screwed down rapidly, causing the diaphragm to bulge with the excess water. This was slowly bled from the system, until the diaphragm was horizontal.

In addition to stress-cell measurement of σ_a, a proving-ring was used to measure axial load in all tests begun with ambient consolidation. For specimens consolidated under K_o conditions, the proving-ring was replaced with the brass bar used in the majority of ATA tests to tranfer load from the machine crosshead to the plunger. Lateral stress was applied and measured in the manner described for ATA tests.

5.3.2 CYL TE TESTS

Unless adequate end lubrication is provided, triaxial extension specimens tend to "neck" at about mid-height.

In two early tests, top and bottom stress-cells were used in conjunction with lubricated end membranes. In each case maximum lateral contraction occurred adjacent to the top stress-cell diaphragm. Apart from affecting stress measurements, the contraction eventually, at large strain during the second test, caused the stress-cell to burst. Therefore in all subsequent tests, axial stress was measured at the bottom only, and a rigid platten used at the top of the specimen (Fig. 5.4).

Usually, in this type of extension test, the tensile force in the plunger is measured using a proving-ring, either inside or outside the cell, and an appropriate cross-sectional area assumed in order to calculate the deviator stress. The effect of bushing friction is far more significant than in triaxial compression testing, and hence an internal proving-ring is essential, unless the frictional loss can be accurately evaluated.

Stress-cell measurement of σ_a is direct, and therefore immune from such errors.

The bottom stress-cell was that used in the cylindrical triaxial compression tests, and was de-aired and sealed as described in the previous section.

5.3.3 CUB TC TESTS

The ATA end stress-cells were used in all cuboidal triaxial compression tests to measure σ_a at the top and bottom of the specimen. External proving-ring measurements of axial load were also taken throughout each test, and therefore it was possible to estimate the effect of bushing friction at any value of axial strain.

5.4 MEASUREMENT OF STRAINS

No attempts were made to measure lateral strains during any of the tests described in this chapter. However, after the majority of cylindrical triaxial tests, in both extension and compression, the profile of the specimen was determined by measuring the mean diameter at ½ in. intervals of specimen height. The average lateral strains at intermediate stages were calculated from measurements of axial and volumetric deformation, after applying the appropriate corrections, (Appendices B and C).

The method used to determine axial deformation in both types of compression test was that used in ATA tests, the deflection of the plunger being measured with respect to a point on the cell top. For triaxial extension tests the dial gauge was inverted and cell displacement in relation to the machine crosshead was determined (Fig. 5.3b). Although direct connection between the top platten and brass bar eliminates the seating error previously associated with the ball-bearing, it is possible that errors in early deflection readings may be greater owing to bedding of the various screw threads. In this respect, the setting up process is critical, and is covered in section 5.6.3.

The volumetric deformation of the specimen, in all three types of test, was determined by subtracting the appropriate membrane penetration correction from the change of volume of the pore-fluid, measured using a 50 ml burette. The membrane penetration tests, reported in Appendix B, were performed using 2.8 in. O.D. specimens, and therefore the correction applied to cylindrical triaxial results was in direct proportion to the specimen height.

In correcting the apparent volumetric deformations of cuboidal specimens, it was assumed that membrane penetration was proportional to surface area, irrespective of specimen shape. A similar assumption

was made for ATA tests.

All deformation corrections were incorporated in the respective computer programs for each type of test.

5.5 SPECIMEN PREPARATION AND MEASUREMENT

5.5.1 SPECIMEN FORMATION

The importance of initial homogeneity of any prepared stress-deformation test specimen was discussed in section 4.4. No attempts were made to measure the distribution of porosity in prepared ATA specimens, and hence assess the degree of homogeneity. However, it was assumed that the chosen method of specimen formation produced deviations from average porosity comparable with those obtained, and measured, during other investigations in which similar processes were used.

5.5.1.1 Cuboidal Specimens

Some reservations were expressed regarding the formation of a cuboidal specimen by deposition from a central circular orifice. However, it was considered that this effect would be minimized by the fact that all particles settled through water, and all but the loosest specimens were subsequently vibrated.

These comments apply equally to all cuboidal triaxial compression specimens tested in this series, which were prepared over a similar range of initial porosity. The formation process was identical to that employed for ATA specimens, and the reader is referred to section 4.5.1 for a complete description.

5.5.1.2 Cylindrical Specimens

Once having been de-aired and sealed into the main cell base, the bottom stress-cell, which was used in the majority of compression tests and all extension tests, was not thereafter disturbed unless repair or replacement of the diaphragm became necessary.

Because drainage in all tests was from the top only, it was important to ensure that no air was trapped in the specimen during its formation. Therefore after sealing the cylindrical membrane to the bottom

stress-cell with O-rings, it was filled with de-aired water to a depth of about ½ in., and manipulated to remove any air-bubbles trapped below the level of the diaphragm. A similar procedure was used when the rigid bottom platten replaced the stress-cell.

The circular lubricated membrane, slightly under 2.8 in. in diameter, was placed in position, and the two halves of the brass cylindrical specimen former were clamped together around the bottom stress-cell. De-aired water supply tubing was then lowered into the former to below the existing water level, and the membrane filled to its brim. The glass funnel, used as the deposition vessel in the preparation of ATA specimens, was connected to the top of the specimen membrane and half filled with de-aired water. The sand, which had been boiled and cooled, was then transferred under water into the funnel and deposited as before.

Although still "heaped" a little towards the centre, the deposited sand surface was an improvement on that obtained for cuboidal specimens. Vibration was applied to the cell base as required, before positioning the top stress-cell, or top platten.

The triaxial compression specimen former was recessed at the "5 in. level". This allowed the top stress-cell unrestricted movement following the application of a small pore suction, thereby reducing the tendency of the specimen to "neck". For this to be successful, it was necessary to finish the sand surface slightly above the 5 in. level.

After placing the filter paper strip around the circumference of the top stress-cell and flooding the surrounds with de-aired water through the drainage system, the specimen membrane was turned back and sealed with O-rings.

The formation process for triaxial extension specimens was essentially the same, except that the specimen former was 2 in. shorter,

being recessed at the "3 in. level". It was particularly important, in this type of test, to ensure that the top platten was horizontal, and hence that the brass bar, used to connect the platten to the loading plunger, was vertical. Even relatively small inclinations may make connection between the bar and plunger impossible (5.6.4).

In both types of cylindrical test, the burette was lowered to apply a negative pore-pressure of about 0.4 lbf/in^2 before removing the former. By dusting the two halves of the former with talc, the tendency for them to adhere to the specimen membrane was greatly reduced, and therefore they could be removed with a minimum of disturbance to the specimen. In all cases the prepared specimen appeared uniform without noticeable necking or surface irregularities.

5.5.2 INITIAL MEASUREMENT

The heights of cuboidal and both types of cylindrical specimens were determined using the technique described in section 4.5.2 for ATA specimens. A height-vernier was used to measure the elevation of the top of the ball-bearing relative to a fixed point on the cell-base, and the specimen height obtained by subtracting the combined elevation of the remaining components relative to the same point. For triaxial extension tests, the top of the brass connecting bar was used as the reference point.

The lateral dimensions of cuboidal specimens were measured, each at fifteen points, with a vernier micrometer, and the mean values calculated. Micrometer measurements were similarly taken of the diameter of cylindrical specimens at five equidistant heights, on two diameters mutually at right angles. In all cases, 0.020 in. was subtracted from the mean diameter to allow for the thickness of the specimen membrane.

The criticisms regarding this method of measurement were discussed

in 4.5.2.

In order to investigate the accuracy of the measurements so obtained, a second method was devised, especially suitable for cylindrical specimens. This was based upon a method described by El-Sohby (1964), in which the volume of water required to fill the cell between two fixed markers was measured.

The upper marker was positioned just below the level of the top of the specimen, vertically above the lower marker, which itself was fixed at a level slightly above the bottom of the specimen. Therefore, the difference between the volumes of water required to fill the cell between the two markers, firstly when the cell was empty, and then when the prepared specimen was present, represented the volume occupied by the specimen. Knowing the distance between the markers, the average diameter of the specimen, over this distance, could be calculated. All the volumes were determined by weighing the water as it emitted from the cell.

In the author's system, the volumes were measured directly, whether water was flowing into or out of the cell, and the number of reference levels was increased from two to twelve.

A vertical line was scribed on the outside of the perspex cell and, beginning from a point 0.10 in. above the level of the bottom stress-cell diaphragm, a series of short horizontal lines were scribed at exactly $\frac{1}{2}$ in. intervals along its length, up to a height of 5.00 in. above the lowest line. An additional horizontal line was scribed 4.80 in. above the lowest line.

The cell was clamped to its base in the usual manner, with the top stress-cell suspended from the plunger, so that the two lengths of polythene capillary-tubing, i.e. the drainage and top stress-cell connections, occupied positions similar to those they would occupy during

a normal cylindrical triaxial compression test. No other components were present within the cell between the elevations of the two extreme $\frac{1}{2}$ in. horizontal graduations.

The volume between consecutive graduations was determined by slowly filling the cell with de-aired water, a paraffin-gauge being used to measure the volume of water admitted. The process was stopped at each graduation in order to take gauge readings. It was important not to "overshoot" the graduations, since removal of water from the cell, although measurable, caused the meniscus to change, leading to significant errors. The paraffin-gauge had been accurately calibrated against a burette for specific directions of the menisci, and therefore it was equally important not to change these at random.

The volume of the "empty" cell was determined using this method. By carrying out the same procedure with a specimen present, the volume occupied by the specimen between graduations could be calculated and hence the average diameter determined.

However, the method could not be relied upon to detect very small differences in the diameter of prepared specimens, between adjacent graduations, prior to deformation. Such differences could well be accounted for by errors in the positioning of the meniscus against each graduation. The intermediate graduations were therefore used primarily to determine the profiles of deformed specimens, after tests taken up to or beyond failure (5.6.2).

In order to estimate the accuracy of initial micrometer gauge diameter measurements, nine prepared cylindrical triaxial specimens were investigated. The volume occupied by each of the specimens between the zero and 4.8 in. graduations was measured. Because the zero graduation was 0.10 in. above the bottom stress-cell, the calculated diameter represented the average value over the middle 4.8 inches of

each 5 in. long specimen. None of the specimens showed noticeable variations in diameter immediately adjacent to the stress-cells.

The membrane thickness was subtracted from each average diameter so determined, and the results are given in Table 5.1, together with the mean values obtained from vernier micrometer readings.

TABLE 5.1

Test Number	Average Diameter (in.)		Error in Initial Volume (%)
	Cell Volume Method	Micrometer Method	
CYL TC 15	2.787	2.784	-0.2
-	2.782	2.788	+0.4
CYL TC 16	2.789	2.788	-0.1
CYL TC 17	2.783	2.789	+0.4
CYL TC 18	2.792	2.789	-0.2
CYL TC 19	2.786	2.783	-0.2
-	2.796	2.786	-0.7
CYL TC 20	2.780	2.773	-0.5
CYL TC 21	2.785	2.789	+0.3

Two sets of legitimate initial measurement data were obtained from tests not subsequently carried through because of apparatus failure during consolidation. The tests were not numbered, since no reliable information on the stress-deformational behaviour of the specimens was obtained.

Assuming that the average diameters determined using the "cell-volume method" are the true values, and that the height measurements are accurate, the percentage errors in initial volumes resulting from micrometer measurements of diameter were calculated. These are shown in the table. The standard deviation, 0.37%, represents an error of

0.002 in initial porosity.

Although repeated measurements of specimen height generally showed differences of much less than 0.1%, this was not indicative of the error involved. The latter depends largely upon bedding of the specimen at each end, and the accuracy with which the height of the assembled components is determined. Therefore, it is conceivable that the errors in height and diameter measurement, the latter from vernier micrometer readings, were of a similar order.

It was concluded that the vernier micrometer method of determining the average diameter of cylindrical specimens was inferior to the alternative cell-volume method. However, the errors were not considered intolerable, compared with those in associated measured quantities. Assuming that the widths of cuboidal specimens measured using the micrometer were subject to similar errors, the method was considered satisfactory and, in the absense of a practicable alternative, fully justified.

5.6 TESTING TECHNIQUE

Following consolidation, the octahedral normal stress was increased to failure in all triaxial compression tests reported in this chapter. In the cylindrical triaxial extension tests, σ_3, and hence σ_{oct}, was decreased to failure.

The stress-deformational behaviour of both cuboidal and cylindrical specimens was investigated for a full range of initial porosities.

5.6.1 CONSOLIDATION

All cuboidal specimens were consolidated under an ambient stress of 10 lbf/in^2, and therefore the value of σ_{oct} at failure was compatible with that in the majority of ATA tests. Variations in behaviour resulting from differences in stress level were investigated by consolidating cylindrical triaxial compression specimens under ambient stresses of 10, 15 and 20 lbf/in^2 respectively. Specimens formed using rigid end plattens were tested in this way, as well as those in which top and bottom stress-cells were used.

In the cylindrical triaxial extension tests, ambient consolidation was taken to a higher stress level, 25 lbf/in^2, so that σ_{oct} at failure would be approximately equal to that, at failure, in compression tests consolidated at 10 lbf/in^2.

Several cylindrical triaxial compression specimens, including one 3 in. long, were consolidated at zero lateral strain, and the values of K_o compared with those obtained, using the ATA, for cuboidal specimens prepared at similar initial porosities.

Ambient consolidation was carried out as follows:-

With the loading plunger restrained, increments of cell pressure, normally 2 or 3 lbf/in^2, were applied to the specimen through the self-compensating mercury system, and the volume changes measured. Ten to

fifteen minutes was allowed for pore-pressure dissipation.

The cuboidal specimen membranes have a relatively large surface area in contact with the end stress-cells. Therefore during consolidation, in ATA and cuboidal triaxial compression tests, it was considered advisable to allow sufficient time for the membrane to bed properly, especially around the edges and corners of the stress-cells, after each stress increment.

Although the problem is less relevant in the testing of cylindrical specimens, bedding of the filter paper used in the top stress-cell circumferential drainage duct may be of similar importance. The effect can be seen in the prepared triaxial extension specimen, shown in Fig. 5.3c, under a mean effective stress of 0.4 lbf/in^2.

No attempt was made to measure axial or lateral deformations during ambient consolidation.

K_o-consolidation was achieved by correlating axial and volumetric strains during strain-controlled axial deformation, as described in section 4.6.1. Corrections for membrane penetration were incorporated in prepared tables of required volume change against deflection dial gauge reading, for several porosities. The volume changes were adjusted to the required values by varying the lateral stress. At regular intervals the axial stresses were recorded on the oscillograph and, at the same time, the remaining measurements were taken. The usual practice was to allow a short time interval after adjustment of the lateral stress, before taking readings.

A rate of axial deformation of 0.0008 in. per min. was used during K_o-consolidation of all cylindrical specimens, three times slower than that used for ATA specimens. This allowed the necessary adjustments to be made with more finesse, and measurements to be taken at closer intervals of axial deformation. However, this strain-rate was unsuitable

for completion of the test, and therefore was increased to 0.004 in. (0.08%) per min., immediately after consolidation.

5.6.2 CYL TC TESTS

Upon reaching the required value of σ_3, using either form of consolidation, the cell pressure was switched to constant mercury pressure control. The majority of tests were continued beyond peak stress ratio, since the appearance of the specimen surface could be observed throughout. In ATA tests, it was necessary to remove the side stress-cells in order to see the σ_y-faces of the specimen, and hence tests had to be concluded at one point of interest.

After cylindrical triaxial tests, the loading plunger was not withdrawn from the specimen, while the lateral stress was reduced to zero. With the air-release valve open, water was then allowed to drain from the cell. The volume of water emitted between each pair of $\frac{1}{2}$ in. cell graduations was measured with a paraffin-gauge, as described in section 5.5.2, the discharge being stopped while each reading was taken. Because the direction of the water meniscus is highly relevant to such measurements, the volume of the "empty" cell between graduations was determined for outward flow as well as inward flow, and the appropriate calibration was used in each situation.

In this way the mean diameter of the specimen was determined at $\frac{1}{2}$ in. intervals of height, enabling a quantitative investigation to be made into its mode of deformation. The results of several such investigations are presented and discussed in Chapter 7.

5.6.3 CYL TE TESTS

All cylindrical triaxial extension tests were concluded at, or immediately after, peak stress ratio. The most difficult stage, from a practical viewpoint, was the transition between the end of consolidation

and the beginning of specimen extension. With the cell filled, prior to consolidation, the loading plunger was located in the upper untapped section of the brass connecting bar (Fig. 5.4), but not connected, so that when the ambient stress was applied, the specimen was not restrained from axial deformation. Unless the top platten was very close to the horizontal, location was impossible without specimen disturbance.

After sufficient time had been allowed for full consolidation under 25 lbf/in^2, the plunger and the brass bar were connected. A second brass bar was used to connect the top of the plunger to the loading crosshead (Fig. 5.3b), where a ball-and-socket joint allowed the assembly to rotate as the plunger was screwed into the lower bar. If not done carefully, the latter process could cause considerable disturbance to the specimen. However, the use of a bottom stress-cell for axial stress measurement was particularly advantageous in this respect, since it allowed any inadvertent stressing of the specimen, either tensile or compressive, to be immediately detected.

When connection was complete, the loading machine motor was started, and the pedestal was lowered until the "slack" had been taken up in the ball-and-socket joint. The bottom stress-cell galvanometer trace, previously positioned in anticipation of stress decrease, responded as soon as this point was reached, since the axial stress became affected. The machine was then stopped, while the axial deflection dial gauge was zeroed, and the initial burette reading taken.

A rate of axial extension of 0.004 in. per min. was applied, a strain-rate of approximately 0.13% per min., until failure was reached. At this point the machine was stopped, but the axial loading assembly was left undisturbed. The cell water was drained, and the specimen profile determined as described for cylindrical triaxial compression

tests (5.6.2).

5.6.4 CUB TC TESTS

The cuboidal triaxial compression tests were performed in essentially the same manner as those on cylindrical specimens, described in section 5.6.2. The rate of axial deformation of 0.004 in. per min. was equivalent to a strain-rate of 0.1% per min.

In one test, a rigid bottom platten was used in conjunction with the top stress-cell, in order to investigate pore-pressure dissipation at the chosen rate of strain (4.2.4). The remaining tests were carried out using both end stress-cells to measure σ_1, and an external proving-ring to measure the corresponding axial loads.

5.7 SUMMARY

This chapter has been concerned with stress-deformation tests carried out, as part of the author's research program, in apparatus other than the ATA.

The same cohesionless soil was used in all three types of axially-symmetrical tests described, and also those performed in the ATA under a variety of stress conditions. Therefore the behaviour of each specimen was significant, not only from the point of view of investigating the mechanical properties of the soil, but also in a partial assessment of the suitability of the ATA for stress-deformation testing.

A convenient basis for comparison was the triaxial compression stress condition, where the side stress-cells of the ATA were superfluous, and yet may have affected specimen behaviour. By testing identical cuboidal specimens in conventional triaxial compression, without the side-cells, their influence could be estimated.

The techniques used in carrying out these tests were described, together with those used in testing cylindrical specimens in both triaxial compression and triaxial extension.

A method was presented with which the average diameter of prepared cylindrical specimens could be determined with an accuracy greater than that obtained from vernier micrometer measurements. However, the errors incurred using the micrometer were shown to be tolerable, especially since a practicable alternative for measuring cuboidal specimens was not available.

A description was given of a similar technique used to determine the profile of cylindrical specimens after test, the results and conclusions from the investigations being deferred until a later chapter.

CHAPTER SIX

ASTON TRIAXIAL APPARATUS TESTS

RESULTS AND DISCUSSION

6.1 INTRODUCTION

The requirements of an apparatus allowing soil specimens to be tested in the laboratory under generalised stress conditions were discussed in Chapter 3, and previous attempts to impose such conditions were reviewed. The Aston Triaxial Apparatus, designed and developed to permit the three principal stresses to be applied independently to a cuboidal specimen, was described in Chapter 4. Some of the test procedures used in carrying out the stress-deformation tests forming part of this research program were outlined, and various other possible stress paths were also mentioned.

This chapter will describe the results obtained from triaxial compression, triaxial extension, plane strain and intermediate-stress tests carried out with this apparatus on specimens of uniform coarse sand (Appendix E) prepared over a range of initial porosities. Test results from the Mk.I apparatus are presented in Appendix G.

The test program is outlined in section 6.2, and the results of ATA TC and ATA PS tests are discussed in 6.3 and 6.4 respectively. Comparisons between the behaviour of specimens in these two series is drawn in the following section before the intermediate-stress and triaxial extension tests are considered in 6.6.

These four major sections are each sub-divided into categories dealing with one particular aspect of soil behaviour. Hence, the results of the consolidation stages, the various stress-strain relationships, and the failure characteristics are treated separately.

The extent to which stress-dilatancy theory is applicable to the

observed behaviour of triaxial compression and plane strain specimens is discussed, and the mode of deformation during all types of ATA test is considered, together with its effect on the end stress-cell measurements.

Information obtained from continuous trace recordings of σ_3 are treated at length in section 6.3.6, though the characteristic variations were common to all test series.

Finally, in section 6.8, the effects of some data corrections are briefly mentioned.

6.2 THE TEST PROGRAM

Table 6.1 shows the program of tests performed, the majority of which were in triaxial compression and plane strain. Some intermediate-stress tests were carried out on dense specimens and one triaxial extension test was also included in the program.

Particularly during the initial usage of the ATA, many tests were unsuccessful and were curtailed after the application of only small strains. Others, though not reaching the peak stress ratio condition, furnished useful information on stress-deformational behaviour, and were therefore included in the consecutive numbering of the tests.

TABLE 6.1

Type of Test	Total Number	Number Reaching Failure	Consol'n	Constant Stress During Shearing	
				σ_1	σ_3
ATA TC	18	11	K_o	4	7
ATA PS	25	21	K_o	12	9
ATA INT	7	6	ambient	1	5
ATA TE	1	1	ambient	1	-

In all tests other than those in plane strain, the intermediate principal stress was constant during the shearing stage. The order in which the tests were performed has not been preserved during the discussion of results, and will be referred to only when strictly relevant, for instance when changes in test procedure have resulted in a change in specimen response.

Many comments apply equally to tests in several of the categories, but are presented only in the earlier sections.

The majority of tests were on specimens prepared at different voids ratios, though the method of formation precluded tests on very loose specimens. The maximum and minimum voids ratios (Appendix E)

were 0.503 and 0.715 respectively. However, the terms "loose" and "dense" will be used liberally to describe the initial states of specimens in relation to the loosest and densest actually tested, rather than in the more specific sense of relative density.

6.3 TRIAXIAL COMPRESSION

This series of tests was carried out primarily to investigate the effect of any undesirable restraint on specimen deformations imposed by the apparatus. All specimens were prepared as described in section 4.5, and their initial dimensions are given in Table 6.2.

TABLE 6.2

ATA Test Number	Mass Solids (gm)	Length (in)	Inter Width (in)	Minor Width (in)	Initial Voids Ratio
TC 1	591.40	4.037	2.344	2.269	0.573
TC 2	595.64	4.057	2.347	2.269	0.575
TC 3	601.23	4.100	2.346	2.273	0.578
TC 4	606.39	4.110	2.346	2.274	0.571
TC 5	566.08	4.084	2.343	2.263	0.648
TC 6	595.72	4.132	2.342	2.259	0.590
TC 7	640.37	4.287	2.344	2.270	0.546
TC 8	599.93	4.194	2.338	2.262	0.605
TC 9	640.42	4.286	2.345	2.263	0.541
TC 10	605.25	4.179	2.336	2.257	0.579
TC 11	584.25	4.166	2.343	2.277	0.649
TC 12	577.83	4.055	2.340	2.264	0.607
TC 13	585.62	4.031	2.339	2.260	0.576
TC 14	610.66	4.159	2.340	2.270	0.570
TC 15	612.00	4.153	2.340	2.262	0.559
TC 16	573.84	4.123	2.340	2.270	0.650
TC 17	627.81	4.178	2.341	2.261	0.528
TC 18	580.47	4.029	2.335	2.271	0.595

The initial voids ratio was calculated from these measurements, and is therefore appropriate to an ambient stress of 0.4 lbf/in^2 resulting from the small pore suction. This quantity was used as a general basis of comparison for the stress-deformational behaviour of specimens in all test series.

6.3.1 CONSOLIDATION

The results of zero lateral strain consolidation (4.6.1), to octahedral normal stress levels of between 15.5 and 21.5 lbf/in^2, are shown in Table 6.3.

TABLE 6.3

ATA Test Number	Initial Voids Ratio	Zero Lateral Strain Consolidation				
		Minor Stress	Major Stress	Volume Strain	Voids Ratio	Stress Ratio
	e_i	$\sigma_y=\sigma_x$	σ_3	ε_{vc}	e_c	$\frac{\sigma_3}{\sigma_1}$
TC 4	0.571	10.20	34.50	0.85	0.558	0.296
TC 5	0.648	11.20	26.10	0.91	0.633	0.429
TC 6	0.590	11.60	31.55	0.98	0.575	0.368
TC 9	0.541	13.30	37.90	0.90	0.527	0.351
TC 10	0.579	12.00	34.85	0.93	0.565	0.344
TC 12	0.607	11.00	27.65	0.93	0.592	0.398
TC 13	0.576	12.00	38.50	1.21	0.557	0.312
TC 15	0.559	10.30	33.10	0.99	0.544	0.311
TC 16	0.650	10.60	27.75	1.16	0.631	0.382
TC 17	0.528	10.10	35.10	0.97	0.513	0.288
TC 18	0.595	9.60	27.25	1.08	0.578	0.352

The major principal stress, σ_3, is the mean value of those recorded by the top and bottom stress-cells at the end of the consolidation stage, and the stress ratio, $\frac{\sigma_3}{\sigma_1}$ $(= K_o)$, has been calculated on this basis.

The encircled points in Fig. 6.6 represent these final K_o values plotted against the initial voids ratio e_i, the scatter being considerable. If, however, the magnitude of K_o is determined from the mean ratio between the principal stresses during the majority of the consolidation stage, the distribution is slightly improved. A curve has been drawn through these points in the figure.

It would not be realistic to calculate K_o from measurements taken over the complete stage, since at small strains the stresses were particularly susceptible to datum and bedding errors, usually resulting in even lower values of this ratio. At the latter end of the stage, however, when the stresses were changing more rapidly, it was frequently necessary to make slightly larger adjustments to the main-cell and side-cell pressures in order to maintain the plane strain condition. Consequently a slightly longer period would have been required for the major principal stress to adjust to such changes. Although attempts were made to even out such adjustments, this process generally had the effect of increasing K_o.

However, all the recorded values were considerably lower than those predicted by Jaky's (1944) equation, i.e. $K_o = 1 - \sin \phi$. This will be discussed in more detail in later sections.

The volumetric strains during K_o-consolidation, ε_{vc}, could not be directly compared because of the variations in stress levels, at the end of the stage, for each test. Therefore the results have been "unified" by dividing each strain by the major principal stress; these quantities are plotted against e_i in Fig. 6.7. Again the points are

scattered.

The volume change of ATA specimens is especially suspect at low stress levels because of the shape of the specimen membrane and the relatively large distances between the ends of the soil specimen and the points at which the membrane is sealed to the top and bottom stress-cells. Although smooth transitions were provided wherever possible over these areas, and generous periods were allowed for the membrane to bed firmly against the stress-cells (4.6.1), it is not surprosing that small volumetric strains at low stress levels show some inconsistency.

Precise investigations of soil compressibility under ambient or K_o-consolidation conditions is not the primary function of the ATA, and would best be performed in one of the several apparatuses more suited to this task. However, the test procedure limited calculated lateral strains, generally to not more than 2% of the volumetric strains, and although the true variation was probably greater in some cases, the main purpose of this stage of the test, viz. to provide intimate contact between plane surfaces of the specimen and the side-cell membranes without undue "exposure", was undoubtedly achieved.

Fig. 6.1b shows a specimen, subsequently tested in plane strain, at the end of K_o-consolidation.

6.3.2. FAILURE CHARACTERISTICS

The most commonly used definition of the "failure" condition for cohesionless soils is that of maximum major to minor principal stress ratio, R_{max}. This has been used for all the stress-deformation tests reported herein, unless otherwise stated.

The peak "angle of internal shearing resistance", $\phi°$, given by $\sin^{-1}\left[\frac{R_{max} - 1}{R_{max} + 1}\right]$, has been plotted against initial voids ratio in Fig. 6.8 and the failure characteristics for each test are given in Table 6.4.

ATA Test Number	Initial Voids Ratio	Conditions at Failure (Peak Stress Ratio)						
		Axial Strain	Volume Strain	Peak Stress Ratio	Volume Strain Rate		Angle Internal Sh'g Res	Dir'n Const. Stress
	e_i	ε_{1f}	ε_{vf}	$\frac{\sigma_1}{\sigma_3}$	$\dot{\varepsilon}_{vf}$	$\sin \phi$	ϕ	
TC 4	0.571	4.97	-0.60	3.814	-0.33	0.585	35.8	x
TC 5	0.648	10.62	-0.17	3.165	-0.10	0.520	31.3	x
TC 6	0.590	7.99	-0.75	3.711	-0.26	0.575	35.1	x
TC 9	0.541	6.70	-1.63	4.041	-0.45	0.603	37.1	x
TC 10	0.579	5.24	-0.59	3.788	-0.36	0.582	35.6	x
TC 12	0.607	7.74	-0.54	3.614	-0.23	0.567	34.5	z
TC 13	0.576	7.34	-0.72	3.905	-0.28	0.592	36.3	z
TC 15	0.559	4.70	-0.55	4.216	-0.44	0.617	38.1	z
TC 16	0.650	10.09	-0.08	3.343	-0.08	0.540	32.7	z
TC 17	0.528	5.43	-0.77	4.396	-0.46	0.629	39.0	x
TC 18	0.595	6.73	-0.54	3.833	-0.29	0.586	35.9	x

TABLE 6.4

A mean curve has been drawn through the failure points from seven tests in which the minor principal stress, σ_x (= σ_y), was held constant and the major principal stress, σ_3, increased to failure, and four tests in which σ_x was decreased to failure with σ_3 constant. The stress level was therefore increasing during shearing in the former tests, and decreasing in the latter.

The maximum deviation from the mean is 1.0°. However, it would appear just admissible to draw different curves through the two sets of test results (the dashed curves in Fig. 6.8). The value of ϕ for the σ_3-constant tests would then exceed that for the σ_x-constant tests by about 0.7° over the full range of e_i.

Although the octahedral normal stress, σ_{oct}, at failure was smaller for the σ_3-constant tests (see Table 6.5), and therefore the increase consistent with the frequently observed curvature of the Mohr-Coulomb envelope at low stress levels, the scatter for each set and the small number of tests render any conclusion tentative.

The volumetric strain rate at failure, $\dot{\varepsilon}_{vf}$, i.e. the gradient of the curve of volumetric strain against major principal strain, is also shown plotted against e_i in Fig. 6.8. No difference is apparent between the results from the two sets of tests, all points lying close to the mean linear curve.

In no case was the volumetric strain rate at failure equal to the maximum rate, and in each test the latter occurred at a smaller axial strain. The dashed curve shows that the ratio of $(\dot{\varepsilon}_v)_{max}$ to $\dot{\varepsilon}_{vf}$ increases from about 1.05 for dense specimens to over 1.50 for loose. The scatter of points about the latter curve is marginally less than before.

TABLE 6.5

ATA Test Number	Initial Voids Ratio e_i	Conditions at Failure (Peak Stress Ratio)				
		Oct'al Normal Stress σ_{oct}	Oct'al Shear Stress τ_{oct}	Oct'al Stress Ratio $\frac{\tau_{oct}}{\sigma_{oct}}$	Oct'al Shear Strain γ_{oct}	Dir'n Const. Stress
TC 4	0.571	19.77	13.53	0.685	7.31	x
TC 5	0.648	19.28	11.43	0.593	15.10	x
TC 6	0.590	22.08	14.83	0.671	11.65	x
TC 9	0.541	26.78	19.07	0.712	10.24	x
TC 10	0.579	23.15	15.77	0.681	7.69	x
TC 12	0.607	14.78	9.73	0.658	11.20	z
TC 13	0.576	19.68	13.69	0.696	10.72	z
TC 15	0.559	16.60	12.16	0.733	7.98	z
TC 16	0.650	14.78	9.17	0.620	14.31	z
TC 17	0.528	21.53	16.17	0.751	8.04	x
TC 18	0.595	18.67	12.83	0.687	9.77	x

Fig. 6.9 shows the major principal strain at failure, ε_{1f}, for each test, and again there is no apparent difference between σ_x- and σ_3-constant test points. However, although there is a clear general trend for the failure strain to be greater in tests on loose specimens, deviations of up to 2% (in ε_{1f}) from the mean curve were apparent. The scatter of the total volumetric strains at failure, ε_{vf}, was of a similar order.

In order to eliminate the effect of any errors in volumetric strain measurements during the consolidation stage (6.3.1), the total volumetric strain during the shearing stage, ε_{vs} ($= \varepsilon_{vf} - \varepsilon_{vc}$), has been plotted against e_i in Fig. 6.9. Again the points are widely

distributed, but the expected tendency for ε_{vs} to increase with density is clear. However, a tentative extrapolation to the maximum voids ratio would predict significant dilatancy of such a specimen during shearing to failure.

In general, the results from this series of tests indicate that the volumetric strain rate at failure is more closely related to initial voids ratio than either the axial or volumetric strain, and that this relationship is independent of whether σ_{oct} is increasing or decreasing.

6.3.3 STRESS-STRAIN CURVES

Typical curves showing the variation of σ_1 and ε_v with the axial strain, ε_1, are presented in Figs. 6.10-12. In each test, the K_o-consolidation stage was concluded at about 1% axial strain.

In tests TC 5 and TC 17, σ_{oct} was increasing during shearing, while in TC 12, σ_1 was held constant and therefore σ_{oct} was decreasing. Fig. 6.10 shows that the increase in σ_1 from the end of consolidation to failure for loose specimens was very gradual, there being several minor fluctuations before a poorly-defined peak was reached at ε_1 = 10.62%. Deformation was continued beyond this point to confirm that the stress ratio was a maximum. It is not surprising, therefore, that there is no clear relationship between ε_{1f} and e_i in Fig. 6.9. The maximum rate of volumetric strain was reached at an axial strain of less than half that at failure, from which point $\dot{\varepsilon}_v$ slowly decreased. For the dense specimen, however, the peak stress ratio was more clearly defined, and $\dot{\varepsilon}_v$ attained its maximum value only just before failure (Fig. 6.11). In test TC 12, σ_3 decreased to an almost constant value, and little increase was observed during an additional axial strain of 3% beyond that at the peak stress ratio.

Only a few of the tests in this series were continued into the post-failure deformation region, and usually only to confirm peak stress

conditions where the stress-strain curve was flat.

In three of the seven tests in which σ_{oct} was increasing, a slight inflexion was observed in the σ_1 v. ε_1 curve shortly after the end of consolidation. An equivalent pattern can be seen in Fig. 6.12, in the σ_3 v. ε_1 curve, though the relatively small overall change in σ_3 tends to conceal the effect. It appears unlikely that this phenomenon can be attributed to apparatus interference (6.3.5), but the cause is unknown.

6.3.4 STRESS-DILATANCY BEHAVIOUR

The stress-dilatancy theory (Rowe 1962, etc.) was described in section 2.2, together with several other theories for the deformational behaviour of cohesionless media under applied stress systems. These were loosely-categorised as particulate mechanics.

The basic stress dilatancy equation $R = D K_f$, or

$$\frac{\sigma_1}{\sigma_3} = \left(1 - \frac{d\varepsilon_v}{d\varepsilon_1}\right) \tan^2\left(45 + \frac{\phi_f}{2}\right),$$

was applied to the triaxial compression test results.

Fig. 6.13 shows R v. D curves for tests TC 9 and TC 16, the former performed on a dense specimen with σ_{oct} increasing, and the latter on a loose specimen with σ_{oct} increasing. The initial point for each test represents the conditions at the end of consolidation, and the vertical arrow indicates the peak stress ratio, R_{max}. The final point is appropriate to the last measurement taken.

At first, the dilatancy factor, D, was calculated from consecutive measurements of the volumetric and axial strain increments, and the resulting curve was seen frequently to fluctuate about a smoother curve in its general direction, i.e. a slight overestimate of one increment was balanced by an underestimate of the next. This effect was regarded as a feature of the sensitivity of the apparatus and measuring systems

rather than a behavioural pattern of the soil. Therefore, since it would have been unrealistic for this to appear in the R v. D plot, a "curve smoothing" procedure was incorporated in the computation of these quantities, two or three measured increments being taken together each time. These are the points shown in Fig. 6.13. The process described was used in all stress-dilatency calculations in this research program.

The parameter ϕ_f has been found, in practice, to vary between a lower limit, ϕ_μ, the friction angle for the material of the particles, and an upper limit, ϕ_{cv}, appropriate to deformation at constant volume, and which is reached after large shear distortion. The relative magnitude of ϕ_f depends upon the specimen porosity, the stress level and the stress path.

For a given stress level, ϕ_μ is regarded as constant, and its value determinable from a simple friction test. Horne (1969) derived a relationship giving ϕ_{cv} in terms of ϕ_μ. Alternatively the former may be determined experimentally at the constant volume condition, when R = K.

In Fig. 6.13, the K_μ-line has been drawn for $\phi_\mu = 27°$, a mean value of those quoted frequently by workers at the University of Manchester for quartz sand, and the K_{cv}-line has been drawn for $\phi_{cv} = 35°$, the corresponding value given by Horne, which has been found to approximate closely to that observed in triaxial compression tests. For the purposes of comparison, a further line (shown dashed) has been drawn for $\phi_\mu = 6.8°$, the friction angle obtained by the author for quartz, from a series of "friction-slider" tests (Appendix E), under submerged conditions.

The K_μ and K_{cv} lines will be shown unlabelled in the majority of subsequent stress-dilatancy graphs.

Figs. 6.14-16 show R v. D curves for the eleven ATA TC tests, the four performed with decreasing σ_{oct} being grouped together in the first

figure. (The experimental points have been omitted to improve clarity).

A fundamental postulate of the stress-dilatancy theory is that deformation is due to relative movement between instantaneously rigid groups of particles sliding at a preferred angle, such that the energy dissipated in internal friction is a minimum. Providing this condition is satisfied, the relationship between R and D will be given by the K_μ-line. Deviations from this lower limit, which have been observed in loose or highly-dilated assemblies, are considered to result from the occurrence of sliding in other than the preferred direction.

Therefore dense specimens may be expected to deform "along" the K_μ-line up to peak stress ratio, and loose specimens to deform along the K_{cv}-line. Each will reach the "critical state", deforming at constant volume without change in stress, at the point D = 1 on the K_{cv}-line. The experimental difficulties associated with post-failure deformation of cohesionless media were discussed in Chapter 2.

Further consideration will be given to the K_o-consolidation of ATA specimens in later sections. However, for the present it will be assumed that the observed magnitude of K_o was in all cases too low, and that Jaky's equation is a reasonable approximation to the genuine value. Assuming also that the stress measurements were accurate, this would imply slight lateral expansion, as $K_o \rightarrow K_a$, the active earth pressure. Such undetected strains would lead to an overestimation of ε_v, and if this effect is considered to apply for a short period after consolidation, the early values of the dilatancy factor D will be underestimates.

The slopes in all but one of the ATA TC tests are initially less than that of the K_μ-line. A correction for the above effect would increase these slopes, and it could then possibly be concluded that the curves followed the lower limit line, during the initial stages only,

for seven of the eleven tests. However, those following initial paths equivalent to higher values of ϕ_f are four of the five densest tests, which is contrary to the behaviour suggested by the stress-dilatancy theory.

After only small increases in stress ratio, the volumetric strain rates became relatively steady at magnitudes close to their maximum, as R increased to near its peak value. In some cases, a significant decrease in D occurred shortly before failure, but this may be a result of the low curvature of the σ_1 v. ε_1 graph and the consequent poor definition of its peak.

Little information on post-failure behaviour was obtained, but it could conceivably be supposed that the curves for all but the two loosest specimens (TC 5 and 16) are directed towards the critical state point.

It may be noted that the behaviour of specimens in σ_{oct}-decreasing tests was no different from that in the remainder. The failure points for all of the tests have been plotted together in Fig. 6.16, and lie between lines representing ϕ_f values of $29\frac{1}{2}°$ and 32°.

From Table 6.4 and Fig. 6.8, it can be seen that the peak strengths of several specimens at the loose end of the initial voids ratio range were considerably lower than the 35° quoted for ϕ_{cv}. The lowest value of ϕ at failure was 31.3°, observed for specimen TC 5, and this decreased further with additional axial strain, even though a constant volume condition was not attained.

Should the genuine value of ϕ_{cv} exist within the range from $29\frac{1}{2}°$ to 32° it would appear that at failure all specimens were deforming in a manner consistent with the upper limit of ϕ_f, postulated for loose or highly-dilated assemblies. This phenomenon may well be connected with the fact that the peak dilatancy rate was reached well before

failure in most tests, and that the points representing D_{max} generally lie much closer to the K_μ line than do the points for R_{max}.

6.3.5 MODE OF SPECIMEN DEFORMATION

The measurement of strains during ATA tests were discussed in section 4.4, where in particular the difficulty of obtaining quantitative information on the distribution of lateral strain was emphasized. All calculations based on measured specimen deformations in the x- and y-directions provide only the overall average strains. This situation is common to the majority of apparatuses in which stresses are applied through flexible surfaces.

The mode of deformation of ATA specimens tested under triaxial compression stress conditions, where lateral strain in the y-direction is large, was of special interest, since specimen restraint resulting from apparatus interference may have had a considerable effect on stress-deformational behaviour.

In order to investigate the shape of specimens at, or shortly after, failure, several attempts were made to measure their lateral dimensions, using a vernier micrometer, in the manner described in section 4.5.2 for initial specimen measurement. Unfortunately few were fully successful, mainly because of the fact that the main-cell and side-cells must be completely removed to allow access to the specimen, and this requires almost complete unloading (a small negative pore-pressure was applied to prevent collapse). Apart from changes in the deformed shape due to unloading and disturbance during dismantling, wrinkling of the specimen membrane invariably occurred, making accurate measurement difficult. However, the results from one of the more successful attempts, ATA TC 6, are shown in Fig. 6.17.

Fifteen width measurements were taken in each lateral direction,

and since no top stress-cell tilting or specimen discontinuities were apparent, it was assumed that deformation was symmetrical in each plane, about the centre-line. Failure was reached at about 8% axial strain, and the test was concluded shortly afterwards. The initial and final dimensions are given in the Table shown overleaf.

The initial measurements in both x- and y-directions were slightly larger towards the bottom and towards the centre of each face, an effect which was more pronounced the looser the specimen.

From the final measurements, it can be seen that lateral expansion at the base of the specimen was approximately twice that at the top for most points in both directions. However, the surfaces remained essentially plane, the maximum difference between centre and "edge" measurements being in the region of 0.025 in.

Based on the average lateral dimensions, the strains in the x- and y-directions were about -4½% and -4% respectively, compared with the average value calculated for axial and volumetric deformations of -4.6%. A more elaborate comparison, based on the overall shape of the specimen surface, would not be justified considering the manner in which the measurements were taken. However, it seems probable that the two lateral strains remained similar during deformation under triaxial compression conditions.

The effect of slight interference from the side stress-cell surrounds at the corners of the specimen could be observed as shallow grooves in the specimen membrane. This was especially evident in tests continued to large strains beyond failure. It would seem reasonable to expect that any significant restraint would seriously affect the stress-strain curves, and therefore be a possible explanation of the slight inflexions observed in some σ_1 v. ε_1 graphs. However, when these occurred, they did so at relatively small strains, generally less than

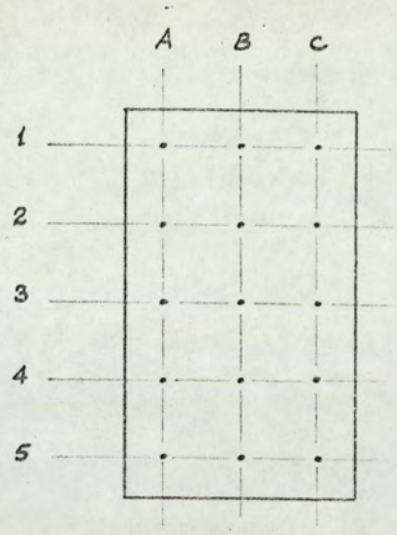

Approximate Positions of Measurement

Initial Dimensions								
	σ_y Planes				σ_x Planes			
	A	B	C	Average	A	B	C	Average
1	2.340	2.336	2.336	2.337	2.257	2.256	2.259	2.257
2	2.337	2.345	2.336	2.339	2.255	2.263	2.254	2.257
3	2.337	2.348	2.341	2.342	2.251	2.262	2.260	2.258
4	2.345	2.351	2.339	2.345	2.257	2.269	2.258	2.261
5	2.350	2.352	2.340	2.347	2.254	2.268	2.265	2.262
Final Dimensions								
	σ_y Planes				σ_x Planes			
	A	B	C	Average	A	B	C	Average
1	2.403	2.423	2.399	2.407	2.299	2.324	2.302	2.308
2	2.430	2.452	2.426	2.436	2.336	2.357	2.336	2.343
3	2.454	2.470	2.446	2.457	2.336	2.370	2.349	2.348
4	2.472	2.492	2.467	2.477	2.358	2.375	2.356	2.363
5	2.477	2.488	2.466	2.477	2.351	2.383	2.352	2.362

half that required for failure, and the subsequent peak strengths were not noticeably different from the average.

It was concluded, therefore, that the effect of apparatus interference on specimen behaviour was slight, and although it would be possible to reduce it further by increasing the initial side-cell membrane exposure, the conditions may not then be representative of those in other types of ATA test.

6.3.6 TOP AND BOTTOM STRESSES

The use of end stress-cells to measure σ_3 directly at the top and bottom surfaces of the specimen eliminates the problem of plunger friction, which is common to many apparatuses, and that of measurement error due to friction on the σ_y-faces, which is peculiar to "three-dimensional" apparatuses similar to the ATA. However, should the specimen deform non-uniformly, the measured stresses at the top and bottom will differ from those at other elevations. Therefore, since the analysis of ATA tests, like that of most stress-deformation tests, is based on the assumption of stress and strain homogeneity, a correction must be applied to the end stress-cell measurements to obtain the average vertical stress.

In all ATA tests, σ_3 was calculated as the mean of the stress-cell values, thus assuming that the corrections appropriate to top and bottom measurements were equal and of opposite sign, and that frictional loss was negligible. The justification for these assumptions will be considered with reference to test ATA TC 6 which was discussed in the foregoing section.

The end stress-cells are enlarged only in the x-direction, and therefore the lateral strain in this direction would be expected to be more uniform than that in the y-direction. From the data in Table 6.6,

it can be seen that this is only marginally so, and that deformation in the y-direction has not been inhibited by the dimensions of the stress-cells. The base of the specimen has expanded to "overlap" the bottom stress-cell, (indicative of the effectiveness of the end lubrication system).

Using the final average measurements taken at elevations 1 and 5, the respective cross-sectional areas at the top and bottom were 5.56 in^2 and 5.85 in^2. These may be compared with the average cross-sectional area, based on the initial dimensions and the axial and volumetric deformations, which was 5.74 in^2, and the average measured value of 5.73 in^2. At failure the top and bottom stresses were 44.5 and 41.6 lbf/in^2 respectively.

If values of σ_3 are calculated separately from the above measurements by multiplying each by the ratio of the appropriate end area to average cross-sectional area (5.74 in^2), stresses of 43.2 and 42.4 lbf/in^2 are obtained. The difference of 0.8 lbf/in^2 may then be regarded as an estimate of the genuine frictional loss, as distinct from the difference between the measured stresses which can be accounted for by variation in the end areas.

The average stress-cell reading of 43.05 lbf/in^2 will, in this case, slightly overestimate the calculated value of 42.8 lbf/in^2. However, the resulting error in ϕ would be only 0.1°, almost certainly less than that from a variety of other sources, discussed in Chapter 4.

An estimate of the coefficient of friction between the side stress-cell and specimen membranes can be made using the 0.8 lbf/in^2 calculated stress difference and the side stress-cell pressure, which in this test was constant at 11.6 lbf/in^2 during the shearing stage. The value of μ obtained, 0.02, is consistent with the results from the series of lubrication tests described in Appendix F.

Although the above analysis of the end stresses at failure, based on measured dimensions before and after test, is approximate, it demonstrates that the mean of the end stress-cell readings is probably sensibly close to the magnitude of the average vertical principal stress, σ_3, even when the specimen does not deform uniformly.

In general, the top and bottom stresses, $(\sigma_1)_t$ and $(\sigma_1)_b$, were similar during the consolidation stage of ATA TC tests. Their magnitude began to deviate significantly from the end of this stage, and some examples of their variation are shown in Fig. 6.18. In test ATA TC 15, σ_3 was held constant by balancing the increase in $(\sigma_1)_t$ with the decrease in $(\sigma_1)_b$. This procedure (4.6.2) was used in all similar tests.

Each point of the σ_1 v. ε_1 is plotted from instantaneous measurements of stress and deformation. However, the use of pressure transducers to relay the induced stress-cell pressures to a recording oscillograph, allows for their continuous measurement over any chosen time-(strain-) increment. Although, in the majority of tests, the recorder was run for short periods only, it was possible to study the minor fluctuations of the stresses from the recorded traces.

Both during consolidation and subsequent deformation prior to peak stress conditions, the recorded curves were basically smooth. Small deviations occurred only occasionally, and were equally reflected in top and bottom traces. In many of the tests, the curves were perfectly smooth over this range, and therefore deviations in other tests could be attributed to slight malfunctioning of the apparatus, the most likely cause being the restraint imposed by the side stress-cell frames on the free downward movement of the top stress-cell.

However, as failure was approached, and for all subsequent deformation, almost continuous fluctuation of the end stresses was observed. Examples of this phenomenon are shown in the recorded traces from an

ATA triaxial compression test, sections of which have been reproduced in Figs. 6.19a,b. This particular test was not included in the general list of ATA TC tests, because of uncertainty regarding the stress-cell calibration figures. However, because lengthy continuous recordings were made of the top and bottom stresses, the results are more suitable for studying the stress variations than those from most other tests.

In each case, the upper trace is that of the top stress-cell taken directly from the oscillograph output. The lower trace, which is that of the bottom stress-cell, has been moved vertically into a convenient position for comparison with the upper trace. In all other respects it is identical with that from the output. Therefore the distance between the traces should not be regarded as indicative of the difference in magnitude of top and bottom stresses.

The encircled numbers in each diaphragm give the approximate magnitude of the average of the end stress-cell measurements, and those at the end of each dashed line are the corresponding axial strains, (ε_1%). Hence the first diagram in Fig. 6.19(a) represents the top and bottom stress-cell traces from $\varepsilon_1 = 0.6\% \rightarrow 0.7\%$, when the average value of σ_1 was about 10 lbf/in^2.

It can be seen that apart from an occasional slight wavering, the traces began to fluctuate significantly and frequently only after about 4% strain, at a stress level close to failure. The maximum amplitude was about 0.2 or 0.3 lbf/in^2 at this stage, increasing to about 0.5 lbf/in^2 after peak stress. It may be noted that all variations occurred simultaneously in the top and bottom traces.

At an axial strain of just over 9.2%, a very sudden drop of about 5 lbf/in^2 occurred, (the calibration factors were different for the two galvanometers and hence the trace movements were not equal), followed

by a progressive build-up of stress to slightly less than its former value. This phenomenon was common to post-failure deformation in almost all of the tests carried out in this research program.

In friction-slider tests on saturated quartz surfaces, the "slip-stick" effect has frequently been demonstrated (Horn and Deere 1962), frictional resistance building up to a peak and then suddenly dropping, causing a short rapid movement of the slider. In this type of experiment, it has been suggested the slip-stick effect is a direct result of the difference between static and kinetic frictional coefficients, and the elastic freedom of the slider. This reasoning has been extended to explain the stress fluctuations observed in conventional stress-deformation tests on saturated sands.

The use of a proving-ring to measure the axial deviator stress in triaxial compression tests has frequently been considered as the cause of this phenomenon. However, in the ATA tests, a proving-ring was not normally used, a rigid brass bar transferring load from the machine crosshead to the plunger.

Skinner's (1969) shear box tests on dry and saturated specimens of glass ballotini showed similar effects to the ATA TC test described above. For each material, the shear load increased smoothly until just before the peak, at which point rapid fluctuations began to occur. It was noted that the magnitudes of the fluctuations were considerably greater for the submerged specimens, and this was associated with greater interparticle friction and the predominance of particle rolling over sliding.

In section 2.2, various theories for the structure of random packings of spheres were discussed; among them was the assumption that small arrays of the densest and loosest packings were present in such a proportion as to give the overall porosity. Extending this idea to

irregular particles, it could be reasoned that the apparent slip-stick effect observed in ATA tests was the result of sudden local failures of small groups of particles, surrounded by other groups at differing porosities. However, although the amplitude of stress fluctuations steadily increased after failure, the very large drops apparent in Fig. 6.19(b), which represent up to 10% of the magnitude of σ_1, appear to be a different, but possibly associated, effect.

A comparison between the two can be seen in the diagram for values of ε_1 between 9.2% and 9.4%. The sudden drop at about 9.25% strain is almost instantaneous and therefore well-defined, whereas that occurring at just over 9.3% strain is much smoother, resembling those at around the peak stress. Clearly the former is not simply a larger version of the latter.

The magnitudes of the large stress changes indicate that the effect is widespread and probably associated with movement along a slip surface. The relatively smooth recovery of the stress curve, occurring over a change in axial strain of about 0.1% may further be associated with the magnitude of such a movement, the masses on each side of the slip damping the rate of overall reponse of the specimen. Assuming a slip occurred along a plane at about $(45 - \frac{\phi}{2})^\circ$ to the vertical, the measured strain increment would be equivalent to a relative displacement of 0.005 in. This may be compared with the mean particle diameter of about 0.030 in., since the latter is likely to be an important factor in such a mechanism.

6.4 PLANE STRAIN

Plane strain tests formed the largest category of all those carried out using the ATA. Specimen preparation was identical with that employed for the ATA triaxial compression tests, and the initial physical properties are given in Table 6.6.

Some of the many previous investigations of soil behaviour in plane strain were discussed in sections 2.4 and 3.3.1. A fundamental difference between the ATA PS tests, performed by the author, and those of most other workers, is the nature of the surface through which the intermediate principal stress is applied.

Rigid plattens, usually lubricated, have commonly been used to constrain specimens from expansion in one lateral direction, and only in a minority of investigations has σ_2 been measured. In all ATA PS tests, σ_2 was applied through the flexible side stress-cell membranes and was therefore known throughout deformation. Because the test conditions were very similar to those in the ATA TC series, direct comparisons of specimen behaviour under the two different stress states were considered to be more reliable than those based on the results of conventional cylindrical triaxial compression tests.

6.4.1 CONSOLIDATION

The conditions at the end of K_o-consolidation are given in Table 6.7, and the magnitude of the stress ratio $\frac{\sigma_3}{\sigma_1}$ is plotted against e_i in Fig. 6.20.

In several tests, e.g. PS 4 and PS 6, alternative systems were tried for maintaining the zero lateral strain condition, but were unsuccessful. These were discussed in section 4.6.1. The procedure used in the large majority of PS tests was that employed for the ATA TC series, and values of K_o obtained from these tests only are shown in

TABLE 6.6

ATA Test Number	Mass Solids (gm)	Length (in)	Inter Width (in)	Minor Width (in)	Initial Voids Ratio
PS 1	566.67	4.050	2.272	2.248	0.580
PS 2	594.49	4.059	2.328	2.249	0.553
PS 3	567.00	4.100	2.315	2.250	0.631
PS 4	550.29	4.128	2.272	2.241	0.656
PS 5	602.92	4.090	2.337	2.260	0.659
PS 6	600.23	4.121	2.334	2.256	0.558
PS 7	615.62	4.100	2.335	2.254	0.521
PS 8	558.28	3.954	2.332	2.259	0.620
PS 9	575.39	4.189	2.340	2.249	0.652
PS 10	577.96	4.062	2.332	2.248	0.599
PS 11	574.14	4.060	2.333	2.257	0.610
PS 12	568.20	4.062	2.329	2.252	0.623
PS 13	575.20	4.071	2.333	2.252	0.615
PS 14	571.79	4.064	2.333	2.252	0.618
PS 15	589.52	4.100	2.337	2.260	0.593
PS 16	605.68	4.181	2.333	2.246	0.577
PS 17	603.81	4.092	2.339	2.256	0.549
PS 18	559.04	4.053	2.332	2.260	0.649
PS 19	596.36	4.209	2.332	2.258	0.615
PS 20	592.15	4.050	2.337	2.263	0.568
PS 21	597.76	4.129	2.337	2.253	0.572
PS 22	592.75	4.270	2.340	2.260	0.641
PS 23	594.10	4.058	2.346	2.256	0.568
PS 24	614.92	4.179	2.336	2.262	0.557
PS 25	564.36	4.040	2.334	2.259	0.621

TABLE 6.7

ATA Test Number	Initial Voids Ratio e_i	Zero Lateral Strain Consolidation					
		Minor Stress $\sigma_y=\sigma_x$	Major Stress σ_3	Volume Strain ε_{vc}	Voids Ratio e_c	Stress Ratio $\frac{\sigma_3}{\sigma_1}$	Oct'al Normal Stress σ_{oct}
PS 1	0.580	10.00	29.85	1.14	0.562	0.335	16.62
PS 2	0.553	11.80	40.25	1.08	0.536	0.293	21.28
PS 3	0.631	11.60	36.65	0.61	0.621	0.316	19.95
PS 4	0.656	14.10	21.75	1.46	0.632	0.649	16.65
PS 6	0.558	10.30	25.55	1.61	0.533	0.404	15.38
PS 7	0.521	12.85	46.05	0.50	0.514	0.279	23.92
PS 8	0.620	15.70	46.25	1.31	0.599	0.340	25.88
PS 9	0.652	14.40	38.50	1.17	0.633	0.374	22.43
PS 10	0.599	15.00	20.00	0.98	0.583	0.750	16.67
PS 11	0.610	15.00	38.40	0.99	0.594	0.390	22.80
PS 12	0.623	13.60	40.60	1.05	0.606	0.335	22.60
PS 14	0.618	10.70	26.75	0.68	0.607	0.400	16.05
PS 15	0.593	11.70	35.00	1.01	0.577	0.334	19.47
PS 16	0.577	12.20	41.75	0.89	0.563	0.292	22.05
PS 17	0.549	13.10	38.15	0.90	0.536	0.344	21.45
PS 18	0.649	9.30	24.20	1.08	0.631	0.359	14.27
PS 20	0.568	11.20	35.05	1.63	0.543	0.320	19.15
PS 21	0.572	10.70	34.60	1.32	0.551	0.309	18.67
PS 22	0.641	10.90	30.20	0.94	0.626	0.361	17.33
PS 23	0.568	14.00	39.15	0.94	0.554	0.358	22.38
PS 24	0.557	10.90	33.95	0.89	0.543	0.322	18.58
PS 25	0.621	11.20	29.00	0.95	0.605	0.386	17.13

the figure. Again, substantially different values were obtained from calculations based on final stresses and mean stresses respectively. The latter were regarded as more appropriate, and therefore the curve has been drawn through these experimental points. The results from the ATA TC and PS series are shown together in Fig. 6.21.

The total volumetric strains during consolidation, divided by the final value of σ_3 have been plotted in Fig. 6.22, and may be compared with those for the ATA TC tests in Fig. 6.7. The scatter is of about the same order, ignoring the uppermost point in the former figure, which represents a test (PS 20) showing uncharacteristic specimen behaviour during subsequent shearing. Reasons for the wide variation in the results were discussed in section 6.3.1.

6.4.2 FAILURE CHARACTERISTICS

The twenty-one ATA PS tests which reached failure are listed in Table 6.8, together with the various strains and stress ratios at this point.

The ratio $\frac{\sigma_2 - \sigma_3}{\sigma_1 - \sigma_3}$ (= b) commonly used to define the relative magnitude of the intermediate principal stress, will vary throughout any plane strain test depending largely on the stress induced by the lateral constraint. Since this must depend upon the packing of the particles, tests in plane strain on specimens of differing porosities will progress along different stress paths. Therefore, while retaining the parameter b to describe a specific relationship between the principal stresses at failure, care must be exercised when comparing the results from plane strain tests with those from "intermediate-stress" tests. This will be considered again in section 6.6.

In Fig. 6.23 the conventionally-defined peak strength, ϕ, has been plotted against e_i for all ATA PS tests, and therefore the magnitude of

TABLE 6.8

ATA Test Number	Initial Voids Ratio e_i	Conditions at Failure (Peak Stress Ratio)								
		Axial Strain ε_{1f}	Volume Strain ε_{vf}	Peak Stress Ratio $\frac{\sigma_1}{\sigma_3}$	Volume Strain Rate $\dot{\varepsilon}_{vf}$	Stress Ratio $\frac{\sigma_2}{\sigma_1+\sigma_3}$	Stress Ratio $\frac{\sigma_2-\sigma_3}{\sigma_1-\sigma_3}$	$\sin\phi$	Angle Internal Sh'g Res ϕ	Dir'n Const. Stress
PS 1	0.580	8.13	-1.21	5.153	-0.28	0.336	0.257	0.675	42.5	z
PS 3	0.631	9.80	-0.47	3.816	-0.06	0.348	0.239	0.585	35.8	z
PS 4	0.656	6.68	+2.15	3.665	-0.09	0.352	0.242	0.571	34.8	z
PS 6	0.558	5.13	+0.75	4.595	-0.52	0.360	0.283	0.643	40.0	z
PS 7	0.521	6.31	-1.28	6.149	-0.49	0.283	0.199	0.720	46.1	z
PS 8	0.620	6.70	+0.88	7.992	-0.19	0.284	0.223	0.778	51.1	z
PS 9	0.652	11.04	+0.17	3.838	-0.10	0.359	0.259	0.587	35.9	z
PS 10	0.599	5.98	-0.57	4.450	-0.30	0.360	0.278	0.630	39.1	z
PS 11	0.610	7.80	-0.67	4.420	-0.20	0.352	0.264	0.631	39.1	z
PS 12	0.623	7.41	-0.18	4.034	-0.15	0.337	0.230	0.603	37.1	z
PS 14	0.618	10.91	-0.70	4.341	-0.10	0.355	0.268	0.626	38.8	x

(cont'd)..

TABLE 6.8 (cont'd)

Number	e_i	ε_{1f}	ε_{vf}	$\frac{\sigma_1}{\sigma_3}$	$\dot{\varepsilon}_{vf}$	$\frac{\sigma_2}{\sigma_1+\sigma_3}$	$\frac{\sigma_2-\sigma_3}{\sigma_1-\sigma_3}$	sin ϕ	ϕ	Const.
PS 15	0.593	6.90	-0.70	4.802	-0.29	0.302	0.191	0.655	40.9	x
PS 16	0.577	5.34	-0.52	4.628	-0.34	0.254	0.118	0.645	40.2	x
PS 17	0.549	5.53	-0.72	5.111	-0.43	0.281	0.175	0.673	42.3	x
PS 18	0.649	9.89	+0.16	3.753	-0.12	0.369	0.274	0.579	35.4	x
PS 20	0.568	8.57	+1.30	5.575	-0.14	0.285	0.191	0.696	44.1	x
PS 21	0.572	7.13	-0.67	4.924	-0.35	0.300	0.198	0.662	41.5	x
PS 22	0.641	10.39	-0.22	4.023	-0.11	0.358	0.264	0.602	37.0	x
PS 23	0.568	7.87	-1.04	5.102	-0.31	0.282	0.177	0.673	42.3	x
PS 24	0.557	7.75	-2.13	5.303	-0.36	0.358	0.291	0.683	43.1	z
PS 25	0.621	9.97	-0.76	4.264	-0.16	0.369	0.288	0.620	38.3	z

the intermediate principal stress is of no importance. A mean curve has been drawn through eight of the nine points representing σ_x-constant tests (σ_{oct}-increasing) and ten of the eleven points shown for σ_3-constant tests. (The variation of σ_{oct} in the latter category will depend largely upon change in σ_2, and therefore in general it will be more convenient to specify which stress was held constant).

The results from tests PS 6 (e_i = 0.558, ϕ = 40.0), and PS 20 (e_i = 0.568, ϕ = 44.1) have been ignored. In the former, the peak strength was 3° lower than that given by the mean curve, and the volumetric strain rate at failure (lower graph) was considerably greater than the average. The reasons for these differences were not obvious from the stress-strain curves, but the behaviour was so untypical that the omission was considered justifiable.

In contrast, test PS 20 exhibited an erratic curve of σ_1 v. ε_1 which was almost certainly caused by apparatus interference. It may be significant that the volumetric strain during consolidation (represented by the uppermost point in Fig. 6.22) was excessive, even allowing for the general scatter of these results. The value of $\dot{\varepsilon}_v$ throughout deformation was very low, and at failure, was less than half that given by the mean $\dot{\varepsilon}_{vf}$ v. e_i curve.

The results from test PS 8 have not been plotted in Fig. 6.23, since ϕ (=51.1°) was 13° in excess of that to be expected for a comparable initial voids ratio. Neither in this test nor in PS 20 and PS 6 were any abnormalities evident when the side stress-cells were removed and the specimen dismantled. The stress-strain curves for these tests are included in Appendix H.

The maximum deviation from the mean curve of ϕ against e_i for the remaining points is 1.4°, and there is no noticeable difference between the results from σ_x-constant and σ_3-constant tests. This would tend to

confirm that the slight increase in ϕ with decreasing stress level, observed in the ATA TC series, was probably not statistically significant. Again the volumetric strain rates at failure have an approximately linear relationship with initial porosity, and apart from the two "worst" points (tests PS 14 and PS 3) at the loose end of the density range, the scatter is less than that in Fig. 6.8. The points disregarded in the ϕ v. e_i plot were also ignored in drawing the $\dot{\varepsilon}_{vf}$ v. e_i curve.

In only three tests of this series did the maximum volumetric strain occur at failure; in the remainder, $(\dot{\varepsilon}_v)_{max}$ was reached before peak stress ratio. The corresponding points and the mean curve of $(\dot{\varepsilon}_v)_{max}$ v. e_i are shown in Fig. 6.23. Although the two curves converge with increasing voids ratio, unlike those for the ATA TC tests, the ratio between the strain rates clearly increases, ranging from about 1.2 to 1.5.

During several of the tests carried out in this series, consolidation deviated considerably from the zero lateral strain condition. Two such tests, PS 7 and PS 8, were disregarded for other reasons. However, the strengths and volumetric strain rates of the others were in general agreement with those of the K_o-consolidated specimens. Other investigators (e.g. Bishop and Eldin (1953) have suggested that the strengths of specimens consolidated under either ambient or K_o conditions were the same. Therefore the ATA PS tests would give tentative support to the more general postulate that the magnitude of the stress ratio $\frac{\sigma_1}{\sigma_3}$, during consolidation, has little effect on ϕ or $\dot{\varepsilon}_{vf}$, providing the principal stresses are not subsequently re-ordered.

In Fig. 6.24 the axial strain at failure, ε_{1f}, and the volumetric strain during the shearing stage, ε_{vs}, are plotted against e_i. By ignoring the values obtained from the more doubtful tests, the wide scatter of points apparent in both graphs can be reduced.

However, although the ε_{vs} v. e_i points then lie reasonably close to the straight line shown, especially for loose specimens, neither relationship is as clear as that between ε_{vf} and e_i. Therefore it is possible only to make the general observation that the axial strain at failure in plane strain increases with initial porosity and that dilatancy during shearing decreases. Extrapolation of the ε_{vs} curve to maximum voids ratio would indicate negligible volume change. There is no discernible difference between the overall behaviour in σ_x-constant and σ_3-constant tests.

Fig. 6.25 shows the variations in the relative magnitudes of the three principal stresses at failure in plane strain for different initial voids ratios. The $\frac{\sigma_1}{\sigma_3}$ v. e_i curve is obviously equivalent to that of ϕ v. e_i in Fig. 6.23.

Two of the more common ratios used to provide information on the intermediate principal stress are represented in the two lower graphs. The most striking feature is the difference between σ_x-constant tests (curves a and c), and the σ_3-constant tests (curves b and d). The points representing PS 7, the densest specimen, are at variance with the others in this respect.

Comparison between Tables 6.7 and 6.9 reveals that the magnitude of σ_{oct} at failure in σ_3-constant tests was, in nearly all cases, very similar to its magnitude at the end of consolidation. Test PS 8 can be ignored for reasons previously discussed, and in PS 10, for which a value of K_o of 0.750 was recorded, the final consolidation stresses were unreliable. In the remaining tests, the overall increase in σ_{oct} was between +1.25 lbf/in^2 and -0.49 lbf/in^2. Obviously the comparison is made between stress conditions at two specific instants, and does not necessarily imply that the entire stress path lies close to an octahedral plane in principal stress space.

TABLE 6.9

ATA Test Number	Initial Voids Ratio e_i	Conditions at Failure $\left(\frac{\sigma_1}{\sigma_3}\right)_{max}$				
		Oct'al Normal Stress σ_{oct}	Oct'al Shear Stress τ_{oct}	Oct'al Stress Ratio $\frac{\tau_{oct}}{\sigma_{oct}}$	Oct'al Shear Strain γ_{oct}	Dir'n Const. Stress
PS 1	0.580	16.17	10.39	0.643	14.28	z
PS 3	0.631	21.20	11.77	0.555	16.39	z
PS 4	0.656	17.25	9.31	0.539	9.21	z
PS 6	0.558	14.72	8.78	0.596	7.77	z
PS 7	0.521	23.55	17.14	0.728	11.37	z
PS 8	0.620	22.72	17.68	0.778	10.23	z
PS 9	0.652	22.35	12.27	0.549	17.89	z
PS 10	0.599	13.98	8.20	0.586	11.83	z
PS 11	0.610	22.72	13.48	0.595	15.36	z
PS 12	0.623	22.88	13.24	0.578	12.25	z
PS 14	0.618	25.82	15.11	0.585	18.39	x
PS 15	0.593	28.47	19.48	0.688	9.15	x
PS 16	0.577	29.10	19.12	0.657	11.84	x
PS 17	0.549	34.18	23.49	0.687	9.62	x
PS 18	0.649	20.17	10.80	0.536	16.02	x
PS 20	0.568	31.57	22.24	0.704	12.95	x
PS 21	0.572	27.43	18.12	0.660	12.19	x
PS 22	0.641	24.78	13.94	0.563	17.15	x
PS 23	0.568	35.25	24.16	0.685	13.71	x
PS 24	0.557	19.12	12.12	0.634	14.43	z
PS 25	0.621	16.82	9.60	0.571	16.91	z

A further relationship between the principal stresses at failure, $\frac{\sigma_2}{\sigma_1 + \sigma_3}$ v. e_i, is shown in Fig. 6.26, and it can be seen that this ratio was very similar in all σ_3-constant tests (except PS 7), the mean value being about 0.35. The small scatter could not be attributed to the overall differences in σ_{oct}, nor to the differences in its magnitude at the end of consolidation and at failure. In the σ_x-constant tests, σ_{oct} increased throughout the shearing stage, and at failure was between 1.32 and 1.65 of its value at the end of consolidation. Although this appears to have had little effect on the three loosest specimens, the remaining points are considerably lower in $\frac{\sigma_2 - \sigma_3}{\sigma_1 - \sigma_3}$, or $\frac{\sigma_2}{\sigma_1 + \sigma_3}$, against e_i plots. There is no direct relationship between these ratios and the magnitude of the changes in σ_{oct}. However, it may be significant that the axial strains at failure for the three loosest specimens were about 10 or 11%, much greater than for the rest. Therefore the shape of the σ_2 v. ε_1 curve could account for the variations in stress ratio for σ_x-constant tests.

Several investigators have attempted to fit empirical expressions to the variations in σ_2 both during deformation and at failure in plane strain. Wood (1958) observed that σ_2 remained approximately equal to $K_o\sigma_1$, and proposed the relationship $\frac{\sigma_2}{\sigma_1 + \sigma_3} = \frac{\cos^2\phi}{2}$. This was amended to $\frac{\cos^2(0.8\phi)}{2}$ by Green (1969) for the failure condition in dense sand. If it is assumed that failure occurs at a b-value of about 0.3, the approximate relationship $\sigma_2 = \sqrt{(\sigma_1\sigma_3)}$ is obtained.

These relationships are plotted against e_i in Fig. 6.26b, using the ϕ v. e_i curve for ATA PS specimens. The theoretical relationships of perfect plasticity, $\sigma_2 = \frac{\sigma_1 + \sigma_3}{2}$, and of Parkin (2.2), $\sigma_2 = \frac{\sigma_1 + \sigma_3}{3}$, are also shown, the latter being applicable to dense media only. All of the curves approximated closely to straight lines in this plot.

Superficial comparison with the ATA PS test results would validate Parkin's expression for tests in which σ_{oct} remained reasonably constant. For σ_x-constant tests, however, the stress ratio for denser specimens was close to that given by Wood's equation. The difference in behaviour in the two types of test, and, in particular, some conclusions that can be drawn from the nature of the σ_2 variations, will be considered in the following section.

Fig. 6.27 shows the relationship between the octahedral stress ratio, $\frac{\tau_{oct}}{\sigma_{oct}}$ (= R_{oct}), and e_i at failure. Unlike the conventional ϕ v. e_i representation, this graph includes the effect of the intermediate principal stress. Because the maximum value of $\frac{\sigma_1}{\sigma_3}$ has been retained to define failure, however, the octahedral stress ratio at this point is not necessarily also at its maximum. In most cases $(R_{oct})_{max}$ was reached at much smaller strains, and the specimen characteristics under these conditions will be discussed in section 6.4.7. In Fig. 6.27, the two dashed curves have been drawn through the points for σ_x- and σ_3-constant tests respectively, though neither relationship is well-defined. Clearly the effect of the magnitude of σ_{oct} must be similar to that previously described.

6.4.3 STRESS-STRAIN CURVES

Figs 6.28-31 show the typical variations in the three principal stresses and σ_{oct}, with axial strain, for both σ_x- and σ_3-constant tests. Curves of ε_v and ε_3 are also given, and the four tests cover a range of initial voids ratios from 0.549 (PS 17) to 0.623 (PS 12). As in the ATA TC test series, the end of the consolidation stage occurred at about 1% axial strain in each case. For σ_3-constant tests, the cell pressure, σ_x, was then adjusted to keep the mean of the end stress-cell readings constant, while the side-cell pressure, σ_y, was varied to balance the null-indicator (4.6.3).

Test PS 12, on a loose specimen, shows that the initial decrease in the minor principal stress was accompanied by a slight decrease in the intermediate principal stress. As σ_3 steadily decreased, σ_2 changed sense, and was increasing at its maximum rate at about the failure point. The subsequent slight increase in σ_3 was accompanied by a decreased rate of increase in σ_2. The total variation in σ_{oct} throughout shearing to failure was less than 1 lbf/in^2.

The dense specimen (PS 24) behaved in a similar manner, but with an exaggerated variation of the intermediate stress. After an initial decrease, during which its magnitude was only slightly greater than σ_3, σ_2 again can be seen to reach a maximum rate of increase at an axial strain just less than that at failure. Because of the nature of the σ_2 variation, the changes in σ_{oct} were greater than for the loose specimen, but still small. Immediately following K_o-consolidation, both specimens began to dilate at a rate very close to the maximum in each case. Little variation in the volumetric strain rate was observed for either specimen during the majority of the shearing stage, although slightly decreased rates occurred close to failure.

All the curves shown in Figs. 6.28,29 are typical of the specimen

behaviour in σ_3-constant tests. Many tests were continued to post-failure strains, but in no instance did the magnitude of σ_2 tend towards the mean of σ_1 and σ_3. Usually its rate of increase with axial strain was seen to decrease after failure and, for looser specimens, its magnitude became almost constant. An exception was the densest specimen, PS 7, in which σ_2 increased at a variable rate after failure, and was increasing rapidly when the test was curtailed.

Although no clear relationship was found between initial voids ratio and the rate of change of σ_2 at failure (when the rates of change of σ_1 and σ_3 were zero), it could be generally stated that the rate was higher for denser specimens. Apart from those tests in which consolidation conditions departed considerably from zero lateral strain, all specimens showed the immediate post-consolidation dilatancy typified by the two tests shown.

The σ_x-constant plane strain tests did not show the same universal response, dilatancy beginning immediately for some specimens, e.g. PS 17, and being preceded by a small compression for others.

It can be seen in Figs 6.30 and 31 that the variation of the major principal stress is similar to that observed in some ATA TC tests, an inflexion in the σ_1 v. ε_1 curves occurring prior to peak stress. The variations in σ_2 are consistent with those in σ_3-constant PS tests, the slope of σ_2 v. ε_1 increasing, slowly at first, to reach a maximum shortly before failure, and becoming zero shortly afterwards. Again the volumetric strain rates were at their greatest before failure, and exhibited significant decrease only at large strains.

Nearly all ATA PS tests were continued beyond failure. However, this always resulted in non-uniformity of specimen deformation, such as that shown in Fig. 6.3 for test PS 15 in which the peak stress was reached at an axial strain of 6.90%. During a test it was not possible

to determine the exact stage at which a slip surface was formed, because the side stress-cells obscured the σ_y faces of the specimen. The mode of deformation of plane strain specimens will be discussed in more detail in section 6.4.5.

It would appear unlikely that the measured post-failure strains were representative of those occurring in local zones, and therefore a detailed analysis of stress-deformational behaviour based on these data would not be justifiable. In the whole of this test series, the axial strains at failure were large. Consequently it was not practicable to greatly exceed these values.

Within the strains applied, however, very few specimens showed any propensity to approach a "critical state". Although in several tests, the volumetric strain rate was becoming very small, and σ_2 was sensibly constant, the $\frac{\sigma_1}{\sigma_3}$ stress ratio continued to decrease, PS 17 being one such example. The conditions at large strains in tests PS 9, 18 and 10 were those most resembling the critical state, but although each yield an approximate value of between 35° and 37° for ϕ_{cv}, similar to that predicted by Horne's theory (2.2) for triaxial compression, it is almost certain that this is fortuitous. Moreover, it may be noted from Table 6.8, that the loosest specimen, PS 4, exhibited a peak strength of 34.8°, which decreased to about 33° at large axial strain. Although lower values were observed in other tests, it is probable that these were the result of severe non-uniformity of the specimen and associated apparatus effects. Therefore it was not possible to determine ϕ_{cv} in this series of tests with any certainty.

Obviously in all σ_x-constant tests σ_{oct} must increase prior to failure, providing the reasonable assumption is made that neither σ_1 nor σ_2 decreases at any stage by other than very small amounts. In both PS 15 and PS 17 inflexions in the σ_{oct} curves are caused primarily

by those in the σ_1 curves; in the former case, the effect is fortified by the nature of the changes in σ_2.

If the series of ATA PS tests is taken in isolation, a probable explanation of this phenomenon must be that, following K_o-consolidation, the test specimen is subjected to a stress path which undergoes a transition between that appropriate to triaxial compression and that appropriate to plane strain. This implies that the slow initial build-up of the lateral deviator stress, $\sigma_2 - \sigma_3$, is uncharactersitic of plane strain and that only at much larger values of ε_1 is deformation confined to y-z planes. This, in turn, implicates the system used to maintain the $\varepsilon_2 = 0$ condition.

In Appendix C, the results of a calibration test for side stress-cell volume change are discussed. Although it is suggested that the errors in the y-direction strains are likely to be small, the difficulties of simulating the exact test conditions in which stress-cell membrane exposure may be important, are pointed out. Therefore it is possible that at small strains following consolidation, the pressure differential across the side stress-cell membranes caused them to expand slightly at the corners of the specimen. However, the magnitude of the expansion was not sufficiently large for its effect to be seen from outside the main-cell.

Fig. 6.1 shows the progressive straining of specimen PS 11. With increasing strain in the x-direction the membrane exposure is reduced and therefore a better approximation to genuine plane strain conditions may be achieved.

The difficulties of determining the specimen dimensions at intermediate stages of a test were discussed in section 6.3.5. Fig. 6.3c,d shows the state of specimen PS 15, subjected to a maximum axial strain 3% in excess of that at failure, after removal of the side-cells. The severe wrinkling of the membrane was characteristic of specimens strained

to failure or beyond. Attempts were made to measure two plane strain specimens shortly after failure and the results will be presented in section 6.4.5. Each showed slight increases in their y-direction dimensions, though the exact causes were difficult to isolate.

It was noted that the magnitudes of K_o, recorded in ATA TC and PS tests were considerably lower than would normally be expected, and that this would be associated with lateral expansion. Therefore, even if it were possible to rely upon the post-test specimen measurements, the proportion of ε_y occurring during the plane strain stage would still be unknown. It is suggested, for the time being, that the inflexions observed in σ_1 and σ_2 curves are the result of small lateral expansions not detectable from mercury thread movement in the null-indicator, and that their effect is more pronounced at small strains. The observed inflexions in the triaxial compression stress-strain curves may not be so explained, and this problem will be reconsidered in subsequent sections.

6.4.4 STRESS-DILATANCY BEHAVIOUR

The plane strain condition, $\varepsilon_2 = 0$, does not disturb the basic stress-dilatancy equation, or the minimum energy principle since the work done in the intermediate principal stress direction is zero. Therefore the dilatancy factor, $\left(1 - \frac{d\varepsilon_v}{d\varepsilon_1}\right)$, reduces to $\frac{-d\varepsilon_3}{d\varepsilon_1}$, and the equation becomes $R = \frac{-d\varepsilon_3}{d\varepsilon_1} K_f$. The variations in K_f, between the lower limit K_μ and the upper limit K_{cv}, for specimens prepared at different initial porosities, are considered to be caused by variations in the angle of interparticle sliding, β.

Wightman (1967) carried out plane strain tests in which it was observed that $K_f \rightarrow K_{cv}$ throughout deformation. It was suggested that the degree of freedom for specimen strains was an important factor

in determining the range of β during any test. Therefore in triaxial compression, the wide choice of planes on which instantaneous sliding can occur allows a sufficient number of contacts to slide at close to the preferred angle β_c. Conversely, plane strain conditions allow a minimum degree of strain freedom, and hence sliding is forced to occur at a wider range of β values, consistent with the upper limit K_{cv}, causing a greater dissipation of frictional energy (6.3.4).

The stress-dilatancy curves, R v. D, for the majority of the ATA PS test series are shown in Figs. 6.32-36. As for the ATA TC tests, the initial point in each curve represents the first set of increments after the end of consolidation. The failure point is indicated with an arrow, and the end point represents the final set of increments. Again every point in Fig. 6.32 was determined from the mean of three measured increments of axial and volumetric strains. A further "smoothing" was achieved by taking the mean gradient of the ε_3 v. ε_1 curve over intervals of 1% axial strain. Unlike the former process, this was considered likely to mask the true specimen behaviour, and therefore the results have not been presented. The magnitudes of $\dot{\varepsilon}_{vf}$ were, however, determined in this way, which accounts for the occasional small differences between the values given in Table 6.8 and those derived from the R v. D graphs.

All the points are shown for two σ_3-constant tests (PS 9 and 25) and one σ_1-constant test (PS 16) in the first figure. They have been omitted in Figs. 6.33,34, in which the remaining σ_3-constant tests are shown, and in Figs. 6.35,36, which show the rest of the σ_1-constant tests. The K_μ and K_{cv} lines are identical with those in Figs. 6.13-16.

In most cases the early portion of the R v. D curve, representing the uncertain conditions immediately after consolidation, should be regarded with caution. In test PS 23, the rate of the continued compression,

and hence the magnitude of D, was such that the initial point appears above the K_{cv}-line. The early increments have been omitted from the PS 10 curve, because of the unusual conditions during consolidation (6.3.1).

If the true initial slopes of the curves are considered to be greater than those shown (6.3.4), it would appear that all but two of the σ_3-constant tests (PS 16 and PS 7) would have followed early paths along the K_μ-line, or just above it. (Test PS 4 has been ignored because of shearing - Appendix H). The exceptions were each dense specimens, PS 7 being the densest tested. This apparent difference in behaviour is even more striking for the σ_1-constant tests, where the curves for the four loosest specimens, PS 9, 25, 18 and 22, all lie very close to the K_μ-line. Curves for the remaining specimens begin progressively further from this line with increasing initial density. Test PS 17 clearly belongs to the latter category, despite the position of its short initial section.

These results are in general agreement with those from the ATA TC series, in which a similar increase in ϕ_f was observed for denser specimens, during the early stages of shearing. Moreover, the same overall pattern is apparent in the R v. D relationships for both series of tests. After reaching a magnitude close to its maximum, the dilatancy factor remained relatively steady throughout the majority of the shearing stage to failure. In all but two of the σ_1-constant tests (Figs. 6.32,35,36) the small changes in D between D_{max} and R_{max} were almost linear, and although the σ_3-constant tests in Figs. 6.32,34 showed the same trend, those in Fig. 6.33 were more wayward. Failure, in almost every case, occurred at a second "peak" of the dilatancy factor, whereupon an immediate and significant decrease in D was observed in tests continued beyond R_{max}. In test PS 3, failure was reached only after a

considerable drop in D, but this may be associated with the poorly-defined peak in its stress-strain curve.

Several specimens were deforming at, or close to, constant volume (D = 1) at the end of the tests. However, all three principal stresses were sensibly constant only in tests PS 9 and 10, though in PS 3, 12 and 18, the stress ratio R was constant. In the remainder, R was continuing to decrease. Clearly the non-uniform behaviour of the specimens at large strains will affect the form of the R v. D curves.

The local dilatancy rate in a failure zone will almost certainly have exceeded the average rate based on overall volume change measurements. This may apply also, but to a lesser extent, to pre-failure deformations. While this argument would explain why the latter portions of the R v. D curves, in several instances, appear to be directed above the critical state point, it would apply equally to those curves directed below this point. Typical of this contradiction are the curves for PS 15 and 17 in Fig. 6.35. However, the stresses were undoubtedly also affected by the non-uniform specimen behaviour, since top stress-cell tilting frequently occurred, possibly giving rise to further apparatus interference. Therefore these differences may not be significant.

Having regard to the possible errors involved in estimating both stresses and strains after failure, these results indicate the possibility of a critical state to which all specimen state paths converge, during plane strain deformation.

It was considered very unlikely that underestimation of the volumetric strain rate would be of a magnitude sufficient to explain the deviations of dense specimens from the K_{cv}-line, during pre-failure deformations. In test PS 7, for instance, D_{max} was reached at an axial strain approximately half that at failure. It would be reasonable to expect that at this stage the average volumetric strains were not

unrepresentative of the volumetric strains at any point within the specimen.

The failure points for all of the tests are shown together in Fig. 6.36, where the upper and lower limit lines are equivalent to ϕ_f values of 39° and 33°. The scatter is much wider than that shown in Fig. 6.16 for the ATA TC series, though it is of interest to note that a mean straight line through these points would lie only a little above the K_{cv}-line.

6.4.5 MODE OF DEFORMATION

The majority of ATA PS tests were continued beyond failure. In most cases specimen deformation became non-uniform, a discontinuity developing along a plane parallel with the y-axis and the top stress-cell commonly tilting. During a test, horizontal discontinuities could be seen at the intersection of the slip surface with the σ_x-faces. A typical example of the specimen appearance is shown in Fig. 6.3. However, it is unlikely that such non-uniformities occurred during pre-failure deformations for the majority of specimens, though the appearance of the σ_x-faces would have been the only visible indication in tests continued to large strains.

Fig. 6.2 shows the state of two plane strain specimens prior to failure, which for PS 17 occurred at $\varepsilon_1 = 5.53\%$, and for PS 25 at $\varepsilon_1 = 9.97\%$. The mode of deformation of the former specimen was typical of the majority of the ATA PS series, lateral expansion in the σ_x-direction occurring predominantly at the base, particularly for loose specimens. Test PS 25 was unusual in that the specimen did not deform symmetrically with respect to the top stress-cell. Probably as a result of poor setting-up, almost all of the lateral expansion at the top was concentrated on the side shown, although the top stress-cell did not tilt.

Few specimens exhibited significant bulging until well after failure, which was testimony to the effectiveness of the end lubrication system. Two specimens were measured after test, PS 1 and PS 18, the former showing the early development of a slip surface, the axial strain at failure having been surpassed by almost 1%. The latter also exhibited a visible slip surface after over 1% additional axial strain. These areas were avoided when taking the final specimen measurements.

The initial average dimensions (Table 6.6), show that the side stress-cell membrane exposure was considerably less for PS 18. A vernier micrometer was used to measure the initial and final local dimensions of each specimen, as described in section 6.3.5 for ATA TC 6, and these are given in Tables 6.10 and 6.11. The same comments apply regarding their accuracy.

For the denser specimen, the average values of ε_x at the top and bottom, computed from the changes in the dimensions of the σ_y-faces, were approximately -6% and -12%, respectively. Specimen PS 18, one of the loosest tested, expanded slightly more at its base, the corresponding values of ε_x being -6% and -13%. In each case the overall average strain in the x-direction, calculated from the mean of the fifteen measurements, was within 1% (in ε_x) of the value determined from volumetric and axial deformations. Considering the manner in which former data was obtained, this must be regarded as fortuitous.

The overall average strain in the ε_y ("constrained") direction was about 0.7% for both tests, which is surprising in view of the greater amount of membrane exposure in test PS 1. Therefore, assuming these results are reliable, and typical of the ATA PS test series, the ratio of the total lateral strains at failure, $\frac{\varepsilon_x}{\varepsilon_y}$, would generally be much greater than 10. However, from the above data, it is impossible to determine the stage of the test during which the majority of the undesired y-direction strain took place.

TABLE 6.10

Initial Dimensions - ATA PS 1								
	σ_y Planes				σ_x Planes			
	A	B	C	Average	A	B	C	Average
1	2.263	2.267	2.262	2.264	2.242	2.243	2.241	2.242
2	2.263	2.269	2.267	2.266	2.236	2.248	2.248	2.244
3	2.267	2.273	2.273	2.271	2.240	2.249	2.250	2.246
4	2.278	2.279	2.277	2.278	2.246	2.256	2.256	2.253
5	2.277	2.278	2.278	2.278	2.252	2.256	2.258	2.255
Final Dimensions								
	σ_y Planes				σ_x Planes			
	A	B	C	Average	A	B	C	Average
1	2.393	2.423	2.403	2.406	2.248	2.260	2.248	2.252
2	2.428	2.456	2.435	2.440	2.250	2.263	2.260	2.258
3	2.488	2.514	2.497	2.500	2.253	2.260	2.275	2.263
4	2.525	2.539	2.524	2.530	2.263	2.268	2.280	2.279
5	2.539	2.550	2.530	2.540	2.265	2.278	2.271	2.271

TABLE 6.11

Initial Dimensions - ATA PS 18								
	σ_y Planes				σ_x Planes			
	A	B	C	Average	A	B	C	Average
1	2.322	2.333	2.325	2.326	2.245	2.251	2.244	2.247
2	2.327	2.336	2.330	2.330	2.244	2.255	2.257	2.252
3	2.332	2.332	2.337	2.334	2.254	2.263	2.259	2.259
4	2.330	2.336	2.324	2.330	2.261	2.268	2.264	2.264
5	2.337	2.344	2.333	2.339	2.278	2.279	2.276	2.278
Final Dimensions								
	σ_y Planes				σ_x Planes			
	A	B	C	Average	A	B	C	Average
1	2.465	2.484	2.473	2.474	2.262	2.261	2.256	2.260
2	2.518	2.562	2.530	2.537	2.258	2.268	2.275	2.267
3	2.577	2.598	2.569	2.581	2.268	2.279	2.280	2.276
4	2.626	2.639	2.620	2.628	2.277	2.269	2.279	2.275
5	2.638	2.663	2.620	2.640	2.298	2.284	2.295	2.292

In view of the low values of K_0 (6.4.1), and the shape of the stress strain curves (6.4.3), it would appear reasonable to assume that significant increments of ε_y occurred only during the consolidation stage and during the early part of plane strain deformation.

6.4.6 TOP AND BOTTOM STRESSES

The variation, with axial strain, of the end stress-cell measurements in the two plane strain tests considered above are shown in Fig. 6.18. Again it was assumed that the mean of the top and bottom stresses was the appropriate value of σ_3 to be used in analyses.

From Table 6.10, the cross-sectional areas at the ends of the PS 1 specimen, shortly after failure, were 5.42 in^2 and 5.76 in^2 respectively. The average area determined from post-test measurement was 5.61 in^2 The final top and bottom stress-cell readings, 31.1 lbf/in^2 and 29.6 lbf/in^2, were corrected for these area differences, in the manner described in section 6.3.6 for ATA TC 6. The corrected stresses were 30.1 lbf/in^2 at the top, and 30.4 lbf/in^2 at the bottom.

Clearly these findings are unacceptable, since the frictional force along the side stress-cell surfaces must always act in sympathy with the bottom stress during a test in which ε_3 is positive. However, in view of the assumptions made, this apparent anomaly is of little significance.

The corresponding analysis for test PS 18, showed the top and bottom cross-sectional areas to be 5.59 in^2 and 6.04 in^2 respectively, and the overall average area 5.84 in^2 After area correction, the final top and bottom stresses (36.2 lbf/in^2 and 33.2 lbf/in^2) became 34.6 and 34.3 lbf/in^2 respectively, consistent with a frictional coefficient of about 0.01, along the side-cell-specimen interface. This would appear to be an underestimate.

Although these calculations, and that in section 6.3.6, are approximate, they indicate that the frictional resistance on the σ_y-faces is small, and the mode of deformation is such that the average end stress-cell reading may be used to determine the magnitude of σ_3.

In a few of the ATA PS tests, the difference between the top and bottom stress measurements became much larger than those shown in Fig. 6.18 for more typical specimens. An extreme example was that of test PS 23, in which the top and bottom stresses, recorded at failure, were 77.6 and 59.8 lbf/in^2 respectively. Even if it were assumed that zero expansion occurred at the top of the specimen, which in fact was not the case, a coefficient of friction in the region of 0.30 would be required to explain this stress difference. Clearly an additional apparatus effect was operative. In general, tests in which the top stress exceeded the bottom by greater than 5 lbf/in^2 were treated with caution, since without quantitative information regarding the mode of deformation, it was impossible to estimate the frictional loss. Such tests were, however, in a small minority.

The nature of the galvanometer traces in the plane strain tests was no different from that described for the ATA TC test series (6.3.6), each trace being very smooth until failure was approached. Again, the almost continuous fluctuations, during post-failure deformation, were punctuated with instantaneous large drops in stress, each being followed by a relatively slow build-up to a stress level slightly lower than before.

6.4.7 OCTAHEDRAL STRESSES

In section 6.4.2, the failure characteristics of all specimens tested in plane strain were discussed assuming that the Mohr-Coulomb criterion for failure was appropriate to this soil. Comparison between

the results from the ATA TC and ATA PS test series will be made in the next section. However, it is clear from Figs. 6.8 and 6.23 that this criterion is inadequate, except possibly for very loose specimens.

Alternative failure theories, which include for the effect of the intermediate principal stress, were reviewed in section 2.4. The Extended von Mises criterion states that failure will occur when the ratio between the octahedral shear and normal stresses, $\frac{\tau_{oct}}{\sigma_{oct}}$ $(= R_{oct})$, reaches a maximum value, dependent upon the material properties.

The stress and strain conditions of all ATA PS specimens at $(R_{oct})_{max}$ are given in Table 6.12, and the latter is plotted against e_i in Fig. 6.37. Tests PS 6, 8 and 20 have been omitted for the reasons previously stated, and the standard deviation of the remaining points from the mean curve is similar to that for the ϕ v. e_i plot. No difference between σ_x-constant and σ_3-constant tests is apparent either in these results or those of the lower graph of $\dot{\varepsilon}_v$ v. e_i, in which overall agreement is excellent.

The volumetric strain rate at $(R_{oct})_{max}$ coincided with $(\dot{\varepsilon}_v)_{max}$ in only three tests, but in about half of the remainder the maximum rate had not yet been reached. For every specimen, the total axial strain was considerably less than that at failure, and although no clear relationship was observed between ε_1 and e_i (Fig. 6.38), this was probably due to the uncertain initial conditions during shearing, and the associated effect on the σ_2 increments, (6.4.3). Obviously the volumetric strains during the shearing stage to maximum octahedral stress ratio (Fig. 6.38) were much less than those to failure. Again it is not surprising that ε_{vs} and e_i were poorly related, and the wide scatter of points in both graphs of Fig. 6.39 probably results from the same cause.

In particular, the values of $b = \left(\frac{\sigma_2-\sigma_3}{\sigma_1-\sigma_3}\right)$ for the two similar specimens PS 17 ($e_i = 0.549$) and PS 21 ($e_i = 0.572$) are of interest.

TABLE 6.12

ATA Test Number	Initial Voids Ratio e_i	Conditions at Maximum Octahedral Stress Ratio $\left(\frac{\tau_{oct}}{\sigma_{oct}}\right)_{max}$											
		Oct'al Normal Stress σ_{oct}	Oct'al Shear Stress τ_{oct}	Oct'al Stress Ratio $\frac{\tau_{oct}}{\sigma_{oct}}$	Oct'al Shear Strain γ_{oct}	Axial Strain ε_1	Volume Strain ε_v	Volume Strain Rate $\dot{\varepsilon}_v$	Stress Ratio $\frac{\sigma_2}{\sigma_1+\sigma_3}$	Stress Ratio $\frac{\sigma_2-\sigma_3}{\sigma_1-\sigma_3}$	Stress Ratio $\frac{\sigma_1}{\sigma_3}$	Equiv't Angle Sh'g Res ϕ_{equiv}	Dir'n Const. Stress
PS 1	0.580	15.67	10.49	0.670	3.42	2.47	+0.78	-0.38	0.221	0.022	3.813	35.7	z
PS 3	0.631	20.02	12.12	0.605	5.92	3.85	+0.46	-0.17	0.242	0.019	3.317	32.5	z
PS 4	0.656	17.05	9.18	0.539	5.66	4.55	+2.30	-0.06	0.303	0.126	3.220	31.7	z
PS 6	0.558	14.28	8.59	0.602	4.88	3.67	+1.42	-0.36	0.285	0.129	4.595	35.4	z
PS 7	0.521	23.05	17.18	0.745	6.99	4.16	-0.24	-0.50	0.228	0.097	5.192	42.6	z
PS 8	0.620	22.33	17.67	0.791	6.64	4.67	+1.24	-0.16	0.236	0.142	6.634	47.6	z
PS 9	0.652	21.83	12.09	0.554	4.92	3.52	+1.04	-0.07	0.277	0.068	3.137	31.1	z
PS 10	0.599	13.25	8.28	0.625	4.16	2.80	+0.52	-0.33	0.244	0.045	3.564	34.2	z
PS 11	0.610	21.68	13.84	0.638	6.21	4.03	+0.32	-0.28	0.240	0.047	3.684	35.0	z
PS 12	0.623	22.15	13.41	0.606	5.59	3.69	+0.54	-0.19	0.270	0.097	3.633	34.6	z
PS 14	0.618	19.93	11.88	0.596	6.58	4.17	+0.28	-0.15	0.262	0.066	3.430	33.3	x

(cont'd)..

TABLE 6.12 (cont'd)

Number	e_i	σ_{oct}	τ_{oct}	$\frac{\tau_{oct}}{\sigma_{oct}}$	γ_{oct}	ε_1	ε_v	$\dot{\varepsilon}_v$	$\frac{\sigma_2}{\sigma_1+\sigma_3}$	$\frac{\sigma_2-\sigma_3}{\sigma_1-\sigma_3}$	$\frac{\sigma_1}{\sigma_3}$	ϕ_{equiv}	Const.
PS 15	0.593	26.58	17.84	0.671	8.80	5.29	-0.20	-0.30	0.261	0.122	4.453	39.3	x
PS 16	0.577	27.38	19.26	0.703	7.50	4.50	-0.19	-0.38	0.232	0.080	4.508	39.6	x
PS 17	0.549	33.33	23.12	0.694	8.59	5.02	-0.48	-0.45	0.269	0.154	5.015	41.9	x
PS 18	0.649	15.18	8.25	0.543	4.46	3.22	+1.01	-0.10	0.260	0.006	2.887	29.0	x
PS 20	0.568	28.57	22.40	0.784	5.48	4.14	+1.64	-0.21	0.200	0.043	5.375	43.3	x
PS 21	0.572	21.88	15.04	0.687	6.28	4.08	+0.47	-0.38	0.220	0.034	4.033	37.1	x
PS 22	0.641	19.80	11.61	0.586	9.01	5.67	+0.31	-0.12	0.267	0.055	3.321	32.5	x
PS 23	0.568	32.33	22.79	0.705	8.25	4.94	-0.22	-0.33	0.245	0.110	4.770	40.8	x
PS 24	0.557	17.58	12.71	0.723	6.48	3.73	-0.47	-0.44	0.207	0.029	4.438	38.7	z
PS 25	0.621	15.95	9.83	0.617	8.57	5.51	+0.10	-0.20	0.244	0.038	3.471	33.6	z

Fig. 6.31 shows that σ_2 began to increase at close to its maximum rate, in the former test, shortly after 2% axial strain. For the second specimen, this did not occur until about 3% axial strain, there being a corresponding inflexion in the σ_1 v. ε_1 curve. Since the magnitudes of ε_1 at $(R_{oct})_{max}$ were similar in each case, it follows that the b values were widely different.

The variations in R_{oct} with γ_{oct}, the octahedral shear strain, for these tests, are shown in Fig. 6.40a, and the results from a further six tests, for specimens with a range of initial densities, are also presented. In each case, the first point represents the end of the consolidation stage. The peaks of these curves are generally less well-defined than those of the more conventional σ v. ε_1 plot, and for the looser specimens in particular, the magnitude of R_{oct} was very close to its maximum for large increments of strain. In test PS 18, the peak occurred at such a small strain after consolidation that σ_2 was barely different from σ_3, as can be seen by the very low value of b in Fig. 6.39. The subsequent increase in σ_2 to failure was very similar to that in σ_1 and therefore this octahedral stress ratio was not exceeded.

No unique value of R_{oct} was indicated for tests taken to large strains.

6.5 COMPARISON OF ATA TC AND ATA PS RESULTS

The similarity of test conditions in the two ATA test series, eliminates many of the errors likely to be incurred when comparing the stress-deformational behaviour of plane strain and triaxial compression specimens of different shapes and sizes tested in different apparatuses.

6.5.1 FAILURE CHARACTERISTICS

Fig. 6.41 shows the peak strengths, ϕ, plotted against initial voids ratio, e_i, the doubtful results, discussed in previous sections, having been omitted. The maximum observed difference in ϕ between any specific ATA TC and PS specimens of comparable initial voids ratios was 7°, and the minimum difference was just over 2°. Although the former comparison agrees with the difference between the two mean curves, the latter does not.

No specimens were formed at either the minimum (0.503) or the maximum (0.715) voids ratios, and therefore it was possible only to estimate the strengths of such specimens by extrapolation of the mean curves. This gave a difference of 7° at e_{min}, and one of 2° at e_{max}. However, in addition to the considerable amount of extrapolation necessary at the higher voids ratio, the behaviour of loose specimens is usually less predictable than that of dense, and the only two triaxial compression specimens looser than e_i = 0.610 showed a strength difference of $1\frac{1}{2}$°. It is conceivable, especially if the upper of the two points is the more reliable, that plane strain and triaxial compression strengths are equal at e_{max}, but any conclusion based only on the test results shown must be tentative. The substantial increase in ϕ for plane strain specimens at e_{min} can be predicted with far greater certainty.

Comparison between Figs. 6.9 and 6.24 indicates little difference between the axial strains at failure. Only for dense specimens did the

σ v. ε_1 curves in both test series exhibit well-defined peaks, those for plane strain specimens generally being sharper than for triaxial compression specimens of similar density. Therefore in many instances the stress ratio R was very close to its maximum value over a range of deformation. In addition, the axial strain at the end of consolidation was marginally different for each specimen. However, possibly the most important factor causing the wide variation in ε_{1f} for the plane strain tests, was the effect of the small initial rates of change of σ_2 associated with slight deviation from the $\varepsilon_2 = 0$ condition (6.4.3). The most likely effect this would have on the stress-strain curves would be to delay attainment of the peak stress ratio. Consequently the values of ε_{1f} in Fig. 6.24 will be overestimates.

A similar argument applied to the volumetric strain ε_{vs} would suggest that volume expansion during shearing in plane strain is less than that in triaxial compression, although there is little difference between the two mean curves.

Fig. 6.42 shows the volumetric strain rates at failure for both test series, and it is emphasized that the curve represents not only the mean through all the test points, but also the mean for the individual ATA TC and PS series. Therefore, for any given initial voids ratio, ε_{vf} appears to be independent of the imposed lateral strain conditions, the magnitude of the total strains at failure, and the value of the peak stress ratio. This will be considered in more detail in section 6.5.3.

6.5.2 STRESS-STRAIN CURVES

Graphs of the principal stresses, and ε_v, against axial strain for each test series were discussed in previous sections. Particular attention was given to the shape of the σ_2 curve, and it was suggested

that its small initial rate of increase after consolidation was associated with a deviation from the plane strain condition. Direct comparisons of the stress-strain curves in triaxial compression and plane strain have been made in Figs. 6.43-47. Only σ_x-constant tests have been considered because of the difficulty of comparing the relatively small changes of σ_x in σ_3-constant tests.

All the curves shown have been taken from the complete graphs presented in previous sections or in Appendix H. Where possible, tests on specimens having similar initial voids ratios, consolidated to similar values of σ_3, have been grouped, and the magnitudes of e_i are given at the end of each σ_1 curve. The curves are shown only from the end of consolidation, and in some cases a slight adjustment has been made so that the axial strains coincide at this point. Unfortunately, even for similar specimens, consolidated to the same σ_3, the values of σ_1 were not necessarily equal (6.3.1), but comparison of the general shapes of the curves remains of interest.

In Fig. 6.43, it can be seen that although the slope of the PS curve was always greater than that of the TC curve, the difference became marked only after about 4% axial strain, with increased rate of change of σ_2. The comparison between the curves in Figs. 6.46 and 6.47 is striking.

In the former, σ_2 for PS 17 increased steadily from the end of consolidation; there is little similarity between the σ_1 curves and only a very slight inflexion in that for the plane strain test. Both plane strain tests in Fig. 6.47 exhibited negligible increases in σ_2 for a prolonged initial period, and the shapes of the σ_1 curves are almost identical with that for TC 5. In each case similarity was lost almost as soon as σ_2 showed a substantially greater rate of increase.

The comparison between Figs. 6.46 and 6.47 is not, in itself,

conclusive, since the specimens were of quite different initial voids ratios. However, Figs. 6.44 and 6.45 show similar trends for denser specimens, with the exception of test PS 23, in which σ_1 increased rapidly during the early stages despite the negligible increase in σ_2. The cause is probably associated with the unusual conditions at the end of consolidation, and with late adjustments to σ_3.

In general, the rate of increase of σ_2 during ATA PS tests was clearly an important factor in determining the nature of the σ_1 v. ε_1 curve, and its initial slow build-up after consolidation appears to be the major cause of the observed inflexions, the test conditions passing through a transitional stage intermediate between triaxial compression and plane strain. However, it does not follow that the early slight deviation from the plane strain condition significantly affected later behaviour, or that the true shape of the σ_2 curve was necessarily linear, though it seems likely that its rate of increase would be greater for denser specimens. Clearly, this is associated with the greater dilatancy rates observed for the latter.

In view of the slight inflexions apparent in some of the ATA TC stress-strain curves (6.3.3), it cannot be stated with certainty that the nature of the variation in σ_2 was fully responsible for those in the ATA PS curves.

6.5.3 STRESS-DILATANCY BEHAVIOUR

The effect of deviations from the $\varepsilon_2 = 0$ will be considered, in connection with the ATA INT tests in section 6.6.4. If it is assumed that the deviations during the early stages of ATA PS tests caused the depressions in the σ_1 curves, the magnitudes of R will have been underestimates. Although the genuine R v. D curves for plane strain would therefore be slightly above those shown in Figs. 6.32-36, itis clear

that none would follow the K_{cv}(upper limit)-line throughout deformation, as has been suggested.

In general, it can be stated only that the mean curve through the failure points lies close to this line, and that after failure, the R v. D curves are directed vaguely towards the critical state point. The results from ATA TC tests on loose specimens, like those in plane strain, suggest that early deformations follow the K_{μ}(lower limit)-line, whereas for denser specimens, greater values of ϕ_f are appropriate. Each observation is contrary to stress-dilatancy theory expectations.

Horne (2.2) has suggested that during deformation of a particulate medium, the degree of induced anisotropy reaches a maximum at the maximum dilatancy rate, which depends upon the initial density. Assuming that the initial structure is destroyed after initial deformation, and therefore that anisotropy depends only upon those newly-formed contacts, the stress and strain-increment ratios were derived:-

$$\frac{\sigma_1}{\sigma_3} = \frac{4m_1}{\pi m_3} \tan\left(45 + \frac{\phi_\mu}{2}\right) \qquad \ldots (1)$$

$$\frac{d\varepsilon_3}{d\varepsilon_1} = \frac{-2m_1}{\pi m_3} \tan\left(45 - \frac{\phi_\mu}{2}\right) \qquad \ldots (2)$$

The term $\frac{4m_1}{\pi m_3}$ is a measure of the degree of induced anisotropy, equivalent to tan α in Rowe's (1962) equation. At the maximum possible rate of dilatancy, it was assumed that the only contacts were those occurring at maximum frequency, giving

$$\left(\frac{m_1}{m_3}\right)_{max} = \frac{\pi}{2} \tan\left(45 + \frac{\phi_\mu}{2}\right).$$

Hence $$R_{max} = 2K \text{ , and } \left(\frac{d\varepsilon_3}{d\varepsilon_1}\right)_{max} = -1.$$

Therefore, an upper limit on D_{max} of 2 was obtained.

Extrapolations of the ATA PS and TC failure curves (Fig. 6.41) to e_{min} gave values of R of 6.52 and 4.68 respectively. Generalising

equations (1) and (2) for ϕ_f, satisfying $\phi_\mu \leq \phi_f \leq \phi_{cv}$, and making Horne's assumption that $\phi_f = \phi_{cv}$ (= 35°) in plane strain, and $\phi_f = \phi_\mu$ (= 27°) in triaxial compression, D values of 1.77 and 1.76, respectively, were obtained. Extrapolation of the mean measured volumetric strain rates at failure (Fig. 6.42) to e_{min} gave a dilatancy factor of 1.57.

Therefore, although Horne's theory predicts the observed equality between the dilatancy factors in triaxial compression and plane strain, it appears to overestimate their magnitude, largely by virtue of overestimating R. However, even using the R values extrapolated from the ATA test results, the predicted dilatancy factors were still greater than those measured.

Clearly, in this analysis much depends on the assumptions regarding ϕ_f, and the chosen magnitudes of ϕ_μ and ϕ_{cv}.

In the majority of ATA tests, D_{max} was reached well before R_{max}, although its subsequent decrease was small, until after failure. A similar analysis based on the maximum observed values of ϕ_f at failure for the densest ATA TC and PS specimens (Fig. 6.16 and 6.36) gave D values of 1.48 in plane strain and 1.44 in triaxial compression. However, the use of equations (1) and (2) at other than the peak dilatancy rate is not strictly valid.

6.5.4 OCTAHEDRAL STRESSES

The relationship between the octahedral stress ratio, R_{oct}, and the initial voids ratio for plane strain specimens was discussed in section 6.4.7, and it was noted that this ratio reached a maximum at an axial strain considerably less than that at failure. In triaxial compression, failure necessarily implies $(R_{oct})_{max}$.

The values given in Table 6.5 have been plotted in Fig. 6.48, against e_i, together with the plane strain points from Fig. 6.37. The corresponding

volumetric strain rates ($\dot{\varepsilon}_v$ for PS, $\dot{\varepsilon}_{vf}$ for TC) are shown in the lower graph.

Although the $(R_{oct})_{max}$ curve for triaxial compression is directly related to ϕ, that for plane strain is not, and therefore there is no reason why these two curves should not coincide over the full range of e_i, especially in view of the different stress conditions at failure and at $(R_{oct})_{max}$ in the latter tests. However, it can be seen that this type of failure criterion is valid only for the dense specimens (say, $e_i < 0.580$). Based on triaxial compression strength, the strength of loose specimens in plane strain would be overestimated by up to 10%.

For values of R_{oct} at failure, $\left(\frac{\sigma_1}{\sigma_3}\right)_{max}$, the mean curve clearly falls even further below the dashed curve in Fig. 6.48 for all initial voids ratios. Consequently a theory based on the octahedral stress ratio at failure would even further overestimate plane strain strength with respect to triaxial compression.

6.6 ATA INT AND ATA TE TESTS

In order to effectively investigate the influence of the intermediate principal stress over a range of b values, it is necessary to detect small differences in stress-deformational behaviour due entirely to this cause. Behavioural differences due to other effects, such as significant discrepancies in e_i, must be eliminated or accurately assessed.

This can be done either by carrying out a large number of tests on specimens of various initial densities for each magnitude of b, and interpolating data for required e_i values, or by reproducing a specific initial density for each test. The former process was used in the ATA TC and PS test series. However, since a great number of ATA INT tests would have been required to fully investigate the effect of σ_2 for a wide range of e_i, it was decided to consider one initial voids ratio only, in this research program. Because of the relative ease with which dense specimens can be reproduced, and their likely accentuated differences in behaviour for each value of b, a value of $e_i = 0.530$ was chosen.

For convenience of comparison, the single ATA TE test has been included with the seven ATA INT tests, and the initial specimen properties are given in Table 6.13. In only two of the eight tests did e_i differ greatly from 0.530, and one of these, INT 5, was curtailed before peak stress because of a side stress-cell failure.

It should be noted that tests INT 1-6 were from category (ii) in Table 4.1 (section 4.6.4), the principal stresses being orientated as in the ATA PS testspreviously described. Test INT 7 was from category (vi), the major principal stress being applied through the side stress-cells and σ_3 reduced to failure, while σ_x was held constant at an intermediate value. The axial stress was also reduced to failure in ATA TE 1, with $\sigma_x = \sigma_y$ constant, the test being from category (vii).

TABLE 6.13

ATA Test Number	Mass Solids (gm)	Length (in)	Inter Width (in)	Minor Width (in)	Initial Voids Ratio
INT 1	589.54	3.940	2.335	2.262	0.533
INT 2	599.53	3.995	2.335	2.266	0.530
INT 3	613.97	4.026	2.356	2.278	0.526
INT 4	601.52	3.987	2.358	2.263	0.534
INT 5	611.10	4.045	2.334	2.262	0.511
INT 6	604.05	4.043	2.337	2.263	0.536
INT 7	597.50	4.016	2.338	2.258	0.535
TE 1	606.32	4.088	2.335	2.263	0.548

6.6.1 CONSOLIDATION

In the ATA PS series, all specimens were consolidated under K_o conditions, in order to restrict exposure of the side stress-cell membrane surfaces. Because the ATA INT specimens were tested along specific stress paths involving various constant values of the deviator stress $(\sigma_2 - \sigma_3)$, little advantage would have been gained by the use of this system.

The first stage of each intermediate-stress test consisted of ambient consolidation to a stress level chosen with a view to obtaining similar values of σ_{oct} at failure for the whole series. The effectiveness of this procedure can be seen in Table 6.15. For tests INT 7 and TE 1, σ_{oct} was necessarily lower because of the restriction placed on the side-cell pressure. The results from both this and the second stage consolidation are given in Table 6.14.

The latter was aimed at establishing values of $(\sigma_2 - \sigma_3)$ which, at failure, would yield a wide range of magnitude of the parameter b. An estimate of the specimen strength was necessary in order to determine an

TABLE 6.14

ATA Test Number	Initial Voids Ratio	Stage One Consolidation			Stage Two Consolidation				
		Ambient Stress	Volume Strain	Voids Ratio	Principal Stresses			Volume Strain	Voids Ratio
	e_i	σ	ε_{vc}	e_c	σ_x	σ_y	σ_3	ε_{vc}	e_c
INT 1	0.533	8.0	0.92	0.520	8.0	14.0	12.9	1.05	0.517
INT 2	0.530	8.0	0.91	0.516	8.0	12.0	13.1	1.09	0.513
INT 3	0.526	6.0	0.80	0.514	6.0	16.0	16.5	1.11	0.509
INT 4	0.534	7.0	0.85	0.521	7.0	14.0	14.9	1.04	0.519
INT 5	0.511	6.0	0.69	0.501	6.0	10.0	10.0	0.81	0.499
INT 6	0.536	6.0	0.73	0.524	6.0	18.0	18.0	1.00	0.520
INT 7	0.535	18.0	1.66	0.510	18.0	21.0	18.0	1.79	0.508
TE 1	0.548	18.0	1.98	0.518	18.0	18.0	18.0	1.98	0.518

approximate value of b, and therefore it was assumed that ϕ in plane strain would not be greatly exceeded, (a conclusion drawn by several investigators - section 2.4). Second stage consolidation in the six σ_3-increasing tests was carried out as described in section 4.6.4.

After applying the ambient stress, axial stress was increased in the strain-controlled manner, at 0.0008 in./min., and, using the end stress-cell recordings to determine the mean value, the side-cell pressure was adjusted to maintain $\sigma_y = \sigma_3$. Since adjustment of σ_y affected σ_3, this process involved some anticipation of the stress increments, and Table 6.14 shows that discrepancies occurred in the early tests, the stresses being equal at the end of the stage in INT 5 and 6 only.

It is easier in the ATA to maintain σ_3 constant by nullifying galvanometer-trace movements than to impose or monitor specific stress increments, mainly because of the difference in end stress-cell calibration factors and the time-lag. However, the stresses given in the table are slightly misleading, since it was only during the latter stages, when changes were more rapid, that noticeable differences occurred. In test INT 1, σ_y was briefly the major principal stress and therefore subsequent re-ordering took place during the shearing stage; the effect on specimen behaviour was considered insignificant. The second stage of test INT 7 comprised a simple increase in σ_y ($= \sigma_1$), at constant cell pressure.

The volumetric strains during first stage consolidation were reasonably consistent, considering the possible errors in measurements of small volume changes (6.3.1). Strains in the y-direction were calculated from the volume change in the side stress-cells, measured using the apparatus described in section 4.4.3. The magnitudes of ε_y during consolidation were determined successfully in tests INT 2-6, and the results are presented in Figs. 6.49-51.

The points have been omitted in Figs. 6.50, 51, for clarity but each curve has been drawn through all the appropriate measured strains. The end of each first stage is marked with an arrow.

The difficulty of accurately measuring axial strains during ambient consolidation were considered in section 4.4.1. No attempt was made to measure ε_3 in this test series. Ambient stress tests by El-Sohby (1964) on various particulate materials have demonstrated that $\frac{\varepsilon_v}{\varepsilon_1} \rightarrow 3$ only for the densest specimens, and that this ratio may be considerably higher for higher initial porosities. All ATA INT specimens were slightly looser than e_{min}, and therefore a value of approximately 3.5 was assumed for $\frac{\varepsilon_v}{\varepsilon_3}$ in order to estimate the axial strain. In addition, ε_x was derived from the other strains. Therefore the stage-one strains are worthy of only superficial consideration. The latter indicates that the relative magnitudes of ε_y were sensible.

During the second stage, in which the axial strain was measured, volumetric strains were small, though the very flat curves shown for ε_v are misleading due to datum errors in ε_3 (6.3.3). For this reason, it was possible to compare ε_y with ε_3 in two tests only, and in each case the value of ε_y was the greater by a factor of ten. Clearly, although it would be expected for lateral compressibility to be the greater, the magnitude of the difference was unacceptable and undoubtedly caused by side-cell membrane bulging.

Because $(\sigma_2 - \sigma_3)$ was constant during the final stage of the test, it was anticipated that the errors from this source would be substantially less.

6.6.2 FAILURE CHARACTERISTICS

The conditions at $\left(\frac{\sigma_1}{\sigma_3}\right)_{max}$ are given in Table 6.15. All values of ϕ have been based on the assumption that the mean end stress-cell value of

TABLE 6.15

ATA Test Number	Initial Voids Ratio	Conditions at Failure - Peak Stress Ratio											
		Axial Strain	Volume Strain	Peak Stress Ratio	Volume Strain Rate	Stress Ratio	Stress Ratio	$\sin \phi$	Angle Internal Sh'g Res	Oct'al Normal Stress	Oct'al Shear Stress	Oct'al Stress Ratio	Oct'al Shear Strain
	e_i	ε_{1f}	ε_{vf}	$\frac{\sigma_1}{\sigma_3}$	$\dot{\varepsilon}_{vf}$	$\frac{\sigma_2}{\sigma_1+\sigma_3}$	$\frac{\sigma_2-\sigma_3}{\sigma_1-\sigma_3}$		ϕ	σ_{oct}	τ_{oct}	$\frac{\tau_{oct}}{\sigma_{oct}}$	γ_{oct}
INT 1	0.533	7.70	-1.21	5.572	-0.26	0.266	0.164	0.696	44.1	22.20	16.03	0.722	18.97
INT 2	0.530	6.85	-1.36	5.000	-0.44	0.250	0.125	0.667	41.8	20.00	14.24	0.712	19.83
INT 3	0.526	3.79	+0.14	6.525	-0.47	0.354	0.302	0.734	47.2	20.38	13.88	0.681	13.90
INT 4	0.534	5.18	-1.49	5.702	-0.58	0.298	0.212	0.702	44.6	20.32	14.17	0.698	18.26
INT 6	0.536	4.11	-0.95	6.033	-0.64	0.426	0.398	0.716	45.7	20.07	12.42	0.619	20.62
INT 7	0.535	7.11	+1.52	5.816	-0.36	0.731	0.828	0.706	44.9	14.20	7.58	0.534	8.53
TE 1	0.548	3.64	+1.81	4.943	-0.58	0.831	1.000	0.665	41.7	13.21	6.77	0.512	18.69

σ_3 was the appropriate axial stress. This will be discussed further in section 6.6.6.

Fig. 6.52 shows these values, plotted against e_i, in relation to the mean curves obtained from ATA TC and PS tests (Fig. 6.41). The short line through each point has been drawn at a gradient consistent with those of the triaxial compression and plane strain curves, enabling the strengths to be "unified" at $e_i = 0.530$. Apart from test TE 1, the maximum adjustment to ϕ was 0.5°. The adjusted strengths are plotted against the parameter b in Fig. 6.53, together with the appropriate values for triaxial compression and plane strain.

Because of the wide scatter of points in the b v. e_i graph for the ATA PS tests (Fig. 6.25), the plane strain strength cannot be placed with any certainty in the ϕ v. b plot. The arrows indicate the likely limits for tests in which an overall increase in σ_{oct} was observed between the end of consolidation and failure. However, even if b were known with certainty, for the failure condition, it is questionable whether the value of ϕ should be directly compared with those obtained in the ATA INT tests, since the stress paths were quite different. Although the strengths of σ_x- and σ_3-constant tests in the ATA TC and PS series were not noticeably different, $\frac{\sigma_1}{\sigma_3}$ was increasing throughout in both and the strain paths were similar. It does not follow that the strain paths for ATA PS and ATA INT specimens reaching failure at the same value of b, would be at all similar (6.6.3).

The volumetric strain rates at failure (Fig. 6.52) are very widely scattered about the mean curve for ATA TC and PS tests.

In the triaxial extension test, deformation became localized as failure was approached. Although the overall dilatancy rate would therefore underestimate that in the failure zone, this would be counteracted by the corresponding error in ε_1. In test INT 7, σ_1 was also applied

through the side-cells and the values of ε_1 must be suspect due to excessive exposure of the membranes. It would appear very probable that the low value of $\dot{\varepsilon}_{vf}$ resulted from overestimation of strain in the y-direction.

Discounting specimen INT 1, in which $(\dot{\varepsilon}_v)_{max}$ was nearly twice as great as $\dot{\varepsilon}_{vf}$, three of the remaining four points could be regarded as within the bounds of experimental variation associated with the mean curve. The point for INT 6 represents an increase of 40% above $\dot{\varepsilon}_{vf}$ from the mean curve, and it may be significant that the value of b (= 0.398) was the highest of those tests giving reliable strain data.

In most cases, little importance should be attached to the measured axial strains at failure which, even allowing for the various measurement errors, seem greatly variable. However, for tests INT 1-6, the increments of ε_1 determined between the end of second-stage consolidation and failure are likely to be accurate, as are those of ε_2. The ratio of these increments $\left(\frac{\varepsilon_2}{\varepsilon_1}\right)_s$ is shown against b in Fig. 6.54.

A typical value of this ratio for an ATA TC specimen of comparable initial porosity would be -0.60, and in triaxial extension its value is theoretically +1.00 for a laterally isotropic material. Overall deformation in the y-direction during the final stage of all five tests was small, though it is interesting to note that at failure all of the specimens were expanding in this direction.

The results from tests INT 3 and 4 show that a zero value of $\left(\frac{\varepsilon_2}{\varepsilon_1}\right)_s$ would not necessarily imply plane strain deformation throughout shearing, and that the corresponding b value would be slightly higher than those observed during the ATA PS series.

6.6.3 STRESS-STRAIN CURVES

Figs. 6.55, 56, show the results from tests giving the lowest and

highest values of b, and in which the major principal stress acted in the z-direction.

The unusual shape of the σ_1 ($= \sigma_2$) v. ε_1 second-stage consolidation curve in test INT 2 is due entirely to a datum error in ε_1, caused by poor centering of the specimen with respect to the loading plunger. Consequently much of the initial measured axial deformation can be attributed to bedding between the countersunk end of the plunger and the ball-bearing.

Both σ_1 curves increase smoothly to failure, which was the case for the majority of ATA INT tests, showing no signs of the inflexions observed in the previous test series.

The curves of ε_2 v. ε_1 are surprisingly similar in view of the large difference in $(\sigma_2 - \sigma_3)$. However, although the strain magnitudes during second-stage consolidation were unreliable, the magnitude of the ε_1 increment was clearly larger in INT 6, allowing for a sensible correction to the INT 2 data, and it would seem reasonable to expect similar values for the ε_2 increments. Therefore the former specimen was likely to have compressed considerably more than the latter in the y-direction, prior to the final stage. If σ_1 and σ_2 had been increased from the end of ambient consolidation at rates such that b was approximately constant throughout shearing, the overall compression in the y-direction would undoubtedly have increased with b.

The shape of all ε_2 curves was similar to those shown, an initial compression being followed by a relatively slow expansion at a rate dictated partly by the magnitude of b.

Both INT 7 and TE 1 (Fig. 6.57) showed a slightly fluctuating σ_3 v. ε_1 curve, as it decreased to failure. However, in view of the small stresses involved, the effect was not considered important. The value of ε_2 ($= \varepsilon_I$) in the former test, being derived from the other strains,

was clearly an underestimate, due largely to non-uniform specimen deformation causing side-cell membrane exposure. In test TE 1, ε_1 and ε_2 were assumed equal, and could therefore be determined from volumetric and axial strains. The ε_v curves were similar in each of these tests, but probably not representative of those for the respective local failure zones.

All tests were stopped shortly after failure, the approximate shape of two specimens at this stage being shown in Figs. 6.4 and 6.5. The stresses were relieved from specimen INT 2 at a very slow rate, but this did not prevent the membrane-wrinkling observed for nearly all specimens, as can be seen from the appearance of the σ_x faces in Figs. 6.4a and b. Specimen TE 1 (Fig. 6.5) "slumped" a little after relief of the stresses. Therefore it was "extended" back to its original axial strain and supported while the photographs and approximate measurements were taken.

6.6.4 STRESS-DILATANCY

For generalised stress and strain conditions, the energy equations of section 2.2 must be amended for the work done in the intermediate principal stress direction.

Assuming that δy is negative, i.e. of the same sense as δx, the energy ratio E, redefined as the ratio of the energy supplied in the major principal direction to the work done in the intermediate and minor principal directions, becomes:-

$$E = \frac{L_1 \delta z}{-(L_2 \delta y + L_3 \delta x)} . \qquad \ldots (1)$$

Therefore the expression for the energy dissipated in internal friction,

$$L_1 \delta z + L_2 \delta y + L_3 \delta x = L_1 \delta z \left(1 - \frac{1}{E}\right) ,$$

remains unchanged with respect to E, but since sliding is no longer confined to x-z planes, an expression for E_{min}, in terms of ϕ_μ only, cannot be obtained. However, in triaxial compression and plane strain,

an observed deviation from the K_μ-line, i.e. the line consistent with $E_{min} = \tan^2(45 + \frac{\phi_\mu}{2})$, does not necessarily invalidate the principle of maximum energy transmission; it may merely indicate that sliding is occurring on planes other than those at the preferred angle, $\beta_c = (45 - \frac{\phi_\mu}{2})$. To overcome this difficulty the existence of a variety of K_f-lines has been postulated for these test conditions, consistent with a value of ϕ_f satisfying $\phi_\mu \leq \phi_f \leq \phi_{cv}$.

There is no reason why this parameter should not be used for generalised stress conditions, provided that the reservations regarding the minimization of E are appreciated.

Using the principle of virtual work, equation 1 becomes:-

$$E = \frac{\sigma_1 d\varepsilon_1}{-(\sigma_2 d\varepsilon_2 + \sigma_3 d\varepsilon_3)} = K_f$$

$$\therefore \sigma_1 d\varepsilon_1 = -(\sigma_2 d\varepsilon_2 + \sigma_3 d\varepsilon_3) K_f$$

$$\therefore \frac{\sigma_1 d\varepsilon_1}{\sigma_3 d\varepsilon_3} = -\left(\frac{\sigma_2 d\varepsilon_2 + \sigma_3 d\varepsilon_3}{\sigma_3 d\varepsilon_3}\right) K_f$$

giving
$$R = \left[T\left(\frac{-d\varepsilon_2}{d\varepsilon_1}\right) + \left(\frac{-d\varepsilon_3}{d\varepsilon_1}\right)\right] K_f, \qquad \ldots (2)$$

where T is the stress ratio $\frac{\sigma_2}{\sigma_3}$,

or,
$$R = D_T K_f , \qquad \ldots (3)$$

where D_T is the generalised dilatancy factor.

In all ATA INT tests, T was constant during the final stage, at a magnitude ranging between 1.5 (INT 2) and 3.0 (INT 6). The stress dilatancy plot of R v. D_T for INT 4 is shown in Fig. 6.60a, where each point represents one set of strain increments. In Figs. 6.60b, 61, these have been omitted.

Discounting the initial dashed parts of these curves, for which the apparent rapid increase in ε_2 was undoubtedly associated with side-cell membrane expansion, the results from tests INT 1, 2 and 4 were not dissimilar to those observed in plane strain. It may be significant that

in these three tests there was an overall expansion in the y-direction, since it was assumed that $d\varepsilon_2$ was negative in the derivation of equation 2.

For compression in the y-direction, the energy ratio becomes:-

$$E = \frac{\sigma_1 d\varepsilon_1 + \sigma_2 d\varepsilon_2}{-\sigma_3 d\varepsilon_3} = K_f \ ,$$

giving

$$R = T\left(\frac{-d\varepsilon_2}{d\varepsilon_1}\right) + \left(\frac{-d\varepsilon_3}{d\varepsilon_1}\right) K_f \ . \qquad \ldots (3)$$

Hence the basic form of the stress-dilatancy equation is lost.

Although all specimens INT 1-6 were expanding in the y-direction during most of the final stage, each exhibited an initial contraction. Therefore the use of equation 2 throughout deformation was not strictly valid for any of these tests. However, this does not account for the very large magnitudes of D_T in test INT 6, which were associated with the high value of T and a rapid decrease in ε_2.

In view of the unreliability of some of the early strain measurements, a more sophisticated treatment was considered unwarranted.

Clearly, a more extensive program of intermediate-stress tests, incorporating a more accurate method of measuring the lateral strains, would be needed in order to draw more definite conclusions regarding generalised stress-dilatancy behaviour, the validity of equations 2 and 3, and the variability of K_f.

6.6.5 MODE OF DEFORMATION

The mode of deformation, in all tests for which σ_3 was the major principal stress, was compatible with that observed in the ATA TC and PS series for dense specimens.

The test INT 2 was stopped after confirming peak stress ratio (Fig. 6.55) and Fig. 6.4c shows the very early development of a possible failure surface (top left to bottom right). Table 6.16 gives the final dimensions of the specimen measured in this condition, and those taken before the test. The average dimension of the σ_x planes changed

TABLE 6.16

Initial Dimensions								
	σ_y Planes				σ_x Planes			
	A	B	C	Average	A	B	C	Average
1	2.327	2.331	2.330	2.329	2.257	2.261	2.259	2.259
2	2.327	2.333	2.335	2.332	2.261	2.265	2.262	2.263
3	2.328	2.337	2.339	2.335	2.263	2.269	2.265	2.266
4	2.331	2.345	2.340	2.339	2.267	2.272	2.268	2.269
5	2.334	2.348	2.338	2.340	2.270	2.278	2.272	2.273
Final Dimensions								
	σ_y Planes				σ_x Planes			
	A	B	C	Average	A	B	C	Average
1	2.368	2.389	2.389	2.382	2.260	2.275	2.254	2.263
2	2.440	2.452	2.447	2.446	2.255	2.270	2.255	2.260
3	2.483	2.499	2.490	2.491	2.264	2.248	2.256	2.256
4	2.472	2.483	2.470	2.475	2.272	2.264	2.274	2.270
5	2.418	2.440	2.429	2.429	2.277	2.255	2.269	2.267

from 2.266 in. to 2.263 in. between initial and final stages, compared with a change to 2.247 in. predicted from ε_y measurements.

It was suggested, in section 6.6.3, that by far the greater proportion of error in ε_y would have occurred during the second-stage consolidation, due to side-cell membrane bulging as $(\sigma_2 - \sigma_3)$ was increased. If the recorded strain during this stage is ignored, and instead it is assumed that the increments of ε_y and ε_3 were equal, the predicted final average dimension of the σ_x-planes would become 2.271 in. Although approximate, this tends to confirm the suggestion that the values of ε_y during most of the final stage were not grossly inaccurate.

Both INT 7 and TE 1 specimens developed "necks" as failure was approached. Fig. 6.5 shows the extent of the non-uniformity in the latter test, although the specimen had been disturbed considerably during dismantling (6.6.3). Measurement of the minimum area showed that this was approximately 91% of the average area derived from ε_v and ε_3. Assuming that the end areas changed negligibly, which is indicated in Fig. 6.5, the minimum area would then be 84% of that at the stress-cell surfaces.

6.6.6 TOP AND BOTTOM STRESSES

The strengths listed in Table 6.15 and plotted, after adjustment, against b in Fig. 6.53 were calculated in the manner described for the ATA TC and PS tests, the mean end stress-cell reading being taken as the appropriate value of σ_3. A check on this assumption, using the dimensions of the INT 2 specimen, reveal that in this case slight overestimation of ϕ would result.

The measured top and bottom stresses, 41.0 and 39.0 lbf/in^2 respectively, after area correction (6.3.6) became 40.0 and 38.8 lbf/in^2. Therefore the assumed value of σ_3 was 0.6 lbf/in^2 greater than that

based on the final measurements, equivalent to an increase in ϕ of 0.3°. A coefficient of friction, for the σ_v-faces, of 0.03 would be consistent with the top and bottom stress difference, in general agreement with the small magnitudes obtained in section 6.3.6 and 6.4.6.

Clearly, the assumption regarding σ_3 would not be valid in tests INT 7 and TE 1, and the order of the errors involved may be determined from the data for TE 1 given in the previous section.

Based on end stress-cell readings, the magnitude of ϕ was 41.7°. When corrected for average cross-sectional area this becomes 39.9°, and if the minimum local area is used, a value of 37.7° is obtained. Therefore, although the top point representing b = 1.0 in Fig. 6.53 is too high, the magnitude of the excess cannot be stated with certainty.

The values of ϕ derived above are shown, after correction for initial voids ratio, in the figure. These were considered to be the probable limits for the strength of a specimen of comparable density deforming more uniformly in triaxial extension. The probable range of ϕ for INT 7 was estimated in a similar manner.

6.6.7 OCTAHEDRAL STRESSES

The ratio between the octahedral shear and normal stresses, R_{oct}, at failure for each ATA INT and TE test is given in Table 6.15. Because only one of the three principal stresses was changing during the final stage in every case, $(R_{oct})_{max}$ necessarily occurred at the same instant as the peak strength, ϕ. This condition is therefore in contrast to that in the plane strain tests.

The octahedral stress ratio has been plotted against b in Fig. 6.58, the points corresponding to those of the ϕ v. b graph (Fig. 6.53). Likewise, three points have been shown for tests INT 7 and TE 1, based on the various cross-sectional area assumptions. The triaxial compression

and plane strain values were interpolated from the results in Fig. 6.48. In none of the intermediate-stress tests were these magnitudes of $(R_{oct})_{max}$ equalled.

The mean curve has been drawn ignoring the plane strain point. In section 6.6.3, the difference between the stress and strain paths for ATA INT and ATA PS specimens, reaching failure at similar magnitudes of b, was pointed out. This may be an important factor in explaining the differences apparent in Fig. 6.58.

6.7 FAILURE CRITERIA

Some of the more common failure criteria which have been suggested for cohesionless particulate media were discussed in section 2.4. Their graphical representation on an octahedral plane in principal stress space was shown in Fig. 2.4, and one segment of such a surface for $e_i = 0.530$, ϕ (triaxial compression) = 38.8°, is given in Fig. 6.59.

Bishop (1966) demonstrated that the von Mises and Tresca criteria were meaningless for cohesionless soils with $\phi > 36.9°$ since, at this point, the respective failure surfaces touch the planes bounding compressive stress space, and with a further increase in ϕ, they penetrate into negative (tensile) stress space. However, these criteria are represented fully, in the figure, for reference purposes.

The vertical axis has been marked σ_1 in order that the results of tests INT 7 and TE 1 may be shown in the same segment. In σ_x-σ_y-σ_3 space, these points would appear in another segment, and therefore this process is valid only if the failure surface may be assumed symmetrical with respect to the x-y-z axes.

Clearly, for dense sand the Mohr-Coulomb criterion substantially underestimates strength for most values of θ between 0° and 60°.

Unfortunately the present practical difficulties which restrict the magnitude of $(\sigma_y - \sigma_x)$ limited the range of b which could be investigated with the same ordering of the principal stresses. For values of $b < 0.4$, the points represent stress conditions at failure which were considered reliable, and the shape of the failure surface appears to be similar to that predicted by Parkin's theory (2.2, 2.4), although the latter tends to overestimate the stresses for the reasons previously discussed. The points for INT 7 and TE 1 were taken from the middle of the range shown in Figs. 6.53, 58, and therefore must be regarded as very approximate. The cylindrical triaxial extension test

results considered in the following chapter provide additional information on soil strength as $b \rightarrow 1$.

It would seem a reasonable assumption that the difference between the experimental results and the Mohr-Coulomb theory, for $b < 0.4$, decreases as the initial porosity increases and the plane strain and triaxial compression values of ϕ become similar. However, it is not certain, from the ATA PS results alone, whether equality would have been achieved at $e_{max.}$ and hence whether the Mohr-Coulomb criterion is strictly valid for any magnitude of e_i for this soil.

6.8 DATA CORRECTIONS

Correction of volume change measurements for membrane penetration (Appendix B), and of axial deformation, for apparatus compression and specimen bedding (Appendix C), were incorporated in the computer processing of the test data.

End stress-cell measurements were, in general, not corrected for variation in specimen cross-sectional area, for the reasons discussed first in section 6.3.6. The lateral stresses were assumed accurate.

The results of membrane strength tests (Appendix D) indicate that the error in ϕ for the majority of ATA tests would be similar for most specimens, and acceptably small. Exceptions to this conclusion would be specimens INT 7 and TE 1 which were elongated in the z-direction. The magnitudes of the necessary corrections to ϕ would probably be in the region of -1°, based on the estimated corrections for cylindrical triaxial extension specimens (Table D.3). From Fig. 6.53 it can be seen that this would lower the dashed line for ATA TE, representing the middle of the "corrected" strength range, to that of the comparable ATA TC specimen. However, in view of the considerable uncertainties resulting from the non-uniform strain conditions, further inspection was not warranted.

6.9 SUMMARY

The analysis of results from the ATA tests, which formed a major part of the author's research program, have been presented and discussed in this chapter.

It was shown, in section 6.3.1, that the apparatus in its present form was not suitable for the precise study of the small deformations occurring during K_o-consolidation. However, one of the primary aims in this stage, for ATA PS tests in particular, was to limit side-cell membrane exposure, and this was satisfactorily achieved.

Comparison between the failure characteristics of specimens tested in plane strain and triaxial compression revealed a difference in ϕ of 7° for low initial voids ratios. Because of the difficulty of preparing very loose specimens, the corresponding increase in ϕ for plane strain could not be stated with equal certainty, though a value of 0° to 2° was estimated. The volumetric strain rates at failure were very similar in ATA TC and PS test series, although in neither case were these rates at a maximum.

The stress-strain curves were compared with particular reference to the inflexions observed in those of σ v. ε_1 during plane strain tests. Slight lateral expansion during the early stages of deformation, and a corresponding slow rate of increase of $(\sigma_2 - \sigma_3)$ was shown to be the major cause.

The stress-dilatancy relationship, R v. D, was found to be characterized by large increments of the stress ratio accompanied by only small changes in the dilatancy factor. There was little evidence to suggest that plane strain specimens deform in accordance with the relationship $R = D\,K_{cv}$.

In ATA PS tests, the maximum octahedral stress ratio, $\left(\frac{\tau_{oct}}{\sigma_{oct}}\right)_{max}$, occurred at strains much less than those at failure and comparison with

the ATA TC series showed that this ratio was similar for high densities only.

Intermediate-stress tests on dense specimens gave strengths up to 2° higher than that in plane strain for a comparable initial voids ratio. A maximum value of ϕ was reached at a b value of approximately 0.3. Although measured strains in the y-direction were unreliable during consolidation, they were considered more accurate for most of the final stage, during which the lateral deviator stress remained constant. However, the erratic stress-dilatancy curves suggest that a more sophisticated method of measuring small increments of ε_y would be desirable.

The doubts concerning stress analysis in tests INT 7 and TE 1 prevented a firm conclusion being reached regarding the shape of the failure surface for b > 0.5. The remaining ATA INT tests appeared to favour a criterion of the form suggested by Parkin's theory.

The deformation of all ATA specimens which were compressed in the z-direction was shown to be reasonably uniform, and to justify the assumptions regarding interpretation of the end stress-cell measurements. Continuous galvanometer trace recording of the top and bottom stresses allowed small fluctuations in their magnitudes to be studied. This was discussed, with reference to triaxial compression tests, in section 6.3.6, but the behaviour was qualitatively similar in all ATA tests.

The results from this test program confirm the overall suitability of the apparatus for the study of soil behaviour under generalised stress conditions. However, for intermediate-stress tests, direct measurement of strain in the x-direction would eliminate some of the errors caused by side-cell membrane expansion. Improvement of the stability of these membranes, either by increasing the rubber thickness along the exposed edges or by using a gauze mesh (Sutherland and

Mesdary 1969), would decrease this effect.

Since the intermediate principal stress is applied in the stress-controlled manner, the ATA is more suitable for imposing specific stress conditions than for monitoring strains.

CHAPTER SEVEN

CYLINDRICAL AND CUBOIDAL TRIAXIAL TESTS

RESULTS AND DISCUSSION

7.1 INTRODUCTION

In Chapter 6 the results from several series of tests performed in the new "three-dimensional" apparatus were analysed and discussed. The current chapter will be concerned with the corresponding analysis of more conventional axially-symmetrical triaxial tests on both cylindrical and cuboidal specimens of the same soil.

All CUB TC and CYL TE specimens were consolidated under ambient stress; in some of the CYL TC tests K_o-consolidation was used. Behaviour during each of these processes is covered in section 7.3.

In the following section, the conditions at peak stress ratio are analysed. Comparisons will be made between the failure characteristics observed in each type of test. The general forms of the stress-strain curves prior to failure are described in section 7.5., where the errors associated with proving-ring measurement of axial stress will be considered.

Section 7.6 deals with stress-dilatancy behaviour. Particular attention will be given to the sources of error in the measurements of incremental stresses and strains, and their relation to the apparent discrepancies between the various test results.

The mode of deformation of cylindrical specimens, and its effect on the measured values of axial stress, will be discussed in sections 7.7 and 7.8. In the analysis of the CYL TE test results, additional corrections, which are insignificant with respect to the CYL TC series, become more important, and these are covered in the penultimate section.

Finally, comparisons will be made between the behaviour of soil specimens in the ATA and in the conventional apparatus, and the overall effectiveness of the new apparatus will be appraised.

7.2 THE TEST PROGRAM

The number of tests in each series is shown in Table 7.1. All the cylindrical specimens were nominally 2.8 in. in diameter. With one exception those for triaxial compression tests were about 5 in. long, and triaxial extension specimens were nominally 3 in. long. The dimensions of all cuboidal specimens were similar to those in the ATA test series (Chapter 6).

Both top and bottom stress-cells (5.3.1) were used in the majority of CYL TC tests, the remainder having rigid plattens either at one or both ends of the specimen. A combination of rigid top platten and bottom stress-cell was employed for all CYL TE tests, and in the CUB TC series the ATA end stress-cells were used. In one CUB TC test, the bottom stress-cell was replaced with the ATA Mk.I bottom platten, allowing pore-pressure to be observed during drained shearing (4.2.4).

The initial physical properties of all specimens are given in Tables 7.2-5.

TABLE 7.1

Type of Test	End Conditions	Consol'n	Total Number	Number Reaching Failure
CYL TC	rigid	ambient	10	9
CYL TC	flexible	ambient	13	10
CYL TC	mixed	ambient	3	2
CYL TC	flexible	K_o	5[1]	5
CYL TE	mixed	ambient	8	8
CUB TC	flexible	ambient	5	5
CUB TC	mixed	ambient	1	1

1 including one 3 in. long

TABLE 7.2

Test Number	Initial Physical Properties				Ambient Consolidation		
	Mass Solids (gm)	Length (in)	Diameter (in)	Initial Voids Ratio	Cell Pressure σ	Volume Strain ε_{vc}	Voids Ratio e_c
CYL TC 1	802.99	5.023	2.790	0.660	20.0	0.66	0.649
CYL TC 2	858.52	5.081	2.798	0.579	20.0	0.49	0.571
CYL.TC 3	879.99	5.051	2.792	0.525	20.0	0.63	0.516
CYL TC 4	851.76	5.005	2.791	0.564	20.0	0.61	0.555
CYL TC 5	845.69	5.139	2.786	0.606	20.0	0.54	0.599
CYL TC 6	844.73	5.045	2.782	0.578	20.0	0.57	0.569
CYL TC 7	889.68	5.129	2.794	0.534	10.0	0.28	0.530
CYL TC 8	870.74	5.019	2.789	0.529	15.0	0.42	0.522
CYL TC 9	896.09	5.082	2.789	0.506	10.0	0.39	0.500
CYL TC 10	851.48	4.878	2.789	0.518	17.8	0.60	0.509
CYL TC 11	889.58	5.108	2.790	0.522	20.0	0.55	0.514
CYL TC 12	851.72	5.080	2.788	0.580	20.0	0.48	0.573
CYL TC 13	864.70	5.082	2.782	0.536	15.0	0.65	0.540
CYL TC 14	836.65	5.027	2.796	0.602	10.0	0.71	0.590
CYL TC 15	835.80	5.011	2.784	0.584	20.0	0.76	0.572
CYL TC 16	862.10	5.143	2.788	0.581	20.0	0.69	0.570
CYL TC 17	869.61	5.058	2.789	0.543	20.0	0.50	0.536
CYL TC 18	825.33	5.067	2.789	0.626	20.0	0.75	0.614
CYL TC 19	856.10	5.026	2.783	0.550	20.0	0.64	0.541
CYL TC 20	798.61	4.962	2.773	0.627	20.0	0.74	0.615
CYL TC 21	850.45	5.004	2.789	0.560	20.0	0.62	0.550
CYL TC 27	861.41	5.086	2.786	0.562	20.0	0.62	0.552
CYL TC 28	828.45	5.030	2.788	0.608	20.0	0.61	0.599

TABLE 7.3

Test Number	Initial Physical Properties					Zero Lateral Strain Consolidation				
	Mass Solids (gm)	Length (in)	Diameter (in)	Initial Voids Ratio	Minor Stress σ_3	Major Stress σ_1	Volume Strain ε_{vc}	Voids Ratio e_c	Stress Ratio $\frac{\sigma_3}{\sigma_1}$	Oct'al Normal Stress σ_{oct}
CYL TC 22	857.06	4.995	2.785	0.540	10.8	31.0	0.73	0.529	0.348	17.53
CYL TC 23	821.70	5.080	2.787	0.633	10.0	21.3	0.63	0.623	0.470	13.77
CYL TC 24	544.60	3.125	2.796	0.530	10.0	27.2	0.49	0.522	0.368	15.73
CYL TC 25	877.25	4.952	2.809	0.519	10.0	30.2	0.51	0.511	0.331	16.73
CYL TC 26	880.31	5.146	2.795	0.557	10.0	25.1	0.69	0.546	0.398	15.03

TABLE 7.4

Test Number	Initial Physical Properties				Ambient Consolidation		
	Mass Solids (gm)	Length (in)	Diameter (in)	Initial Voids Ratio	Cell Pressure σ	Volume Strain ε_{vc}	Voids Ratio e_c
CYL TE 1	535.40	3.204	2.806	0.605	25.0	0.59	0.598
CYL TE 2	543.01	3.182	2.794	0.558	25.0	0.72	0.547
CYL TE 3	515.32	3.050	2.804	0.586	25.0	0.73	0.575
CYL TE 4	543.10	3.155	2.801	0.555	25.0	0.61	0.546
CYL TE 5	541.47	3.172	2.807	0.576	25.0	0.69	0.565
CYL TE 6	497.14	3.082	2.793	0.649	25.0	0.68	0.637
CYL TE 7	525.01	3.174	2.803	0.603	25.0	0.67	0.614
CYL TE 8	545.40	3.162	2.794	0.549	25.0	0.59	0.540

TABLE 7.5

Test Number	Initial Physical Properties					Ambient Consolidation		
	Mass Solids (gm)	Length (in)	Inter Width (in)	Minor Width (in)	Initial Voids Ratio	Cell Pressure σ	Volume Strain ε_{vc}	Voids Ratio e_c
CUB TC 1	592.70	4.113	2.336	2.253	0.582	10.0	0.61	0.572
CUB TC 2	572.64	4.077	2.260	2.257	0.575	10.0	0.46	0.568
CUB TC 3	559.92	4.065	2.232	2.294	0.614	10.0	0.72	0.602
CUB TC 4	606.85	4.099	2.336	2.258	0.548	10.0	0.35	0.542
CUB TC 5	607.35	4.108	2.356	2.252	0.557	10.0	0.38	0.553
CUB TC 6	580.40	4.017	2.334	2.253	0.578	10.0	0.56	0.570

7.3 CONSOLIDATION

Five specimens of the CYL TC series were consolidated under zero lateral strain conditions. The first stage of all other tests consisted of ambient consolidation and these will be considered together in the following section.

7.3.1 AMBIENT CONSOLIDATION

A maximum ambient stress of 25 lbf/in^2 was used for all CYL TE specimens. In most CYL TC tests this was 20 lbf/in^2, but several were carried out at lower stresses. All CUB TC specimens were consolidated at 10 lbf/in^2.

The volumetric strains during consolidation are given in Table 7.2, 4, 5, and are plotted against e_i in Figs. 7.5 and 7.6. The CYL TC specimens consolidated to 20 lbf/in^2 showed a wide scatter, though this was slightly less for those with end stress-cells. A tentative curve has been drawn through all the points, and this is reproduced in Fig. 7.6 where the remaining results are shown.

By far the best relationship between ε_{vc} and e_i was that for the CUB TC tests. However, for loose specimens the strains were of a similar magnitude to those shown in Fig. 7.5 for twice the consolidation pressure. The distribution of CYL TE results was about the same as that in the latter figure. As a whole, these results are contrary to what might be expected.

The cuboidal specimens, subject to the same errors as the ATA specimens (6.3.1), exhibited surprisingly consistent strains, though it is probably significant that their magnitudes were relatively high. At low stresses, specimen membrane bedding against the end stress-cells was liable to be greater for higher initial porosities.

It was anticipated that compression of the gauze and filter paper

in the drainage channel of the cylindrical top platten, or top stress-cell, would be small and consistent. Although this factor cannot be isolated from others, such as bedding of the end plattens, or stress-cells, and compression of the lubricated membranes and O-rings, additional information may be obtained from the membrane penetration test results (Appendix B).

All of these specimens were prevented from significant axial compression, during ambient stressing, by a rigid rod passing down the centre. Both end plattens were rigid. It would be reasonable to assume that the compression of the end membranes, between the end plattens and the coaxial rod, was similar for all specimens, at comparable pressures. The volume changes for ambient stresses of less than 5 lbf/in^2 were erratic, but between 5 and 80 lbf/in^2 much more consistent results were obtained.

Since the consolidation stresses for all the triaxial tests were relatively small, any initial errors would cause greater variability in the overall volume changes. This appears to have been the case for both CYL TC and TE specimens, the major cause probably being compression of the filter paper.

Axial strains were not measured during ambient consolidation; the difficulties of obtaining accurate measurements were discussed in sections 4.6 and 5.6. In order to make comparisons with K_o-consolidated specimens, it was assumed that $\varepsilon_1 = \frac{\varepsilon_v}{3}$. This assumption is likely to overestimate ε_1, particularly for loose specimens for which marked initial cross-anisotropy has been observed by several investigators. However, the overall axial strain at failure was found to be greatly variable.

7.3.2 K_o-CONSOLIDATION

Five CYL TC specimens were consolidated at zero lateral strain, using the method described in section 5.6.1. The results are shown in Table 7.3, and in Fig. 7.7 the stress ratio, $\frac{\sigma_3}{\sigma_1}$, and the "unified" volumetric strain, $\frac{\varepsilon_{vc}}{\sigma_1}$, are plotted against the initial voids ratio.

In the upper graph, the measured values of K_o are compared with Jaky's (1944) expression, $K_o = (1 - \sin \phi)$, the magnitude of ϕ being that observed at failure for each specimen. Unlike the ATA results, the differences between the values of K_o based on mean and final stress measurements are slight, and Fig. 7.8 shows that deviations from straight lines representing constant stress ratios were small, except during the early strains.

The relationship between $\frac{\varepsilon_{vc}}{\sigma_1}$ and e_i in Fig. 7.7 is poor, and cannot be explained by significant deviations from the K_o condition. In each case the maximum lateral strain was only a few percent of the measured axial deformation. However, the possibility of ε_1 datum errors cannot be excluded. Although the use of the end stress-cells allowed contact between the loading plunger and the specimen to be observed, errors could still have resulted from eccentricity of contact, leading to over-compensation of ε_v and a consequent overestimation of K_o. In this test series, however, there appeared to be no such correlation of stress ratio and strain errors, and the major sources of the latter were probably those described in section 7.3.1.

In view of the wide scatter in both ambient and K_o-consolidation strains, the magnitudes of K_o are surprisingly consistent, and although the majority of tests were on relatively dense specimens, the results tend to support the $(1 - \sin \phi)$ approximation.

7.4 FAILURE CHARACTERISTICS

7.4.1 CYL TC TESTS

The conditions at failure for all cylindrical triaxial compression specimens are given in Tables 7.6 and 7.7, where the twenty-four tests reaching failure have been split into three groups: those in which proving-ring measurements only were used in computing the stresses (i.e. where there were two rigid end plattens), those in which stress-cells were also used, and those in which consolidation was carried out under K_o conditions, again using end stress-cells. In the latter series, the proving-ring was removed in order that the rate of deformation should be constant. This greatly facilitated the consolidation process.

Two sets of failure characteristics are shown in Table 7.7, based on peak proving-ring measurements and peak stress-cell recordings, respectively. The values of ϕ, calculated on these bases, are plotted against e_i in Fig. 7.9, where it can be seen that the effect of plunger friction would lead to overestimations of between 1.5° and 3.8°, with an average of 2.0°. However, this does not necessarily represent the error in stress measurement, since the strains at "failure" were different in each case. No difference was apparent for loose and dense specimens in this respect, the errors being erratic.

The points determined from stress-cell measurements of σ_1 all lie within a range of 0.8° from the mean curve, a. Another dashed curve, b, has been drawn through the five points representing K_o-consolidated specimens, and there appears to be a considerable increase in the peak strengths of the three densest specimens, relative to curve a.

The magnitude of ϕ calculated for the 3 in. long specimen (CYL TC 24, ϕ = 39.0°) was of doubtful accuracy, owing to some uncertainty regarding the area correction (7.7), and the stress-strain curve for test

TABLE 7.6

Test Number	Initial Voids Ratio e_i	End Cond'ns	Axial Strain ε_{1f}	Volume Strain ε_{vf}	Volume Strain Rate $\dot{\varepsilon}_{vf}$	$\sin \phi$	Angle Internal Sh'g Res ϕ
CYL TC 1	0.660	rigid	12.44	-0.33	-0.07	0.551	33.4
CYL TC 3	0.525	rigid	5.53	-1.76	-0.56	0.642	39.9
CYL TC 4	0.564	rigid	5.57	-1.33	-0.39	0.613	37.8
CYL TC 5	0.606	rigid	4.33	-0.41	-0.24	0.577	35.2
CYL TC 6	0.578	rigid	3.78	-0.68	-0.41	0.597	36.7
CYL TC 7	0.534	rigid	9.66	-3.09	-0.38	0.633	39.3
CYL TC 8	0.529	rigid	8.46	-2.43	-0.42	0.642	40.0
CYL TC 9	0.506	rigid	7.71	-3.16	-0.42	0.660	41.3
CYL TC 10	0.518	rigid	6.45	-1.84	-0.41	0.658	41.1
CYL TC 22	0.540	flexible	4.90	-0.45	-0.30	0.640	39.8
CYL TC 23	0.633	flexible	2.25	+0.66	-0.16	0.546	33.1
CYL TC 24	0.530	flexible	4.69	-1.43	-0.52	0.629	39.0
CYL TC 25	0.519	flexible	4.19	-0.79	-0.56	0.652	40.7
CYL TC 26	0.557	flexible	4.66	-0.03	-0.34	0.596	36.6

TABLE 7.7

Test Number	Initial Voids Ratio e_i	End Cond'ns	Conditions at Failure (Peak Stress Ratio)									
			Proving-Ring Measurements					End Stress-Cell Measurements				
			Axial Strain ε_{1f}	Volume Strain ε_{vf}	Volume Strain Rate $\dot{\varepsilon}_{vf}$	sin ϕ	Angle Internal Sh'g Res ϕ	Axial Strain ε_{1f}	Volume Strain ε_{vf}	Volume Strain Rate $\dot{\varepsilon}_{vf}$	sin ϕ	Angle Internal Sh'g Res ϕ
CYL TC 11	0.522	mixed[1]	5.13	-1.69	-0.57	0.645	40.2	4.89	-2.12	-0.57	0.625	38.7
CYL TC 13	0.536	mixed[2]	6.51	-1.43	-0.35	0.633	39.3	5.19	-1.63	-0.34	0.602	37.0
CYL TC 14	0.602	flexible	3.53	+1.23	-0.21	0.595	36.5	3.53	+0.52	-0.20	0.574	35.0
CYL TC 15	0.584	flexible	5.02	-0.59	-0.35	0.594	36.4	4.08	-0.99	-0.36	0.575	35.1
CYL TC 16	0.581	flexible	5.66	-0.84	-0.31	0.593	36.4	3.58	-0.80	-0.35	0.570	34.8
CYL TC 17	0.543	flexible	8.66	-2.01	-0.38	0.617	38.1	6.38	-1.63	-0.38	0.595	36.5
CYL TC 18	0.626	flexible	8.11	-0.17	-0.11	0.581	35.5	9.25	-1.06	-0.12	0.551	33.4
CYL TC 19	0.550	flexible	8.69	-0.76	-0.23	0.630	39.0	8.12	-1.27	-0.23	0.596	36.6
CYL TC 20	0.627	flexible	7.37	+0.26	-0.15	0.577	35.2	4.23	+0.07	-0.17	0.548	33.2
CYL TC 21	0.560	flexible	8.11	-0.80	-0.17	0.648	40.4	6.06	-1.06	-0.22	0.596	36.6

1 rigid top platten, bottom stress-cell

2 top stress-cell, rigid bottom platten

CYL TC 22 showed an uncharacteristic drop in σ_1 prior to failure. Therefore it is possible that the difference between the two curves a and b was not statistically significant, and the solid curve has been drawn through all the reliable points.

Fig. 7.10 shows the results from the conventional rigid-end tests together with the proving-ring points repeated from Fig. 7.9. Discounting the result from CYL TC 21, the maximum deviation from the mean curve is about 1.0°, but in all cases the magnitude of ϕ was much greater than that given by the stress-cell measurements from tests CYL TC 11-21. The lower graph in Fig. 7.10 shows a wide variation of volumetric strain rates at the point of failure based on proving-ring measurements. However, the "stress-cell points", plotted in Fig. 7.9, were little better in this respect, which was surprising in view of the good correlation between $\dot{\varepsilon}_{vf}$ and e_i observed in ATA TC and PS tests.

There was no discernible difference between the results from tests carried out at 10, 15 and 20 lbf/in^2 in any of the above graphs.

Figs. 7.11 and 7.12 show the axial strains at failure and the volumetric strain during shearing for all CYL TC tests. There was little correlation between ε_{1f} and e_i. In tests where both proving-ring and stress-cells were used, the latter almost invariably reached a peak at a smaller strain which, discounting tests CYL TC 18, 19 and 23, ranged between about 4% and 6%. Tests 18 and 23 exhibited unusual stress-strain curves, the former having two distinct peaks, and although the specimen in test 19 was dense, a very flat curve of σ_1 v. ε_1 was observed in the failure region. It would appear, therefore, that the axial strain at failure is not an important factor in cylindrical triaxial compression tests, but its variability is not as great as proving-ring measurements would suggest.

Since all specimens were dilating at failure, the smaller values

of ε_{1f} associated with stress-cell measurements imply smaller volumetric strains during shearing (Fig. 7.12). In addition to the tests mentioned above, CYL TC 14 showed a large continued compression after the end of the consolidation stage. Since this specimen was not particularly loose, the results must be regarded as doubtful. The mean curve through the remaining stress-cell points would still predict a substantical compression during shearing for a specimen prepared at e_{max}. However, an examination of the volumetric strain curves for tests CYL TC 20 and 23, those closest to $\varepsilon_{vs} = 0$, reveals that both specimens were dilating rapidly at failure, and that ε_{vs} was low only by virtue of the small axial strain recorded at failure. Therefore no great significance should be placed on the mean curve at the loose end of the initial voids range.

7.4.2 CYL TE TESTS

Eight cylindrical triaxial extension specimens were tested to failure, by decreasing the axial stress, σ_3, while the radial stress, σ_1, was held constant (5.6.3). The manner in which the specimens deformed will be considered in section 7.7. For the present, it will be assumed that the mode of deformation was such that the average cross-sectional area at failure was the appropriate value to be used in stress calculations. The conditions at failure are given in Table 7.8.

The mean curve of ϕ v. e_i is shown in Fig. 7.13, together with the corresponding relationship for the CYL TC test series. Only the loosest specimen, CYL TE 6, exhibited a peak strength in accordance with the triaxial compression value, the remainder having greater magnitudes. The densest specimen tested, CYL TE 8, showed an increase of $5\frac{1}{2}°$ in ϕ, but although an extrapolation to e_{min} would predict an 8° increase, this depends to a large extent on the chosen slope of the mean curve through the points for the four strongest specimens. However, an

increase somewhere in excess of 6° is clearly indicated.

The average major principal strain, ε_1, at failure has been plotted against e_i in Fig. 7.14, and although this strain was not uniform, the results are more consistent than those for the CYL TC specimens, and show greater magnitudes for looser specimens. The corresponding axial extension strains, ε_3, ranged between about 6% and 10%, considerably larger than the compression strains in the CYL TC tests.

TABLE 7.8

Test Number	Initial Voids Ratio e_i	Conditions at Failure (Peak Stress Ratio)				
		Major Strain ε_{1f}	Volume Strain ε_{vf}	Volume Strain Rate $\dot{\varepsilon}_{vf}$	sin ϕ	Angle Internal Sh'g Res ϕ
CYL TE 1	0.605	4.11	+0.43	-0.69	0.599	36.8
CYL TE 2	0.558	2.55	-0.05	-0.87	0.661	41.4
CYL TE 3	0.586	4.64	+0.93	-0.74	0.608	37.4
CYL TE 4	0.555	2.94	+0.07	-0.91	0.655	40.9
CYL TE 5	0.576	3.35	-0.04	-0.85	0.650	40.5
CYL TE 6	0.649	5.25	+2.49	-0.14	0.545	33.0
CYL TE 7	0.603	3.22	+1.02	-0.37	0.584	35.7
CYL TE 8	0.549	3.63	+0.46	-0.78	0.676	42.5

Despite these apparently high rates of volume change at failure, the overall volumetric strains during the shearing stage (Fig. 7.14) were low, and a substantial overall compression would be predicted for a specimen initially at the maximum voids ratio.

Such phenomena are almost certainly the result of localized deformations and consequent underestimation of local volume changes when determined from overall measurements.

7.4.3 CUB TC TESTS

Six cuboidal triaxial compression tests were carried out on specimens having the same physical characteristics as those in the ATA series. In addition to top and bottom stress-cells, a proving-ring was used to measure axial load. The conditions at failure, given in Table 7.9, are shown graphically in Figs. 7.15 and 16.

All proving-ring values of ϕ were between 2° and 3° greater than those determined from the stress-cell measurements. The latter curve was found to be in very good agreement with the results from cylindrical specimens, whereas the proving-ring values were consistently above the corresponding CYL TC curve.

In half of the tests, the axial strain at failure (Fig. 7.16) was the same for both stress-cell and proving-ring measurements, and all but one of the stress-cell points (CUB TC 2) fall within a band similar to that shown in Fig. 7.11. Again the magnitudes of ε_{vs} are dictated by those of ε_{1f}, and no general conclusion can be drawn.

In both the CYL TC and CUB TC test series, the maximum dilatancy rate occurred prior to failure for the majority of specimens, a trend observed in nearly all ATA tests. However, discounting the points which were palpably unreliable, the scatter in the graph of $\dot{\varepsilon}_{vf}$ v. e_i was markedly greater for the cylindrical specimens. The extent to which this was governed by the relative proportions of the specimen dimensions will be considered in section 7.7.

TABLE 7.9

		Conditions at Failure (Peak Stress Ratio)									
		Proving-Ring Measurements					End Stress-Cell Measurements				
Test Number	Initial Voids Ratio e_i	Major Strain ε_{1f}	Volume Strain ε_{vf}	Volume Strain Rate $\dot{\varepsilon}_{vf}$	sin ϕ	Angle Internal Sh'g Res ϕ	Axial Strain ε_{1f}	Volume Strain ε_{vf}	Volume Strain Rate $\dot{\varepsilon}_{vf}$	sin ϕ	Angle Internal Sh'g Res ϕ
CUB TC 1	0.582	4.35	-0.08	-0.37	0.614	37.9	4.35	-0.08	-0.37	0.572	34.9
CUB TC 2	0.575	3.62	-0.69	-0.47	0.621	38.4	2.38	-0.06	-0.49	0.591	36.2
CUB TC 3	0.614	8.79	+0.40	-0.16	0.599	36.8	5.69	+0.89	-0.17	0.558	33.9
CUB TC 4	0.548	4.12	-0.94	-0.39	0.639	39.7	4.12	-0.94	-0.39	0.610	37.6
CUB TC 5	0.557	3.91	-0.54	-0.38	0.641	39.9	3.91	-0.54	-0.38	0.605	37.2
CUB TC 6	0.578	5.54	-0.42	-0.31	0.624	38.6	3.64	+0.16	-0.31	0.586	35.9

7.5 STRESS-STRAIN CURVES

Typical stress-strain and volume change curves for each of the three test series are shown in Figs. 7.17-22.

Tests CYL TC 11 and 20 were the densest and loosest specimens, respectively, for tests in which both proving-ring and stress-cells were used. Fig. 7.17a shows that the dense specimen began dilating soon after the beginning of the shearing stage at a rate which varied very little for strains up to and beyond failure. The stress-cell curve, $(\sigma_1)_{sc}$ v. e_i, showed certain fluctuations which were not apparent from the proving-ring measurements. However, this was unusual; for most tests, the two curves were generally of similar form, but divergent.

The initial concave section of the σ_1 v. ε_1 curve, at the beginning of the shearing stage in test CYL TC 20 (Fig. 7.17b), was caused by poor centering of the specimen relative to the loading plunger, leading to a datum error in ε_1. This effect is reflected in the volumetric strain curve, and is unlikely to be of serious consequence unless the initial strain increments are of interest (7.6). The approximate magnitude of the necessary correction to the overall axial strain is evident from the two curves shown.

The volumetric strain rate decreased continuously during post-failure deformation, but even at 16% axial strain $\dot{\varepsilon}_{vf}$ was 0.16. In test CYL TC 17, a much greater strain was applied with a similar result (Appendix H). However, in both cases, specimen deformation was grossly non-uniform at this stage, and therefore large variations in local dilatancy rates were to be expected.

The percentage error in the deviator stress at failure in these two tests was about 8%. From all the results in this series, it was clear that bushing friction varied greatly with the axial strain of the specimen, even though the conventional precautions of cleaning and

lightly greasing the plunger were undertaken before each test. Therefore the use of a constant deviator stress friction correction is unlikely to yield satisfactory results, even for pre-failure deformations.

The stress-strain curves for a K_o-consolidated specimen are shown in Fig. 7.18. No proving-ring was used. The significance of the corrected- , σ_1, and uncorrected- , $(\sigma_1)_{un}$, major principal stress curves will be discussed in section 7.8. The magnitudes of volumetric compression following consolidation were generally less than for specimens consolidated under ambient stress, but otherwise no consistent differences were apparent between the two series of tests.

Figs. 7.19 and 20 show the results from two triaxial extension tests. The σ_3 v. ε_1 curves are very similar for both loose (CYL TE 7) and dense specimens, but although the volumetric strain curves are of the same form, the dilatancy rates and the overall volume expansion were much greater for CYL TE 4. In all cases, the ε_v v. ε_1 curves exhibited a smooth transition between initial compression and expansion, and the maximum dilatancy rate occurred towards the end of each test.

The results from CUB TC tests were qualitatively similar to those for cylindrical triaxial compression, though Figs. 7.21 and 22 indicate the greater plunger friction error (7.4.3).

7.6 STRESS-DILATANCY BEHAVIOUR

7.6.1 CYL TC TESTS

The relationship between the stress ratio R, $(= \frac{\sigma_3}{\sigma_2})$, and the dilatancy factor D, $(= 1 - \frac{d\varepsilon_v}{d\varepsilon_1})$, for test CYL TC 4 is shown in Fig. 7.23. The lower and upper limit lines, K_μ and K_{cv}, of the stress-dilatancy theory (2.2) have been drawn for ϕ_f values of 27° and 35° respectively, and are identical with those shown in the R v. D graphs of Chapter 6.

Many of the tests were continued to axial strains well in excess of that at failure, but in no instance did the specimen show signs of reaching a constant volume deformation condition.

The peak strength of the loosest specimen tested using end stress-cells (CYL TC 20) was 33.2°. Between failure and an axial strain of 9%, this decreased by about $\frac{1}{2}$°, and although a further large drop occurred, the strains were severely non-uniform at that stage. Therefore, ignoring the ε_v v. ε_1 curve, a value of ϕ_{cv} of about 32° may be more realistic.

A similar inspection of the σ_1 v. ε_1 curve for the loosest K_o-consolidated specimen would give about 30°.

These figures are close to those suggested by the results from ATA TC tests, for which better approximations to the constant volume condition were observed. Clearly the value of ϕ_{cv} determined from ϕ_μ, using Horne's theory, is almost certainly too high. However, it has been preserved in all of the following stress-dilatancy plots to assist comparison with the ATA curves.

Each point in Fig. 7.23 was determined from stress and strain increments in the manner described for ATA tests (6.3.4), and similarly the points have been omitted in subsequent graphs to avoid confusion of the various curves. However, with the exceptions mentioned below, every curve passes through all of the points determined from these increments.

The first two increments in Fig. 7.23 illustrate a phenomenon

common to many of the tests in this series. Following ambient consolidation, bedding between the various components as the deviator stress was first applied caused overestimation of ε_1, and hence of the dilatancy factor. The effect can also be seen in the σ_1 v. ε_1 curve for CYL TC 4 (Appendix H). Although corrections were made for bedding errors, very slight eccentricity of the plunger, as it was brought into contact with the top ball-bearing would be sufficient to cause a radical increase in D. The dashed curves equivalent to those in Fig. 7.23 have been omitted in the other graphs.

Figs. 7.24-26 show the results from rigid end-platten CYL TC tests, and therefore the values of R. particularly during the latter stages, are excessive. However, the early parts of the R v. D curves for seven out of the nine tests lie on, or just above, the K_μ-line. Of the remaining two tests, CYL TC 6 and 9, the latter exhibited unusual stress-strain behaviour throughout deformation.

For every curve the maximum dilatancy rate precedes failure.

The σ_1 v. ε_1 graph for CYL TC 10 indicates a greater than average friction error. Therefore the failure points for this test and for CYL TC 9 have been omitted from Fig. 7.24, where the remainder are shown. All lie between $31° \leq \phi_f \leq 34°$.

The results from the ten cylindrical triaxial compression tests in which both proving-ring and stress-cells were used are presented in Figs. 7.27-30. For test CYL TC 16 (Fig. 7.27), the difference between the stress-dilatancy curves calculated on these two bases is illustrated. The effect of the error in R resulting from proving-ring measurement is most pronounced in the region of failure and beyond, and in particular, the slopes of the post-failure R v. D curves are quite different. The remaining graphs in this section have all been derived from stress-cell measurements of σ_1.

Again the early portions of the R v. D curves plot close to the K_μ-line. Test CYL TC 13 was the only one in which lower ϕ_f values were observed, but specimen behaviour was erratic throughout deformation. The curves for the four loosest specimens, CYL TC 14, 18, 15 and 20, all showed a curious pre-failure kink, associated with noticeable changes in the dilatancy rate (see Fig. 7.17b), the cause of which was unknown. A few of the specimens with rigid ends showed similar tendencies.

After failure, the specimen response was varied, but in most cases, D was almost certainly overestimated, owing to strain non-uniformity. In addition, the magnitude of R was probably underestimated, the combined effect causing almost all of the curves to be directed well below the critical state point. An extreme example was that of test CYL TC 17, which was continued to very large strains.

The curves for CYL TC 19 and 21 are the only ones lying close to the K_{cv}-line, given by $\phi_{cv} = 35°$, and in both cases the specimen was relatively dense. From Fig. 7.9 it can be seen that the values of ε_{vf} for these specimens were substantially lower than the mean curve, due largely to the relatively high values of ε_{1f}.

The stress-dilatancy graphs for the K_o-consolidated specimens are shown in Figs. 7.31 and 32. In each case, the initial part of each curve follows a path, well above the K_μ-line, consistent with a ϕ_f value of about 31° or 32°. In four of the five tests, the peak dilatancy rate was not reached until after failure. The remaining test, CYL TC 22, can be disregarded for the reasons given in section 7.4.1.

All the failure points are shown, in Fig. 7.30, to fall within K_f-lines consistent with $\phi_f = 30°$ and 34°, respectively. If the more doubtful tests are disregarded, the upper limit becomes 32°. The corresponding range for the rigid end-platten tests was 31° to 34°. Assuming that a correction of -2° is appropriate for errors in the proving-ring

values of R, the failure condition for the majority of cylindrical triaxial compression specimens is in accordance with $29° \leq \phi_f \leq 32°$. These results compare well with those from the ATA TC test series (6.3.4).

7.6.2 CYL TE TESTS

In triaxial extension, $\sigma_2 = \sigma_1$ and $\varepsilon_2 = \varepsilon_1$; therefore the energy ratio (2.2) becomes

$$E = \frac{2\sigma_1 d\varepsilon_1}{-\sigma_3 d\varepsilon_3} ,$$

leading to the modified stress-dilatancy equation

$$\frac{\sigma_1}{\sigma_3} = \left(1 - \frac{d\varepsilon_v}{2d\varepsilon_1}\right) \tan^2\left(45 + \frac{\phi_f}{2}\right) ,$$

or more conveniently, in terms of the axial strain increment $d\varepsilon_3$,

$$R = \frac{1}{1 - \left(\frac{d\varepsilon_v}{d\varepsilon_3}\right)} K_f . \qquad \ldots (1)$$

The symbol D has been preserved for the above modified dilatancy factor, in preference to $\frac{1}{D}$ sometimes used, which requires D to be defined as $(1 - \frac{d\varepsilon_v}{d\varepsilon_a})$.

Alternatively, equation 1 may be derived from equation 3 in section 6.6.4, as a special case of the generalised stress-dilatancy relationship for which $T = R$ and $d\varepsilon_2 = d\varepsilon_1$.

The characteristic shape of the volumetric strain curves in all of these tests was noted in section 7.5 (Figs. 7.19 and 7.20). After ambient consolidation, the rapid decrease in σ_3 was accompanied by a steady continued compression, followed by a smooth transition to dilatancy. The rate of dilatancy $\dot{\varepsilon}_{vf}$, defined as the rate of change of volumetric strain with respect to the major (radial) principal strain, increased continuously to failure.

The mode of deformation of the CYL TE specimens will be considered

fully in the following section. However, it is clear that localized deformations, such as the formation of the "neck" commonly associated with triaxial extension testing, would cause the magnitudes of ε_3 and ε_v in the "failure" zone to be underestimated, if based on overall measurements. The resulting errors would increase with deformation.

The effect on the derived values of ε_1 in the CYL TE test series will obviously depend on the relative magnitude of the above errors, but it is probable that these too will be increasingly underestimated with increasing deformation.

Clearly, the relationship between $\dot{\varepsilon}_{vf}$ and e_i, shown for both CYL TE and CYL TC results in Fig. 7.13, is of little significance when comparing specimen behaviour in the two types of tests. Because of the different form of the energy ratio, E, the dilatancy factors for triaxial compression and extension are $(1 - \frac{d\varepsilon_v}{d\varepsilon_1})$ and $(1 - \frac{d\varepsilon_v}{2d\varepsilon_1})$ respectively, and therefore twice the magnitude of $\dot{\varepsilon}_{vf}$ might be expected for the latter.

Fig. 7.13 shows that this proportion was generally exceeded, which may be consistent with the greater values of R observed for most densities in triaxial extension.

The stress-dilatancy curves of R v. D are shown in Figs. 7.33-36 for the eight CYL TE tests carried out. Clearly, they will be affected by the errors in the measured strain-increments described above.

During the initial stages of shearing the measured volumetric strains were probably representative of those throughout the specimen, and therefore the major source of error would have been in the axial strain measurements. A similar conclusion was reached for triaxial compression tests. The effect on the R v. D curves is likely to be similar, since an overestimation of $d\varepsilon_3$, in equation 1, caused by bedding of the tension components, would give excessive values of D.

The curves for every specimen show this tendency.

For the three densest specimens, CYL TE 2, 4 and 8, the latter portions of the curves fall above the K_{cv}-line. At this stage of the test, the average rate of dilatancy was almost certainly less than that in localized failure zones. Although this would have been partly offset by a greater localized axial strain, the overall effect probably cuased an underestimation of D. The same argument would apply to the looser specimens, but the magnitudes of such errors were likely to have been less.

The combined effect of these two phenomena would increase the slope of the R v. D curves, as Figs. 7.33-36 clearly show.

Qualitative correction suggests that the form of the true curves would be similar to that observed for the majority of CYL TC tests, the initial portions following a path close to the K_{μ}-line and the failure points plotting within a comparable range of ϕ_f values.

7.6.3 CUB TC TESTS

Fig. 7.37 and 38 show that only two of the cuboidal specimens tested in triaxial compression deformed in accordance with $\phi_f = \phi_{\mu}$ for any significant range of deformation. Each was dense. The remainder deviated considerably during the initial stages, but each curve showed a tendency to become closer to the K_{μ}-line until failure was approached. In most tests, the maximum rate of dilatancy occurred prior to peak stress ratio.

The failure points, shown together in Fig. 7.37, were bounded by the K_f-lines consistent with ϕ values of $29\frac{1}{2}°$ and 32°.

7.7 MODE OF DEFORMATION

7.7.1 CYL TC TESTS

With one exception, the CYL TC specimens tested in this series were nominally 5 in. in length and 2.8 in. in diameter, a ratio of approximately 1.8 : 1. Whether rigid plattens or top and bottom stress-cells were used, each specimen was lubricated with a membrane smeared with silicone grease. For the single 3 in. long specimen, CYL TC 24, double membrane-grease sandwiches were used. The efficiency of such lubrication and its effect on the deformation of the specimen have been discussed in previous sections (3.3.1, etc.).

The difficulties of obtaining quantitative information on the deformed shape of a stress-controlled boundary were indicated in section 5.5.2, and a method was described by which the approximate profile of cylindrical specimens could be determined at the end of a test, with a minimum of disturbance. This method was used for CYL TC and CYL TE specimens. In addition, photographs were taken at various stages of deformation during several tests. Figs. 7.1 and 7.2 show the states of two specimens prior to and just after failure, and at large axial strains.

In Fig. 7.1c, the CYL TC 21 specimen is shown after removal of the axial load. This was accompanied by a characteristic axial elongation and lateral contraction, which ruled out vernier micrometer gauge measurement for obtaining the specimen dimensions at failure.

Figs. 7.39 and 40 show half-sections of eight CYL TC specimens determined at the end of their respective tests, which in most cases was shortly after failure. Both rigid and flexible end conditions are represented, and the initial voids ratios range between 0.506 (CYL TC 9) and 0.626 (CYL TC 18).

Despite the lubrication provided, in none of these tests did any

noticeable expansion occur immediately adjacent to the stress-cells or end-plattens at either the top or the bottom. In the majority of tests, the radial bulge was displaced slightly below the mid-height of the specimen, though in tests CYL TC 9 and 19, the reverse was the case. The latter were each dense specimens. In general, the "uniformity" of bulging was considered to indicate that the method of preparation gave a reasonable degree of homogeneity. The average lateral strains determined from these measurements were generally in good agreement with the values calculated from volumetric and axial deformations.

The profiles of specimens CYL TC 17 and 24 are shown in Fig. 7.41. The former was tested to a very large axial strain (34%), primarily to observe its volume change characteristics. However, it is of interest to note the reluctance of the specimen to expand at the ends, particularly in the zone immediately adjacent to the top stress-cell.

In contrast, the deformed shape of the 3 in. long specimen, CYL TC 24, more closely resembled a right cylinder, and end expansion began at quite small strains, the specimen overlapping the edges of the stress-cells. It is very probable that the use of enlarged end plattens would have further improved the uniformity of lateral expansion. Although lubrication was improved by the provision of a double membrane-grease sandwich, this was not considered to be of great significance, in view of the consistent end expansions noted during the ATA test series where only one membrane was used. In this respect, it would appear that the ratio of length to maximum horizontal dimension, i.e. the diagonal, is of more significance than the length to width ratio. For the ATA specimens, these ratios were approximately 1.25 and 1.75 respectively.

Clearly the mode of deformation of "long" cylindrical triaxial specimens is not greatly affected by the provision of "free ends", a

conclusion reached by several investigators. It does not follow, however, that the overall uniformity of stresses and strains within the specimen are similarly unaffected (3.3.1).

The testing of "short" specimens throughout the CYL TC series would undoubtedly have improved the strain uniformity, providing an efficient end lubrication system were used in conjunction with enlarged stress-cell surfaces. At the present stage of development, this could be achieved only by increasing the peripheral flange area, thereby decreasing the effectiveness of the stress-cell system. Although a small overlap of the ATA cuboidal stress-cells was allowed in the y-direction, the shape of the diaphragms and the fact that the perpendicular flanges remained covered tended to improve their stability.

7.7.2 CYL TE TESTS

It was found necessary to measure axial stress only at the bottom of the "short" triaxial extension specimens.

Figs. 7.3 and 7.4 show the development of lateral strain in two CYL TE tests, and half-sections of all eight specimens, determined at the end of each test using the "cell-volume" method, are given in Figs. 7.42 and 43. In every case, lateral contraction occurred adjacent to the rigid top platten. During preliminary testing, in which both end stress-cells were used, this effect caused a failure of the top component.

Only in test CYL TE 6, on the loosest specimen, did a similar contraction occur at the bottom stress-cell, though its magnitude was relatively small (Fig. 7.3). The remaining specimens developed a minimum cross-sectional area at about three-quarter height. However, the deformed shapes were not sufficiently irregular for this region to be described as a "neck".

The effect of the variation in specimen cross-section on the axial stress calculations will be considered in section 7.8.2.

Single greased membranes were used at each end of all CYL TE specimens, reinforcing the conclusion that inefficient lubrication was not responsible for the absence of end movement in the CYL TC series.

7.7.3 CUB TC TESTS

Lateral expansion occurred at both ends of all six cuboidal triaxial compression specimens. In the y-direction this caused the stress-cell surfaces to be slightly overlapped. The difficulties of determining the final dimensions of these specimens have been discussed previously, and in this test series no satisfactory measurements were obtained. However, the mode of deformation was similar to that described for ATA TC specimens, and the enlargement of the end stress-cells in the x-direction appeared to assist end expansion.

In every test, the lateral strains increased towards the bottom of the specimen, but in most cases, for pre-failure conditions, the degree of bulging was small. In common with both CYL TC and CYL TE test series, failure planes were not usually apparent, unless tilting of the top stress-cell occurred. The latter effect was not possible during triaxial extension tests.

7.8 TOP AND BOTTOM STRESSES

Because the end stress-cell system involves direct measurement of stress rather than of load, knowledge of the variation of specimen cross-sectional area is probably more important than in the more conventional systems.

For all ATA tests described in the previous chapter, it was assumed that the mean of the recorded top and bottom stresses was the appropriate value of σ_3 to be used in the stress analysis. Justification for this assumption was presented by relating stress-cell measurements with quantitative information regarding the mode of specimen deformation. All the axial stresses in the CUB TC tests were calculated on the same basis. However, for both of the cylindrical triaxial test series this was clearly unacceptable.

7.8.1 CYL TC TESTS

In section 7.7.1, it was shown that all 5 in. long specimens bulged centrally with negligible end expansion. In consequence, the stress-cell measurements would have been significantly greater than the average vertical stress. Therefore a correction was applied by multiplying both top and bottom measured stresses by the ratio between the end area and the average area calculated from volumetric and axial strains.

The effect of this correction was shown for specimen CYL TC 26 in Fig. 7.18, the lower curve representing the corrected value of σ_1. Clearly the difference was small during the early stages before significant bulging occurred. However, at failure the use of uncorrected stress-cell measurements would have resulted in an error of 0.9° in ϕ.

In every stress-strain curve for CYL TC tests, the area correction has been applied to σ_1. A single exception was test CYL TC 24, carried

out on a 3 in. long specimen, for which noticeable end expansion occurred. Because the end stress-cells were overlapped, the average vertical stress could not be determined with any certainty, and therefore the results were less reliable than those from tests on long specimens.

7.8.2 CYL TE TESTS

In all but one of the triaxial extension tests, no discernible expansion occurred at the bottom of the specimen (Figs. 7.42, 43). The axial stress was not measured at the top, and therefore a correction was applied to the bottom stress-cell measurement, in the manner described for CYL TC tests, to determine the average minor principal stress. Since the average area is less than that at the ends, the magnitude of σ_3 will be increased, as shown in Figs. 7.19 and 7.20.

The corrected and uncorrected values of ϕ have been plotted in Fig. 7.44, the difference varying between about 2° for loose specimens and 1° for dense specimens.

A further set of points is shown for strengths based on the minimum cross-sectional area of each specimen, determined from the final profiles. Since no well-defined "neck" was formed in any of the specimens, there would be little justification in using this data for comparison with the results of triaxial compression tests. However, additional corrections assume greater importance at the low stress levels of the CYL TE series, and these will be considered in the next section.

7.9 DATA CORRECTIONS

The area corrections discussed in the previous sections were incorporated in computer programs, together with the corrections for membrane penetration and the apparatus calibration factors. Tests carried out to determine the effect of specimen membrane strength are described in Appendix D.

Table D.2 shows that the corrections to ϕ for three CYL TC tests and two CUB TC tests were negligible. However, a similar analysis of triaxial extension data (Table D.3) indicated that far greater errors would result from ignoring this effect. Because the membrane is elongated, the deviator stress correction is negative.

In all previous test series, the effect of specimen self-weight was insignificant, especially since any error would have been consistent for tests carried out at similar stress levels. For all CYL TE tests the axial stress, σ_3, was measured at the bottom only, and since this stress was reduced to failure, its magnitude at peak stress ratio was much lower than that in CYL TC tests. These two factors combine to greatly increase the importance of self-weight.

The increase in vertical stress from top to bottom of the 3 in. × 2.8 in. dia. CYL TE specimens was approximately 0.2 lbf/in^2, and therefore half of this must be subtracted from the corrected stress-cell measurement of σ_3 in order to determine its average value. Clearly this partially counteracts the effect of the membrane strength correction, as shown in Table 7.10.

The combined correction was applied to the results of all CYL TE tests, and the final values of ϕ are compared with the mean curve from the cylindrical triaxial compression series in Fig. 7.45.

TABLE 7.10

Test Number	Uncorrtd ϕ	Membrane strength correction	Self-weight correction	Corrected ϕ
CYL TE 1	36.8	-0.9	+0.4	36.3
CYL TE 2	41.4	-0.8	+0.4	41.0
CYL TE 3	37.4	-0.9	+0.3	36.8
CYL TE 4	40.9	-0.7	+0.4	40.6
CYL TE 5	40.5	-0.9	+0.4	40.0
CYL TE 6	33.0	-0.9	+0.4	32.5
CYL TE 7	35.7	-0.6	+0.4	35.5
CYL TE 8	42.5	-0.8	+0.5	42.2

7.10 COMPARISON WITH ATA RESULTS

The primary purpose in carrying out the triaxial test series described in the previous sections was to assist the assessment of the new apparatus for generalised stress and strain testing. Several comparisons between the results from tests in the ATA and in the more conventional apparatus have been made; others were implied. In this section, the more important aspects of such comparisons are summarized.

7.10.1 CONSOLIDATION

In none of the test series described were the consolidation stages carried out in a fully satisfactory manner, due largely to errors in measured volume changes below about 5 lbf/in^2. Since the majority of tests were performed at relatively low stress levels, such errors assumed greater importance.

However, the values of K_o determined from five CYL TC tests were in good agreement with the frequently-suggested approximation $(1 - \sin \phi)$, which confirmed that lateral expansion had occurred during the "K_o"-consolidation of ATA TC and PS specimens. A comparison between the mean curves is given in Fig. 7.46, together with that for $(1 - \sin \phi)$ derived from the ϕ v. e_i relationship for CYL TC tests.

7.10.2 FAILURE CHARACTERISTICS

The relationship between the peak strength ϕ and e_i is shown for all six test series in Fig. 7.47. The range of strengths observed for the ATA INT tests as the parameter b varied between 0.125 and 0.398 are given for the "unified" initial voids ratio, 0.530. All necessary corrections have been applied to the measured data.

For the majority of the range of e_i, the ATA TC strengths were marginally greater than those obtained from the CYL TC series, the maximum difference being about 0.6°. However, it may be that part of this

difference could be accounted for by the shape of the respective specimens, since the CUB TC specimens also showed a slight increase in ϕ. Although the ATA TC curve is shown in full for initial voids ratios in the region of 0.650, there was a wide discrepancy in the results from tests on the two loosest specimens. Therefore it is quite probable that the true relationship between ϕ and e_i would have a curvature similar to that for the CYL TC specimens.

Allowing for experimental scatter, these three sets of results show excellent agreement, which was considered to indicate that the ATA imposes a minimum of restraint on cuboidal specimens deforming under triaxial compression stress conditions. Since it is under these conditions that specimen expansion in the y-direction is likely to be a maximum, for the usual orientation of the principal stresses, the possibility of additional restraint during ATA INT or PS tests must be remote.

The curve of ϕ v. e_i for ATA PS tests was linear and well above the three triaxial compression curves for the whole of the initial density range investigated. However, an extrapolation of the CYL TC curve, probably the more reliable curve for loose specimens, would predict equality of triaxial compression and plane strain curves at about the maximum voids ratio.

The CYL TE results, after all necessary corrections had been applied, were in agreement with the triaxial compression values for loose specimens only, after which a rapid increase was apparent. Extrapolation to the minimum voids ratio would indicate possible agreement between plane strain and triaxial extension strengths. At e_i = 0.530 a difference of 1° in ϕ would be obtained.

If this value of ϕ, for b = 1, is used in conjunction with the results from the ATA INT tests 1-6, and the two doubtful results from INT 7 and ATA TE 1 are disregarded, the intersection of the failure

surface with an octahedral plane in principal stress space approximates very closely to the form predicted by Parkin's theory (2.2). A similar conclusion was reached by Green (1969). This was, however, based on cuboidal triaxial extension test results, since significantly lower strengths were obtained for cylindrical specimens.

The axial strains at failure in ATA tests were more variable, and generally slightly greater, than those observed during the CYL TC and CUB TC tests, but since there was very little correlation between ε_{1f} and e_i for any series, this was not considered to be of great importance. A similar conclusion was reached regarding the volumetric strains during shearing. However, the volumetric strain rate at failure, $\dot{\varepsilon}_{vf}$, was found to be a far more significant parameter for the triaxial compression and plane strain tests.

The respective relationships between $\dot{\varepsilon}_{vf}$ and e_i are given in Fig. 7.49.

From energy considerations it was shown, in section 7.6.2 that for triaxial extension the corresponding dilatancy rate should be expressed as $\frac{d\varepsilon_v}{2d\varepsilon_1}$, or $\frac{\dot{\varepsilon}_{vf}}{2}$; this curve is also given.

The scatter of points about the mean curve for ATA TC and PS tests was small (Fig. 6.42), whereas that for the CYL TC series was very much greater (Fig. 7.10). With one exception, the CUB TC results were more consistent, and if this single test were ignored, the mean curve would approximate closely to that for the ATA specimens. Therefore, it would appear that the size and shape of the specimen was important in this respect.

The modes of deformation of the various specimens have been discussed in detail, and will be summarized in section 7.10.4. All of the cuboidal specimens deformed in a reasonably uniform manner up to peak stress ratio. In most cases, lateral expansion was greatest

towards the base, but occurred over the full specimen height. The mean of the lateral strain at the two ends of the specimen was shown to be similar to the average lateral strain calculated from overall measurements. In contrast, none of the "long" CYL TC specimens expanded at the top or bottom. Therefore, it is probable that the local strains were far more variable in the latter, and consequently the magnitudes of $\dot{\varepsilon}_{vf}$ calculated from overall measurements of axial and volumetric strains must be considered less representative of local conditions. These specimens also showed less tendency to approach the constant volume state at large strains.

It is of interest to note that the scatter of points for the "short" CYL TE specimens, in a plot of $\frac{\dot{\varepsilon}_{vf}}{2}$ against e_i, would be similar to that for the ATA results in Fig. 7.49.

7.10.3 STRESS-DILATANCY BEHAVIOUR

The most consistent common features of the stress-dilatancy behaviour in the three triaxial compression test series were the upper and lower K_f-lines bounding the failure points in the R v. D relationships. This necessarily follows from the agreement between the values of ϕ and of $\dot{\varepsilon}_{vf}$ for ATA TC, CYL TC and CUB TC tests, discussed in the previous section. The corresponding values of ϕ_f were found to lie between $29\frac{1}{2}^\circ$ and 32°.

It was suggested, in several sections, that the assumed magnitude of ϕ_{cv} was considered to be about 32°.

Many specimens deformed, during the initial stages, in a manner consistent with $\phi_f = \phi_\mu$ ($= 27^\circ$), and very few R v. D curves plotted below this line. Therefore, it was concluded that the difference between ϕ_μ and ϕ_{cv}, predicted by Horne's theory, was excessive.

Direct comparisons between the ATA TC results and those from the

CYL TC and CUB TC series over a full range of deformation were limited because of the different consolidation processes used and their effect on subsequent behaviour. This applies particularly to comparisons between the two series of tests on cuboidal specimens.

After "K_o"-consolidation, the ATA TC curves of R v. D showed a tendency to follow or approach the K_μ-line before reaching a maximum dilatancy rate (Fig. 6.13, etc.). The dilatancy factor, D, then changed very little until just before failure. The early parts of the CUB TC curves, however, deviated considerably from this line in half of the tests (Figs. 7.37, 38), and showed no sustained dilatancy rate.

The CYL TC specimens behaved similarly, but with a greater preference for the K_μ-line during initial deformation. Noticeable exceptions were the K_o-consolidated specimens, for which ϕ_f was several degrees higher throughout the shearing stage.

It is probable that the effects of non-uniform strain distribution (7.10.2) were significant in all CYL TC tests.

There was little consistent evidence from these three test series to indicate that loose and dense specimens behaved differently, with respect to K_f. However, a few ATA TC results suggested higher ϕ_f-values for dense specimens, which was contrary to the general postulates of the stress-dilatancy theory.

7.10.4 MODE OF DEFORMATION

The most significant difference between the deformation of cuboidal and "long" cylindrical specimens was degree of movement of the soil adjacent to the end stress-cells.

For all ATA specimens, and those in CUB TC tests, noticeable end expansion occurred and, in consequence, the overall strains were more uniform. In contrast, the CYL TC specimens, exhibited negligible end

expansion.

Since the lubrication system was identical, it was clear that the proportion of the specimen dimensions was an important factor. This was confirmed by the end expansions observed in the CYL TE series, where the initial length to diameter ratio was about 1.1, compared with that of 1.8 for the CYL TC tests.

For ATA specimens, the length to minimum width ratio was similar to the latter figure, and therefore it would appear very unlikely that this ratio is significant in determining the mode of deformation. The ratio of length to maximum horizontal dimension, which was about 1.25, is probably the critical factor for cuboidal specimens.

The observed end expansions were considered to be indicative of end lubrication efficiency (Appendix F).

7.11 SUMMARY

This chapter has been concerned with the results and analysis of tests carried out in apparatus other than the ATA.

Although none of the consolidation processes were precise, it was confirmed that the values of K_o from ATA tests were low, and that $(1 - \sin \phi)$ was a reasonable approximation to the CYL TC results (7.3.2).

At failure, the peak strength of cuboidal and cylindrical triaxial compression specimens were very similar over a range of initial voids ratios (7.4.1). However, after all reasonable corrections had been applied to the results of CYL TE tests, the values of ϕ were considerably greater for dense specimens (7.4.2), and an extrapolation to e_{min} would predict strengths similar to those in the ATA PS series. In section 7.5, it was shown that errors of greater than 10% would have resulted from the measurement of deviator stress by proving-ring only.

Although many CYL TC and CUB TC specimens tended to deform in accordance with $\phi_f \rightarrow \phi_\mu$, in a stress-dilatancy plot of R v. D, the results from the latter series in particular were variable, and showed little correlation with initial voids ratio. The curves for CYL TE specimens were probably subject to greater errors due to local strain non-uniformities, but qualitative correction suggested a similar pattern of behaviour (7.6).

In section 7.7, the ratio of the maximum vertical to maximum horizontal dimension was shown to be the more important factor in determining the mode of deformation of cuboidal specimens, providing end lubrication is adequate. Corrections to the end stress-cell measurements of axial stress were essential for CYL TC tests, in which negligible end expansions occurred, and for CYL TE tests, where stress was measured at the bottom only (7.8). Membrane strength and specimen self-weight were also

shown to be significant for the latter series (7.9).

Finally, in section 7.10, comparisons were made with the results from the ATA series, and it was concluded that the new apparatus imposed negligible restraint on specimen deformation during tests in which σ_y was the intermediate principal stress.

CHAPTER EIGHT

SUMMARY AND CONCLUSIONS

The majority of this research program has been concerned with investigation of the mechanical properties of a cohesionless soil under a variety of stress and strain conditions.

In order to carry out tests in which the intermediate principal stress could be independently controlled, a new apparatus was designed for testing cuboidal soil specimens. The problems encountered in the development of this apparatus and the manner in which they were overcome were discussed fully in Chapter 4.

A combination of one strain-controlled and two stress-controlled boundaries was used. Although this ensured that the two pairs of vertical boundaries were uniformly stressed, it was later shown that at large lateral deviator stresses, undesirable expansion of the side stress-cell membranes caused appreciable errors in the measurements of ε_y. Since the magnitude of the other lateral strain, ε_x, was derived from these values, there was no redundancy of measured quantities which would allow the errors to be determined.

In order to establish the effect of friction along the σ_y-faces of the specimen, and to eliminate errors in the deviator stress resulting from plunger friction, it was considered necessary to measure the axial stress, σ_3, at both top and bottom. The surfaces of the stress-cells, designed to fulfill this objective, were largely flexible, and therefore also had the effect of reducing rigid boundary constraint.

The procedures used in the triaxial compression, plane strain and intermediate-stress tests carried out by the author were described, and further types of ATA tests, involving alternative orientation of the principal stresses were discussed. The major fundamental limitation on

the stress paths that can be applied in this apparatus is that $(\sigma_y - \sigma_x)$ must not be negative. The testing of specimens under certain other stress and strain conditions may necessitate complex experimental procedures, but the success of these tests would depend largely on the dexterity of the operators.

In Chapter 5, cylindrical and cuboidal triaxial compression tests and cylindrical triaxial extension tests, carried out on specimens of the same soil, were described. The stresses and strains were determined using similar techniques.

Corrections for membrane penetration, elasticity of the apparatus and compression of the lubricated end membranes were applied to all ATA and conventional test results. Membrane strength and specimen self-weight were shown to be significant only in the CYL TE series.

The analyses of results discussed in Chapters 6 and 7 are of particular interest when considered together, since the primary objective in carrying out the more conventional triaxial test program was to allow a reliable assessment of the new apparatus to be made.

Previous attempts to impose generalised stress or strain conditions have frequently resulted in considerable interference with the natural deformation of the specimen. An obvious example is that of Ko and Scott's (1967) apparatus, where the rigid metal frame separating three pairs of flexible diaphragms totally constrained the cubical specimens along its twelve edges. The problems of mutual interference at the edges of three pairs of rigid strain-controlled boundaries, together with the uncertainties regarding boundary stress uniformity, render this type of apparatus even less feasible, unless the stress distribution can be determined.

Comparisons between the strengths and stress-strain characteristics of the ATA TC, CYL TC and CUB TC specimens were excellent, and therefore

it was concluded that the degree of interference imposed by the new apparatus was negligible.

From quantitative consideration of the deformed shape of several ATA specimens at failure, it was shown that the frictional forces on the σ_y faces were small. Although these calculations were necessarily approximate, the average magnitude of the frictional coefficient, μ, was of the same order as that determined from the special tests described in Appendix F. The observed lateral expansion of ATA specimens adjacent to both top and bottom stress-cells was regarded as indicative of the efficiency of end lubrication, though it is probable that the value of μ was greater than that along the σ_y faces.

The results from plane strain tests on dense sand revealed an increase in ϕ of 7° above that for all triaxial compression specimens at comparable voids ratios. This decreased linearly with density, and it was estimated that at e_{max}, any difference would be very small.

Detailed consideration was given to the pre-failure stress-strain relationships observed in the ATA PS tests. With few exceptions, the curves of σ_1 and σ_2 against axial strain in σ_x-constant tests showed marked inflexions. These were present in the σ_3 curves of σ_3-constant tests, but were less clear because of the lower stress level.

During the initial stages after consolidation, the σ_1 curves were found to be very similar to those obtained for similar specimens in ATA TC tests. The range of agreement was found generally to coincide with the slow build-up of the lateral deviator stress $(\sigma_2 - \sigma_3)$.

Measurements of two specimens after removal of the side stress-cells confirmed that a positive strain in the y-direction had taken place. The results from K_o-consolidation of several CYL TC specimens suggested that lateral expansion must also have occurred during the first stage of ATA tests. Therefore it was impossible to estimate the

magnitude of ε_y during the shearing stage. It is not certain that these slight deviations from the plane strain condition were wholly responsible for the observed inflexions in the σ_1 v. ε_1 curves, or for the nature of the variations in σ_2. However, it is clear that expansion of the side stress-cell compartments is a considerable hindrance to the testing of ATA specimens under strict plane strain conditions.

Certain practical remedies could be taken to reduce this effect to a minimum, but because of the stress-controlled nature of the σ_y boundaries, the ATA must be considered more suitable for applying specific stress conditions. This was done in the ATA INT test series, in order to investigate the influence of the intermediate principal stress on the behaviour of dense specimens. However, lateral strain measurements were found to be subject to serious errors for large magnitudes of the parameter b. This further prevented tests being carried out, with the usual orientation of the principal stresses, at b-values greater than about 0.5.

In two tests, the major principal stress was applied in the y-direction and the axial stress, σ_3, was decreased to failure. The two lateral stresses were made equal in test ATA TE 1, an axially-symmetrical extension test, and for ATA INT 7, σ_y was increased slightly above the main-cell pressure to provide a b-value of just over 0.8. Although this reduced the magnitude of $(\sigma_y - \sigma_x)$, the specimen strains were considerably less uniform than in the previous tests, and measurements of the major principal strain, ε_y, were particularly suspect.

A maximum strength in the intermediate-stress tests was obtained for a magnitude of b of approximately 0.3. The increase in ϕ above its triaxial compression value was approximately 8°; the plane strain strength was 2° lower. The influence of σ_2 on soil strength was clearly greater for b-values less than that at failure in plane strain. However, because

of the uncertainties regarding the area corrections necessary in tests INT 7 and ATA TE 1 no definite conclusions could be reached, from this data alone, on an appropriate failure criterion.

The cylindrical triaxial extension specimens deformed in a more uniform manner, and the final profiles were determined using the "cell-volume" method. Because no appreciable necking occurred, it was not considered justifiable to use the minimum cross-sectional areas in determining the stress ratios at failure. After all other corrections, triaxial extension strengths were found to be much greater than the corresponding triaxial compression values for most of the density range.

Using the value of ϕ in cylindrical triaxial extension at an initial voids ratio comparable with the "unified" intermediate-stress value (0.530), a failure criterion of the form given by Parkin's theory would be appropriate. However, this would apply only for dense specimens, since the variation of triaxial extension strength with initial voids ratio was shown to be quite different from that in plane strain. Moreover, the above theory is strictly applicable only to the densest arrangements of particles.

For all test series, consideration was given to the relationship between the principal stress ratio, R, and the incremental strains in the form of the parameter D.

At failure the volumetric strain rates, $\dot{\varepsilon}_{vf}$, in ATA TC and PS tests were found to be in excellent agreement. Although the CUB TC values were similar, the results from cylindrical triaxial compression tests were considerably more variable. It was concluded that this phenomenon was associated with the less uniform mode of deformation observed for "long" specimens. Clearly, the measured strain increments would be similarly affected, but probably to a lesser extent, during the majority of pre-failure deformation.

Other reservations were presented regarding the measurements of these increments in ATA TC, ATA PS and CYL TE tests. However, the curves of R v. D show similar trends in all tests. Initial deformations were found to follow, or be directed towards, the K_μ-, lower limit, line. With the exception of those tested in cylindrical triaxial extension, all specimens reached maximum dilatancy rate prior to peak stress ratio. In most plane strain tests, D varied very little from this point until just before failure. A similar pattern of behaviour was apparent for the ATA TC specimens.

The most noticeable factor common to all axially-symmetrical tests was the tendency for failure to be reached at a ϕ_f-value of between $29\frac{1}{2}^\circ$ and 32°. This was considered to be a better approximation to ϕ_{cv} than the value suggested by Horne's theory, assuming $\phi_\mu = 27^\circ$.

Generalised forms of the stress-dilatancy equation were derived for $\sigma_1 > \sigma_2 > \sigma_3$. However, because the lateral strains in some of the intermediate-stress tests were seriously in error, it was not possible to draw definite conclusions regarding their validity. For tests in which there was an overall expansion in the y-direction during the final stage, the R v. D curves were similar to those in plane strain, but since the increments of ε_2 varied in sign, the application of a single stress-dilatancy equation was not strictly justifiable.

In general, while it may be concluded that a more accurate system of measuring the two lateral strains would enhance the scope of the new apparatus, it clearly fulfills many of the objectives discussed in Chapter 3.

The application of three independent, uniform principal stresses to the boundaries of a cuboidal soil specimen, without inhibiting its freedom to deform to large strains, has been made possible.

The end stress-cell system of axial stress measurement has further

reduced the uncertainties associated with more conventional methods, and has allowed the shear forces on the vertical surfaces of the specimen to be estimated.

Continuous galvanometer trace recordings of the top and bottom stresses have also allowed small fluctuations in their magnitude to be studied, and this may have considerable significance in particulate theories of stress-deformational behaviour.